Workshop on the Standard Model and Beyond

August 28 - September 8, 2021

Highlights from ATLAS

Louis FAYARD (IJCLab Orsay)

on behalf of the ATLAS Collaboration

- ***Historical introduction , Setting the stage***
- ***Results***
- ***Future of ATLAS , Run-3 , HL-LHC***
- ***Conclusions***
- ***Backup***

LHCP2021
The Ninth Annual Conference on Large Hadron Collider Physics

see also recent conferences

EPS HEP2021 VIRTUAL EDITION

***Presentations** by Stéphane Willocq, Kerstin Tackmann (EPS) Manuella Vincter (LHCP)*

https://indico.desy.de/event/28202/contributions/102714/attachments/67623/84294/ATLAS-Highlights-2021-07-27-v4.pdf

https://indico.desy.de/event/28202/contributions/102731/attachments/67620/84257/EPS-Higgs.pdf

https://indico.cern.ch/event/905399/contributions/4099244/attachments/2259199/3834217/talk_LHCP21_Vincter.pdf

and listen to future conferences

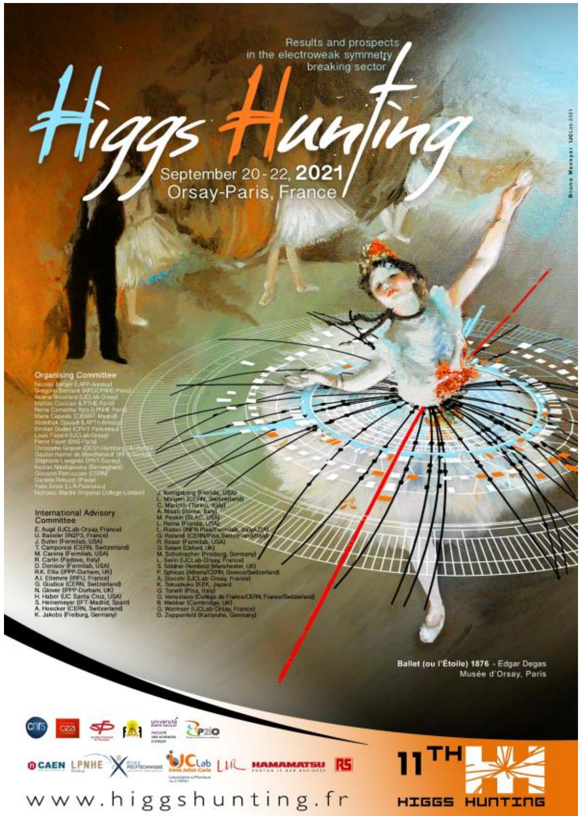

Large number of results !

(however remember that Run-2 ended in 2018 and that there is no new data ⇒ Some results with full run 2 dataset were already available and presented at Corfu 2019)

I will be selective with only few details !

For more results : look at backup and references

I will insist more strongly on strategy and results than on phenomenological interpretations

Rien n'est cru si fermement que ce que l'on sait le moins

Nothing is believed more strongly that which we know the least

Montaigne, Essais

Other relevant presentations (with ATLAS results) this year at Corfu

Higgs studies in ATLAS and CMS ***(Paul Asmuss)***

SUSY searches in ATLAS and CMS ***(Pablo Matorras Cuevas)***

DM in ATLAS and CMS ***(Andreas Albert)***

Exotics and BSM in ATLAS and CMS (non-DM, non-SUSY searches)
(Ann-Kathrin Perrevoort)

Top physics in ATLAS and CMS ***(James Michael Keaveney)***

SM (EW+QCD) measurements in ATLAS and CMS ***(Kostas Kordas)***

I thank the organizers, in particular Georges and I am really sorry not being this year at Corfu

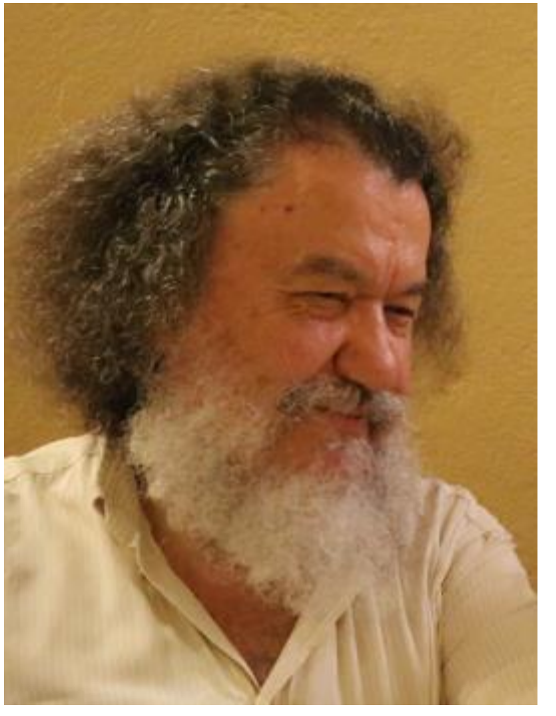

♪ ***Historical introduction , Setting the stage***

♪ ***Results***

♪ ***Future of ATLAS , Run-3 , HL-LHC***

♪ ***Conclusions***

♪ ***Backup***

Spontaneous Symmetry breaking

The Brout-Englert-Higgs mechanism

The LHC

in a 

1950 Ginzburg-Landau (Meissner-Ochsenfeld effect → London penetration length ~ W mass
→ Pippard coherence length ~ H mass)
1959 Nambu
1960 Goldstone, Gell-Mann Levy, NJL
1961 Schwinger
1962 Anderson
1964 Brout, Englert, Higgs, Guralnik, Hagen, Kibble
1967 Weinberg, Salam Faddeev, Popov
1970 Glashow, Iliopoulos,
Maiani, 't Hooft, Veltman, BRST…..

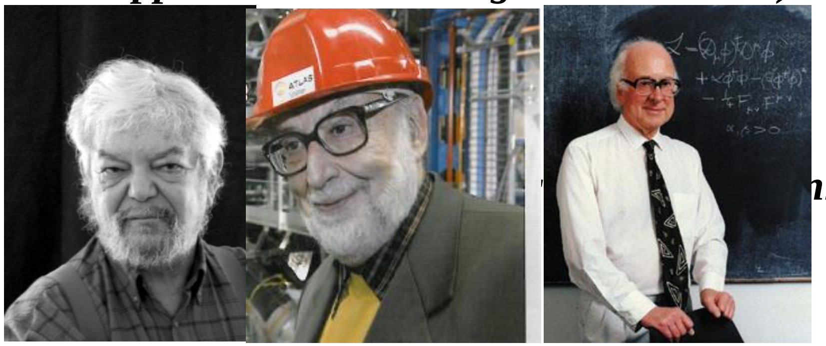

particles of mass $\sqrt{-2\mu_0^2}$

1983 Rubbia, van der Mee … *discovery of W and Z at CERN*
1984 Spiro …

Lausanne

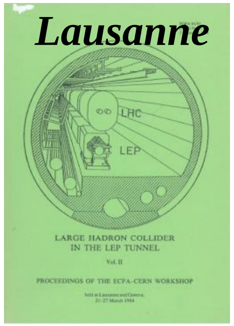

1989 constructio…
beginning o…

1992 ← LOI of 'lar…
1994 ← TP of ATL…
1995 discovery o…
1996 ← approval o…
1998 ←
approval o… …CE)
1999 ← ATLAS Ph… …P data ended in 2000

2006 ← CMS Physi…
2008 ← ATLAS Ex…
2010 ← start-up at…

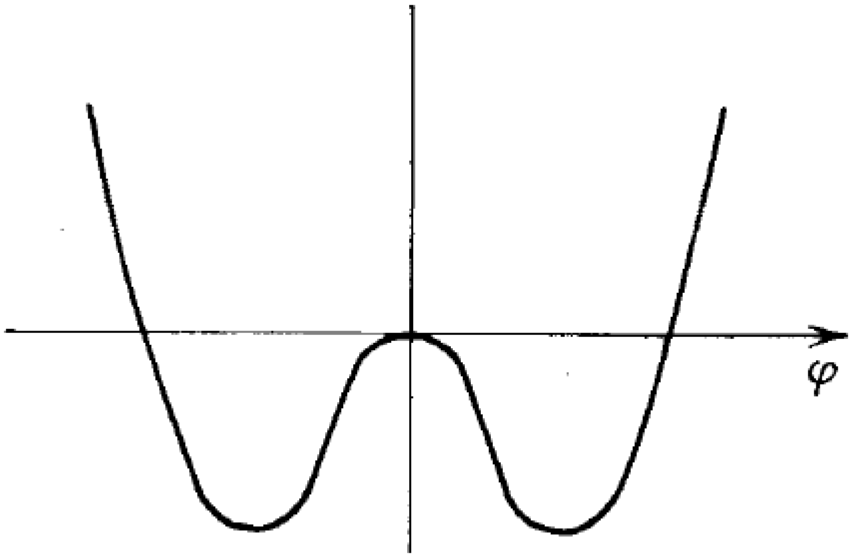

$$\frac{\mu_0^2}{2}\varphi^2 + \frac{\lambda_0}{24}\varphi^4$$

2012 ← 4th July discovery of boson (m ~ 125 GeV) *Tevatron data ended in Sept 2011*
2013 ← boson like properties Nobel prize to Englert and Higgs
2014

2008

10th september 2008 : first beams around
19th september 2008 : incident

14 months of major repairs and consolidation
New Quench Protection system

2009

20th november 2009 : first beams around (again)
december 2009 : collisions at 2.36 TeV cms

January 2010 : decided scenario 2010-11 7 TeV cms
instead of 14 TeV

2010

30th march 2010 : first collisions at 7 TeV cms
august 2010 : luminosity of 10^{31} cm^{-2} s^{-1}

may 2011 : luminosity > 10^{33} cm^{-2} s^{-1}
november 2011 : integrated luminosity ~ 5 fb^{-1}
13^{th} december 2011 : first 'signal' around 126 GeV

2011

march 2012 : start again at 8 TeV
(50 ns between bunches)
4^{th} July 2012 : evidence for a new boson
(8 TeV integrated luminosity ~ 6 fb^{-1})

2012

(Standard-Model) boson-like properties
peak luminosity 7 10^{33} cm^{-2} s^{-1}
integrated luminosity ~ 5+ 20 fb^{-1}

end of Run-1

2013

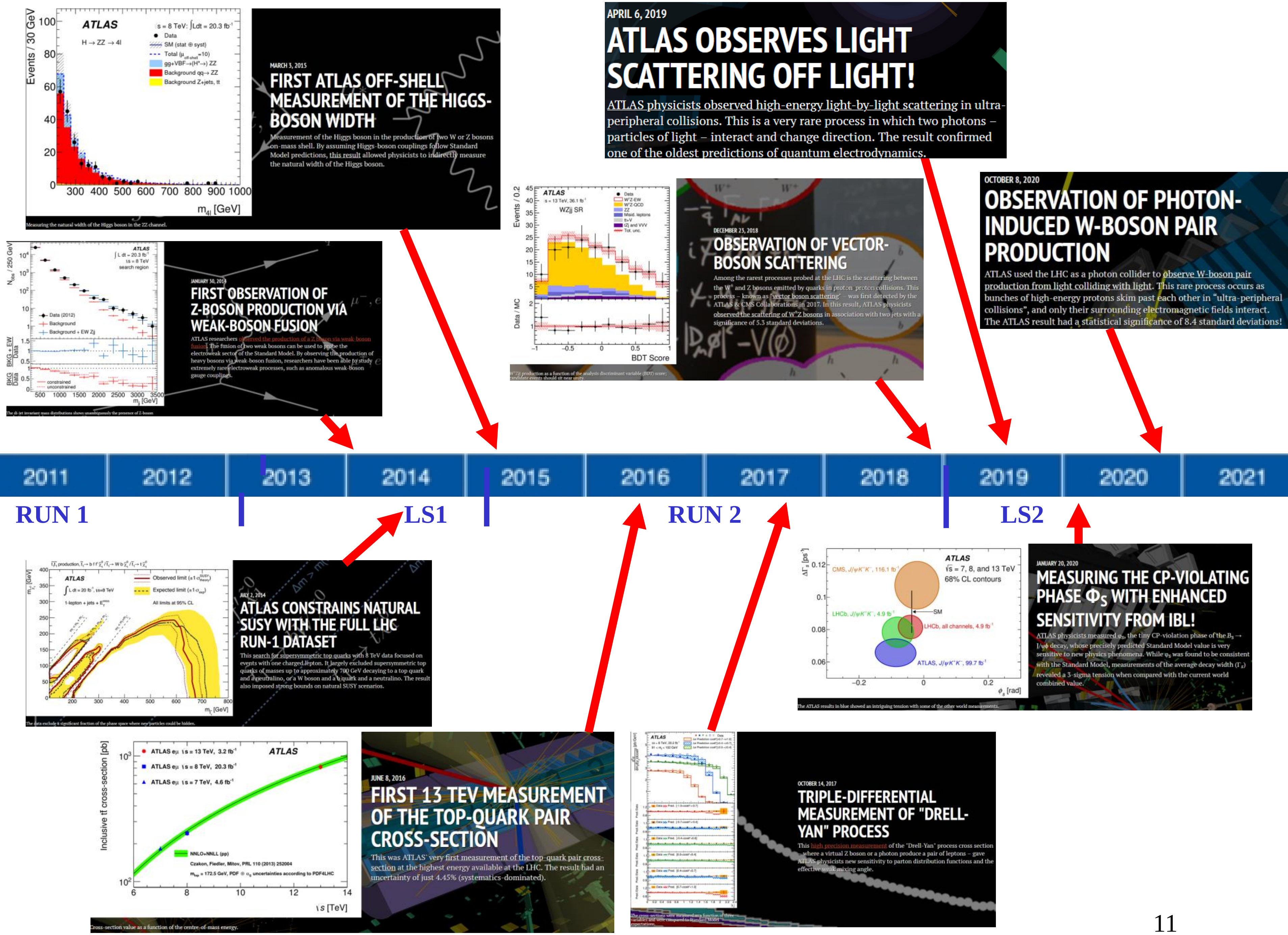

https://cdn.knightlab.com/libs/timeline3/latest/embed/index.html?source=1fq4odmMyOeDTyGewycfgVwdet8NIixzWI6tMHC30nv8&font=Default&lang=en&initial_zoom=2&height=800)

Muon Spectrometer ($|\eta|<2.7$) : air-core toroids (B ~ 0.5 / 1T in barrel/ end-cap) with gas-based muon chambers Muon trigger and measurement with momentum resolution < 10% up to E_μ ~ 1 TeV

Run-1 ATLAS detector

Length : ~ 46 m
Radius : ~ 12 m
Weight : ~ 7000 tons
~10^8 electronic channels
3000 km of cables

3-level trigger reducing the rate from 40 MHz to ~1200 Hz

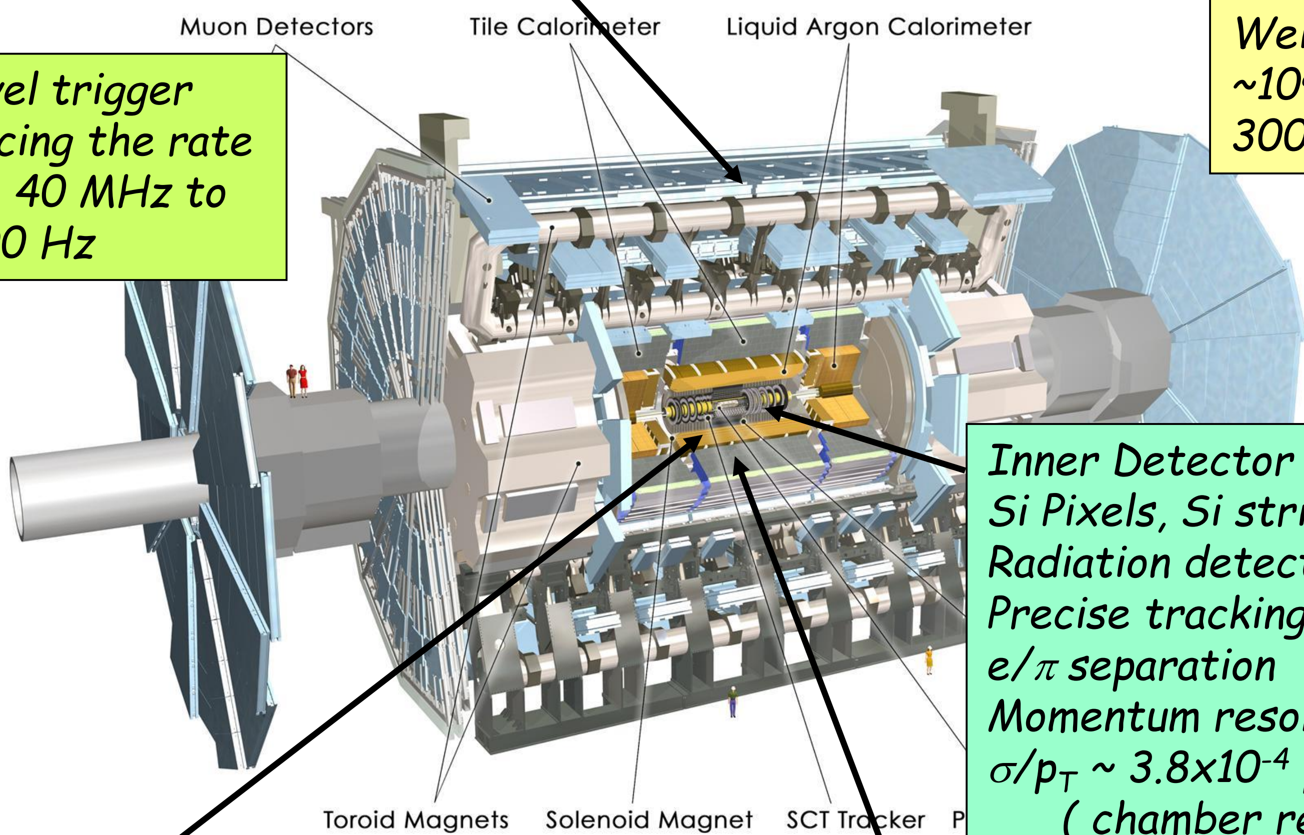

Inner Detector ($|\eta|<2.5$, B=2T):
Si Pixels, Si strips, Transition Radiation detector (straws)
Precise tracking and vertexing,
e/π separation
Momentum resolution:
$\sigma/p_T \sim 3.8\times10^{-4}\, p_T(\text{GeV}) \oplus 0.015$
(chamber resolution $\oplus$ MS)

EM calorimeter: Pb-LAr Accordion
e/γ trigger, identification and measurement
E-resolution: $\sigma/E \sim 10\%/\sqrt{E}$

HAD calorimetry ($|\eta|<5$): segmentation, hermeticity
Fe/scintillator Tiles (central), Cu/W-LAr (fwd)
Trigger and measurement of jets and missing E_T
E-resolution: $\sigma/E \sim 50\%/\sqrt{E} \oplus 0.03$

ATLAS in Run-2

New detectors in Run-2:

- Innermost pixel layer IBL, 3.4cm from interaction point
- Forward proton detectors (one arm in 2016, 210m from IP)

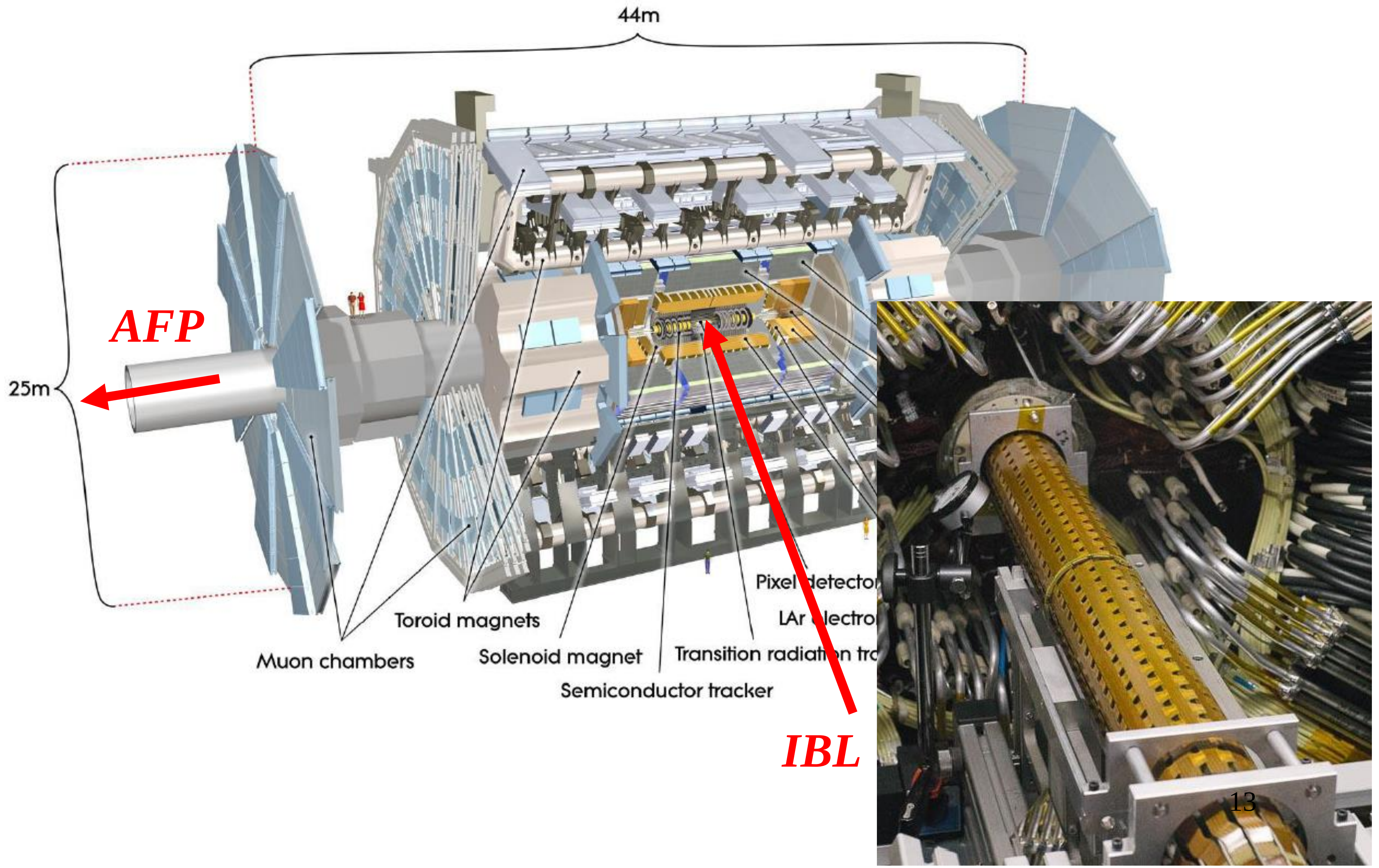

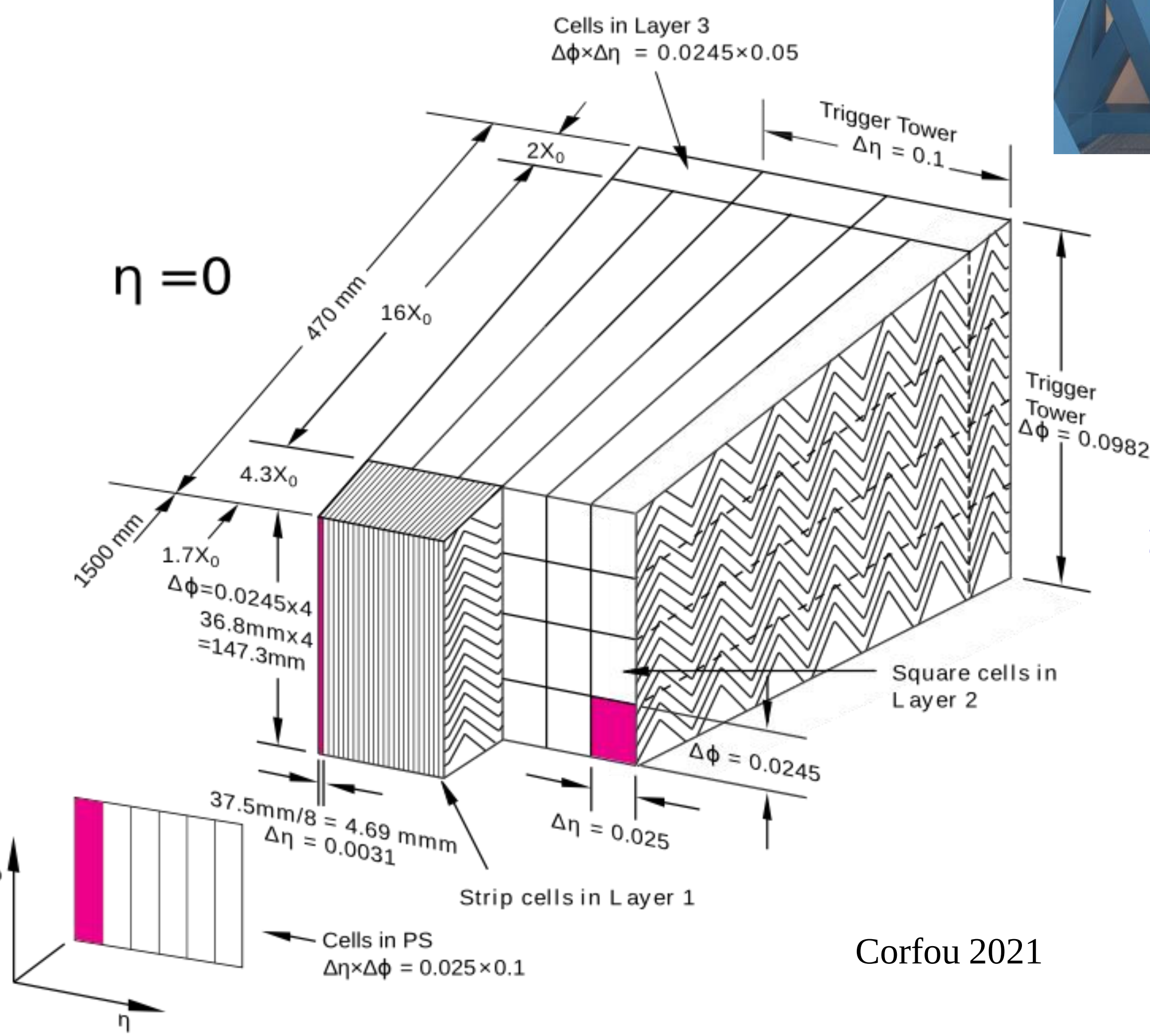

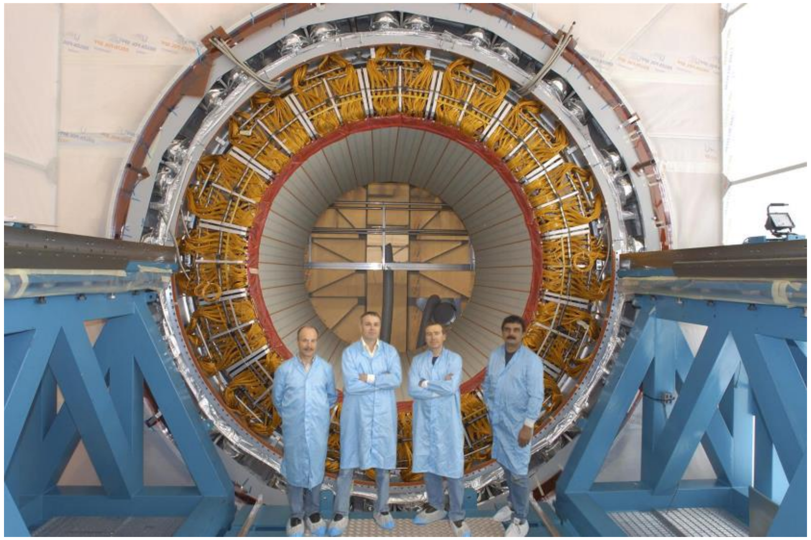

transverse and longitudinal segmentation of the EM ATLAS** (Liquid Argon) **accordion calorimeter

(very stable - about 200 000 channels)

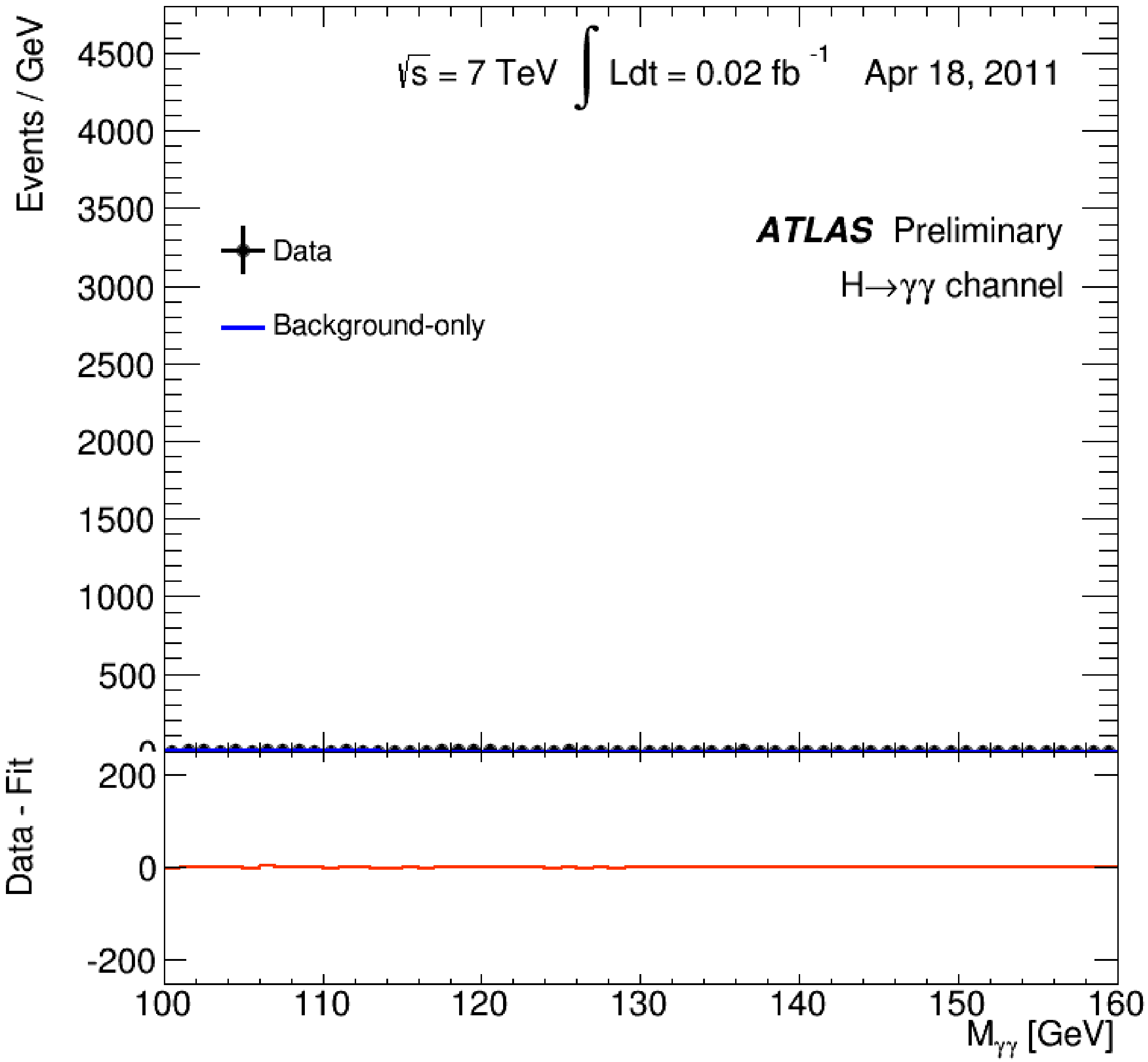
$\sqrt{s}$ = 7 TeV $\int$ Ldt = 0.02 fb^{-1} Apr 18, 2011
ATLAS Preliminary
H→γγ channel
Data
Background-only
Events / GeV
4500
4000
3500
3000
2500
2000
1500
1000
500
0
Data - Fit
200
0
-200
100
110
120
130
140
150
160
$M_{\gamma\gamma}$ [GeV]

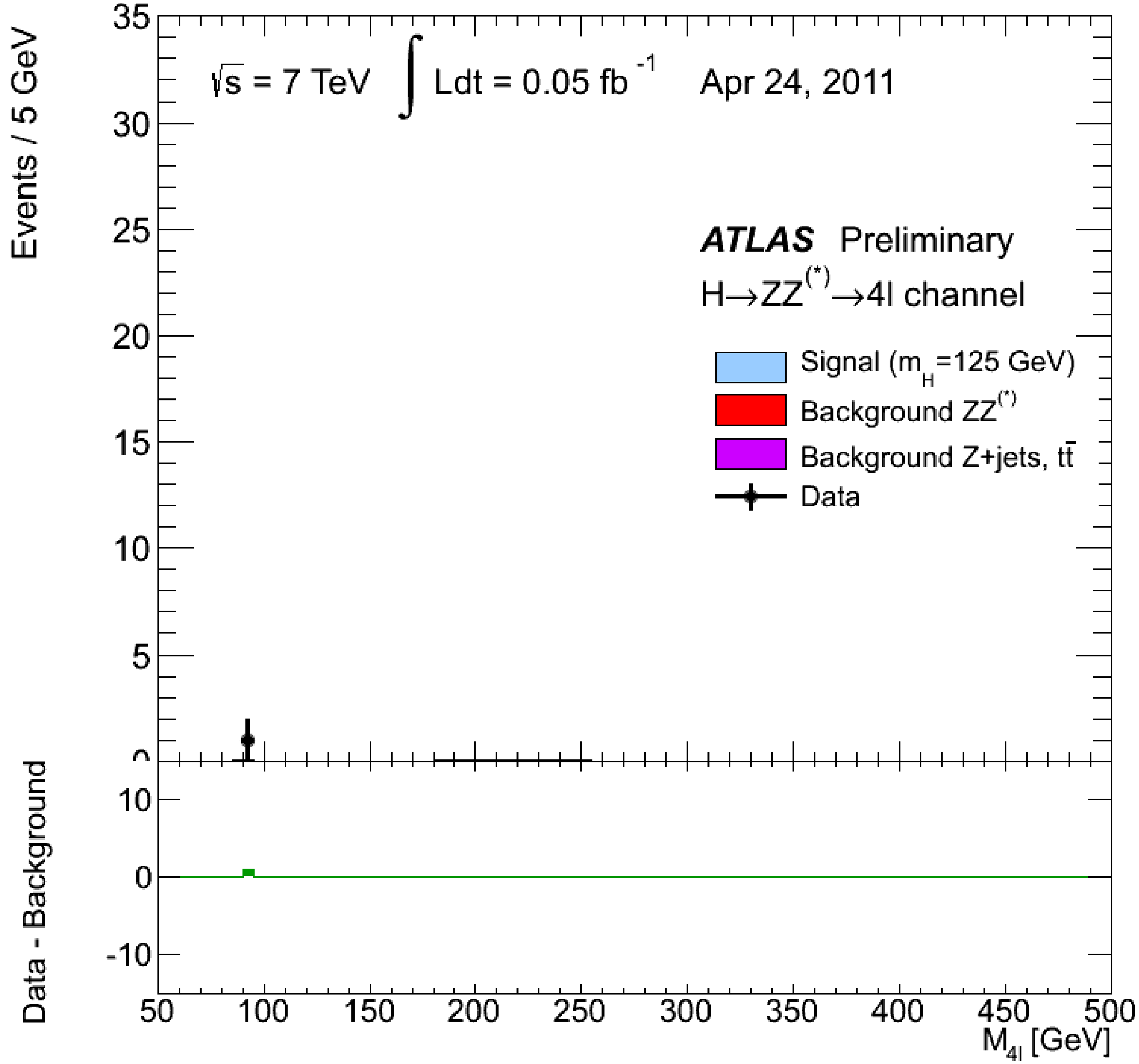
Events / 5 GeV
√s = 7 TeV ∫ Ldt = 0.05 fb-1 Apr 24, 2011
ATLAS Preliminary
H→ZZ(*)→4l channel
Signal (mH=125 GeV)
Background ZZ(*)
Background Z+jets, tt̄
Data
Data - Background
M4l [GeV]

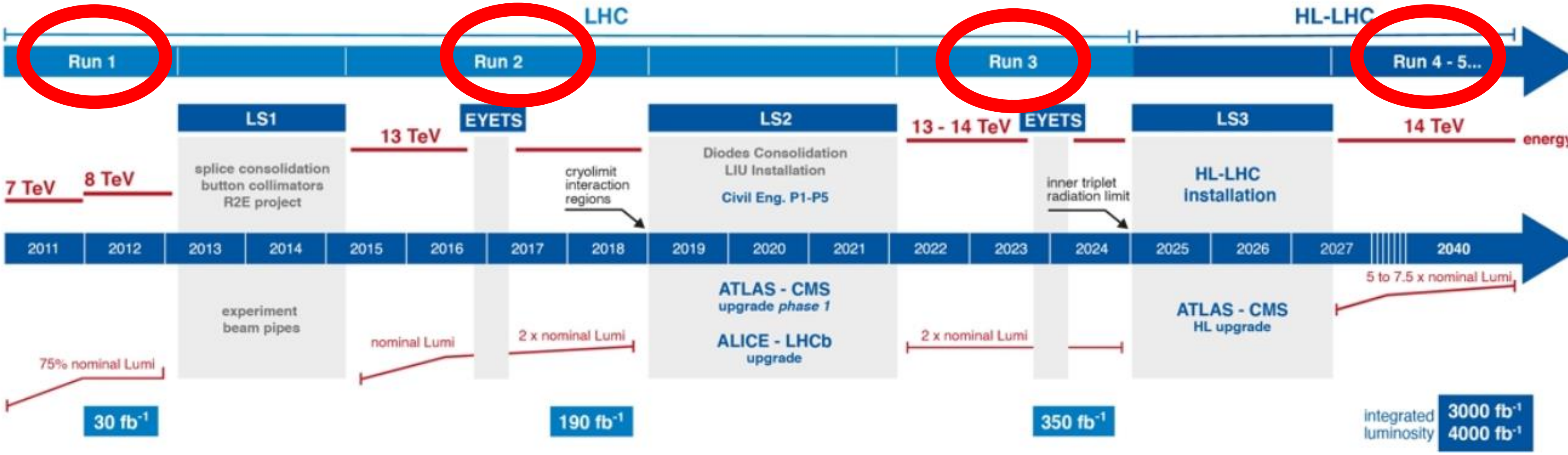

discovery of H boson

now

Official planning above . It will probably change soon

- ♪ *Historical introduction , Setting the stage*
- ♪ ***Results***
- ♪ *Future of ATLAS , Run-3 , HL-LHC*
- ♪ *Conclusions*
- ♪ *Backup*

♪ Results

- ***detector***
- ***SM (including multibosons and VBS)***
- ***BSM***
- ***(B-E)H***

short summary

1 > ***No new physics (yet)*** *outside the discovery of the H boson*

2 > ***We are entering an era of precision physics***

Large sample of various particles produced in Run-2

W bosons	*27*	10^9
Z bosons	*8*	10^9
$t\bar{t}$	*1.3*	10^8
$b\bar{b}$	*80*	10^{12}
BEH bosons	*8*	10^6

♪ ***Results***

- ***detector***
- ***SM (including multibosons and VBS)***
- ***BSM***
- ***(B-E)H***

Integrated pp luminosity during Run-2

Also collected Pb-Pb p-Pd Xe-Xe data

low μ data for high precision W physics

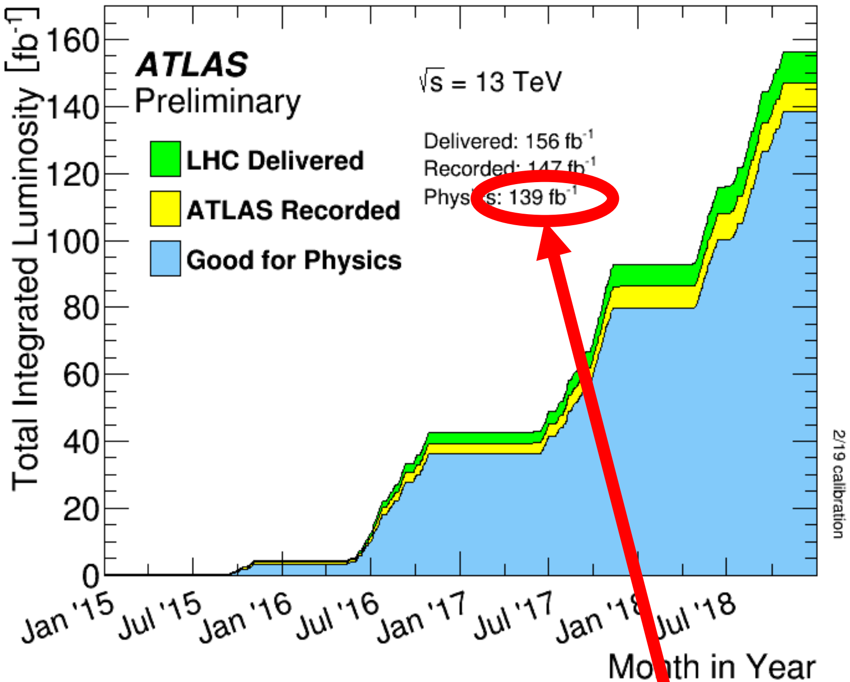

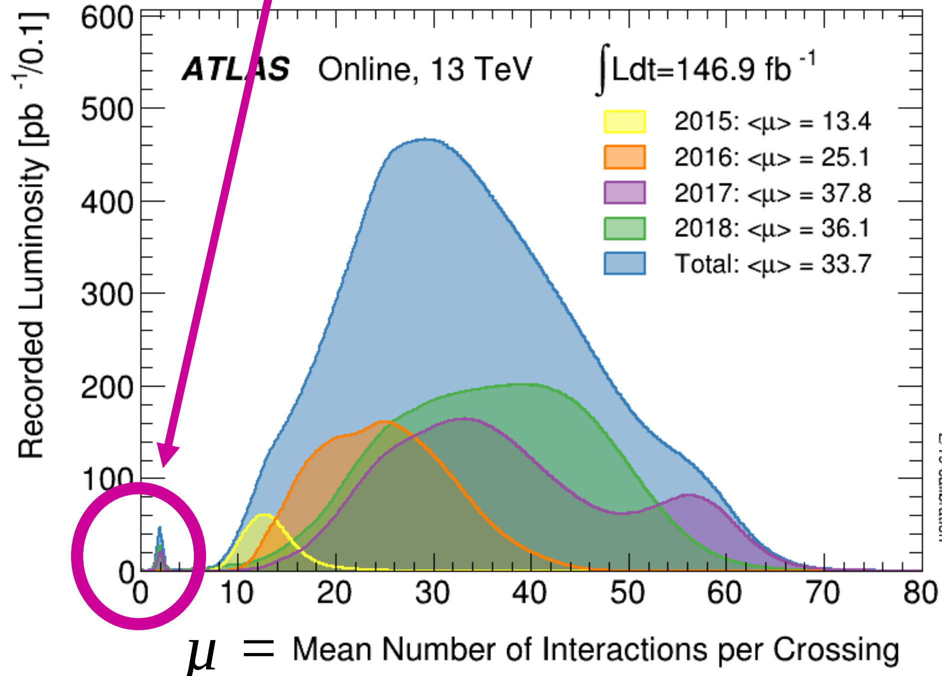

measured to 1.7% precision

(ATLAS-CONF-2019-021)

High-luminosity comes with a challenge

All dogmas need to be revisited

Like the fact that the response of the calorimeter is constant w.r.t time

for instance current in detector ~ I ~ μ

(there are also short time-scale variations due to T change)

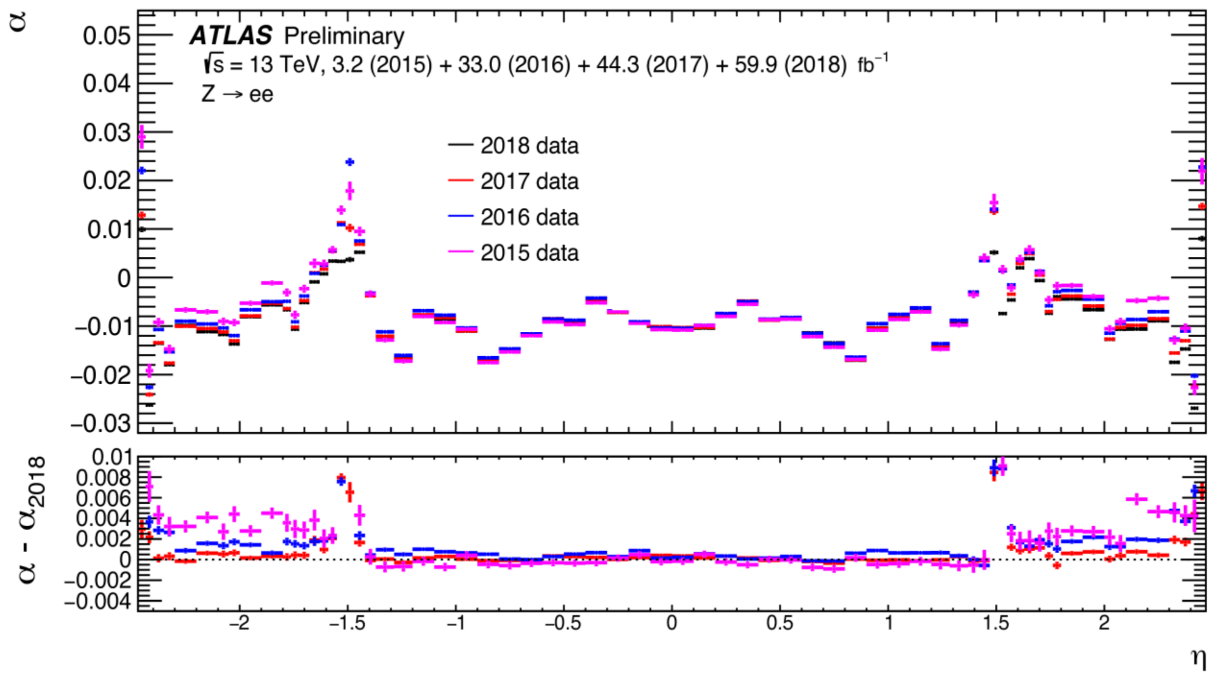

energy mis-calibration defined by α_i $E^{\mathrm{data}} = E^{\mathrm{MC}}(1+\alpha_i)$

We have a lot of data in order to make precise calibrations

But the needs for precision physics are very important !

https://atlas.web.cern.ch/Atlas/GROUPS/PHYSICS/PLOTS/EGAM-2019-01/fig_02a.png

♪ ***Results***

- ***detector***
- ***SM (including multibosons and VBS)***
- ***BSM***
- ***(B-E)H***

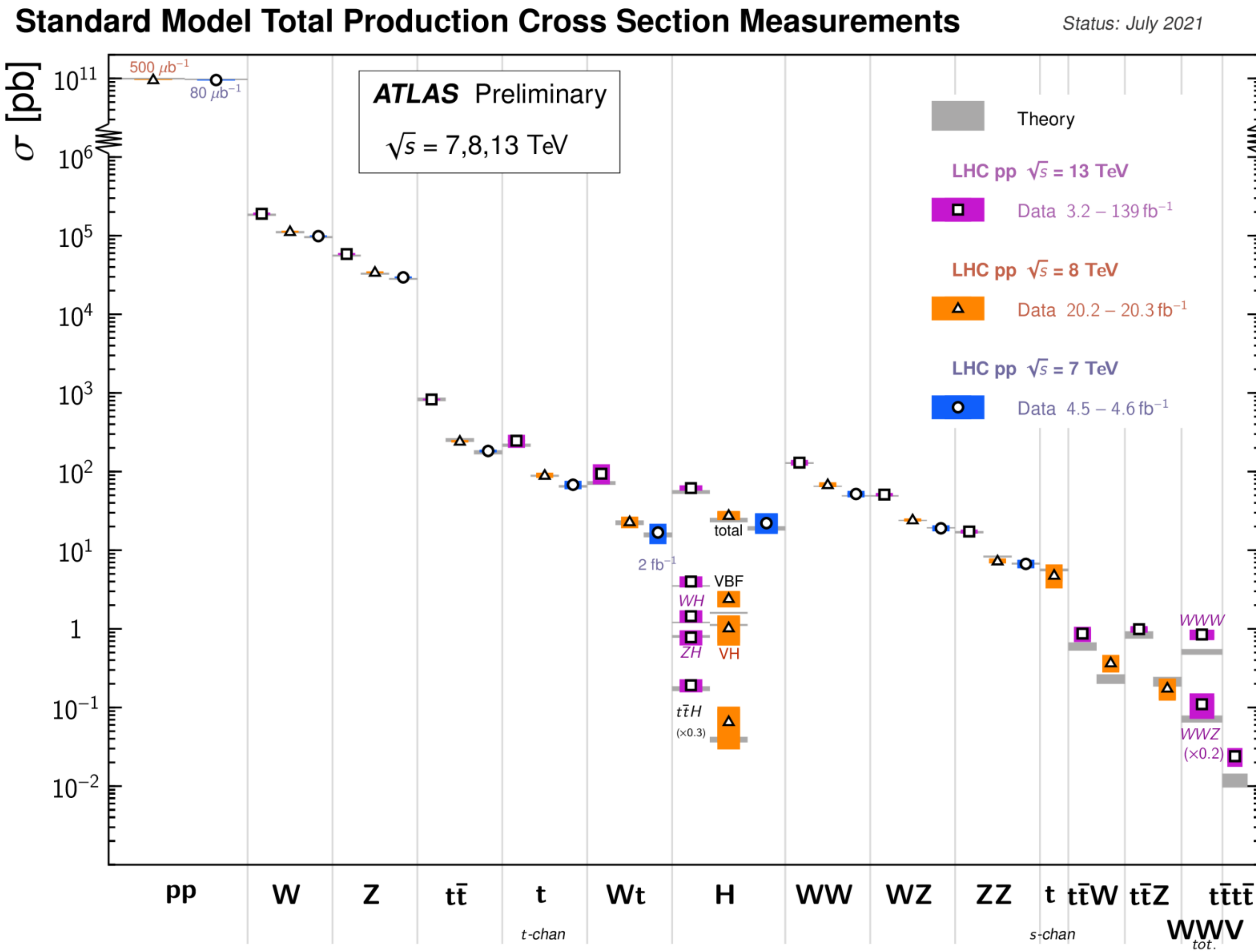

Theory agrees so far with the measured cross sections on 15 orders of magnitude

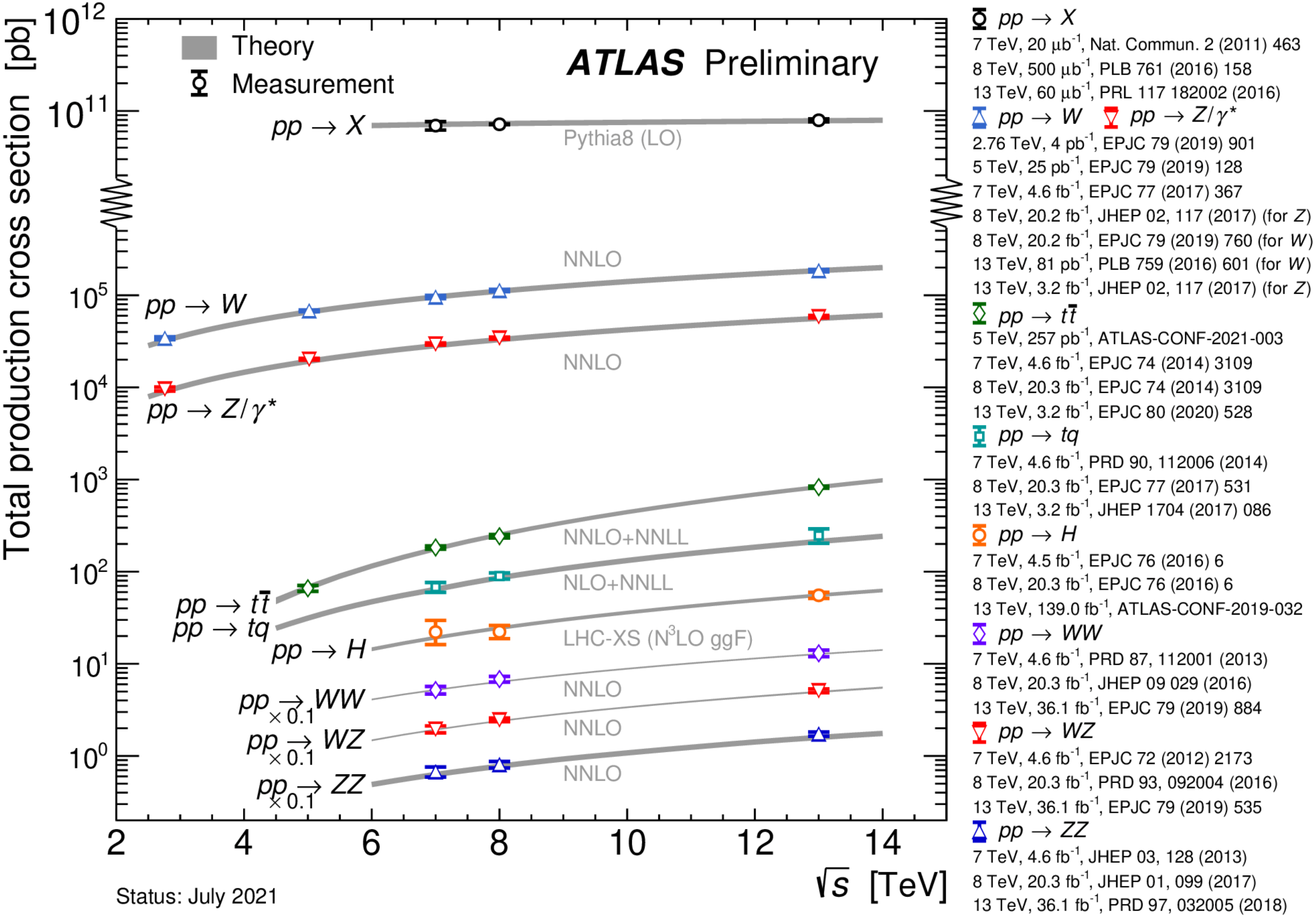
Total production cross section [pb]
Theory
Measurement
ATLAS Preliminary
pp → X
Pythia8 (LO)
NNLO
pp → W
NNLO
pp → Z/γ*
NNLO+NNLL
NLO+NNLL
pp → tt̄
pp → tq
pp → H
LHC-XS (N3LO ggF)
NNLO
pp → WW ×0.1
NNLO
pp → WZ ×0.1
NNLO
pp → ZZ ×0.1
√s [TeV]
Status: July 2021
pp → X
7 TeV, 20 μb-1, Nat. Commun. 2 (2011) 463
8 TeV, 500 μb-1, PLB 761 (2016) 158
13 TeV, 60 μb-1, PRL 117 182002 (2016)
pp → W pp → Z/γ*
2.76 TeV, 4 pb-1, EPJC 79 (2019) 901
5 TeV, 25 pb-1, EPJC 79 (2019) 128
7 TeV, 4.6 fb-1, EPJC 77 (2017) 367
8 TeV, 20.2 fb-1, JHEP 02, 117 (2017) (for Z)
8 TeV, 20.2 fb-1, EPJC 79 (2019) 760 (for W)
13 TeV, 81 pb-1, PLB 759 (2016) 601 (for W)
13 TeV, 3.2 fb-1, JHEP 02, 117 (2017) (for Z)
pp → tt̄
5 TeV, 257 pb-1, ATLAS-CONF-2021-003
7 TeV, 4.6 fb-1, EPJC 74 (2014) 3109
8 TeV, 20.3 fb-1, EPJC 74 (2014) 3109
13 TeV, 3.2 fb-1, EPJC 80 (2020) 528
pp → tq
7 TeV, 4.6 fb-1, PRD 90, 112006 (2014)
8 TeV, 20.3 fb-1, EPJC 77 (2017) 531
13 TeV, 3.2 fb-1, JHEP 1704 (2017) 086
pp → H
7 TeV, 4.5 fb-1, EPJC 76 (2016) 6
8 TeV, 20.3 fb-1, EPJC 76 (2016) 6
13 TeV, 139.0 fb-1, ATLAS-CONF-2019-032
pp → WW
7 TeV, 4.6 fb-1, PRD 87, 112001 (2013)
8 TeV, 20.3 fb-1, JHEP 09 029 (2016)
13 TeV, 36.1 fb-1, EPJC 79 (2019) 884
pp → WZ
7 TeV, 4.6 fb-1, EPJC 72 (2012) 2173
8 TeV, 20.3 fb-1, PRD 93, 092004 (2016)
13 TeV, 36.1 fb-1, EPJC 79 (2019) 535
pp → ZZ
7 TeV, 4.6 fb-1, JHEP 03, 128 (2013)
8 TeV, 20.3 fb-1, JHEP 01, 099 (2017)
13 TeV, 36.1 fb-1, PRD 97, 032005 (2018)

definition of μ (signal strength)

$$\mu = (\sigma \, . \, BR) \, / \, (\sigma \, . \, BR)_{SM}$$

called ***signal strength***

B-physics

$B_c^+ \to J/\psi D_s^+ \; B_c^+ \to J/\psi D_s^{*+}$

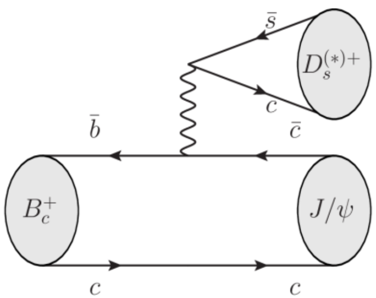

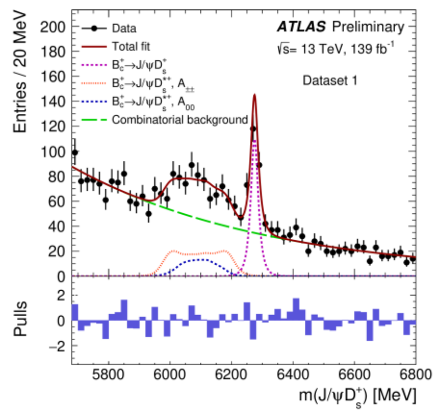

ATLAS-CONF-2021-046

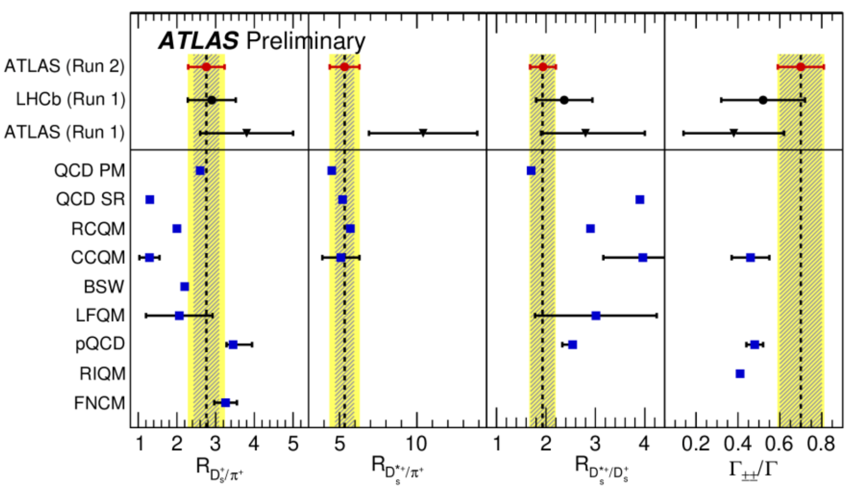

Eur. Phys. J. C 81 (2021) 342
arXiv:2001.07115

Measurement of the CP-violating phase ϕ_s in $B_s^0 \to J/\psi\phi$ decays

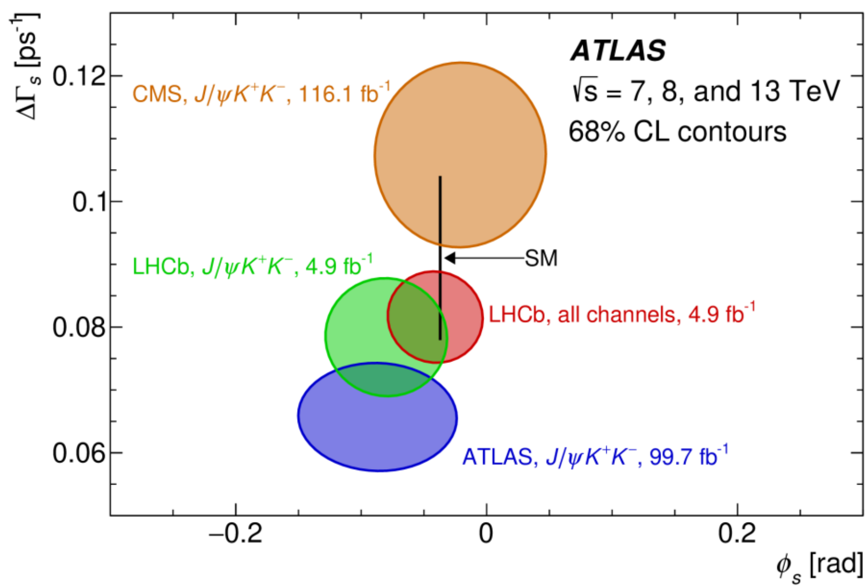

top-quark pair events with a high p_T top quark

Test SM at high p_T^{top}, where deviations expected from BSM

SM predictions at NNLO QCD + NLO EW

l+jets channel: $t\bar{t} \to Wb\,Wb \to \ell\nu b\, qq'b$

P_T (top)> 355 GeV

Reduce jet energy scale by using mass of hadronic top

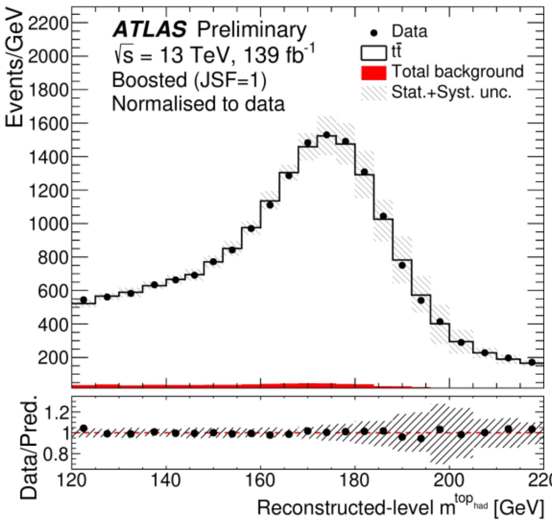

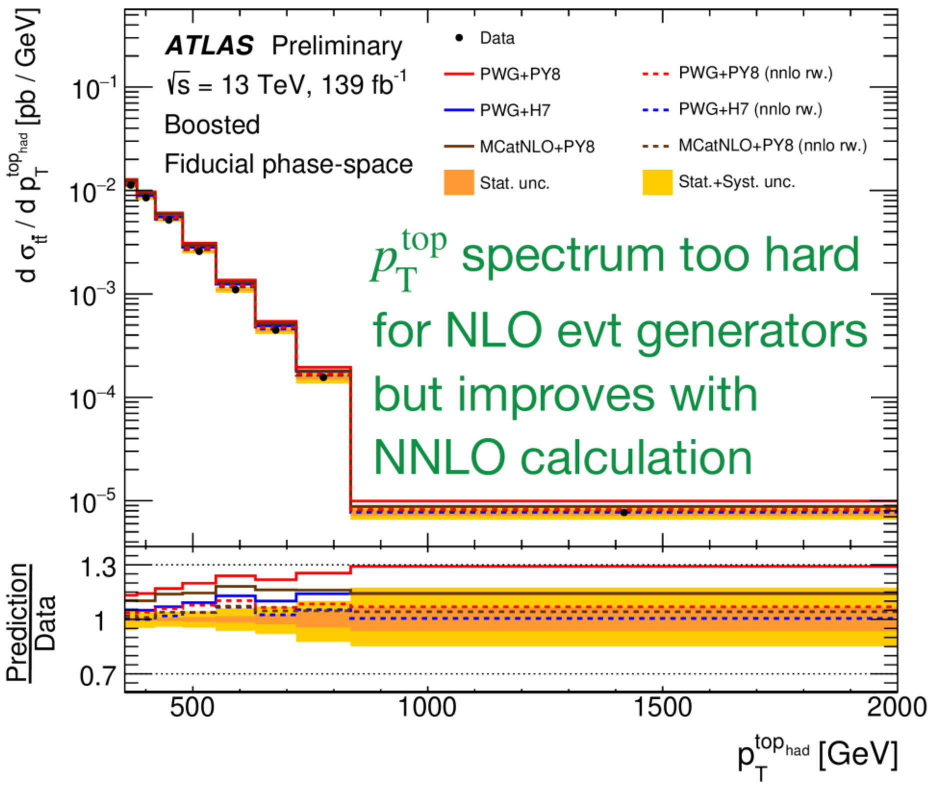

p_T^{top} spectrum too hard for NLO evt generators but improves with NNLO calculation

arXiv:2106.11683
Eur.Phys.J.C 80 (2020) 11, 1085

Measurement of $t\bar{t}t\bar{t}$ production cross section

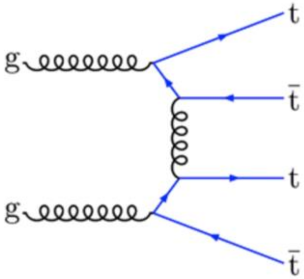

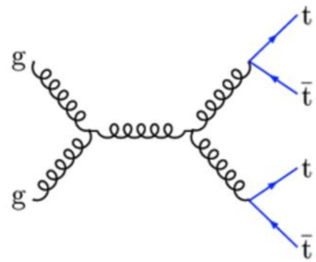

13 TeV, 139 fb^{-1}
$t\bar{t}t\bar{t}$ 1 ℓ / 2 ℓ OS (ℓ = e,μ)
[57% of $t\bar{t}t\bar{t}$ events]

13 TeV, 139 fb^{-1}
$t\bar{t}t\bar{t}$ 2 ℓ SS / 3 ℓ (ℓ = e,μ)
[13% of $t\bar{t}t\bar{t}$ events]

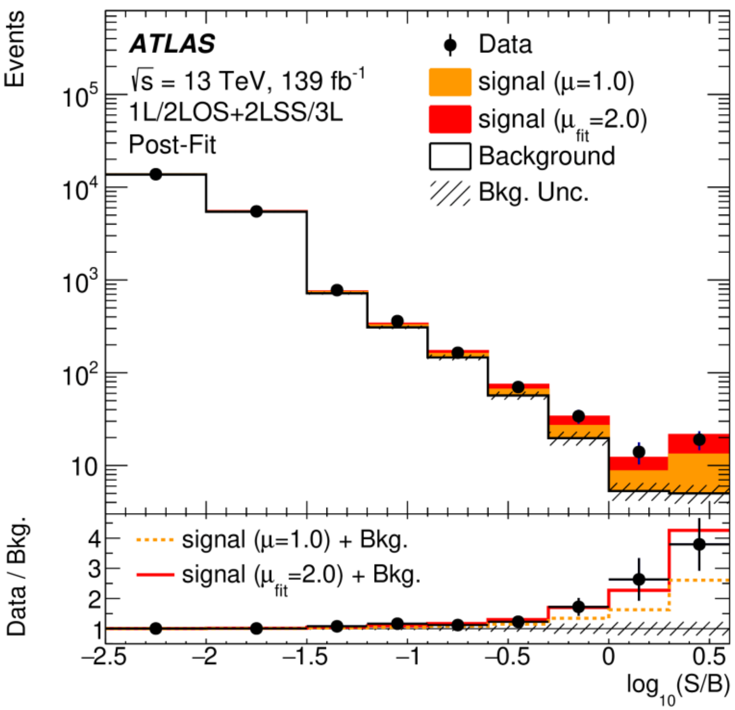

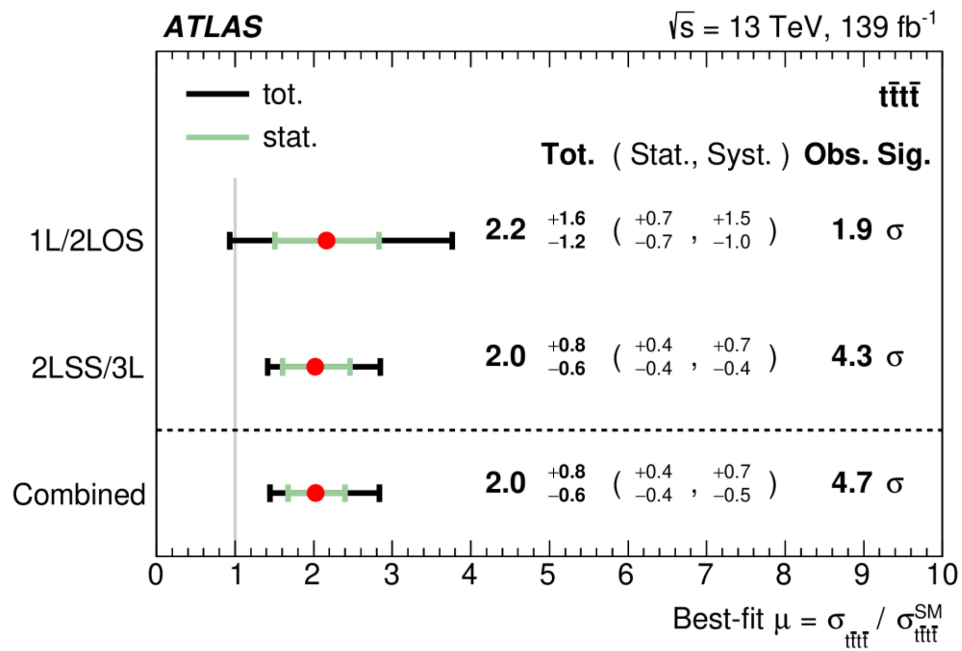

Prediction: $\sigma_{t\bar{t}t\bar{t}} = 12.0 \pm 2.4$ fb (NLO, incl EW corrs.)

Result: $\sigma_{t\bar{t}t\bar{t}} = 26 \pm 8\,(\text{stat.}) \pm^{15}_{13}\,(\text{syst.})$ **fb,** 1.9 obs. (1.0 exp.) σ

4.7 σ obs. (2.6 σ exp.) above bkg-only hypothesis

ATLAS-CONF-2021-039

WWW production

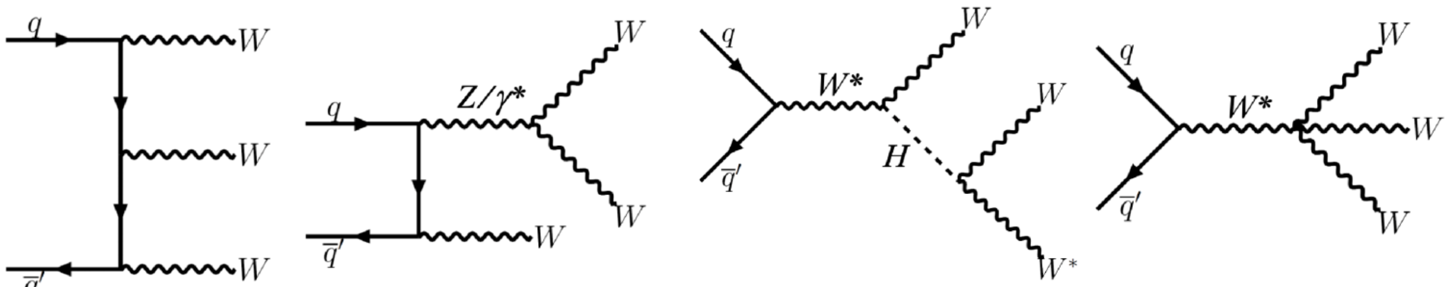

Channels: $W^{\pm}W^{\pm}W^{\mp} \rightarrow \ell^{\pm}\nu\,\ell^{\pm}\nu\,qq'$ with $\ell = e, \mu$

$\rightarrow \ell^{\pm}\nu\,\ell^{\pm}\nu\,\ell^{\mp}\nu$

Main bkg: $WZ \rightarrow \ell\nu\,\ell\ell$ estimated w/ control regions

Signal extracted w/ BDTs for 2ℓ and 3ℓ channels

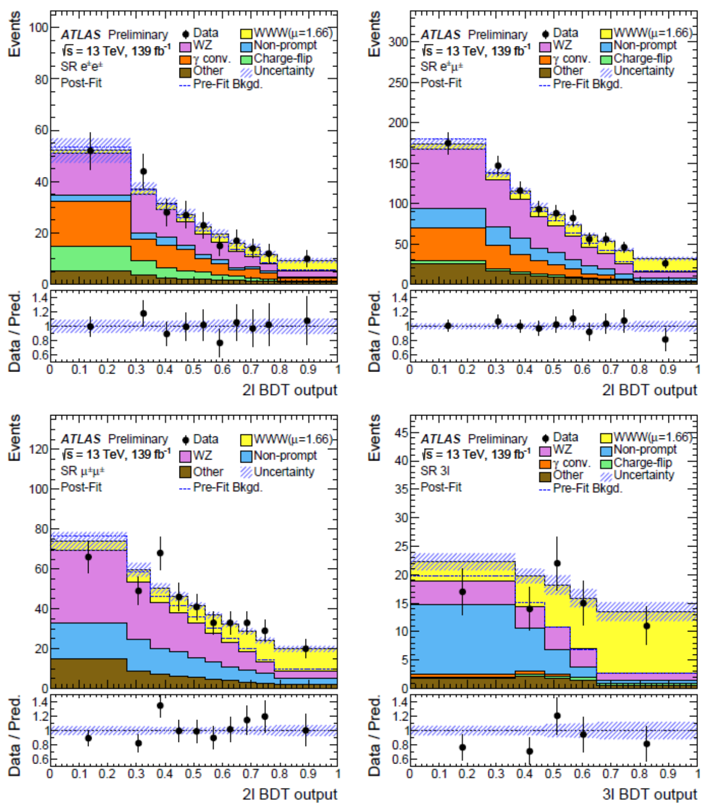

First *WWW* observation with significance of $8.2\,\sigma\,(5.4\,\sigma)$ obs (exp)

$$\sigma(pp \rightarrow W^{\pm}W^{\pm}W^{\mp}) = 850 \pm 100\,(\text{stat}) \pm 80\,(\text{syst})\ \text{fb}$$

$$\text{signal strength}: 1.66 \pm 0.28$$

SM for WWW + WH : 511 ± 42 fb at NLO QCD

Z boson with high p_T jets

ATLAS-CONF-2021-033

Test SM in events w/ $Z(\rightarrow ee, \mu\mu)$ and ≥ 1 jet with $p_T > 100$ GeV

Measure cross section in more extreme phase space
collinear vs back to back

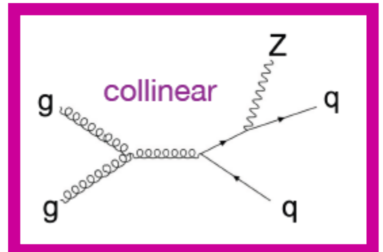

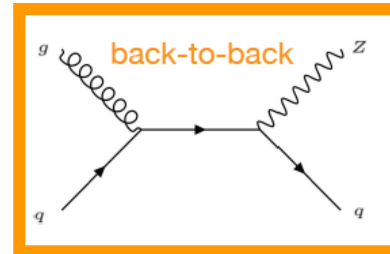

Latest SHERPA 2.2.11 and MG5_aMC + Py8 (FxFx) provide improved modeling esp. in collinear region and at high p_T

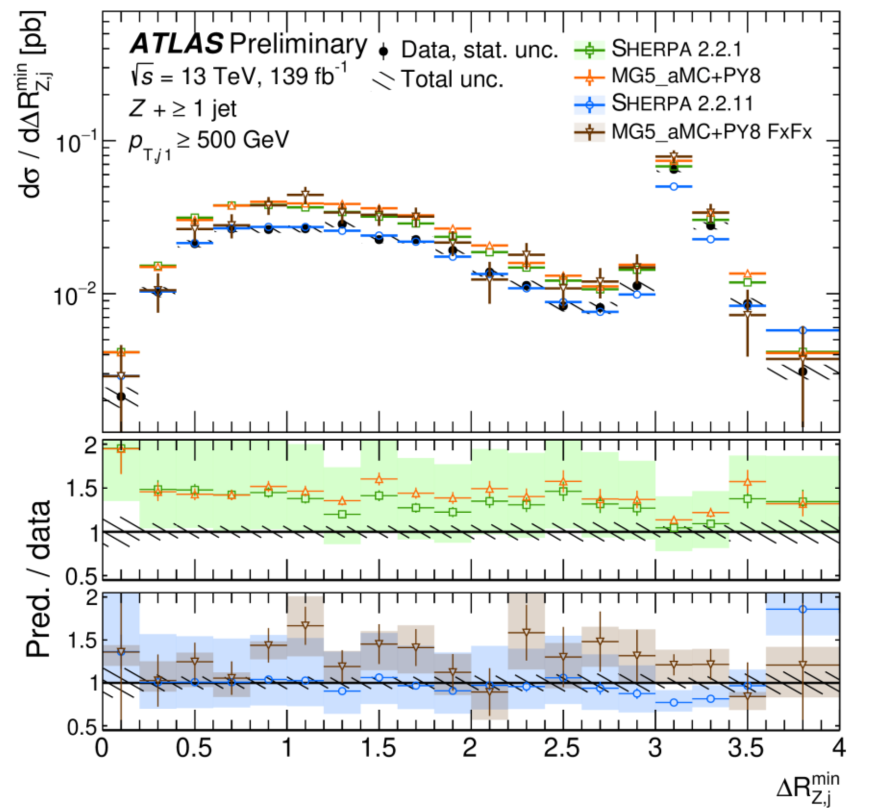

Process	Generator	Order pQCD
$Z\rightarrow \ell\ell$ (ℓ=e, μ, τ)	SHERPA v.2.2.1	0-2p NLO, 3-4p LO
$Z\rightarrow \ell\ell$ (ℓ=e, μ)	MG5_aMC+PY8 CKKWL	0-4p LO
$Z\rightarrow \ell\ell$ (ℓ=e, μ)	SHERPA v.2.2.11	0-2p NLO, 3-5p LO
$Z\rightarrow \ell\ell$ (ℓ=e, μ)	MG5_aMC+PY8 FxFx	0-3p NLO

EW precision measurements
W mass m_W

7 TeV data

Eur.Phys.J. C78 (2018) no.2, 110,
Erratum: Eur.Phys.J. C78 (2018) no.11, 898

One wants to have measurements with uncertainties close to the results of the EW fit $m_W = 80354 \pm 7$ ***MeV***

arXiv:1803.01853

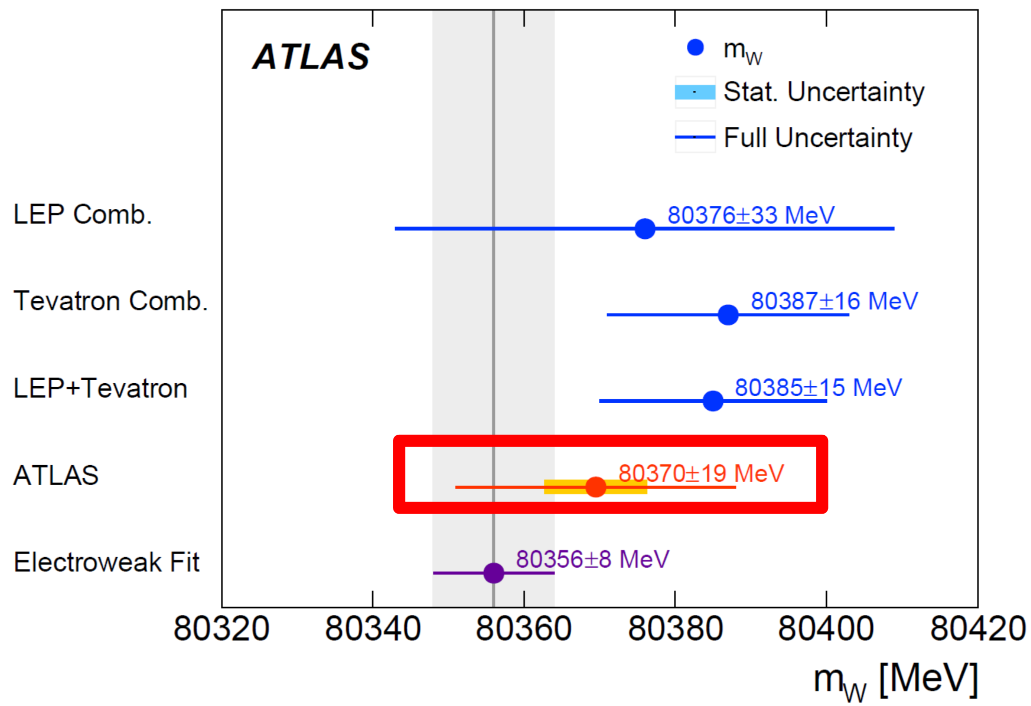

ATL-PHYS-PUB-2021-032

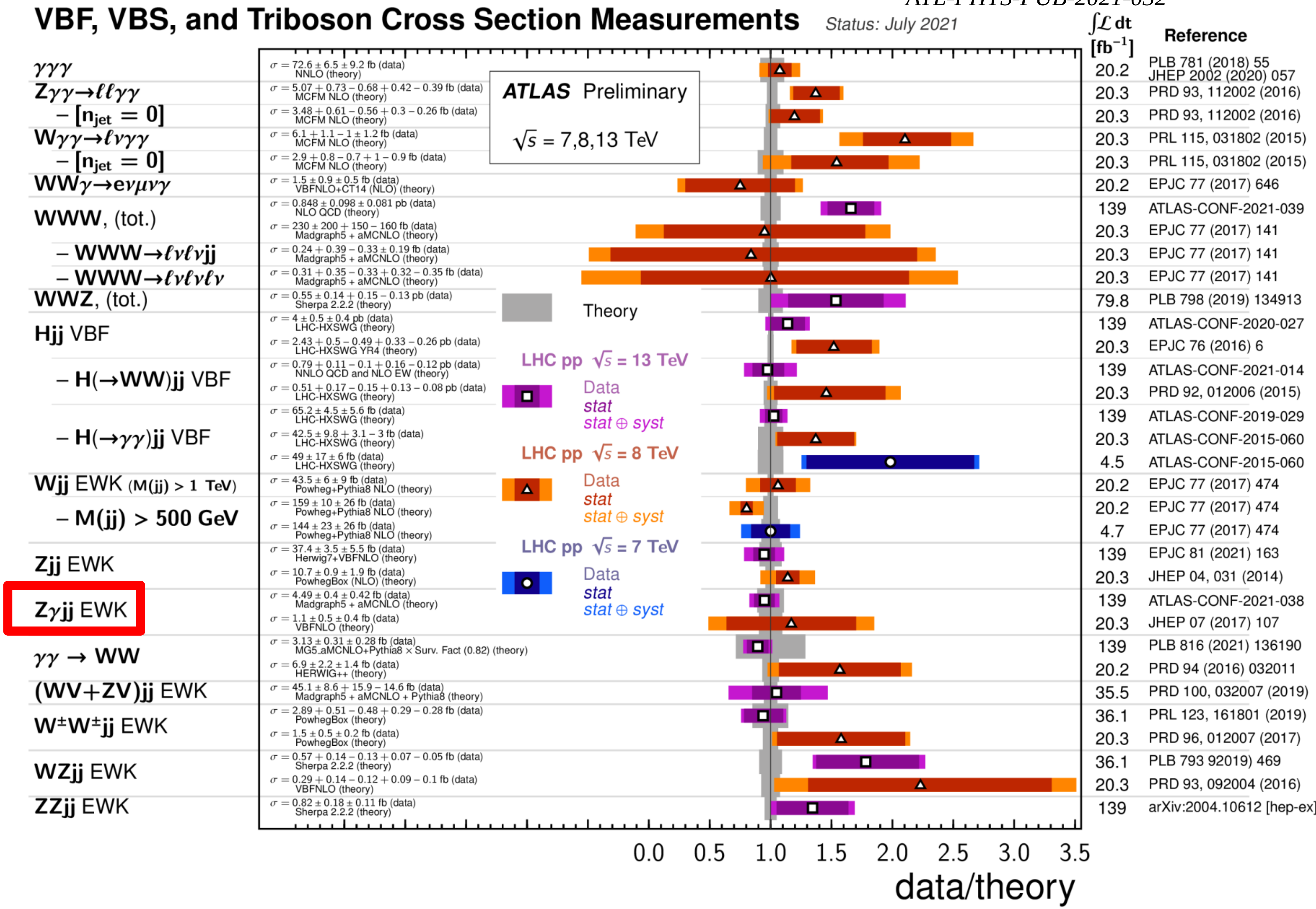

All EW VVjj observed : most recent one is Zγjj

$Z(\rightarrow ll)\,\gamma jj$ EW

CERN-EP-2021-137 ATLAS-CONF-2021-038

cubic and quartic couplings

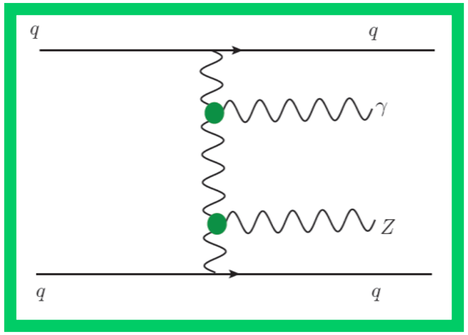

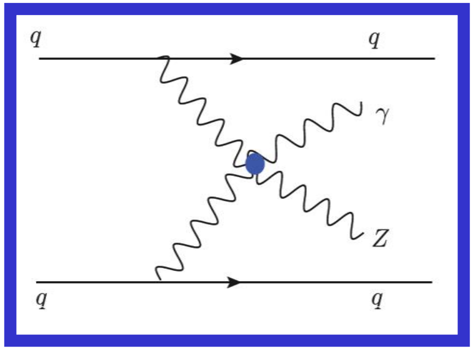

jets with large mass and rapidity gap

Signal strength for $Z\gamma jj$ EW production (rel. to LO prediction)

$$\mu_{\rm EW} = 0.95 \pm 0.08\,({\rm stat}) \pm 0.11\,({\rm syst})$$

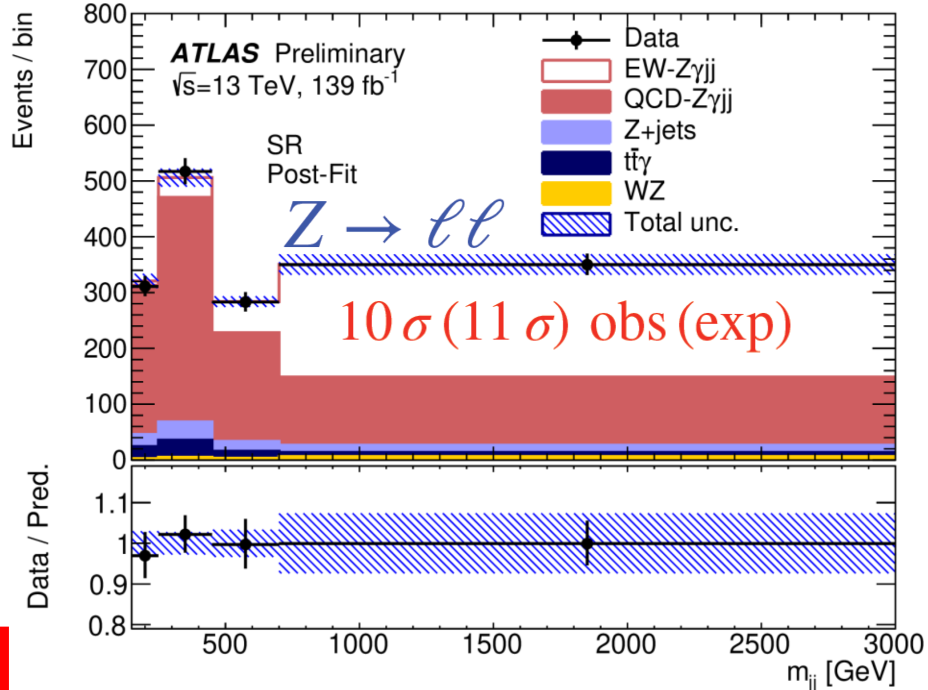

Z (→νν) γ j j EW

CERN-EP-2021-137

5.2 σ (5.1 σ) obs (exp)

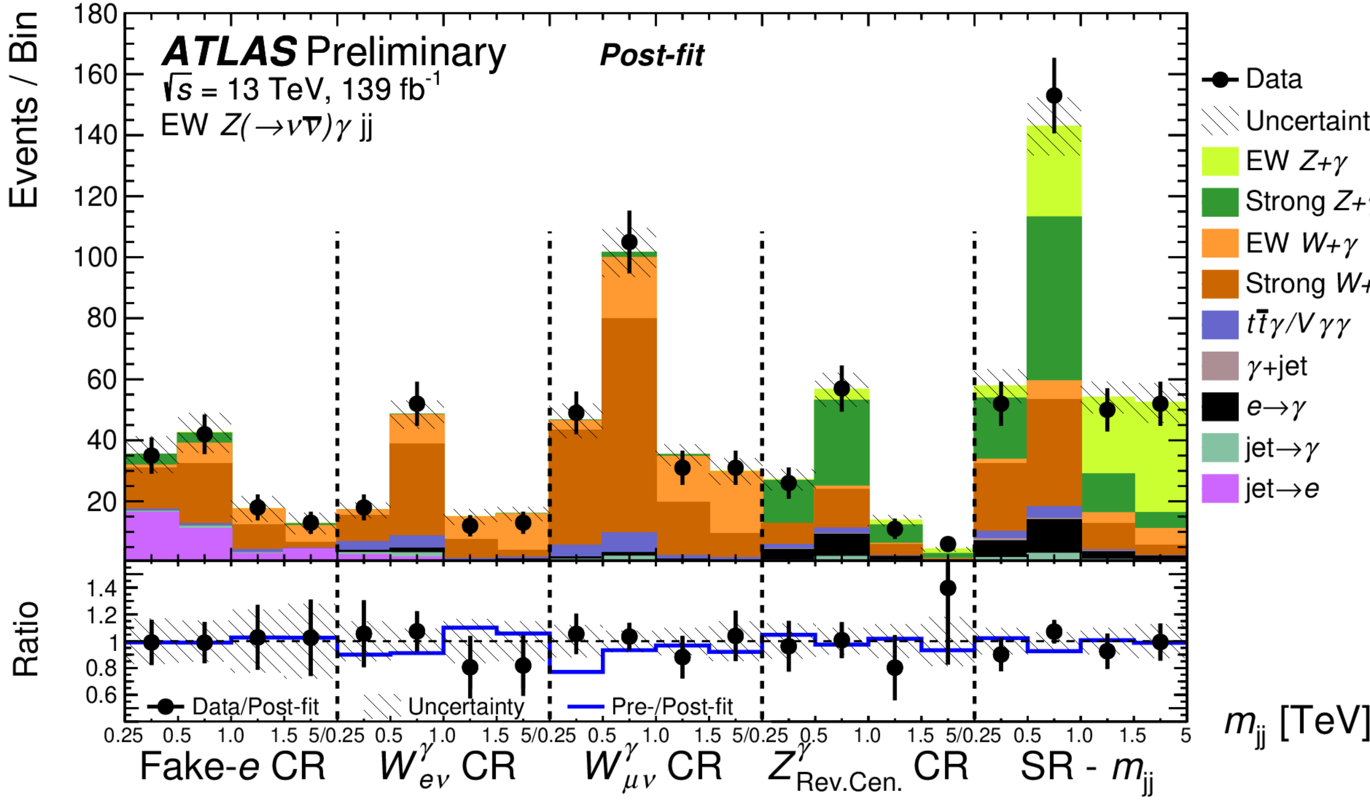

Signal strength

$$\mu_{\mathrm{EW}} = 1.03 \pm 0.16\,(\mathrm{stat}) \pm 0.19\,(\mathrm{syst})$$

This analysis is also setting limits on H→ inv and H → γ+dark-γ BRs

ATLAS-CONF-2021-004

♪ ***Results***

- * ***detector***
- * ***SM (including multibosons and VBS)***
- * ***BSM***
- * ***(B-E)H***

ATL-PHYS-PUB-2021-019

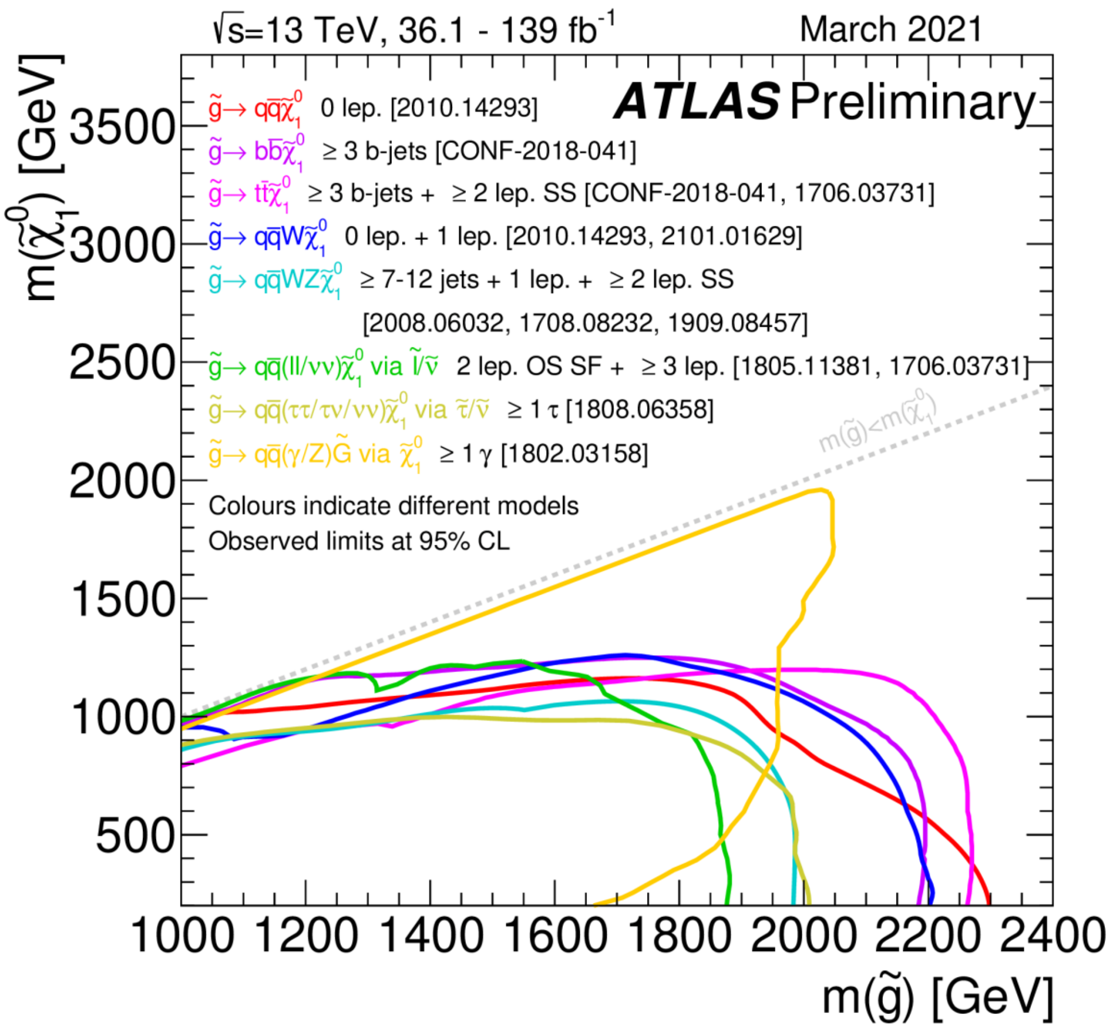

ATLAS SUSY Searches* - 95% CL Lower Limits

June 2021

SUSY

ATL-PHYS-PUB-2021-019

ATLAS Preliminary

$\sqrt{s}$ = 13 TeV

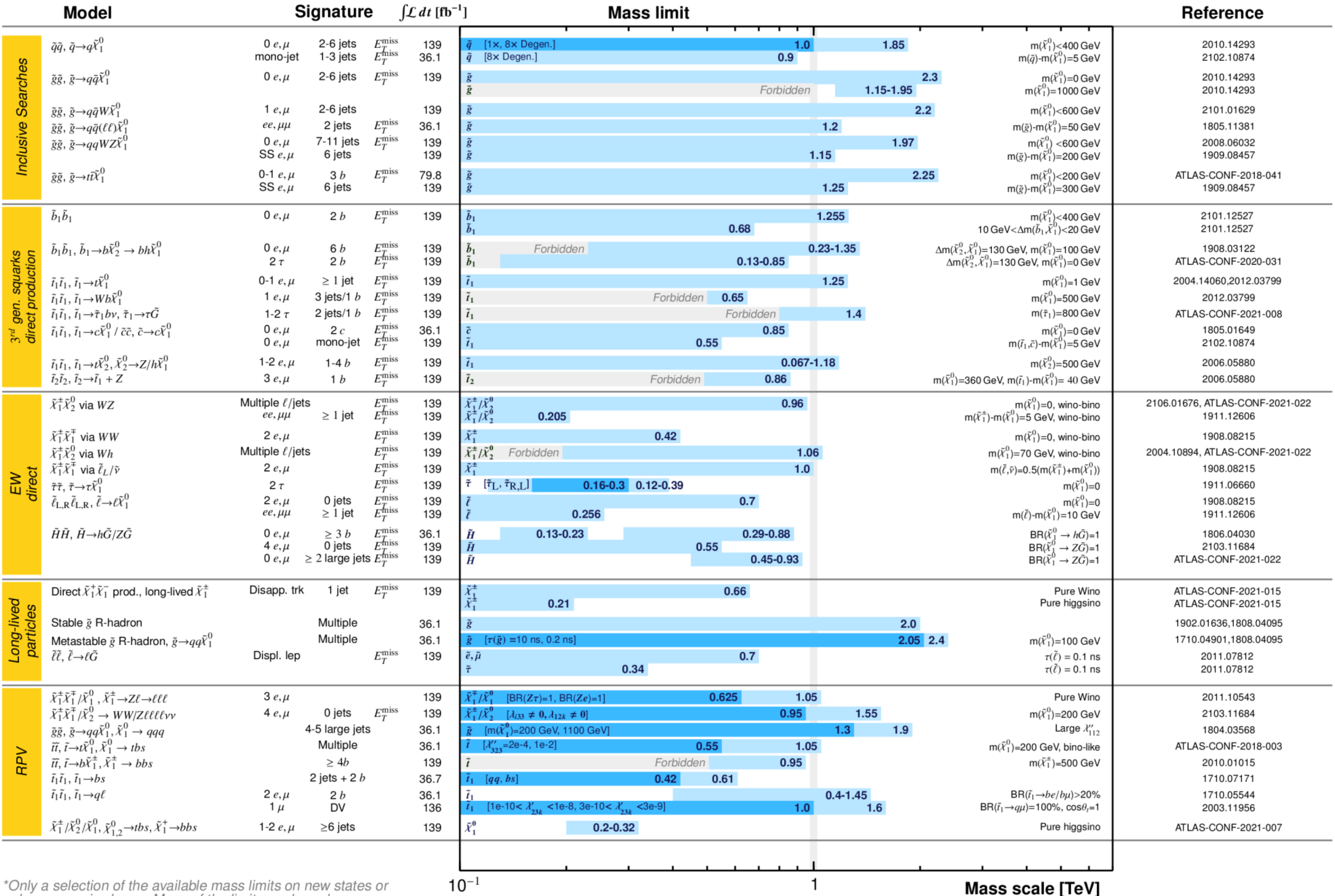

*Only a selection of the available mass limits on new states or phenomena is shown. Many of the limits are based on simplified models, c.f. refs. for the assumptions made.

SUSY Electroweak

arXiv:2108.07586

Electroweakinos with mass ~0.1—1 TeV well motivated:

Neutralino LSP as dark matter, naturalness problem, muon g-2 anomaly

Target mass splitting between NLSP and LSP > 400 GeV

First SUSY EW search with fully hadronic final state using large-R jets tagged as W/Z or H jets

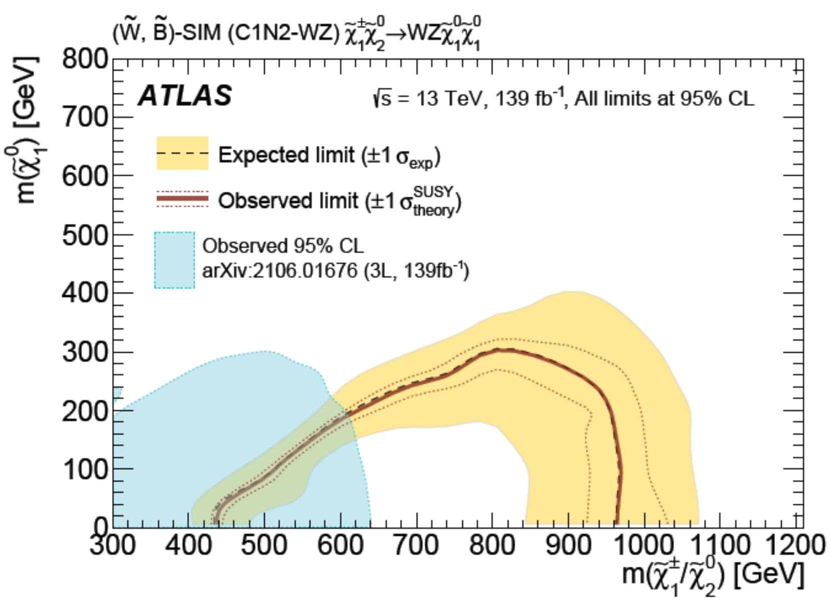

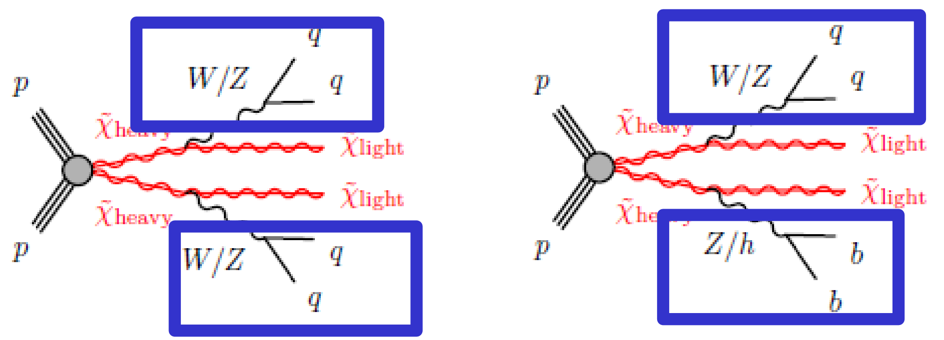

Strongest limits at high electroweakino mass

Flavour anomalies and vector leptoquarks

Recent results from B decays indicate deviations from lepton-flavor universality

- $R(K^{(*)}) = \dfrac{\mathscr{B}(B \to K^{(*)}\mu^+\mu^-)}{\mathscr{B}(B \to K^{(*)}e^+e^-)}$ and $R(D^{(*)}) = \dfrac{\mathscr{B}(B \to D^{(*)}\tau\nu)}{\mathscr{B}(B \to D^{(*)}\ell\nu)}$ (with $\ell = e, \mu$) both disagree w/ SM at ~3σ

- Vector leptoquarks a potential explanation

(diagrams by LHCb and D.Zanzi)

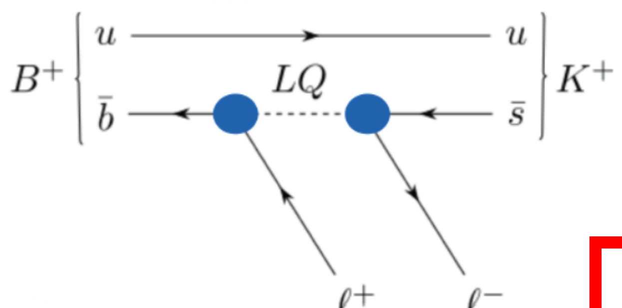

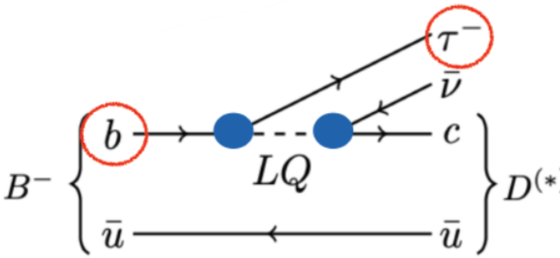

Search for LQ pair production

$m(\mathrm{LQ}_3^\mathrm{V}) > 1.8$ TeV
for $\mathscr{B}(\mathrm{LQ}_3^\mathrm{V} \to b\tau) \sim 0.5$

https://atlas.web.cern.ch/Atlas/GROUPS/PHYSICS/PAPERS/SUSY-2019-18/

some summary plots for scalar LQs can be found in ATL-PHYS-PUB-2021-017

See also ATLAS-CONF-2021-008

Lepton Flavor Violation in Z decays (eμ , eτ , μτ)

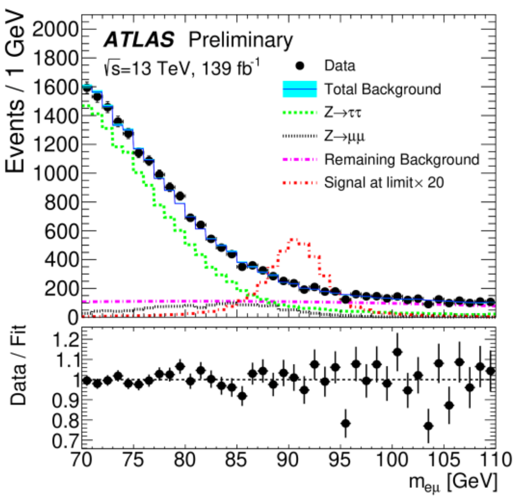

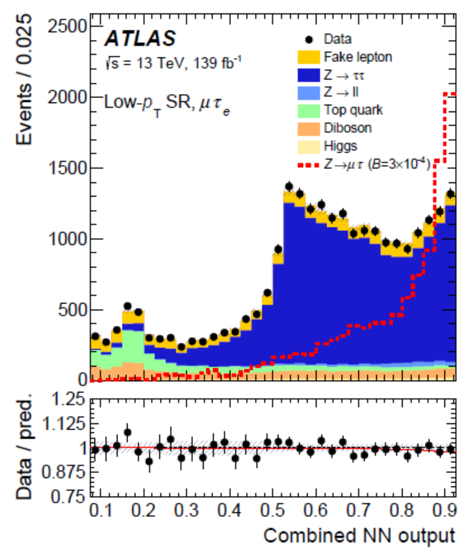

ATLAS-CONF-2021-042

arXiv:2105.12491

© S.Willocq EPS21

Upper limits at 95% CL	ATLAS	LEP
B(Z —> e μ)	0.34 × 10^{-6}	1.7 × 10^{-6} (OPAL)
B(Z —> e τ)	5.0 × 10^{-6}	9.8 × 10^{-6} (OPAL)
B(Z —> μ τ)	6.5 × 10^{-6}	12 × 10^{-6} (DELPHI)

LEP limits surpassed by factors of 5 ($Z \to e\mu$) and 2 ($Z \to e\tau, \mu\tau$)

these limits are stat-limited, so they will continue to improve with more luminosity

Heavy particle searches

Motivated by hierarchy problem
—> new physics at TeV scale

Heavy Gauge Boson with RH couplings

Deep NN top tagger using jet substructure

Discriminant: m_{tb}

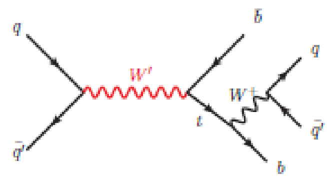

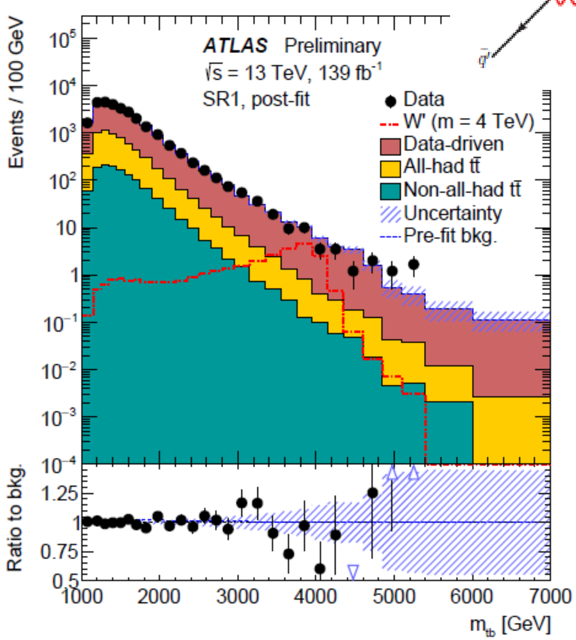

ATLAS-CONF-2021-043

$$m(W'_R) > 4.4\ \text{TeV}\ (4.1\ \text{TeV})$$

obs (exp)

Vector-like top quark

e/μ Z/H b tagged large/small R jets

Discr.: $m_{\text{eff}} = \sum p_{T_i} + E_T^{\text{miss}}$

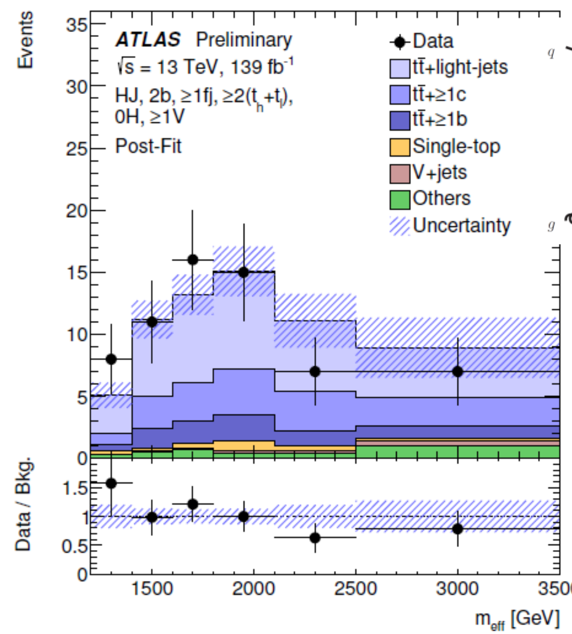

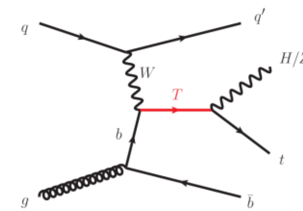

ATLAS-CONF-2021-040

$$m(T) > 1.8\ \text{TeV}\ (1.5\ \text{TeV})$$

obs (exp)

for coupling $\kappa \geq 0.5$

ATLAS Heavy Particle Searches* - 95% CL Upper Exclusion Limits

Status: July 2021

ATLAS Preliminary

$\int \mathcal{L}\, dt = (3.6 - 139)\ \mathrm{fb}^{-1}$ $\sqrt{s} = 8, 13$ TeV

	Model	ℓ, γ	Jets†	E_T^{miss}	$\int \mathcal{L}\, dt [\mathrm{fb}^{-1}]$	Limit		Reference
Extra dimensions	ADD $G_{KK} + g/q$	$0\ e, \mu, \tau, \gamma$	$1-4$ j	Yes	139	M_D 11.2 TeV	$n = 2$	2102.10874
	ADD non-resonant $\gamma\gamma$	$2\ \gamma$	–	–	36.7	M_S 8.6 TeV	$n = 3$ HLZ NLO	1707.04147
	ADD QBH	–	2 j	–	37.0	M_{th} 8.9 TeV	$n = 6$	1703.09127
	ADD BH multijet	–	≥3 j	–	3.6	M_{th} 9.55 TeV	$n = 6$, $M_D = 3$ TeV, rot BH	1512.02586
	RS1 $G_{KK} \to \gamma\gamma$	$2\ \gamma$	–	–	139	G_{KK} mass 4.5 TeV	$k/\overline{M}_{Pl} = 0.1$	2102.13405
	Bulk RS $G_{KK} \to WW/ZZ$	multi-channel			36.1	G_{KK} mass 2.3 TeV	$k/\overline{M}_{Pl} = 1.0$	1808.02380
	Bulk RS $G_{KK} \to WV \to \ell\nu qq$	$1\ e, \mu$	2 j / 1 J	Yes	139	G_{KK} mass 2.0 TeV	$k/\overline{M}_{Pl} = 1.0$	2004.14636
	Bulk RS $g_{KK} \to tt$	$1\ e, \mu$	≥1 b, ≥1J/2j	Yes	36.1	g_{KK} mass 3.8 TeV	$\Gamma/m = 15\%$	1804.10823
	2UED / RPP	$1\ e, \mu$	≥2 b, ≥3 j	Yes	36.1	KK mass 1.8 TeV	Tier (1,1), $\mathcal{B}(A^{(1,1)} \to tt) = 1$	1803.09678
Gauge bosons	SSM $Z' \to \ell\ell$	$2\ e, \mu$	–	–	139	Z' mass 5.1 TeV		1903.06248
	SSM $Z' \to \tau\tau$	$2\ \tau$	–	–	36.1	Z' mass 2.42 TeV		1709.07242
	Leptophobic $Z' \to bb$	–	2 b	–	36.1	Z' mass 2.1 TeV		1805.09299
	Leptophobic $Z' \to tt$	$0\ e, \mu$	≥1 b, ≥2 J	Yes	139	Z' mass 4.1 TeV	$\Gamma/m = 1.2\%$	2005.05138
	SSM $W' \to \ell\nu$	$1\ e, \mu$	–	Yes	139	W' mass 6.0 TeV		1906.05609
	SSM $W' \to \tau\nu$	$1\ \tau$	–	Yes	139	W' mass 5.0 TeV		ATLAS-CONF-2021-025
	SSM $W' \to tb$	–	≥1 b, ≥1 J	–	139	W' mass 4.4 TeV		ATLAS-CONF-2021-043
	HVT $W' \to WZ \to \ell\nu qq$ model B	$1\ e, \mu$	2 j / 1 J	Yes	139	W' mass 4.3 TeV	$g_V = 3$	2004.14636
	HVT $Z' \to ZH$ model B	0-2 e, μ	1-2 b	Yes	139	Z' mass 3.2 TeV	$g_V = 3$	ATLAS-CONF-2020-043
	HVT $W' \to WH$ model B	$0\ e, \mu$	≥1 b, ≥2 J		139	W' mass 3.2 TeV	$g_V = 3$	2007.05293
	LRSM $W_R \to \mu N_R$	$2\ \mu$	1 J	–	80	W_R mass 5.0 TeV	$m(N_R) = 0.5$ TeV, $g_L = g_R$	1904.12679
CI	CI $qqqq$	–	2 j	–	37.0	Λ 21.8 TeV η_{LL}^-		1703.09127
	CI $\ell\ell qq$	$2\ e, \mu$	–	–	139	Λ 35.8 TeV η_{LL}^-		2006.12946
	CI $eebs$	$2\ e$	1 b	–	139	Λ 1.8 TeV	$g_* = 1$	2105.13847
	CI $\mu\mu bs$	$2\ \mu$	1 b	–	139	Λ 2.0 TeV	$g_* = 1$	2105.13847
	CI $tttt$	$\geq 1\ e, \mu$	≥1 b, ≥1 j	Yes	36.1	Λ 2.57 TeV	$\lvert C_{4t} \rvert = 4\pi$	1811.02305
DM	Axial-vector med. (Dirac DM)	$0\ e, \mu, \tau, \gamma$	$1-4$ j	Yes	139	m_{med} 2.1 TeV	g_q=0.25, g_χ=1, $m(\chi)$=1 GeV	2102.10874
	Pseudo-scalar med. (Dirac DM)	$0\ e, \mu, \tau, \gamma$	$1-4$ j	Yes	139	m_{med} 376 GeV	g_q=1, g_χ=1, $m(\chi)$=1 GeV	2102.10874
	Vector med. Z'-2HDM (Dirac DM)	$0\ e, \mu$	2 b	Yes	139	m_{med} 3.1 TeV	tanβ=1, g_Z=0.8, $m(\chi)$=100 GeV	ATLAS-CONF-2021-006
	Pseudo-scalar med. 2HDM+a	multi-channel			139	m_{med} 560 GeV	tanβ=1, g_χ=1, $m(\chi)$=10 GeV	ATLAS-CONF-2021-036
	Scalar reson. $\phi \to t\chi$ (Dirac DM)	0-1 e, μ	1 b, 0-1 J	Yes	36.1	m_ϕ 3.4 TeV	y=0.4, λ=0.2, $m(\chi)$=10 GeV	1812.09743
LQ	Scalar LQ 1[st] gen	$2\ e$	≥2 j	Yes	139	LQ mass 1.8 TeV	$\beta = 1$	2006.05872
	Scalar LQ 2[nd] gen	$2\ \mu$	≥2 j	Yes	139	LQ mass 1.7 TeV	$\beta = 1$	2006.05872
	Scalar LQ 3[rd] gen	$1\ \tau$	2 b	Yes	139	LQ_3^u mass 1.2 TeV	$\mathcal{B}(LQ_3^u \to b\tau) = 1$	ATLAS-CONF-2021-008
	Scalar LQ 3[rd] gen	$0\ e, \mu$	≥2 j, ≥2 b	Yes	139	LQ_3^u mass 1.24 TeV	$\mathcal{B}(LQ_3^u \to t\nu) = 1$	2004.14060
	Scalar LQ 3[rd] gen	$\geq 2\ e, \mu, \geq 1\ \tau$	≥1 j, ≥1 b	–	139	LQ_3^d mass 1.43 TeV	$\mathcal{B}(LQ_3^d \to t\tau) = 1$	2101.11582
	Scalar LQ 3[rd] gen	$0\ e, \mu, \geq 1\ \tau$	$0-2$ j, 2 b	Yes	139	LQ_3^d mass 1.26 TeV	$\mathcal{B}(LQ_3^d \to b\nu) = 1$	2101.12527
Heavy quarks	VLQ $TT \to Zt + X$	2e/2μ/≥3e,μ	≥1 b, ≥1 j	–	139	T mass 1.4 TeV	SU(2) doublet	ATLAS-CONF-2021-024
	VLQ $BB \to Wt/Zb + X$	multi-channel			36.1	B mass 1.34 TeV	SU(2) doublet	1808.02343
	VLQ $T_{5/3} T_{5/3} \vert T_{5/3} \to Wt + X$	2(SS)/≥3 e, μ	≥1 b, ≥1 j	Yes	36.1	$T_{5/3}$ mass 1.64 TeV	$\mathcal{B}(T_{5/3} \to Wt)$= 1, $c(T_{5/3}Wt)$= 1	1807.11883
	VLQ $T \to Ht/Zt$	$1\ e, \mu$	≥1 b, ≥3 j	Yes	139	T mass 1.8 TeV	SU(2) singlet, κ_T= 0.5	ATLAS-CONF-2021-040
	VLQ $Y \to Wb$	$1\ e, \mu$	≥1 b, ≥1 j	Yes	36.1	Y mass 1.85 TeV	$\mathcal{B}(Y \to Wb)$= 1, $c_R(Wb)$= 1	1812.07343
	VLQ $B \to Hb$	$0\ e,\mu$	≥2b, ≥1j, ≥1J	–	139	B mass 2.0 TeV	SU(2) doublet, κ_B= 0.3	ATLAS-CONF-2021-018
Excited fermions	Excited quark $q^* \to qg$	–	2 j	–	139	q^* mass 6.7 TeV	only u^* and d^*, $\Lambda = m(q^*)$	1910.08447
	Excited quark $q^* \to q\gamma$	$1\ \gamma$	1 j	–	36.7	q^* mass 5.3 TeV	only u^* and d^*, $\Lambda = m(q^*)$	1709.10440
	Excited quark $b^* \to bg$	–	1 b, 1 j	–	36.1	b^* mass 2.6 TeV		1805.09299
	Excited lepton ℓ^*	$3\ e, \mu$	–	–	20.3	ℓ^* mass 3.0 TeV	$\Lambda = 3.0$ TeV	1411.2921
	Excited lepton ν^*	$3\ e, \mu, \tau$	–	–	20.3	ν^* mass 1.6 TeV	$\Lambda = 1.6$ TeV	1411.2921
Other	Type III Seesaw	2,3,4 e, μ	≥2 j	Yes	139	N^0 mass 910 GeV		ATLAS-CONF-2021-023
	LRSM Majorana ν	$2\ \mu$	2 j	–	36.1	N_R mass 3.2 TeV	$m(W_R) = 4.1$ TeV, $g_L = g_R$	1809.11105
	Higgs triplet $H^{\pm\pm} \to W^\pm W^\pm$	2,3,4 e, μ (SS)	various	Yes	139	$H^{\pm\pm}$ mass 350 GeV	DY production	2101.11961
	Higgs triplet $H^{\pm\pm} \to \ell\ell$	2,3,4 e, μ (SS)	–	–	36.1	$H^{\pm\pm}$ mass 870 GeV	DY production	1710.09748
	Higgs triplet $H^{\pm\pm} \to \ell\tau$	$3\ e, \mu, \tau$	–	–	20.3	$H^{\pm\pm}$ mass 400 GeV	DY production, $\mathcal{B}(H_L^{\pm\pm} \to \ell\tau) = 1$	1411.2921
	Multi-charged particles	–	–	–	36.1	multi-charged particle mass 1.22 TeV	DY production, $\lvert q \rvert = 5e$	1812.03673
	Magnetic monopoles	–	–	–	34.4	monopole mass 2.37 TeV	DY production, $\lvert g \rvert = 1 g_D$, spin 1/2	1905.10130

Legend: $\sqrt{s}$ = 8 TeV; $\sqrt{s}$ = 13 TeV partial data; $\sqrt{s}$ = 13 TeV full data

Axis: 10^{-1}, 1, 10 — Mass scale [TeV]

*Only a selection of the available mass limits on new states or phenomena is shown.

†Small-radius (large-radius) jets are denoted by the letter j (J).

♪ ***Results***

- ***detector***
- ***SM (including multibosons and VBS)***
- ***BSM***
- ***(B-E)H***

The (Brout-Englert-) Higgs = BEH boson(s)

1 Additional BEH bosons (and exotic decays)

2 The SM BEH boson

see back-up ($H \rightarrow bb$ $H \rightarrow l\, l\, \gamma$, $H \rightarrow Z\, \gamma$ ..)

3 Search for a pair of BEH bosons

1 Additional BEH bosons

General recipe : SM Higgs Doublet + Additional Field = Additional H bosons

SM + 1 additional H doublet = 2HDM (Two Higgs Doublet Model) that corresponds to 5 physical Higgs bosons

h, H, A, H^+, H^-

Four variants to couple SM fermions to the 2HDs

Coupling scale factor	Type I	Type II	Lepton-specific	Flipped
κ_V	$\sin(\beta-\alpha)$			
κ_u	$\cos(\alpha)/\sin(\beta)$			
κ_d	$\cos(\alpha)/\sin(\beta)$	$-\sin(\alpha)/\cos(\beta)$	$\cos(\alpha)/\sin(\beta)$	$-\sin(\alpha)/\cos(\beta)$
κ_ℓ	$\cos(\alpha)/\sin(\beta)$	$-\sin(\alpha)/\cos(\beta)$	$-\sin(\alpha)/\cos(\beta)$	$\cos(\alpha)/\sin(\beta)$

JHEP 1511 (2015) 206

MSSM $\subset$ type II HDM .. Numerous benchmark models like hMSSM

1 Additional BEH bosons

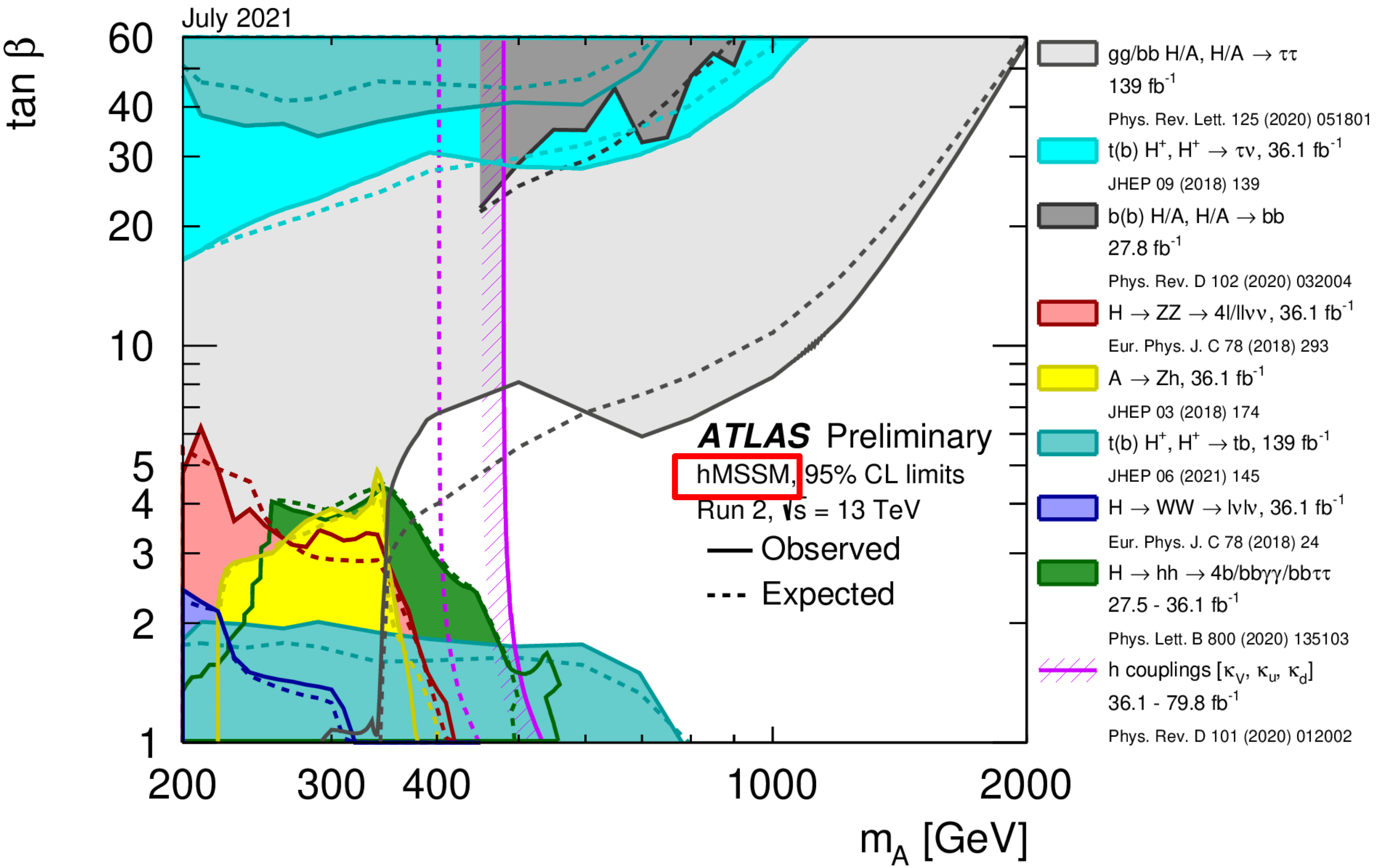

ATL-PHYS-PUB-2021-030

1 Additional BEH bosons $\gamma\gamma$ excess at 95 GeV
(same situation than 2 years ago)

***comparison between CMS and ATLAS results** (Sven Heinemeyer)*

CMS PAS HIG-17-013

20 fb^{-1} (8 TeV) + 36 fb^{-1} (13 TeV)

ATLAS-CONF-2018-025

80 fb^{-1} (13 TeV)

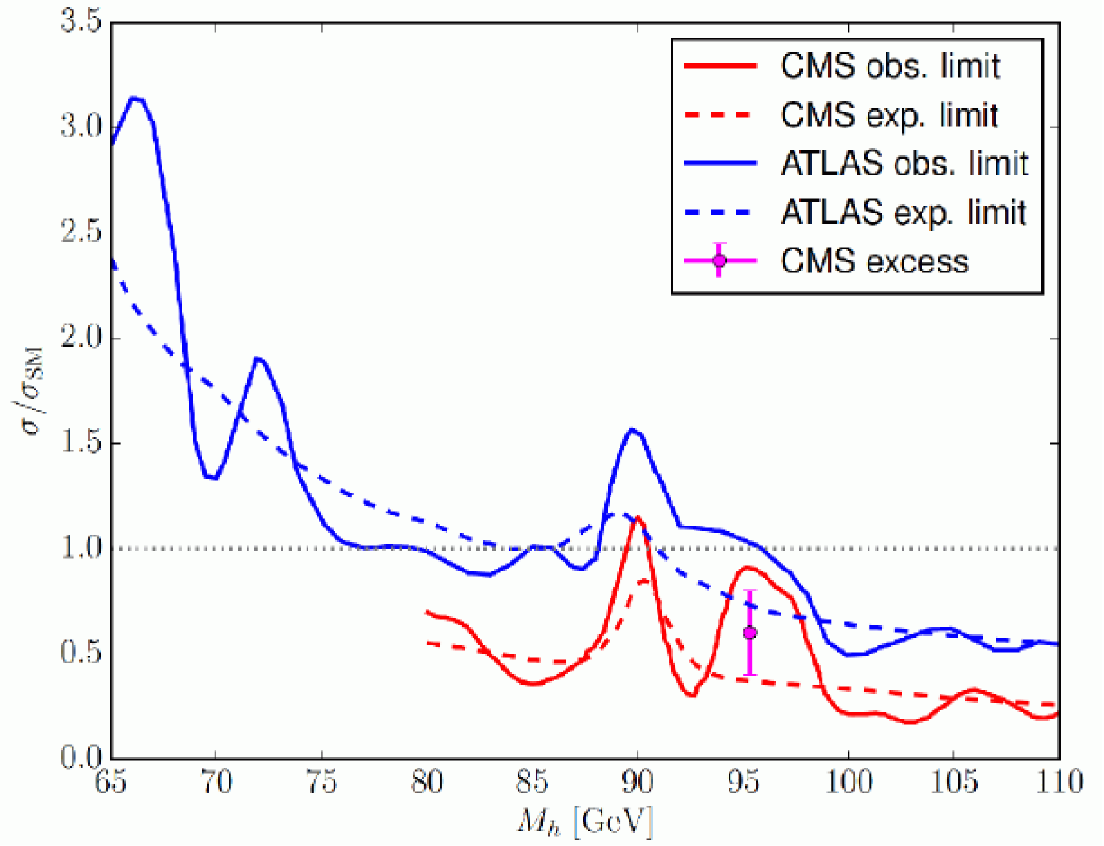

1 *exotic decays of standard BEH boson*

Higgs portal / Hidden sector models predict exotic Higgs decays to LLP s

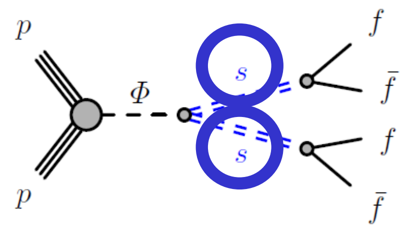

Require 2 DVs:
0 events observed
w/ 0.32 +/- 0.05
expected bkg

BF(Φ(125)—>*ss*) =10%
excluded for cτ(*s*) in range
4 cm — 7.8 m
for m(s) = 5 GeV

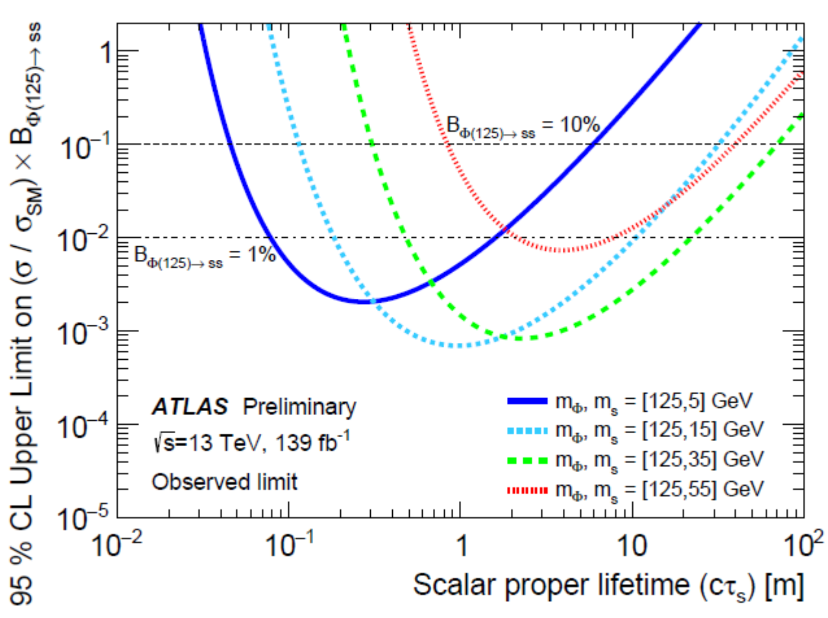

2 The SM BEH boson executive summary

9 years after the discovery we have now a much clearer picture of the BEH boson properties

♠ *It is spin 0 and its interactions with bosons are mainly CP-even*

♠ *We know its mass at < 0.2% accuracy*

BEH boson couples to mass ➔ couplings to be measured

► *Observation of all main production modes (ggF, VBF, VH, ttH)*

Increasing precision in all measurements

► *bosonic sector : inclusive measurement at ~10% precision differential measurements probing extended phase space with increasing accuracy*

► *fermionic sector : 3rd generation (τ, t, b) established with uncertainties approaching ~ 20% level . Most promising channel for 2^{nd} generation is $H \rightarrow \mu\mu$*

2 The SM BEH boson

A.Djouadi Phys.Rept.457:1-216

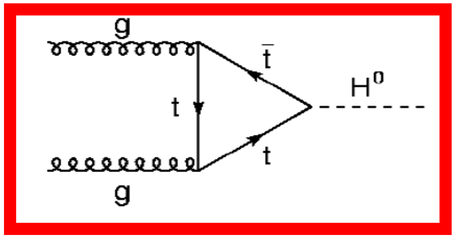

GF $H \to WW, ZZ, \gamma\gamma, (bb), \tau\tau$

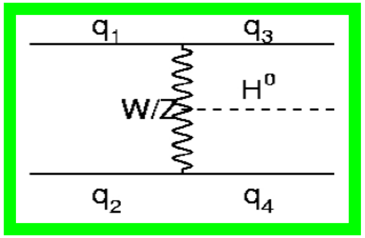

VBF $H \to WW, ZZ, \gamma\gamma, bb, \tau\tau$

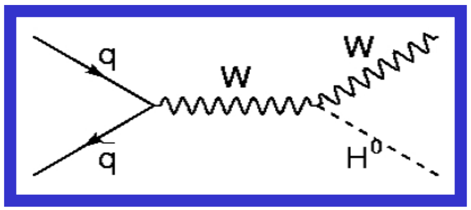

WH, ZH $H \to WW, \gamma\gamma, bb$

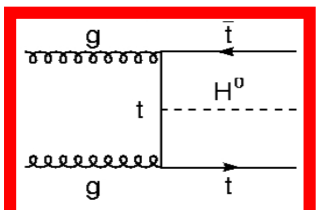

ttH $H \to WW, \gamma\gamma, \tau\tau, ZZ, bb$

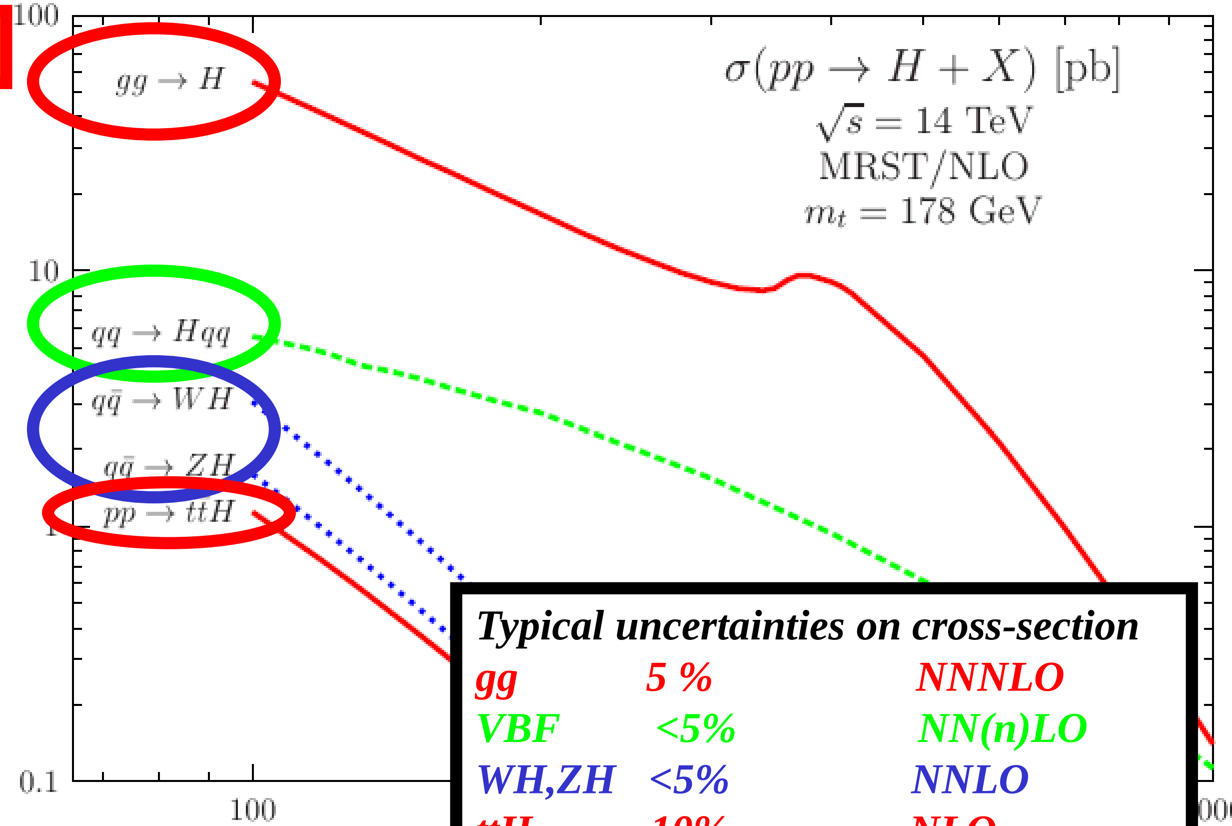

Typical uncertainties on cross-section

gg	5 %	NNNLO
VBF	<5%	NN(n)LO
WH,ZH	<5%	NNLO
ttH	10%	NLO

These production cross sections have to be used with the decays **bb , ττ , WW , ZZ , γγ**

channels with good mass resolution

2 The SM BEH boson

A.Djouadi Phys.Rept.457:1-216

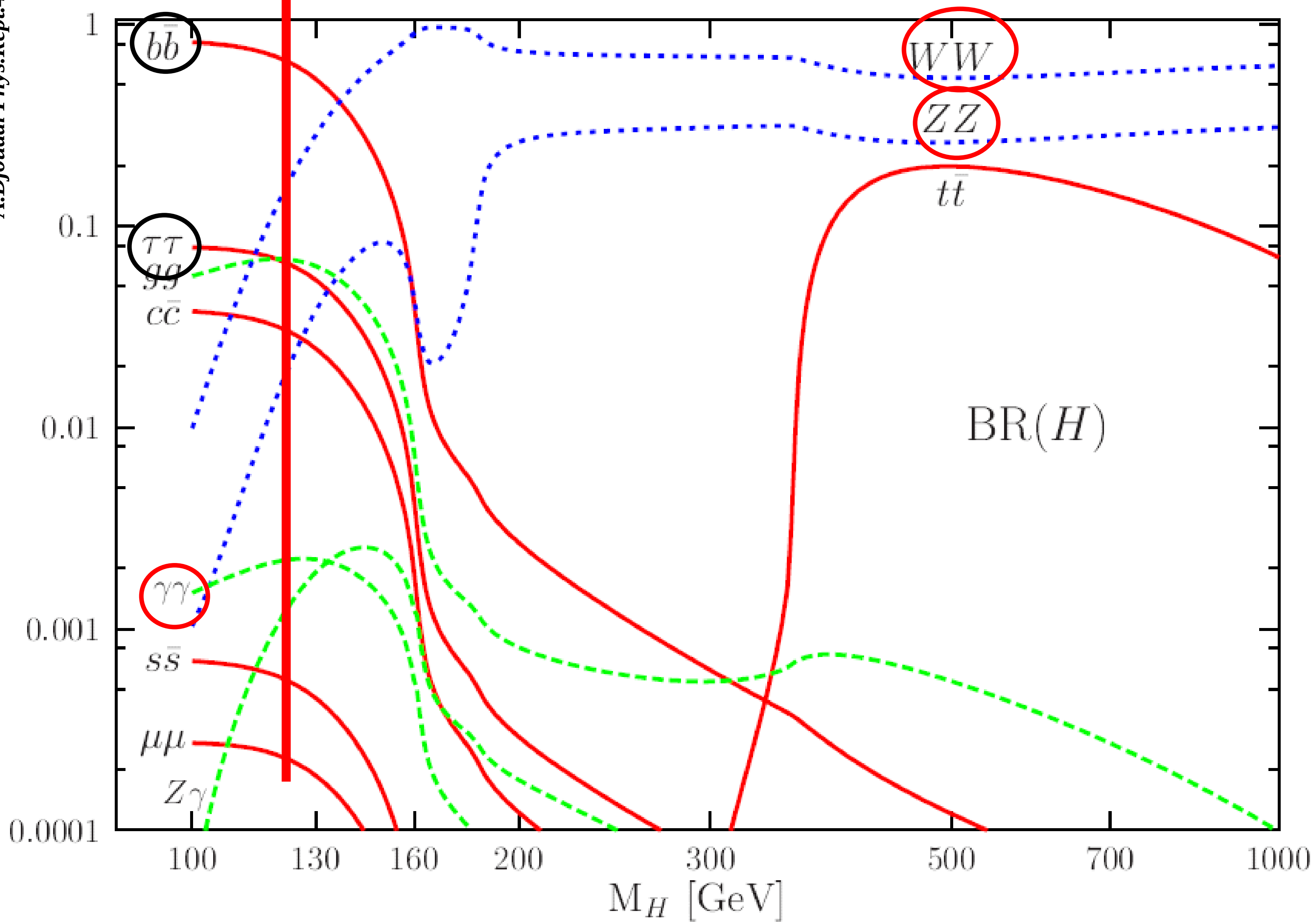

2 The SM BEH boson The H mass

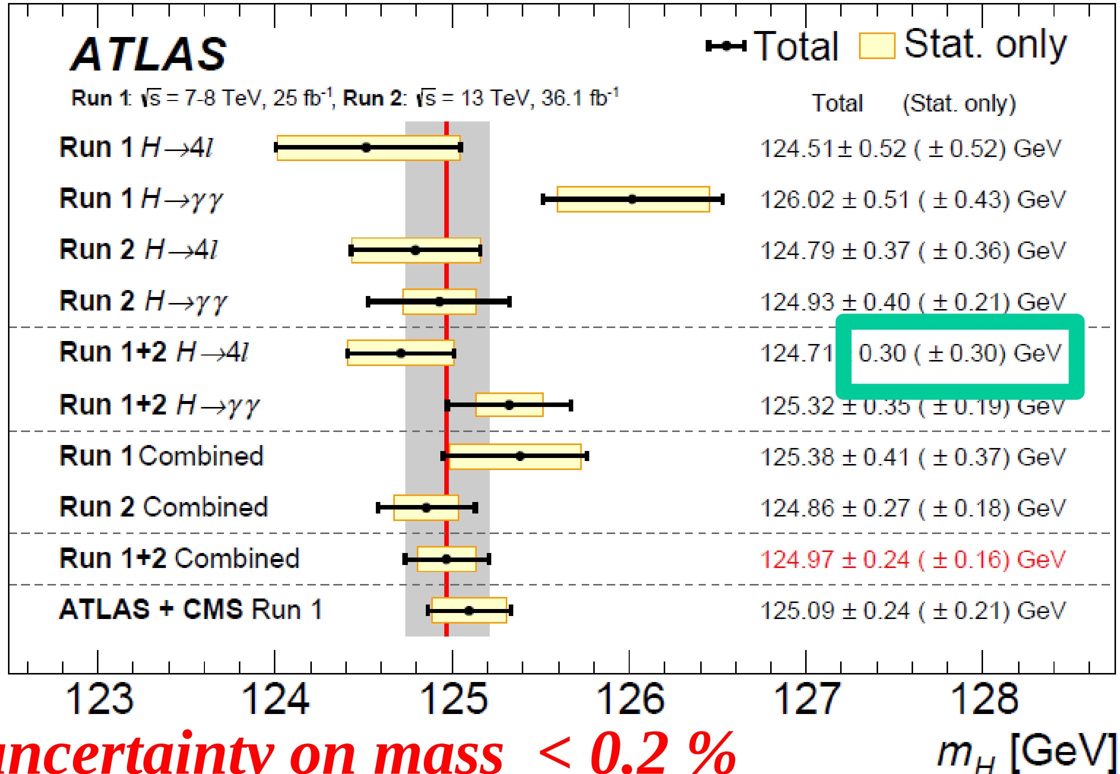

Phys. Lett. B 784 (2018) 345

uncertainty on mass < 0.2 %

Remember ATLAS has an uncertainty on W mass of 19 MeV *Eur.Phys.J. C78 (2018) no.2, 110*

note that $\Delta m_H = 0.1$ GeV $\rightarrow \Delta(BR(H\rightarrow ZZ)) / BR(H\rightarrow ZZ) \sim 1\%$

At longer term uncertainty will be dominated by 4l

(for $H\rightarrow \gamma\gamma$: need to extrapolate from e to γ !)

note : new CMS measurements Phys. Lett. B 805 (2020) 135425

2 The SM BEH boson $t\,t\,H \quad H \rightarrow \gamma\gamma$

Phys.Rev.Lett. 125 (2020) 6, 061802

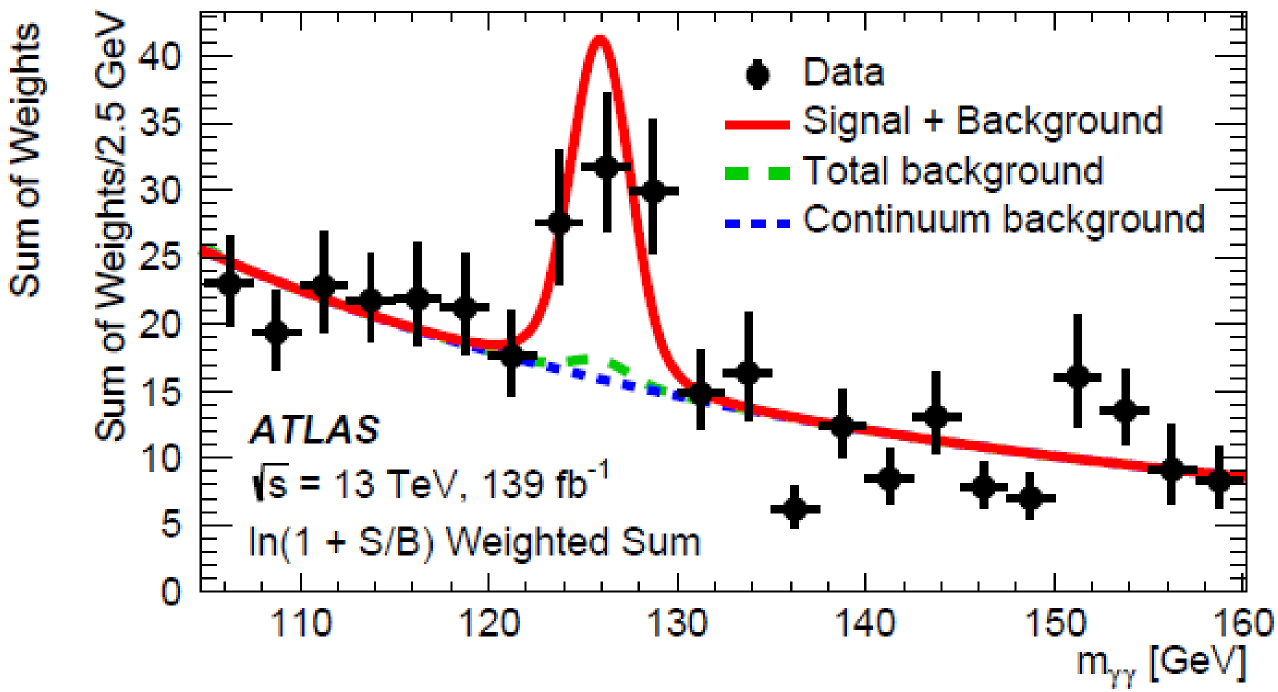

Assuming a CP-even coupling, the $t\bar{t}H$ process is observed with a significance of 5.2 standard deviations

4.4 expected

contraints on CP admixture

2 The SM BEH boson $H \to \tau\tau$

$$\mathscr{B}(H \to \tau\tau) = 6.3\,\%$$

Expt. challenge: 2-4 neutrinos in final state, poor mass resolution

Multiple BDTs used to suppress $Z \to \tau\tau$ and $t\bar{t}$ background, and categorize event purity for each production mechanism

Dominant $Z \to \tau\tau$ background from MC, controlled with $Z \to \ell\ell$ data via kinematic embedding procedure

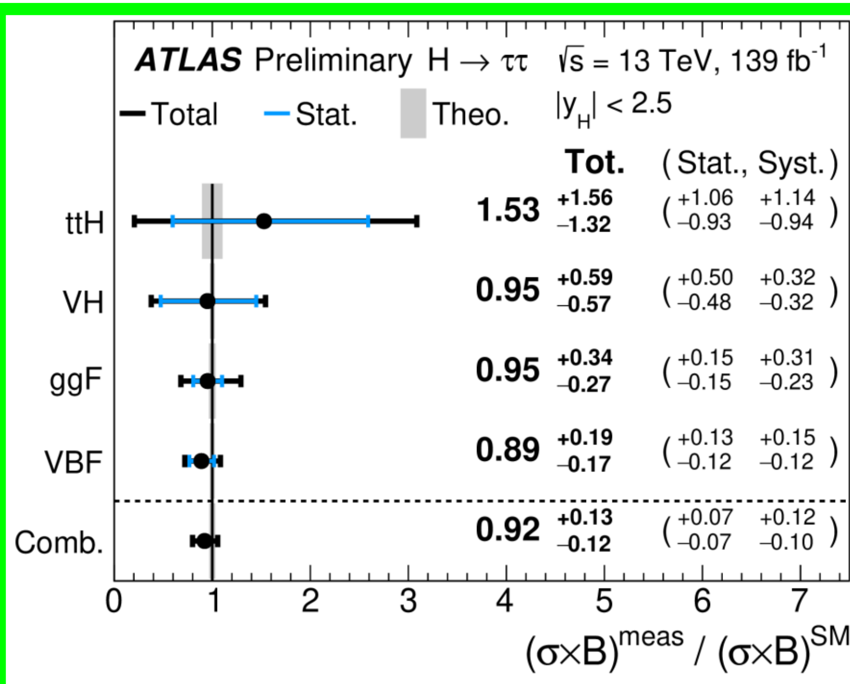

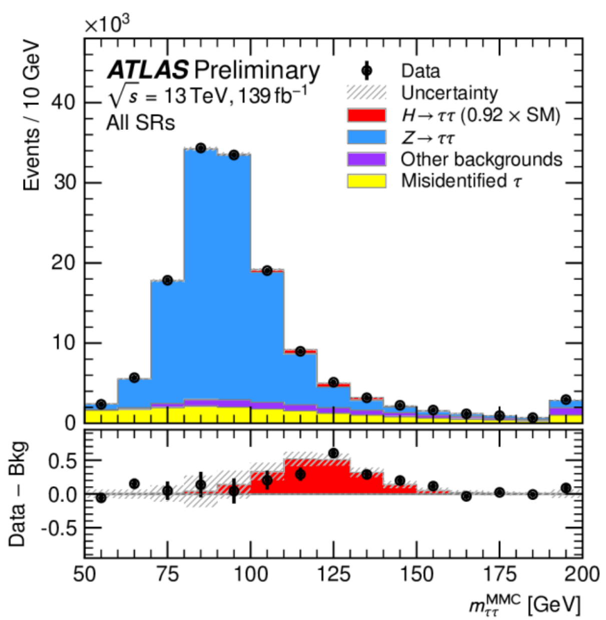

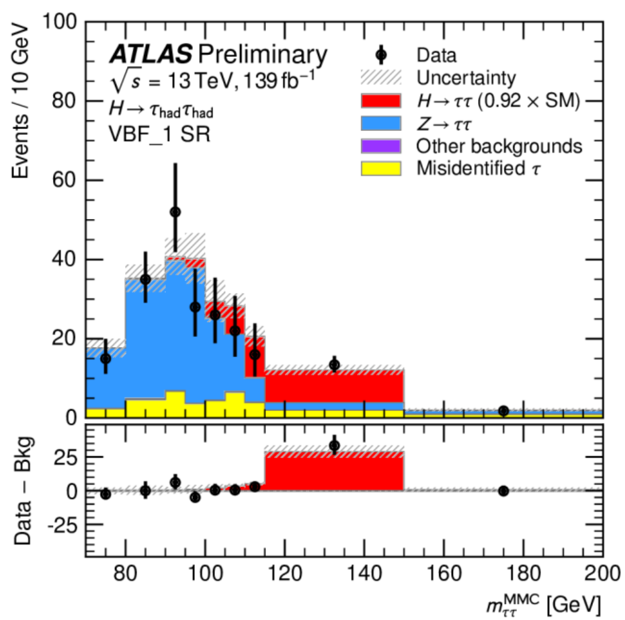

ggF significance

$3.9\,\sigma\,(4.6\,\sigma)$ obs (exp)

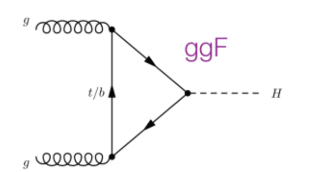

VBF significance

$5.3\,\sigma\,(6.2\,\sigma)$ obs (exp)

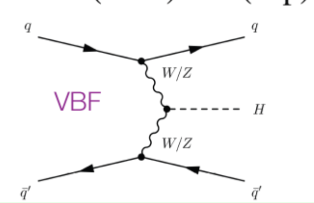

2 The SM BEH boson $H \to cc$ $H \to \mu\mu$

ATLAS-CONF-2021-021

Phys. Lett. B 812 (2021) 135980 arXiv:2007.07830

$H \to cc$

Target VH production

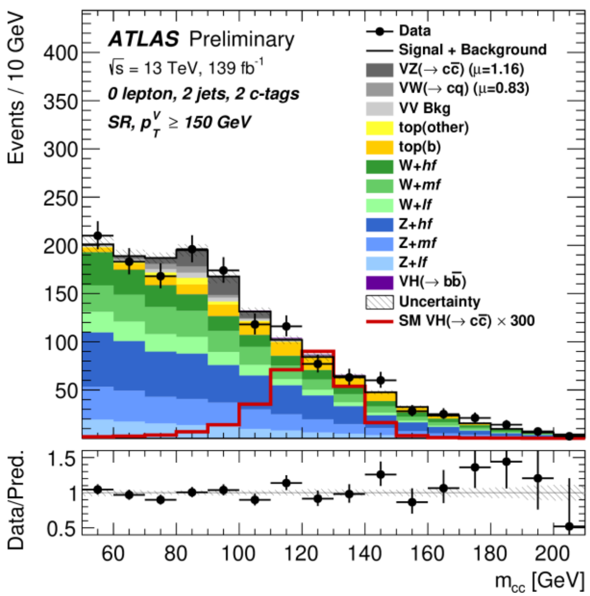

$VH(\to cc) < 26\,(31)\,\sigma_{SM}$ obs (exp)

$H \to \mu\mu$

Good signal resolution, smoothly falling background dominated by $Z \to \mu\mu$

$m_{\mu\mu}$ shape parametrized

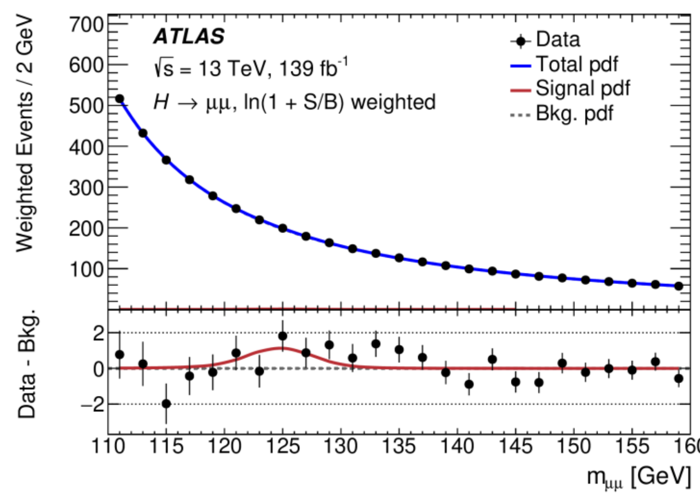

significance: 2 σ obs. (1.7 σ exp.)

2 The SM BEH boson $H \to 4l$ $H \to \gamma\gamma$

Full Run-2

$H \to 4l$

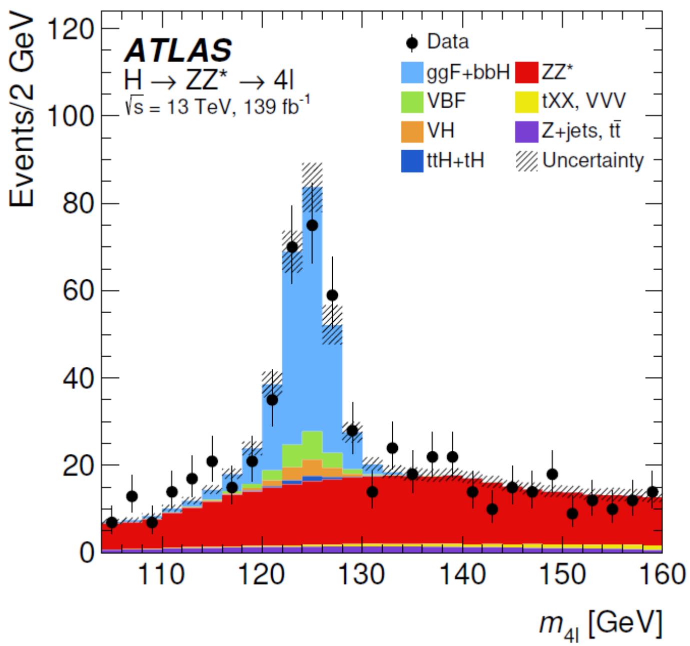

$$\mu = 1.01 \pm 0.08(\text{stat.}) \pm 0.04(\text{exp.}) \pm 0.05(\text{th.}) = 1.01 \pm 0.11$$

Eur. Phys. J. C 80 (2020) 957

Full Run-2

$H \to \gamma\gamma$

ATLAS-CONF-2020-026

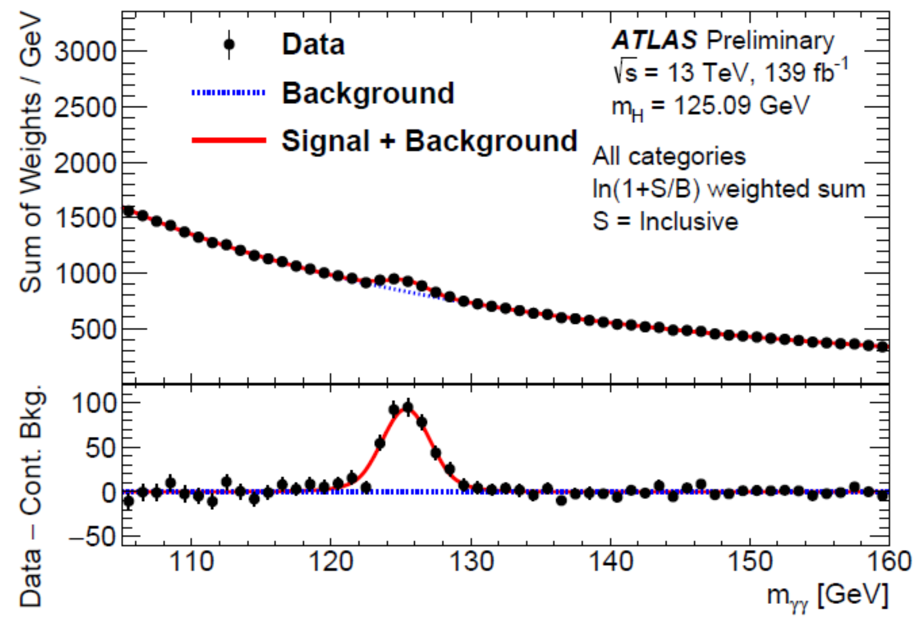

$$(\sigma \times B_{\gamma\gamma})_{\text{obs}} = 127 \pm 10 \text{ fb} = 127 \pm 7 \text{ (stat.)} \pm 7 \text{ (syst.) fb}$$

$$(\sigma \times B_{\gamma\gamma})_{\text{exp}} = 116 \pm 5 \text{ fb}$$

constraint on charm coupling through pT distribution

($gg \to H$ and $c\bar{c} \to H$) ATLAS-CONF-2019-029

Coefficient	Observed 95% CL limit	Expected 95% CL limit
κ_c	[−19, 24]	[−15, 19]

syst (background modelling + energy resolution + …. = stat !

arXiv:1907.06131

arXiv:1909.10235

$H \rightarrow ee, e\mu, e\tau, \tau\mu$

no evidence for $H \rightarrow ee$ ☺

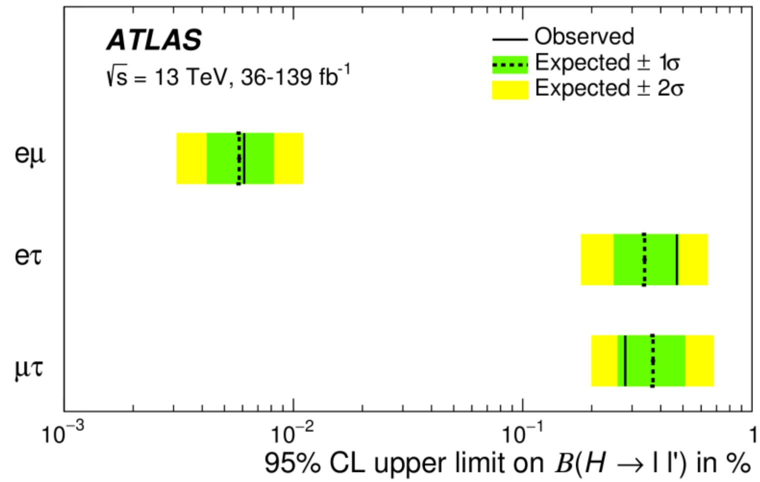

$BR(H \rightarrow ee) < 3.6_{obs}\ (3.5)_{exp}\ 10^{-4}$

2 The SM BEH boson H combination

$$\mu = 1.06 \pm 0.07 = 1.06 \pm 0.04\,(\text{stat.}) \pm 0.03\,(\text{exp.}) {}^{+0.05}_{-0.04}\,(\text{sig. th.}) \pm 0.02\,(\text{bkg. th.})$$

ATLAS-CONF-2020-027

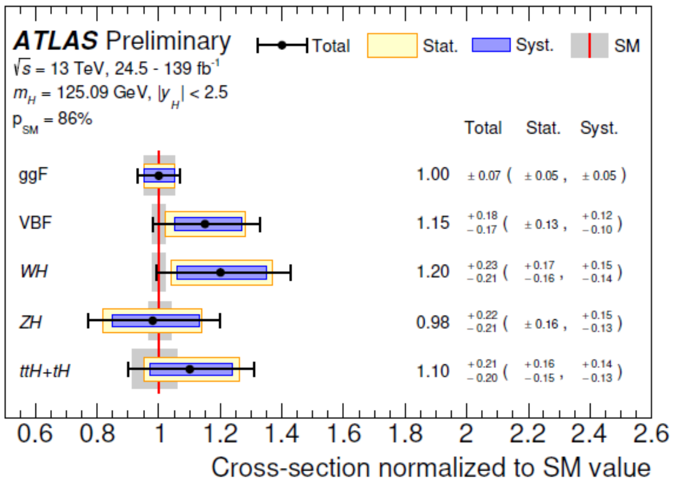

assumption of SM branching fractions

13 TeV

up to 140 fb^{-1}

iconic H plot

The SM BEH mechanism predicts relations between couplings and masses

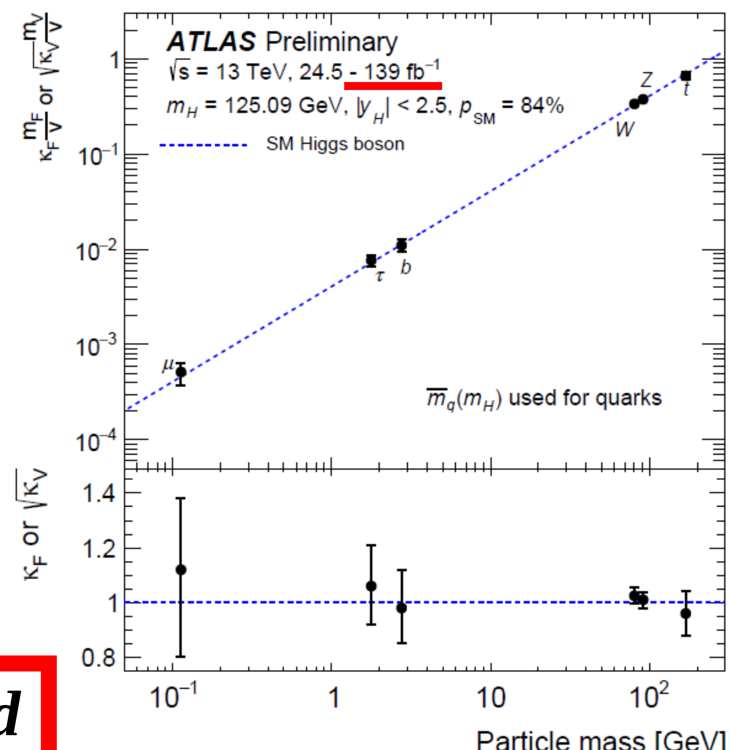

checked

There are other results (STXS , interpretations)

SEE BACKUP

ATLAS-CONF-2020-053

2 *The SM BEH boson H combination*

with the

large statistics

we are able to compute a large number of individual cross sections

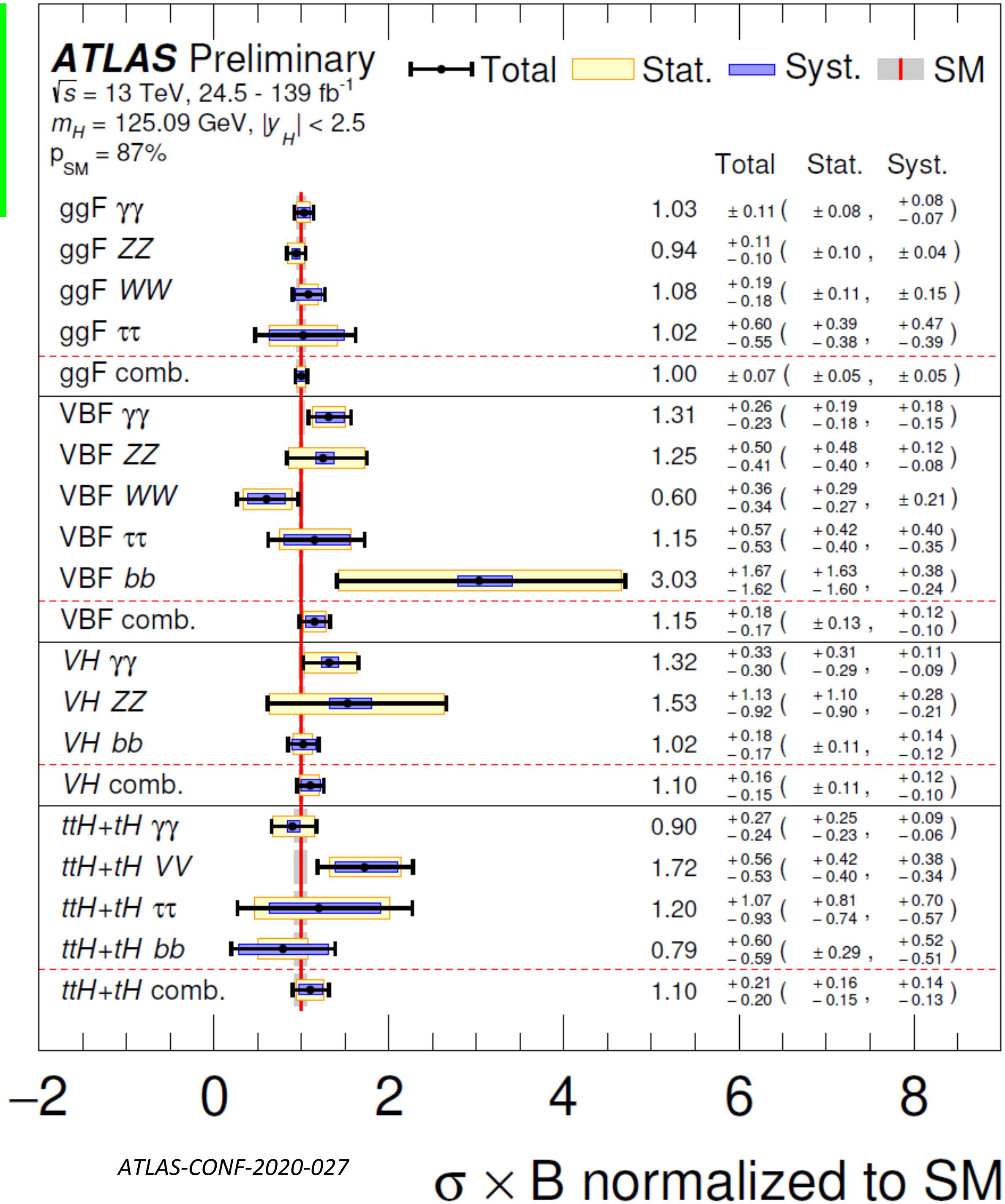

ATLAS-CONF-2020-027

2 The SM BEH boson H combination

and in some extreme kinematic regions

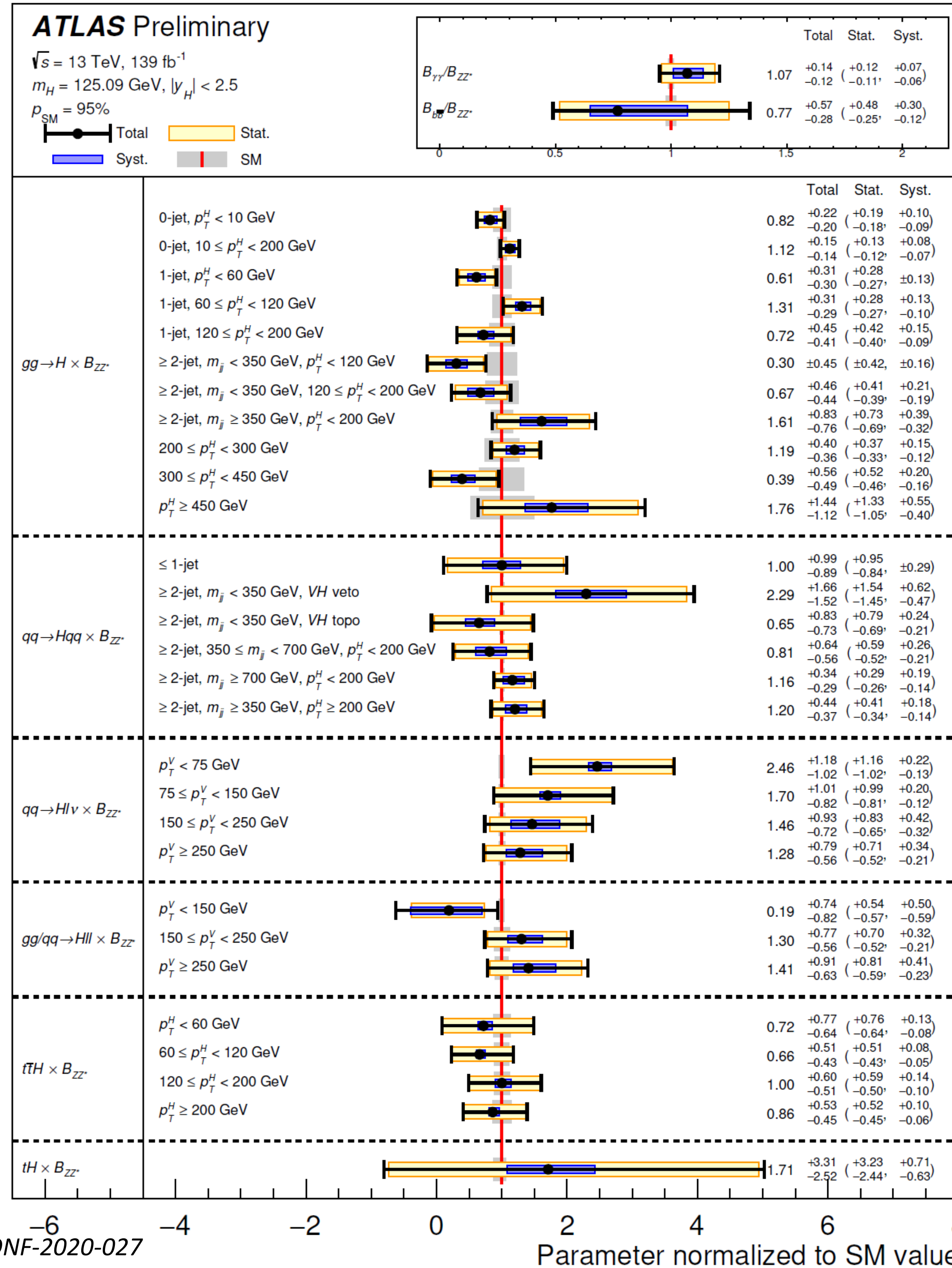

ATLAS-CONF-2020-027

2 *The SM BEH boson H combination*

allow some simple physics interpretations (coupling modifiers)

ATLAS-CONF-2020-027

$$\kappa_j^2 = \frac{\sigma_j}{\sigma_j^{SM}} \quad \text{or} \quad \kappa_j^2 = \frac{\Gamma_j}{\Gamma_j^{SM}}.$$

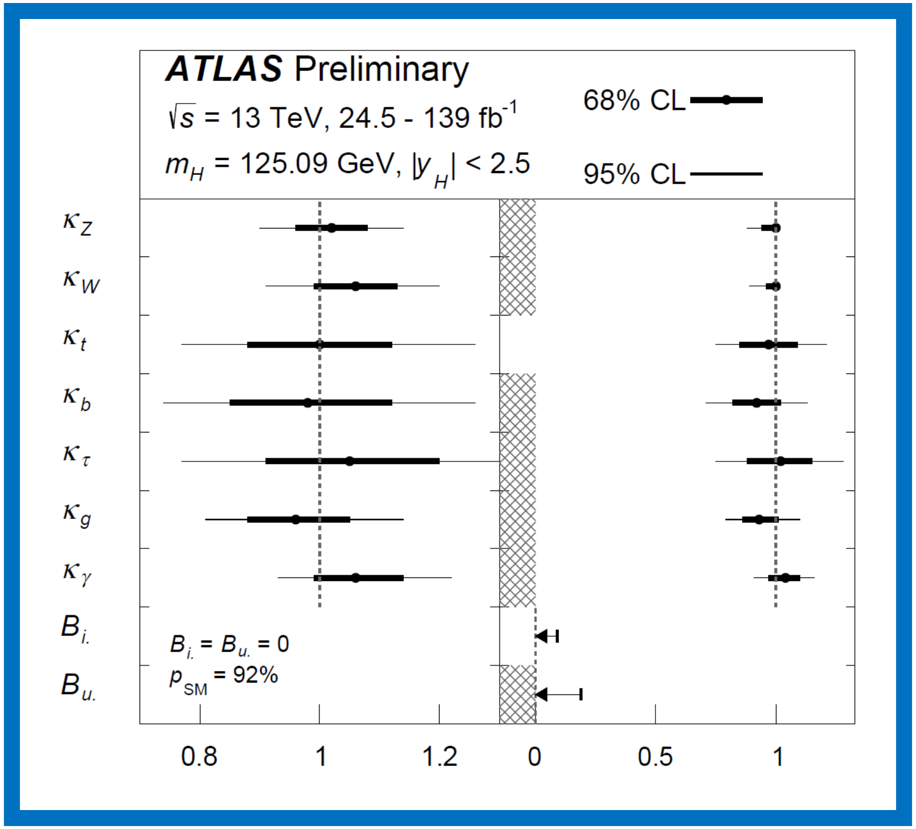

and more complicated physics interpretations

Standard Model Effective Field Theory (SMEFT) operators and corresponding Wilson coefficients

Several MSSM benchmark scenarios

ATLAS-CONF-2020-053

2 The SM BEH boson invisible decays

SM BR($H \to 4\nu$) ~ 1.2 10^{-3}

« Old » Combination

ATLAS-CONF-2020-052

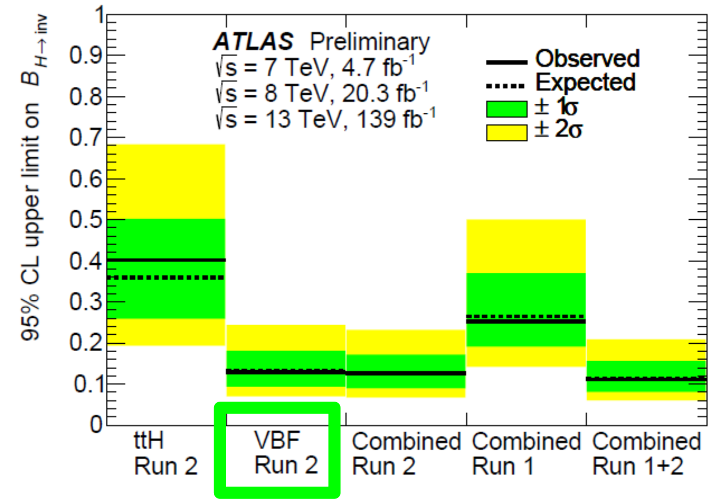

$\mathcal{B}(H \to \text{inv}) <$ 11% obs. (11% exp.) at 95% CL

$Z \to ll$ H inv

ATLAS-CONF-2021-029

Experimental signature: $Z \to \ell\ell + E_T^{miss}$

ZZ background estimated from $ZZ \to 4\ell$ CR

$\mathcal{B}(H \to \text{inv}) <$ 18% obs. (18% exp.) at 95% CL

assuming SM H production

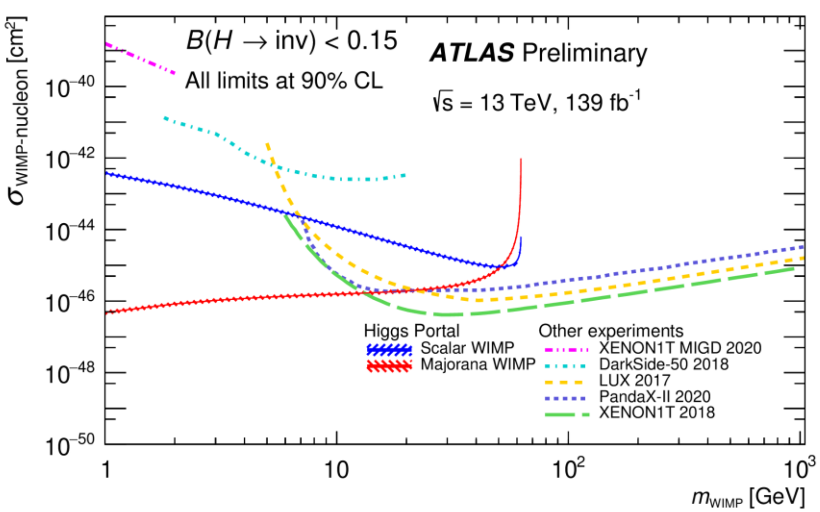

DM interpretation

as limit on WIMP-nucleon scattering in Higgs portal model

Complementary to direct DM searches

3 Search for a pair of BEH bosons

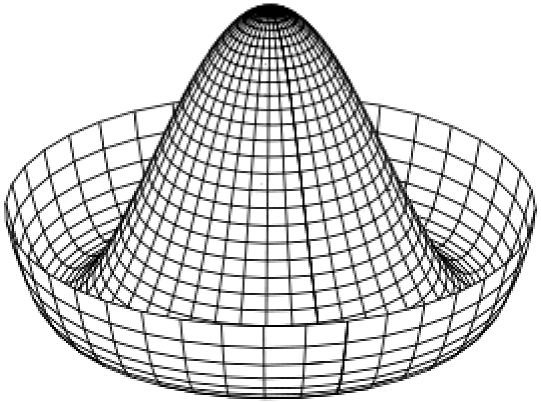

After discovering the Higgs boson, the ultimate probe of the Standard Model is to fully measure the Higgs potential.

$\Phi \rightarrow v + h$

$$V(\phi) = \frac{1}{2}\mu^2\phi^2 + \frac{1}{4}\lambda\phi^4 = \lambda v^2 h^2 + \lambda v h^3 + \frac{1}{4}\lambda h^4$$

mass term

$\frac{1}{2} m_h^2 h^2$

self coupling terms

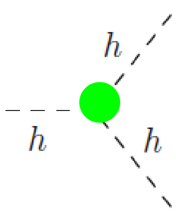

3 Search for a pair of BEH bosons

Standard Model

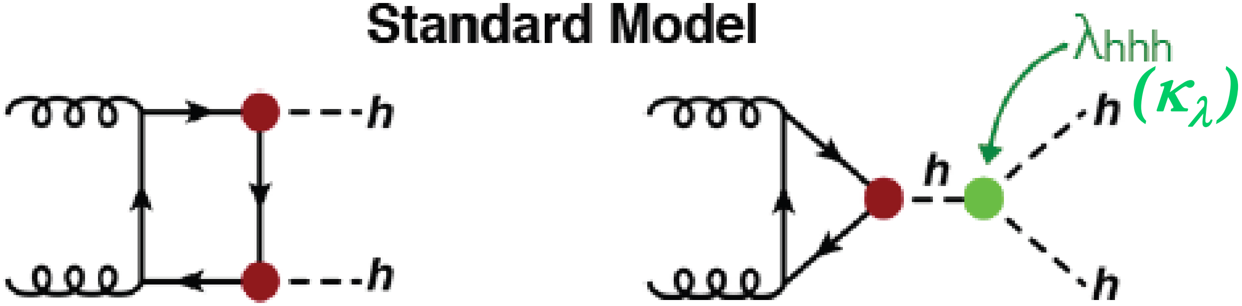

33.4 fb @ 13 TeV (significant destructive interference)

Beyond Standard Model

Resonant

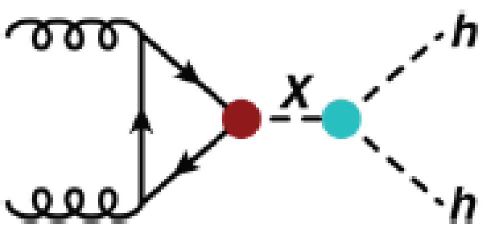

KK gravitons, heavy higgs, …

Non-resonant

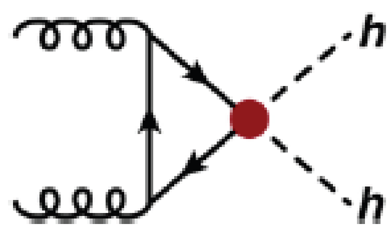

tthh vertex, coloured scalars, …

3 Search for a pair of BEH bosons

ATL-PHYS-PUB-2021-031

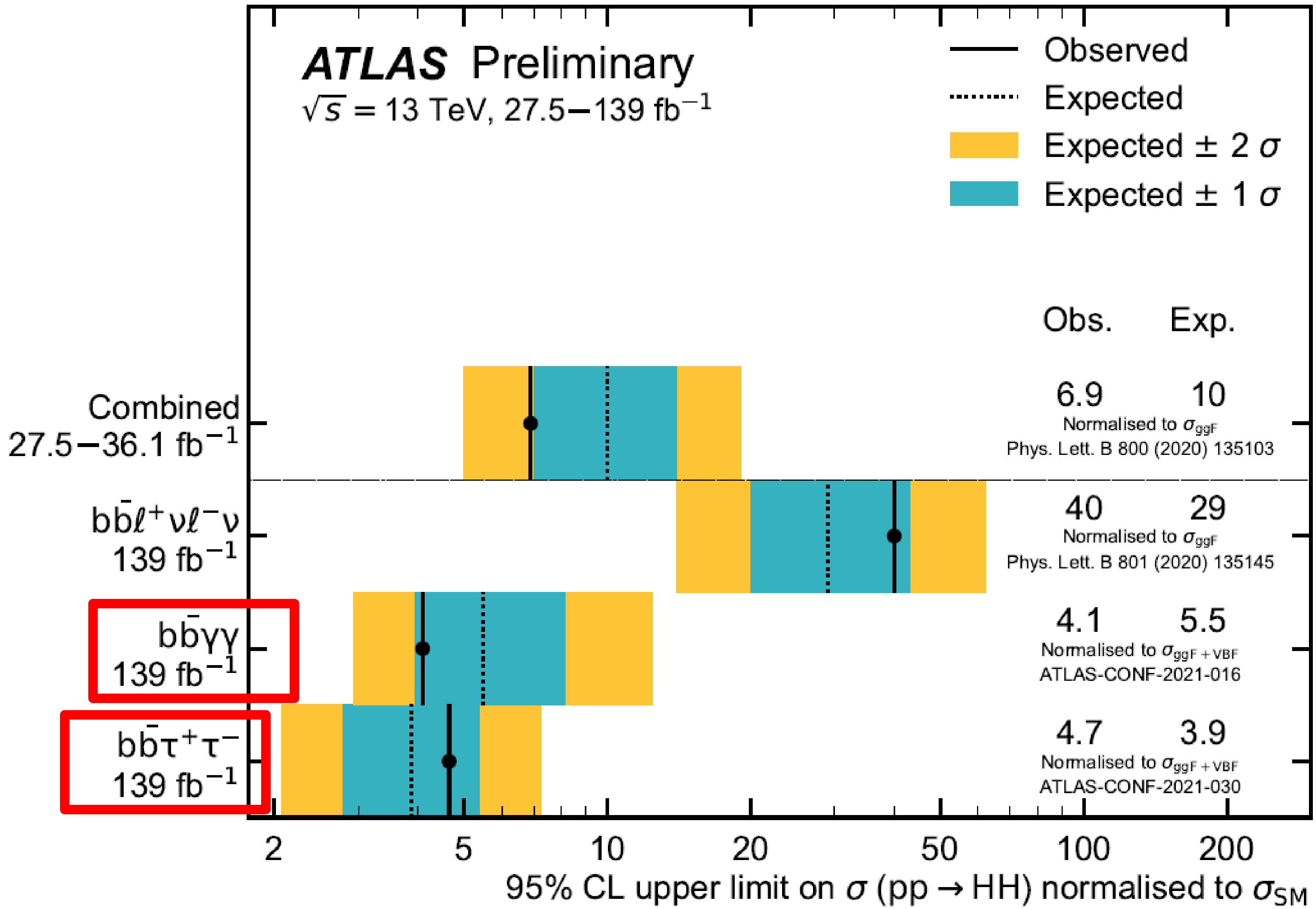

3 Search for a pair of BEH bosons

HH → bb ττ

ATLAS-CONF-2021-030

Using $\tau_{\rm had}\tau_{\rm had}$ and $\tau_{\rm had}\tau_{\rm lep}$ decay channels with significantly improved $\tau_{\rm had}$ efficiencies

Variety of sizeable backgrounds: $t\bar{t}$, V+jets, VV, multijet, single Higgs, fake τ

- Estimated from simulation and data

Signal extracted from fits to multivariate discriminants

$\sigma(pp \to HH \to b\bar{b}\tau\tau) < 4.7\ (3.9) \times$SM obs. (exp.) at 95% CL

HH → bb γγ

ATLAS-CONF-2021-016

Events categorized by $m_{b\bar{b}\gamma\gamma}$ and a multivariant discriminant

Low and high $m_{b\bar{b}\gamma\gamma}$ regions sensitive to large and smaller $|\kappa_\lambda|$

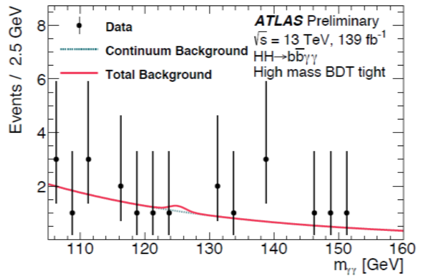

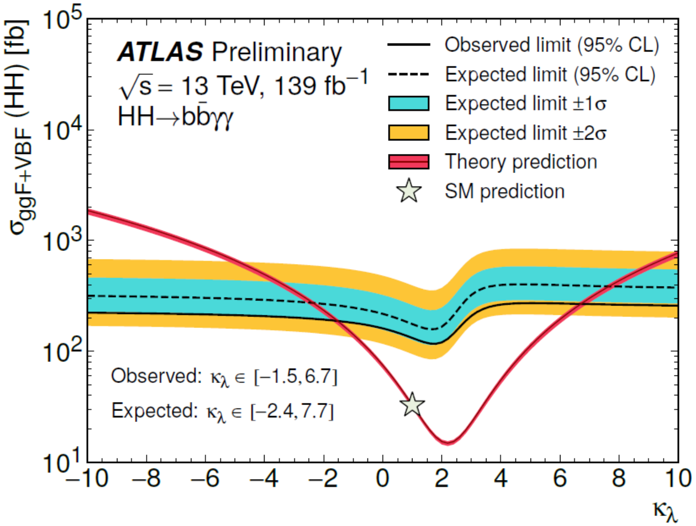

$\sigma(pp \to HH \to b\bar{b}\gamma\gamma) < 4.1\ (5.5) \times$SM obs. (exp.) at 95% CL

$-1.5 < \kappa_\lambda < 6.7$ obs.
($-2.4 < \kappa_\lambda < 7.7$ exp.) at 95% CL

- ♪ *Historical introduction , Setting the stage*
- ♪ *Results*
- ♪ ***Future of ATLAS , Run-3 , HL-LHC***
- ♪ *Conclusions*
- ♪ *Backup*

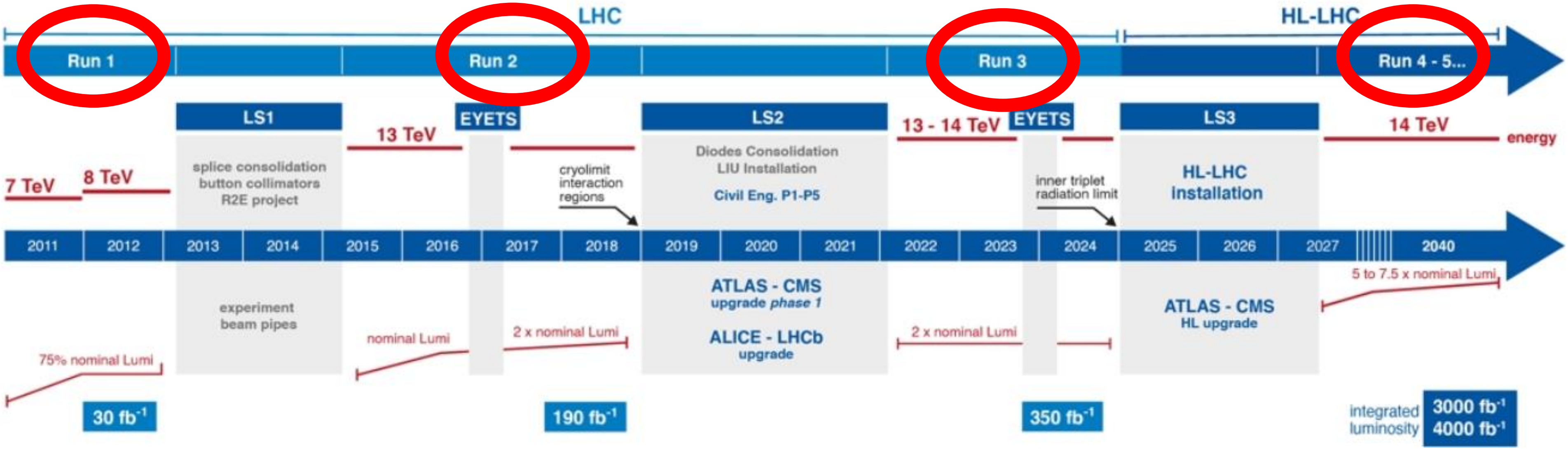

discovery
of H boson

now

Official planning above . Most probably one additional year for Run 3 and a longer delay for LS3

ATLAS Phase-I Upgrade (during LS2)

(i) Liquid Argon Calorimeter Electronics

Aim to improve the Level-1 calorimeter decision for Run 3 and beyond
(enhanced jet-rejection and pile-up subtraction)

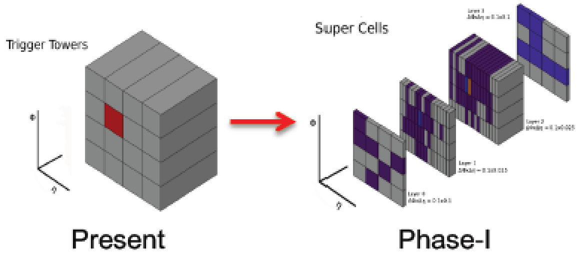

(ii) Trigger / DAQ upgrade

Take full advantage of the finer segmentation available with LAr electronics upgrade, and improved muon trigger information (NSW)

(iii) Muon System: New Small Wheel

Replacement of the inner muon stations in the endcap regions of the detector;
→ reduced muon fake trigger rate, preserve position resolution and efficiency at HL-LHC

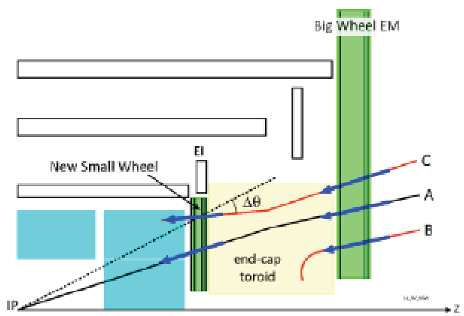

ATLAS Phase-II Upgrade (during LS3)

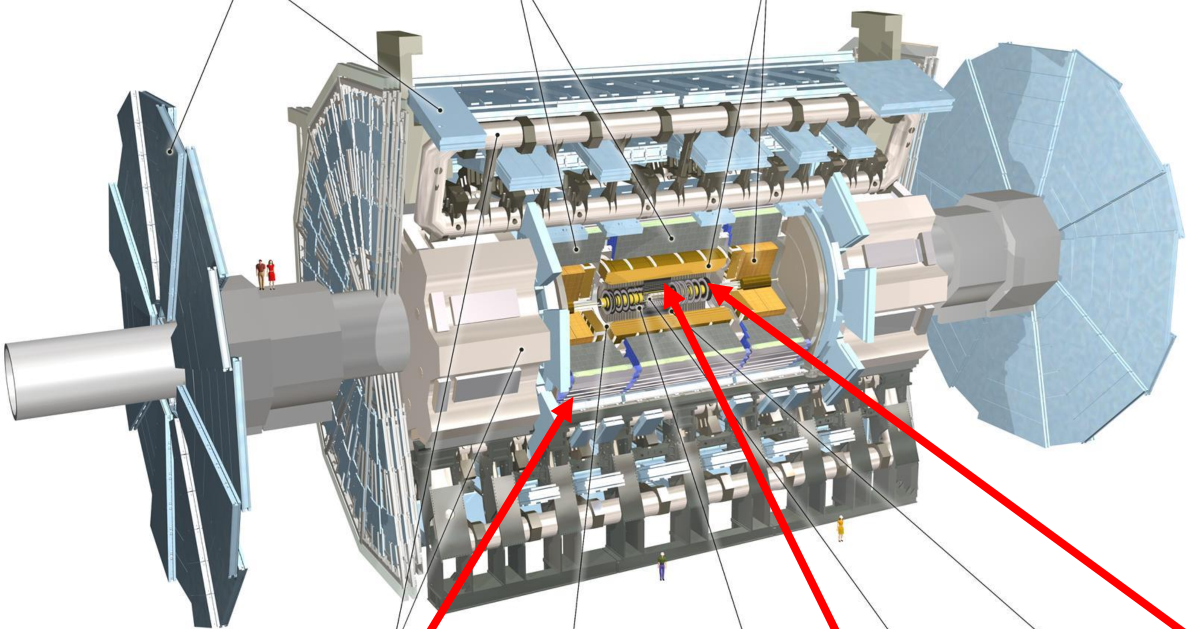

Upgraded Trigger and Data Acquisition System:

- L0: 1 MHz
- Improved High-Level Trigger

Electronics Upgrade :

- LAr Calorimeter
- Tile Calorimeter
- Muon system

New Inner Tracking Detector (all silicon tracker, up to $|\eta| = 4$)

High granularity timing detector $2.4 < |\eta| < 4$

New muon chambers in the inner barrel region

It is very hard to predict, especially the future.

N.Bohr

H

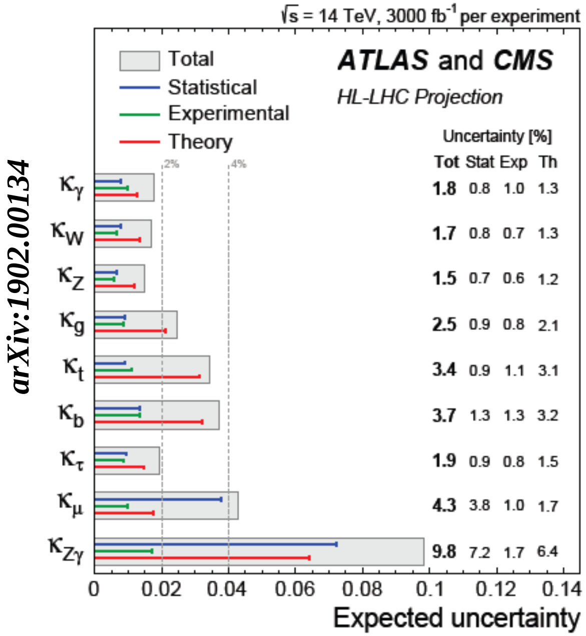

$$\kappa_j^2 = \sigma_j / \sigma_j^{\mathrm{SM}}$$

$\Delta\, m_W$

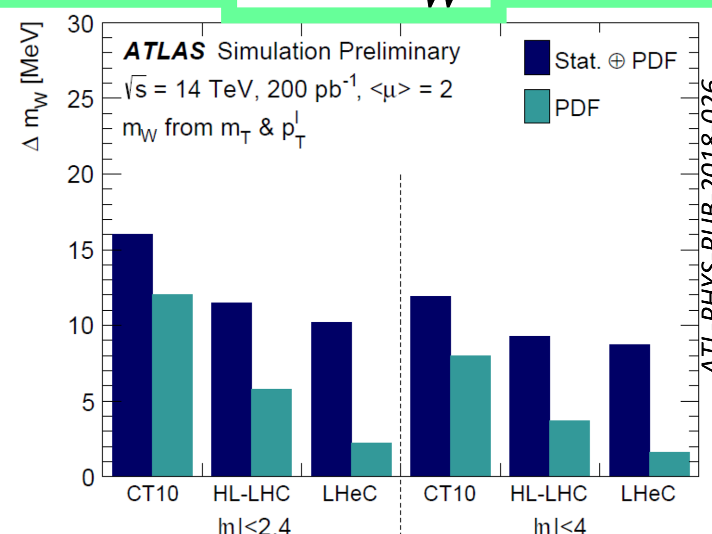

will require special runs

HH

Sensitivity to hh direct search

50% uncertainty on $\kappa_3 \equiv \frac{\lambda_3}{\lambda_3^{\mathrm{SM}}}$

self coupling normalized to SM

3000 fb^{-1}

arXiv:1905.03764

- ♪ ***Historical introduction , Setting the stage***
- ♪ ***Results***
- ♪ ***Future of ATLAS , Run-3 , HL-LHC***
- ♪ ***Conclusions***
- ♪ ***Backup***

- ***Fantastic Run-2 dataset , thanks to the outstanding performance of the LHC and ATLAS***

- ***During Run-3 emphasis on precision***

- ***< 5% of the data that will be delivered by HL-LHC***
  $\Rightarrow$ ***a lot to do !***

Thanks for your attention

Thanks to the Corfu organizers

In particular to Georges
who I met 40 years ago ..

Wait for next year and
George's fest !

- ♪ ***Historical introduction , Setting the stage***
- ♪ ***Results***
- ♪ ***Future of ATLAS , Run-3 , HL-LHC***
- ♪ ***Conclusions***
- ♪ ***Backup***

- ♪ ***Historical introduction , Setting the stage***
- ♪ ***Results***
- ♪ ***Future of ATLAS , Run-3 , HL-LHC***
- ♪ ***Conclusions***
- ♪ ***Backup***

- ♪ *Historical introduction , Setting the stage*
- ♪ ***Results***
- ♪ *Future of ATLAS , Run-3 , HL-LHC*
- ♪ *Conclusions*
- ♪ *Backup*

♪ ***Results***

- ***detector***
- ***SM (including multibosons and VBS)***
- ***BSM***
- ***(B-E)H***

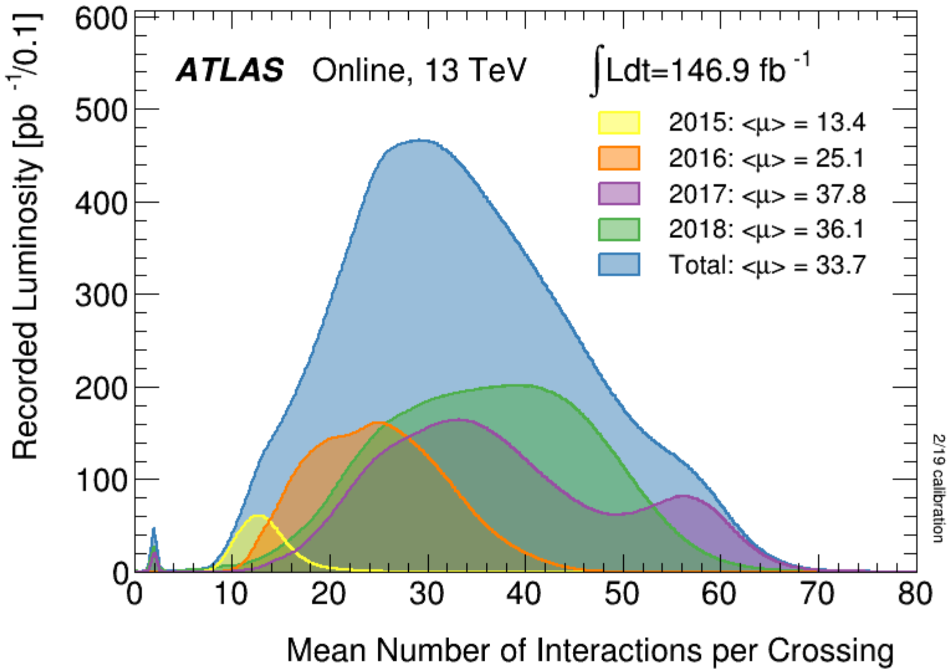

Δ t= 25 ns

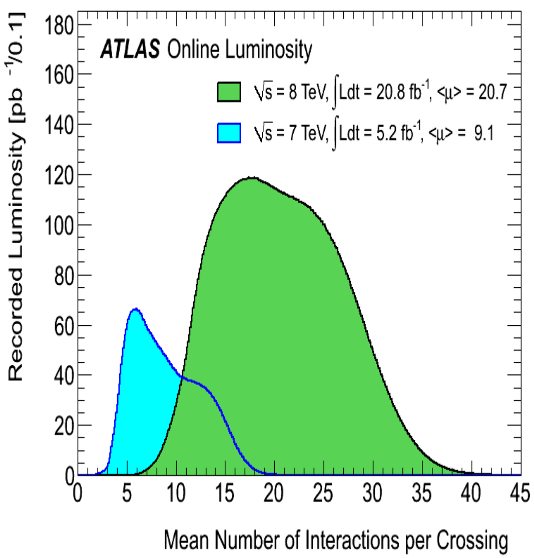

Δ t= 50 ns

***Pile up** increases at higher energy (higher luminosity + higher cross sections)*
→
Experiments have requested 25 ns** (instead of 50 ns) **operation at 13 TeV

But if the time constant is larger than 50 ns (i.e integrating time of the LAr calorimeter) then the pile-up is independent of the bunch spacing (for a given luminosity)

M. Lamont, IPAC'13

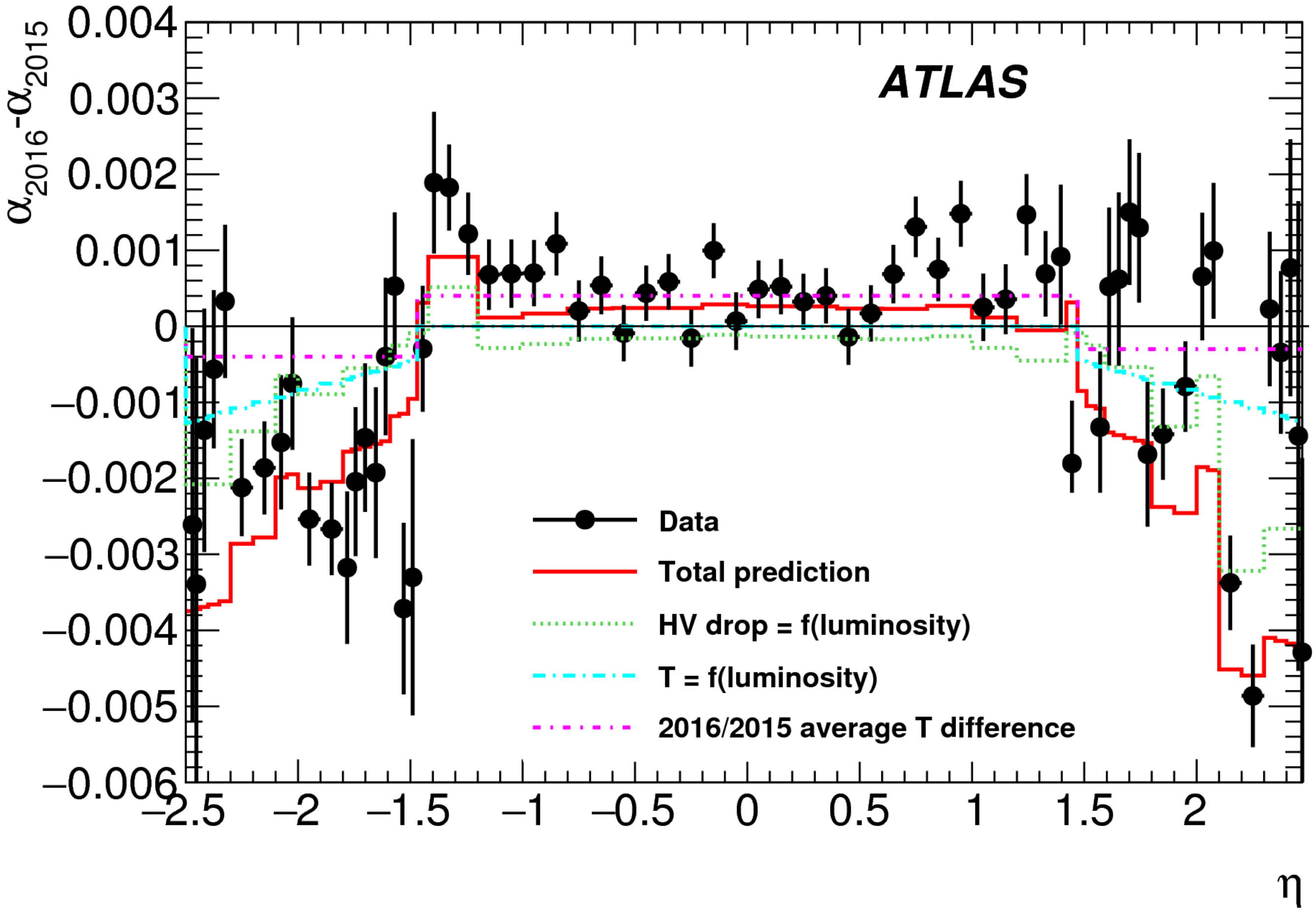

JINST 14 (2019) no.03, P03017

Comparison between the energy scale corrections derived from $Z\rightarrow ee$ events in 2015 and 2016 as a function of η. *The difference of the energy scales measured in the data are compared with predictions taking into account the luminosity-induced high-voltage reduction and LAr temperature changes as well as the small overall difference in LAr temperature between 2015 and 2016*

additional constant term c as a function of eta

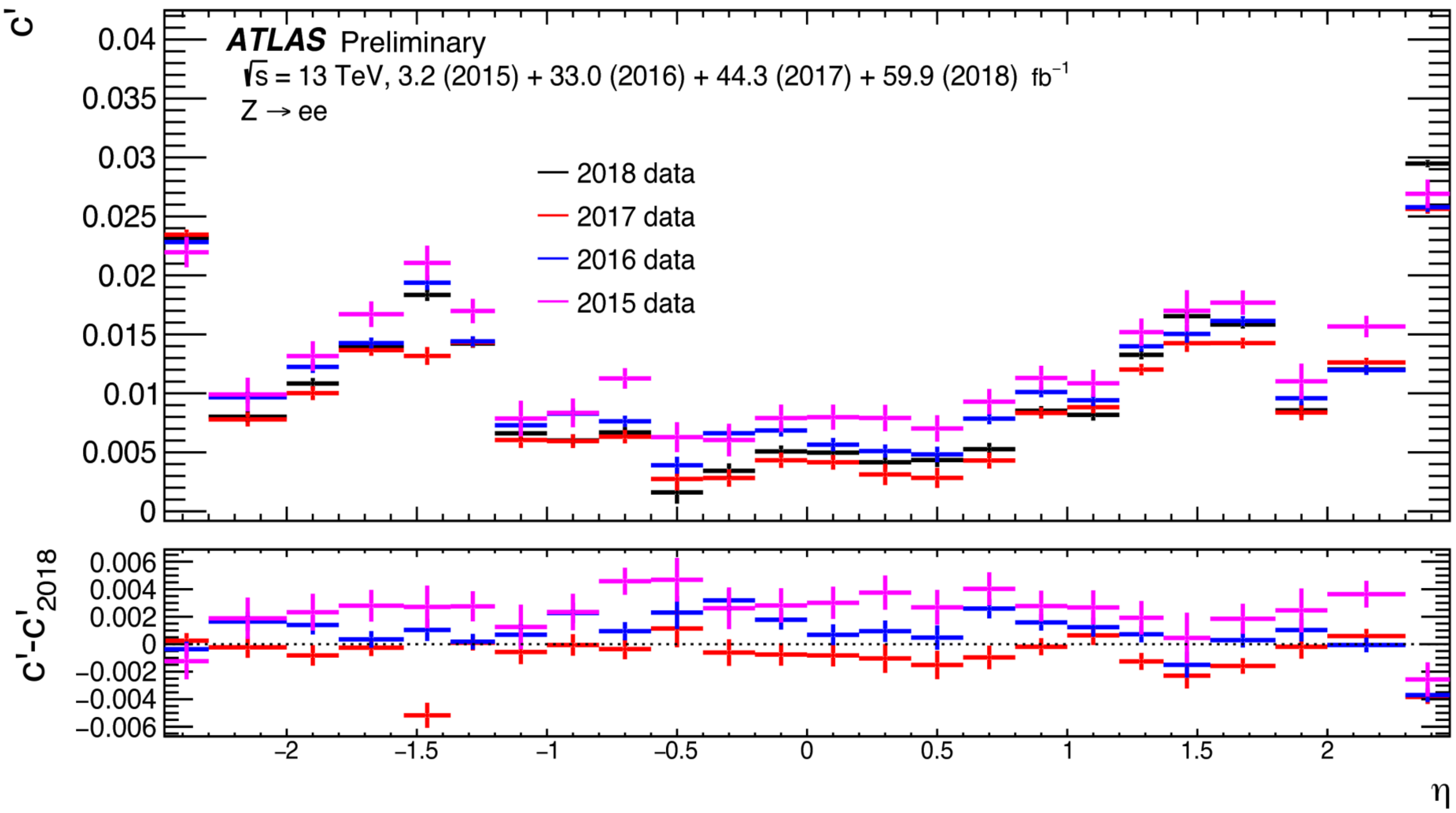

https://atlas.web.cern.ch/Atlas/GROUPS/PHYSICS/PLOTS/EGAM-2019-01/fig_02b.png

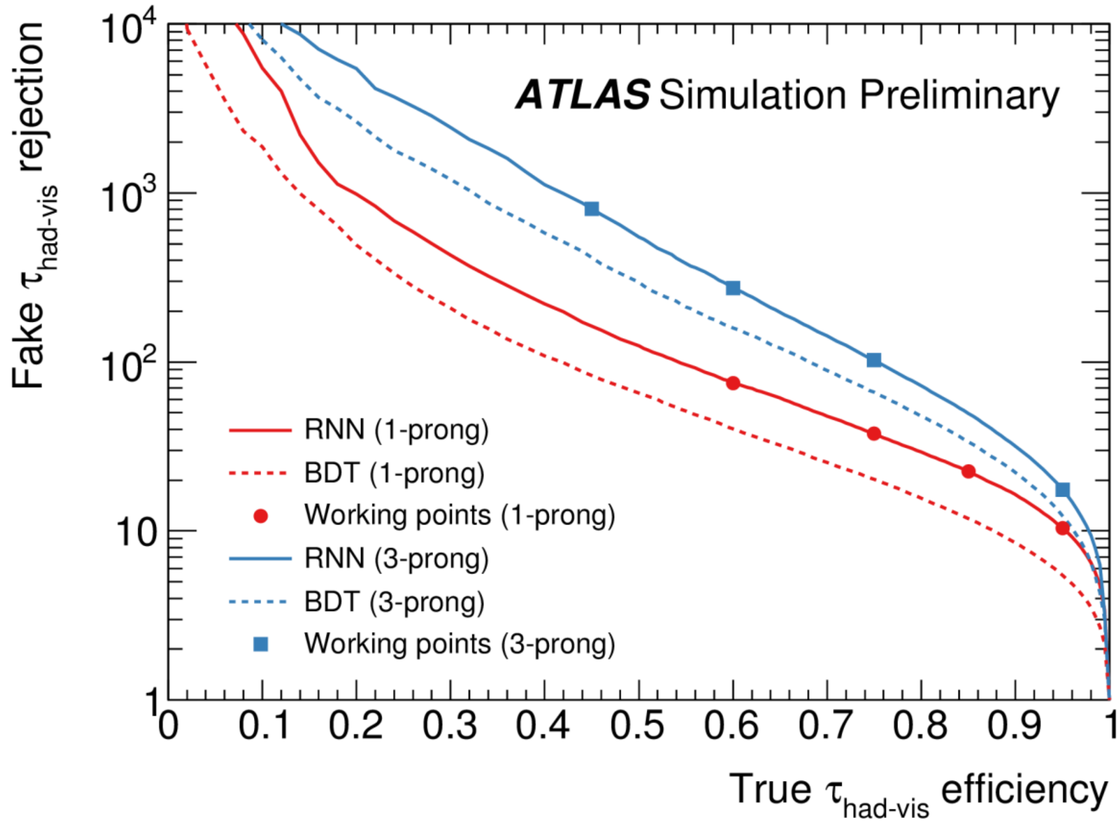

ATL-PHYS-PUB-2019-033

Figure 4: Rejection power for quark and gluon jets misidentified as $\tau_{\text{had-vis}}$ (fake $\tau_{\text{had-vis}}$) depending on the true $\tau_{\text{had-vis}}$ efficiency. Shown are the curves for 1-prong (red) and 3-prong (blue) $\tau_{\text{had-vis}}$ candidates using the RNN-based (full line) and the BDT-based (dashed line) identification algorithms. The markers indicate the four defined working points *Tight*, *Medium*, *Loose* and *Very loose* with increasing signal selection efficiencies.

♪ ***Results***

- ***detector***
- ***SM (including multibosons and VBS)***
- ***BSM***
- ***(B-E)H***

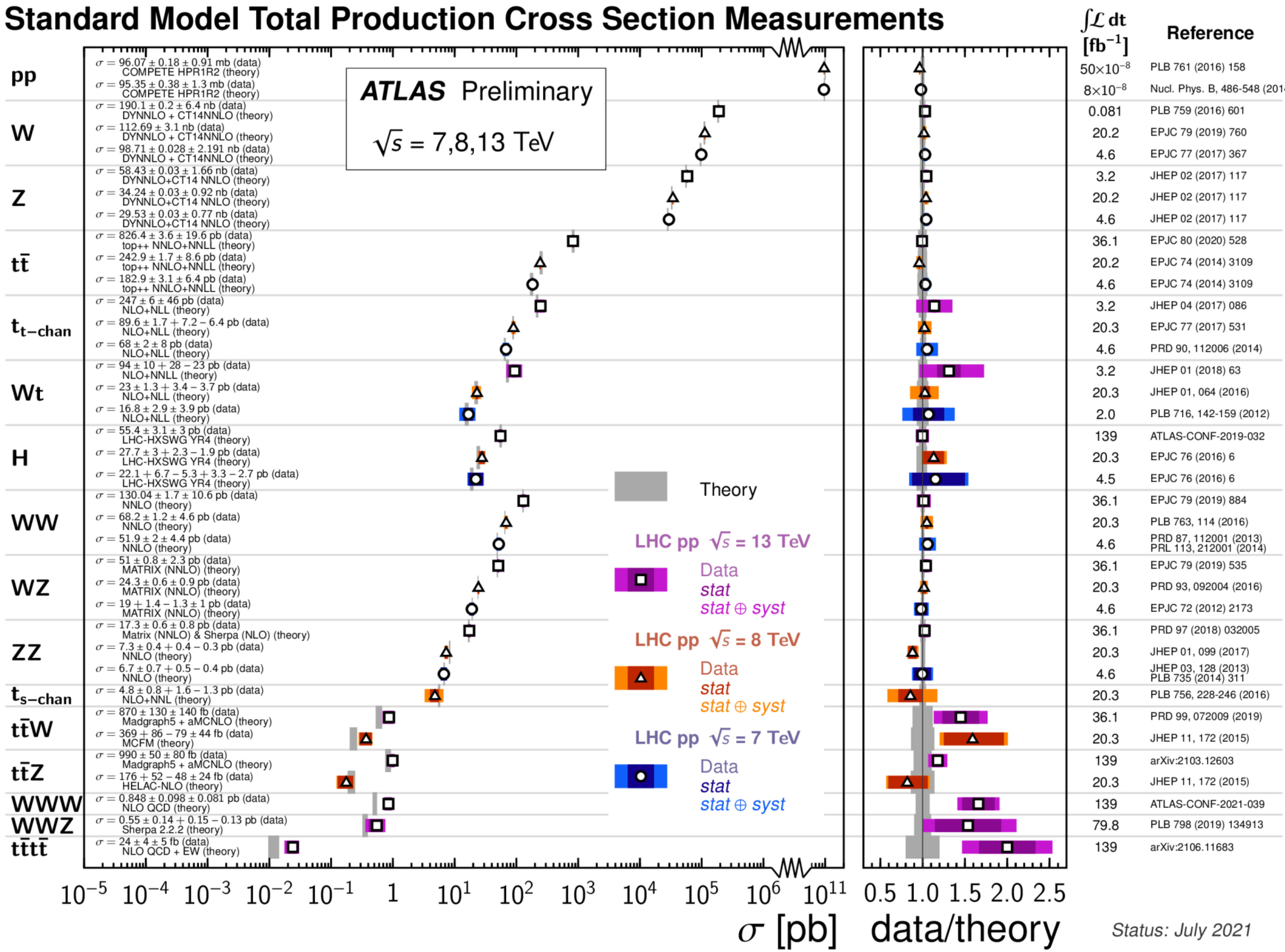
Standard Model Total Production Cross Section Measurements
ATLAS Preliminary
√s = 7,8,13 TeV
∫ℒ dt [fb⁻¹]
Reference
Status: July 2021
pp
σ = 96.07 ± 0.18 ± 0.91 mb (data) COMPETE HPR1R2 (theory) 50×10⁻⁸ PLB 761 (2016) 158
σ = 95.35 ± 0.38 ± 1.3 mb (data) COMPETE HPR1R2 (theory) 8×10⁻⁸ Nucl. Phys. B, 486-548 (2014)
W
σ = 190.1 ± 0.2 ± 6.4 nb (data) DYNNLO + CT14NNLO (theory) 0.081 PLB 759 (2016) 601
σ = 112.69 ± 3.1 nb (data) DYNNLO + CT14NNLO (theory) 20.2 EPJC 79 (2019) 760
σ = 98.71 ± 0.028 ± 2.191 nb (data) DYNNLO + CT14NNLO (theory) 4.6 EPJC 77 (2017) 367
Z
σ = 58.43 ± 0.03 ± 1.66 nb (data) DYNNLO+CT14 NNLO (theory) 3.2 JHEP 02 (2017) 117
σ = 34.24 ± 0.03 ± 0.92 nb (data) DYNNLO+CT14 NNLO (theory) 20.2 JHEP 02 (2017) 117
σ = 29.53 ± 0.03 ± 0.77 nb (data) DYNNLO+CT14 NNLO (theory) 4.6 JHEP 02 (2017) 117
tt̄
σ = 826.4 ± 3.6 ± 19.6 pb (data) top++ NNLO+NNLL (theory) 36.1 EPJC 80 (2020) 528
σ = 242.9 ± 1.7 ± 8.6 pb (data) top++ NNLO+NNLL (theory) 20.2 EPJC 74 (2014) 3109
σ = 182.9 ± 3.1 ± 6.4 pb (data) top++ NNLO+NNLL (theory) 4.6 EPJC 74 (2014) 3109
tt−chan
σ = 247 ± 6 ± 46 pb (data) NLO+NLL (theory) 3.2 JHEP 04 (2017) 086
σ = 89.6 ± 1.7 + 7.2 − 6.4 pb (data) NLO+NLL (theory) 20.3 EPJC 77 (2017) 531
σ = 68 ± 2 ± 8 pb (data) NLO+NLL (theory) 4.6 PRD 90, 112006 (2014)
Wt
σ = 94 ± 10 + 28 − 23 pb (data) NLO+NNLL (theory) 3.2 JHEP 01 (2018) 63
σ = 23 ± 1.3 + 3.4 − 3.7 pb (data) NLO+NLL (theory) 20.3 JHEP 01, 064 (2016)
σ = 16.8 ± 2.9 ± 3.9 pb (data) NLO+NLL (theory) 2.0 PLB 716, 142-159 (2012)
H
σ = 55.4 ± 3.1 ± 3 pb (data) LHC-HXSWG YR4 (theory) 139 ATLAS-CONF-2019-032
σ = 27.7 ± 3 + 2.3 − 1.9 pb (data) LHC-HXSWG YR4 (theory) 20.3 EPJC 76 (2016) 6
σ = 22.1 + 6.7 − 5.3 + 3.3 − 2.7 pb (data) LHC-HXSWG YR4 (theory) 4.5 EPJC 76 (2016) 6
WW
σ = 130.04 ± 1.7 ± 10.6 pb (data) NNLO (theory) 36.1 EPJC 79 (2019) 884
σ = 68.2 ± 1.2 ± 4.6 pb (data) NNLO (theory) 20.3 PLB 763, 114 (2016)
σ = 51.9 ± 2 ± 4.4 pb (data) NNLO (theory) 4.6 PRD 87, 112001 (2013) PRL 113, 212001 (2014)
WZ
σ = 51 ± 0.8 ± 2.3 pb (data) MATRIX (NNLO) (theory) 36.1 EPJC 79 (2019) 535
σ = 24.3 ± 0.6 ± 0.9 pb (data) MATRIX (NNLO) (theory) 20.3 PRD 93, 092004 (2016)
σ = 19 + 1.4 − 1.3 ± 1 pb (data) MATRIX (NNLO) (theory) 4.6 EPJC 72 (2012) 2173
ZZ
σ = 17.3 ± 0.6 ± 0.8 pb (data) Matrix (NNLO) & Sherpa (NLO) (theory) 36.1 PRD 97 (2018) 032005
σ = 7.3 ± 0.4 + 0.4 − 0.3 pb (data) NNLO (theory) 20.3 JHEP 01, 099 (2017)
σ = 6.7 ± 0.7 + 0.5 − 0.4 pb (data) NNLO (theory) 4.6 JHEP 03, 128 (2013) PLB 735 (2014) 311
ts−chan
σ = 4.8 ± 0.8 + 1.6 − 1.3 pb (data) NLO+NNL (theory) 20.3 PLB 756, 228-246 (2016)
tt̄W
σ = 870 ± 130 ± 140 fb (data) Madgraph5 + aMCNLO (theory) 36.1 PRD 99, 072009 (2019)
σ = 369 + 86 − 79 ± 44 fb (data) MCFM (theory) 20.3 JHEP 11, 172 (2015)
tt̄Z
σ = 990 ± 50 ± 80 fb (data) Madgraph5 + aMCNLO (theory) 139 arXiv:2103.12603
σ = 176 + 52 − 48 ± 24 fb (data) HELAC-NLO (theory) 20.3 JHEP 11, 172 (2015)
WWW
σ = 0.848 ± 0.098 ± 0.081 pb (data) NLO QCD (theory) 139 ATLAS-CONF-2021-039
WWZ
σ = 0.55 ± 0.14 + 0.15 − 0.13 pb (data) Sherpa 2.2.2 (theory) 79.8 PLB 798 (2019) 134913
tt̄tt̄
σ = 24 ± 4 ± 5 fb (data) NLO QCD + EW (theory) 139 arXiv:2106.11683
Theory
LHC pp √s = 13 TeV
Data
stat
stat ⊕ syst
LHC pp √s = 8 TeV
Data
stat
stat ⊕ syst
LHC pp √s = 7 TeV
Data
stat
stat ⊕ syst
10⁻⁵ 10⁻⁴ 10⁻³ 10⁻² 10⁻¹ 1 10¹ 10² 10³ 10⁴ 10⁵ 10⁶ 10¹¹
σ [pb]
0.5 1.0 1.5 2.0 2.5
data/theory

Standard Model Production Cross Section Measurements

Status: July 2021

ATLAS Preliminary

$\sqrt{s}$ = 5, 7, 8, 13 TeV

Model	E_{CM} [TeV]	$\int\mathcal{L}\,dt[fb^{-1}]$	Measurement	Theory	Reference
pp	8	50×10^{-8}	$\sigma = 96.07 \pm 0.18 \pm 0.91$ mb	$\sigma = 99.55 \pm 2.14$ mb (COMPETE HPR1R2)	PLB 761 (2016) 158
pp	7	8×10^{-8}	$\sigma = 95.35 \pm 0.38 \pm 1.3$ mb	$\sigma = 97.26 \pm 2.12$ mb (COMPETE HPR1R2)	Nucl. Phys. B, 486-548 (2014)
W	13	0.081	$\sigma = 190.1 \pm 0.2 \pm 6.4$ nb	$\sigma = 184.9 + 6 - 6.1$ nb (DYNNLO + CT14NNLO)	PLB 759 (2016) 601
W	8	20.2	$\sigma = 112.69 \pm 3.1$ nb	$\sigma = 110.919889503 \pm 3.7$ nb (DYNNLO + CT14NNLO)	EPJC 79 (2019) 760
W	7	4.6	$\sigma = 98.71 \pm 0.028 \pm 2.191$ nb	$\sigma = 95.9 \pm 2.9$ nb (DYNNLO + CT14NNLO)	EPJC 77 (2017) 367
Z	13	3.2	$\sigma = 58.43 \pm 0.03 \pm 1.66$ nb	$\sigma = 55.96 + 1.5 - 1.7$ nb (DYNNLO+CT14 NNLO)	JHEP 02 (2017) 117
Z	8	20.2	$\sigma = 34.24 \pm 0.03 \pm 0.92$ nb	$\sigma = 32.94 + 0.8 - 0.92$ nb (DYNNLO+CT14 NNLO)	JHEP 02 (2017) 117
Z	7	4.6	$\sigma = 29.53 \pm 0.03 \pm 0.77$ nb	$\sigma = 28.31 + 0.68 - 0.8$ nb (DYNNLO+CT14 NNLO)	JHEP 02 (2017) 117
$t\bar{t}$	13	36.1	$\sigma = 826.4 \pm 3.6 \pm 19.6$ pb	$\sigma = 832 + 40 - 45$ pb (top++ NNLO+NNLL)	EPJC 80 (2020) 528
$t\bar{t}$	8	20.2	$\sigma = 242.9 \pm 1.7 \pm 8.6$ pb	$\sigma = 252.9 + 13.3 - 14.5$ pb (top++ NNLO+NNLL)	EPJC 74 (2014) 3109
$t\bar{t}$	7	4.6	$\sigma = 182.9 \pm 3.1 \pm 6.4$ pb	$\sigma = 177 + 10 - 11$ pb (top++ NNLO+NNLL)	EPJC 74 (2014) 3109
t_{t-chan}	13	3.2	$\sigma = 247 \pm 6 \pm 46$ pb	$\sigma = 217 \pm 10$ pb (NLO+NLL)	JHEP 04 (2017) 086
t_{t-chan}	8	20.3	$\sigma = 89.6 \pm 1.7 + 7.2 - 6.4$ pb	$\sigma = 87.8 + 3.4 - 1.9$ pb (NLO+NLL)	EPJC 77 (2017) 531
t_{t-chan}	7	4.6	$\sigma = 68 \pm 2 \pm 8$ pb	$\sigma = 64.6 + 2.7 - 2$ pb (NLO+NLL)	PRD 90, 112006 (2014)
Wt	13	3.2	$\sigma = 94 \pm 10 + 28 - 23$ pb	$\sigma = 71.7 \pm 3.9$ pb (NLO+NNLL)	JHEP 01 (2018) 63
Wt	8	20.3	$\sigma = 23 \pm 1.3 + 3.4 - 3.7$ pb	$\sigma = 22.4 \pm 1.5$ pb (NLO+NLL)	JHEP 01, 064 (2016)
Wt	7	2.0	$\sigma = 16.8 \pm 2.9 \pm 3.9$ pb	$\sigma = 15.7 \pm 1.1$ pb (NLO+NLL)	PLB 716, 142-159 (2012)
H	13	139	$\sigma = 55.4 \pm 3.1 \pm 3$ pb	$\sigma = 55.6 \pm 2.5$ pb (LHC-HXSWG YR4)	ATLAS-CONF-2019-032
H	8	20.3	$\sigma = 27.7 \pm 3 + 2.3 - 1.9$ pb	$\sigma = 24.5 + 1.3 - 1.8$ pb (LHC-HXSWG YR4)	EPJC 76 (2016) 6
H	7	4.5	$\sigma = 22.1 + 6.7 - 5.3 + 3.3 - 2.7$ pb	$\sigma = 19.2 + 1 - 1.4$ pb (LHC-HXSWG YR4)	EPJC 76 (2016) 6
H VBF, $\|y_H\| < 2.5$	13	139	$\sigma = 4 \pm 0.5 \pm 0.4$ pb	$\sigma = 3.51 + 0.08 - 0.07$ pb (LHC-HXSWG)	ATLAS-CONF-2020-027
H VBF	8	20.3	$\sigma = 2.43 + 0.5 - 0.49 + 0.33 - 0.26$ pb	$\sigma = 1.6 \pm 0.04$ pb (LHC-HXSWG YR4)	EPJC 76 (2016) 6
VH	8	20.3	$\sigma = 1.03 + 0.37 - 0.36 + 0.26 - 0.21$ pb	$\sigma = 1.12 \pm 0.03$ pb (NNLO(QCD)+NLO(EW))	JHEP 12 (2017) 024
WH, $\|y_H\| < 2.5$	13	139	$\sigma = 1.45 + 0.2 - 0.19 + 0.18 - 0.17$ pb	$\sigma = 1.204 \pm 0.024$ pb (Powheg Box NLO(QCD))	ATLAS-CONF-2020-027
ZH, $\|y_H\| < 2.5$	13	139	$\sigma = 0.78 \pm 0.13 + 0.12 - 0.1$ pb	$\sigma = 0.797 + 0.033 - 0.026$ pb (Powheg Box NLO(QCD))	ATLAS-CONF-2020-027
$t\bar{t}H$	13	139	$\sigma = 640 \pm 90 \pm 80$ fb	$\sigma = 590 + 30 - 50$ fb (LHCHXSWG NLO QCD + NLO EW)	ATLAS-CONF-2020-027
$t\bar{t}H$	8	20.3	$\sigma = 220 \pm 100 \pm 70$ fb	$\sigma = 133 + 8 - 13$ fb (LHCHXSWG NLO QCD + NLO EW)	PLB 784 (2018) 173
WW	13	36.1	$\sigma = 130.04 \pm 1.7 \pm 10.6$ pb	$\sigma = 128.4 + 3.2 - 2.9$ pb (NNLO)	EPJC 79 (2019) 884
WW	8	20.3	$\sigma = 68.2 \pm 1.2 \pm 4.6$ pb	$\sigma = 65 + 1.2 - 1.1$ pb (NNLO)	PLB 763, 114 (2016)
WW	7	4.6	$\sigma = 51.9 \pm 2 \pm 4.4$ pb	$\sigma = 49.04 + 1.03 - 0.88$ pb (NNLO)	PRD 87, 112001 (2013), PRL 113, 212001 (2014)
WZ	13	36.1	$\sigma = 51 \pm 0.8 \pm 2.3$ pb	$\sigma = 49.1 + 1.1 - 1$ pb (MATRIX (NNLO))	EPJC 79 (2019) 535
WZ	8	20.3	$\sigma = 24.3 \pm 0.6 \pm 0.9$ pb	$\sigma = 23.92 \pm 0.4$ pb (MATRIX (NNLO))	PRD 93, 092004 (2016)
WZ	7	4.6	$\sigma = 19 + 1.4 - 1.3 \pm 1$ pb	$\sigma = 19.34 + 0.3 - 0.4$ pb (MATRIX (NNLO))	EPJC 72 (2012) 2173
ZZ	13	36.1	$\sigma = 17.3 \pm 0.6 \pm 0.8$ pb	$\sigma = 16.9 + 0.6 - 0.5$ pb (Matrix (NNLO) & Sherpa (NLO))	PRD 97 (2018) 032005
ZZ	8	20.3	$\sigma = 7.3 \pm 0.4 + 0.4 - 0.3$ pb	$\sigma = 8.284 + 0.249 - 0.191$ pb (NNLO)	JHEP 01, 099 (2017)
ZZ	7	4.6	$\sigma = 6.7 \pm 0.7 + 0.5 - 0.4$ pb	$\sigma = 6.735 + 0.195 - 0.155$ pb (NNLO)	JHEP 03, 128 (2013), PLB 735 (2014) 311
t_{s-chan}	8	20.3	$\sigma = 4.8 \pm 0.8 + 1.6 - 1.3$ pb	$\sigma = 5.61 \pm 0.22$ pb (NLO+NNL)	PLB 756, 228-246 (2016)
$t\bar{t}W$	13	36.1	$\sigma = 870 \pm 130 \pm 140$ fb	$\sigma = 600 \pm 72$ fb (Madgraph5 + aMCNLO)	PRD 99, 072009 (2019)
$t\bar{t}W$	8	20.3	$\sigma = 369 + 86 - 79 \pm 44$ fb	$\sigma = 232 \pm 32$ fb (MCFM)	JHEP 11, 172 (2015)
$t\bar{t}Z$	13	139	$\sigma = 990 \pm 50 \pm 80$ fb	$\sigma = 840 \pm 90$ fb (Madgraph5 + aMCNLO)	arXiv:2103.12603
$t\bar{t}Z$	8	20.3	$\sigma = 176 + 52 - 48 \pm 24$ fb	$\sigma = 215 \pm 30$ fb (HELAC-NLO)	JHEP 11, 172 (2015)
WWW	13	139	$\sigma = 0.848 \pm 0.098 \pm 0.081$ pb	$\sigma = 0.511 \pm 0.042$ pb (NLO QCD)	ATLAS-CONF-2021-039
WWZ	13	79.8	$\sigma = 0.55 \pm 0.14 + 0.15 - 0.13$ pb	$\sigma = 0.358 \pm 0.036$ pb (Sherpa 2.2.2)	PLB 798 (2019) 134913
$t\bar{t}t\bar{t}$	13	139	$\sigma = 24 \pm 4 \pm 5$ fb	$\sigma = 12 \pm 2.4$ fb (NLO QCD + EW)	arXiv:2106.11683

Standard Model Production Cross Section Measurements

Status: July 2021

ATLAS Preliminary

$\sqrt{s}$ = 5, 7, 8, 13 TeV

Model	E_{CM} [TeV]	$\int\mathcal{L}\,dt[fb^{-1}]$	Measurement	Theory	Reference
pp	8	50×10^{-8}	$\sigma = 96.07 \pm 0.18 \pm 0.91$ mb	$\sigma = 99.55 \pm 2.14$ mb (COMPETE HPR1R2)	PLB 761 (2016) 158
pp	7	8×10^{-8}	$\sigma = 95.35 \pm 0.38 \pm 1.3$ mb	$\sigma = 97.26 \pm 2.12$ mb (COMPETE HPR1R2)	Nucl. Phys. B, 486-548 (2014)
pp inelastic	13	6×10^{-8}	$\sigma = 79.3 \pm 2.9$ mb	$\sigma = 78.4 \pm 2$ mb (Schuler/Sjöstrand)	PRL 117, 182002 (2016)
pp inelastic	8	50×10^{-8}	$\sigma = 71.73 \pm 0.15 \pm 0.69$ mb	$\sigma = 73 \pm 2$ mb (Schuler/Sjöstrand)	PLB 761 (2016) 158
pp inelastic	7	8×10^{-8}	$\sigma = 71.34 \pm 0.36 \pm 0.83$ mb	$\sigma = 71.5 + 20 - 2$ mb (Schuler/Sjöstrand)	Nucl. Phys. B, 486-548 (2014)
Incl. jet **R**=0.4, **|y| < 3.0**	13	3.2	$\sigma = 1845 \pm 4 + 119 - 120$ nb	$\sigma = 1997 + 152 - 208$ nb (NLOJet++, CT14)	JHEP 09 (2017) 020
Incl. jet **R**=0.4, **|y| < 3.0**	8	20.2	$\sigma = 726.4 \pm 1.1 + 42.7 - 41.8$ nb	$\sigma = 800 + 59 - 100$ nb (NLOJet++, CT14)	JHEP 09 (2017) 020
Incl. jet **R**=0.4, **|y| < 3.0**	7	4.5	$\sigma = 563.9 \pm 1.5 + 55.4 - 51.4$ nb	$\sigma = 569.8 + 29.5 - 46.3$ nb (NLOJet++, CT10)	JHEP 02, 153 (2015)
Dijet **R**=0.4, **|y| < 3.0, y* < 3.0**	13	3.2	$\sigma = 321 \pm 0.8 + 18.6 - 19$ nb	$\sigma = 340 + 17 - 54$ nb (NLOJet++, CT14)	JHEP 09 (2017) 020
Dijet **R**=0.4, **|y| < 3.0, y* < 3.0**	7	4.5	$\sigma = 86.87 \pm 0.26 + 7.56 - 7.2$ nb	$\sigma = 86.9 + 4.7 - 12.4$ nb (NLOJet++, CT10)	JHEP 05, 059 (2014)
γ	13	3.2	$\sigma = 399 \pm 0.4 \pm 16$ pb	$\sigma = 352 + 36 - 30$ pb (JETPHOX+MMHT2014 (NLO))	PLB 2017 04 072
γ	8	20.2	$\sigma = 56.8 \pm 0.1 + 5.8 - 5.6$ nb	$\sigma = 52.2 \pm 7$ nb (PETER (NLO+N^3LL))	JHEP 06 (2016) 005
γ	7	4.6	$\sigma = 359 \pm 3 + 22 - 16$ pb	$\sigma = 308 \pm 40$ pb (JETPHOX (NLO))	PRD 89, 052004 (2014)
γ [njet ≥ 1]	13	3.2	$\sigma = 300 \pm 0.4 \pm 12$ pb	$\sigma = 319 + 55 - 46$ pb (SHERPA (NLO))	PLB 780 (2018) 578
γ [njet ≥ 1]	8	20.2	$\sigma = 134 \pm 0.1 \pm 4$ pb	$\sigma = 128 + 11 - 9$ pb (JETPHOX (NLO))	Nucl. Phys. B, 918 (2017) 257
γ [njet ≥ 2]	8	20.2	$\sigma = 30.4 \pm 0.04 \pm 1.8$ pb	$\sigma = 29.2 + 2.8 - 2.7$ pb (NLOBlackhat+CT10)	Nucl. Phys. B, 918 (2017) 257
γ [njet ≥ 3]	8	20.2	$\sigma = 8.7 \pm 0.02 \pm 0.8$ pb	$\sigma = 9.5 + 0.9 - 1.2$ pb (NLOBlackhat+CT10)	Nucl. Phys. B, 918 (2017) 257
$\sigma^{fid}(W \to e\nu, \mu\nu)$	13	0.081	$\sigma = 8.03 \pm 0.01 \pm 0.23$ nb	$\sigma = 7.82 + 0.26 - 0.3$ nb (DYNNLO + CT14NNLO)	PLB 759 (2016) 601
$\sigma^{fid}(W \to e\nu, \mu\nu)$	8	20.2	$\sigma = 5247 \pm 0.6 \pm 111$ pb	$\sigma = 5120 \pm 142$ pb (DYNNLO + CT14NNLO)	EPJC 79 (2019) 760
$\sigma^{fid}(W \to e\nu, \mu\nu)$	7	4.6	$\sigma = 4.911 \pm 0.001 \pm 0.092$ nb	$\sigma = 4.777 + 0.12 - 0.14$ nb (DYNNLO + CT14NNLO)	EPJC 77 (2017) 367
$\sigma^{fid}(W \to e\nu, \mu\nu)$	5	0.025	$\sigma = 3.667 \pm 0.016 \pm 0.084$ nb	$\sigma = 3.58 \pm 0.11$ nb (DYNNLO + CT14NNLO)	EPJC 79 (2019) 128
W [njet ≥ 1]	8	20.2	$\sigma = 564.71 \pm 0.24 \pm 72.13$ pb	$\sigma = 584 + 8 - 37$ pb (Sherpa 2.2.1 NLO)	JHEP 05 (2018) 077
W [njet ≥ 1]	7	4.6	$\sigma = 493.8 \pm 0.5 \pm 45.1$ pb	$\sigma = 474.22 \pm 0.84$ pb (Blackhat)	EPJC 75 (2015) 82
W [njet ≥ 2]	8	20.2	$\sigma = 128.35 \pm 0.12 \pm 20.39$ pb	$\sigma = 126.5 + 2.1 - 14.4$ pb (Sherpa 2.2.1 NLO)	JHEP 05 (2018) 077
W [njet ≥ 2]	7	4.6	$\sigma = 111.7 \pm 0.2 \pm 12.2$ pb	$\sigma = 111.98 \pm 0.44$ pb (Blackhat)	EPJC 75 (2015) 82
W [njet ≥ 3]	8	20.2	$\sigma = 26.38 \pm 0.06 \pm 5.34$ pb	$\sigma = 23.6 + 1.3 - 5$ pb (Sherpa 2.2.1 NLO)	JHEP 05 (2018) 077
W [njet ≥ 3]	7	4.6	$\sigma = 21.82 \pm 0.1 \pm 3.23$ pb	$\sigma = 23.47 \pm 0.22$ pb (Blackhat)	EPJC 75 (2015) 82
W [njet ≥ 4]	8	20.2	$\sigma = 5.47 \pm 0.03 \pm 1.47$ pb	$\sigma = 5 + 0.5 - 1.4$ pb (Sherpa 2.2.1 NLO)	JHEP 05 (2018) 077
W [njet ≥ 4]	7	4.6	$\sigma = 4.241 \pm 0.056 \pm 0.885$ pb	$\sigma = 4.67 \pm 0.06$ pb (Blackhat)	EPJC 75 (2015) 82
W [njet ≥ 5]	8	20.2	$\sigma = 1.107 \pm 0.013 \pm 0.423$ pb	$\sigma = 1.1 + 0.13 - 0.38$ pb (Sherpa 2.2.1 NLO)	JHEP 05 (2018) 077
W [njet ≥ 5]	7	4.6	$\sigma = 0.877 \pm 0.032 \pm 0.301$ pb	$\sigma = 0.933 \pm 0.027$ pb (Blackhat)	EPJC 75 (2015) 82
W [njet ≥ 6]	8	20.2	$\sigma = 0.22 \pm 0.006 \pm 0.121$ pb	$\sigma = 0.239 + 0.03 - 0.084$ pb (Sherpa 2.2.1 NLO)	JHEP 05 (2018) 077
W [njet ≥ 6]	7	4.6	$\sigma = 0.199 \pm 0.019 \pm 0.11$ pb		EPJC 75 (2015) 82
W [njet ≥ 7]	8	20.2	$\sigma = 0.041 \pm 0.003 \pm 0.032$ pb	$\sigma = 0.052 + 0.007 - 0.02$ pb (Sherpa 2.2.1 NLO)	JHEP 05 (2018) 077
W [njet ≥ 7]	7	4.6	$\sigma = 0.041 \pm 0.0068 \pm 0.031$ pb		EPJC 75 (2015) 82
$\sigma^{fid}(Z \to ee, \mu\mu)$	13	3.2	$\sigma = 776 \pm 1 \pm 18$ pb	$\sigma = 744 + 22 - 28$ pb (DYNNLO+CT14 NNLO)	JHEP 02 (2017) 117
$\sigma^{fid}(Z \to ee, \mu\mu)$	8	20.2	$\sigma = 506 \pm 0.2 \pm 11$ pb	$\sigma = 486 + 13.6 - 16$ pb (DYNNLO+CT14 NNLO)	JHEP 02 (2017) 117
$\sigma^{fid}(Z \to ee, \mu\mu)$	7	4.6	$\sigma = 451 \pm 0.4 \pm 8.8$ pb	$\sigma = 432 + 12.5 - 13.8$ pb (DYNNLO+CT14 NNLO)	JHEP 02 (2017) 117
$\sigma^{fid}(Z \to ee, \mu\mu)$	5	0.025	$\sigma = 374.5 \pm 3.4 \pm 7.9$ pb	$\sigma = 356 + 9 - 10$ pb (DYNNLO + CT14NNLO)	EPJC 79 (2019) 128
Z [njet = 1]	13	139	$\sigma = 11.84 \pm 0.0081 \pm 0.57$ pb	$\sigma = 11.17 + 2.2 - 1.3$ pb (Sherpa (NLO QCD+ NLO EW corr))	ATLAS-CONF-2021-033
Z [njet ≥ 1]	7	4.6	$\sigma = 68.84 \pm 0.13 \pm 5.15$ pb	$\sigma = 64.8 \pm 3.1$ pb (Blackhat)	JHEP 07, 032 (2013)
Z [njet = 2]	13	139	$\sigma = 1.97 \pm 0.0039 \pm 0.098$ pb	$\sigma = 1.807 + 0.69 - 0.39$ pb (Sherpa (NLO QCD+ NLO EW corr))	ATLAS-CONF-2021-033
Z [njet ≥ 2]	7	4.6	$\sigma = 15.05 \pm 0.06 \pm 1.51$ pb	$\sigma = 14.9 \pm 0.4$ pb (Blackhat)	JHEP 07, 032 (2013)
Z [njet = 3]	13	139	$\sigma = 0.201 \pm 0.0014 \pm 0.015$ pb	$\sigma = 0.186 + 0.11 - 0.058$ pb (Sherpa (NLO QCD+ NLO EW corr))	ATLAS-CONF-2021-033
Z [njet ≥ 3]	7	4.6	$\sigma = 3.09 \pm 0.03 \pm 0.4$ pb	$\sigma = 3.1 \pm 0.14$ pb (Blackhat)	JHEP 07, 032 (2013)
Z [njet = 4]	13	139	$\sigma = 0.0227 \pm 0.00044 \pm 0.0023$ pb	$\sigma = 0.0234 + 0.015 - 0.0083$ pb (Sherpa (NLO QCD+ NLO EW corr))	ATLAS-CONF-2021-033
Z [njet ≥ 4]	7	4.6	$\sigma = 0.65 \pm 0.01 \pm 0.11$ pb	$\sigma = 0.646 \pm 0.031$ pb (Blackhat)	JHEP 07, 032 (2013)
Z [njet = 5]	13	139	$\sigma = 0.0028 \pm 0.00015 \pm 0.00031$ pb	$\sigma = 0.00326 + 0.0022 - 0.0012$ pb (Sherpa (NLO QCD+ NLO EW corr))	ATLAS-CONF-2021-033
Z [njet ≥ 5]	7	4.6	$\sigma = 0.135 \pm 0.006 \pm 0.027$ pb		JHEP 07, 032 (2013)
Z [njet ≥ 6]	13	139	$\sigma = 0.000338 \pm 5.3e-05 \pm 5.5e-05$ pb	$\sigma = 0.000511 + 0.00034 - 0.00019$ pb (Sherpa (NLO QCD+ NLO EW corr))	ATLAS-CONF-2021-033
Z [njet ≥ 6]	7	4.6	$\sigma = 0.0253 \pm 0.00265 \pm 0.00595$ pb		JHEP 07, 032 (2013)
Z [njet ≥ 7]	7	4.6	$\sigma = 0.0062 \pm 0.001456 \pm 0.00214$ pb		JHEP 07, 032 (2013)
$t\bar{t}$	13	36.1	$\sigma = 826.4 \pm 3.6 \pm 19.6$ pb	$\sigma = 832 + 40 - 45$ pb (top++ NNLO+NNLL)	EPJC 80 (2020) 528
$t\bar{t}$	8	20.2	$\sigma = 242.9 \pm 1.7 \pm 8.6$ pb	$\sigma = 252.9 + 13.3 - 14.5$ pb (top++ NNLO+NNLL)	EPJC 74 (2014) 3109
$t\bar{t}$	7	4.6	$\sigma = 182.9 \pm 3.1 \pm 6.4$ pb	$\sigma = 177 + 10 - 11$ pb (top++ NNLO+NNLL)	EPJC 74 (2014) 3109
$t\bar{t}$	5	0.3	$\sigma = 66 \pm 4.5 \pm 1.6$ pb	$\sigma = 68.2 + 5.2 - 5.3$ pb (NNLO+NNLL QCD)	ATLAS-CONF-2021-003
$t\bar{t}$ [$n_{jet} = 4$]	7	4.7	$\sigma = 3.76 \pm 0.05 \pm 0.27$ pb		JHEP 01, 020 (2015)
$t\bar{t}$ [$n_{jet} = 5$]	7	4.7	$\sigma = 1.72 \pm 0.04 \pm 0.16$ pb		JHEP 01, 020 (2015)
$t\bar{t}$ [$n_{jet} = 6$]	7	4.7	$\sigma = 0.611 \pm 0.024 \pm 0.083$ pb		JHEP 01, 020 (2015)
$t\bar{t}$ [$n_{jet} = 7$]	7	4.7	$\sigma = 0.161 \pm 0.007 \pm 0.033$ pb		JHEP 01, 020 (2015)
$t\bar{t}$ [$n_{jet} \geq 8$]	7	4.7	$\sigma = 0.0425 \pm 0.004 \pm 0.012$ pb		JHEP 01, 020 (2015)
t_{t-chan}	13	3.2	$\sigma = 247 \pm 6 \pm 46$ pb	$\sigma = 217 \pm 10$ pb (NLO+NLL)	JHEP 04 (2017) 086
t_{t-chan}	8	20.3	$\sigma = 89.6 \pm 1.7 + 7.2 - 6.4$ pb	$\sigma = 87.8 + 3.4 - 1.9$ pb (NLO+NLL)	EPJC 77 (2017) 531
t_{t-chan}	7	4.6	$\sigma = 68 \pm 2 \pm 8$ pb	$\sigma = 64.6 + 2.7 - 2$ pb (NLO+NLL)	PRD 90, 112006 (2014)
Wt	13	3.2	$\sigma = 94 \pm 10 + 28 - 23$ pb	$\sigma = 71.7 \pm 3.9$ pb (NLO+NNLL)	JHEP 01 (2018) 63
Wt	8	20.3	$\sigma = 23 \pm 1.3 + 3.4 - 3.7$ pb	$\sigma = 22.4 \pm 1.5$ pb (NLO+NNLL)	JHEP 01, 064 (2016)
Wt	7	2.0	$\sigma = 16.8 \pm 2.9 \pm 3.9$ pb	$\sigma = 15.7 \pm 1.1$ pb (NLO+NNLL)	PLB 716, 142-159 (2012)
t_{s-chan}	8	20.3	$\sigma = 4.8 \pm 0.8 + 1.6 - 1.3$ pb	$\sigma = 5.61 \pm 0.22$ pb (NLO+NNL)	PLB 756, 228-246 (2016)
tZj	13	139	$\sigma = 97 \pm 13 \pm 7$ fb	$\sigma = 102 + 5 - 2$ fb (Madgraph5 + aMCNLO (NLO))	JHEP 07 (2020) 124

Standard Model Production Cross Section Measurements

Status: July 2021

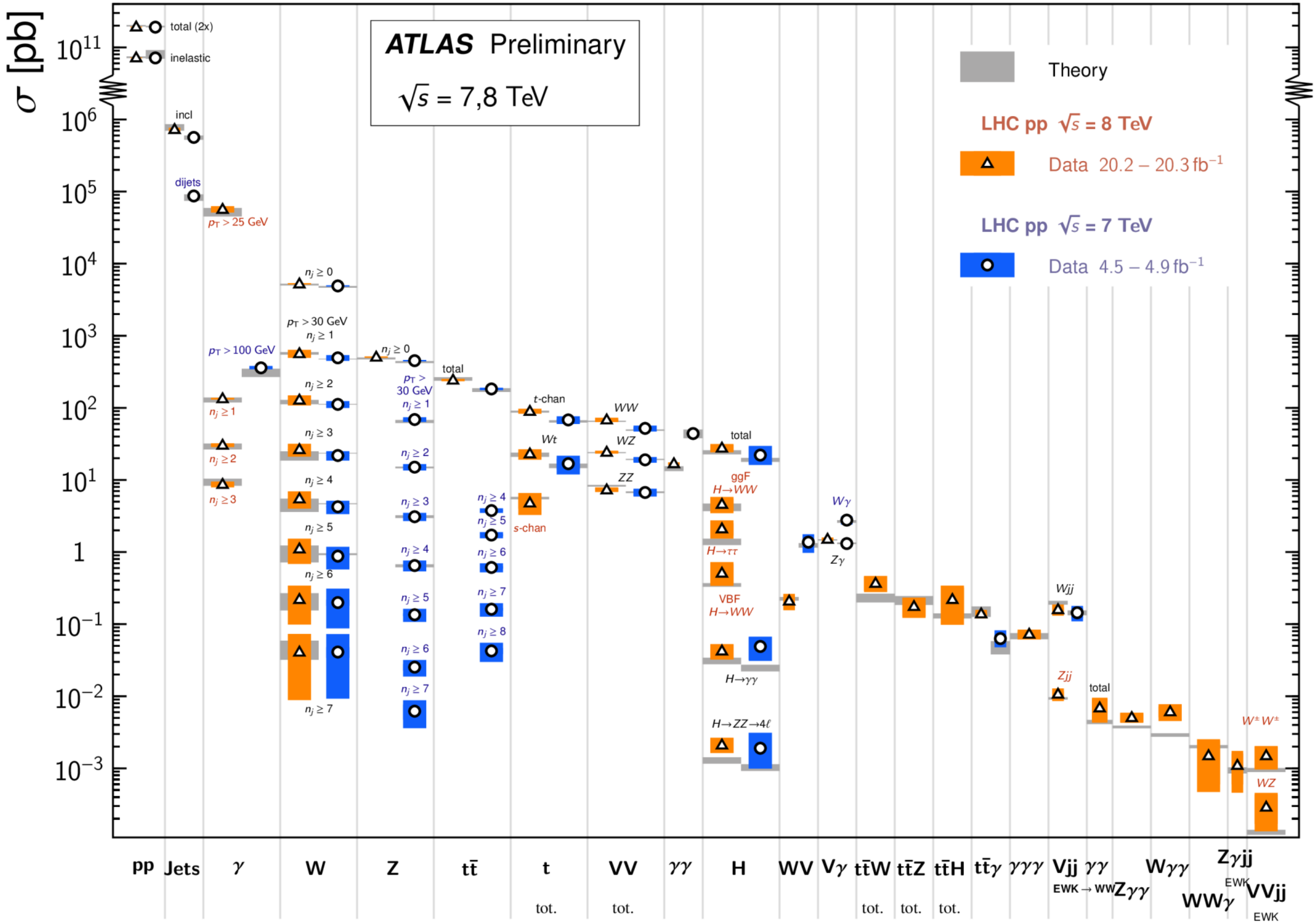

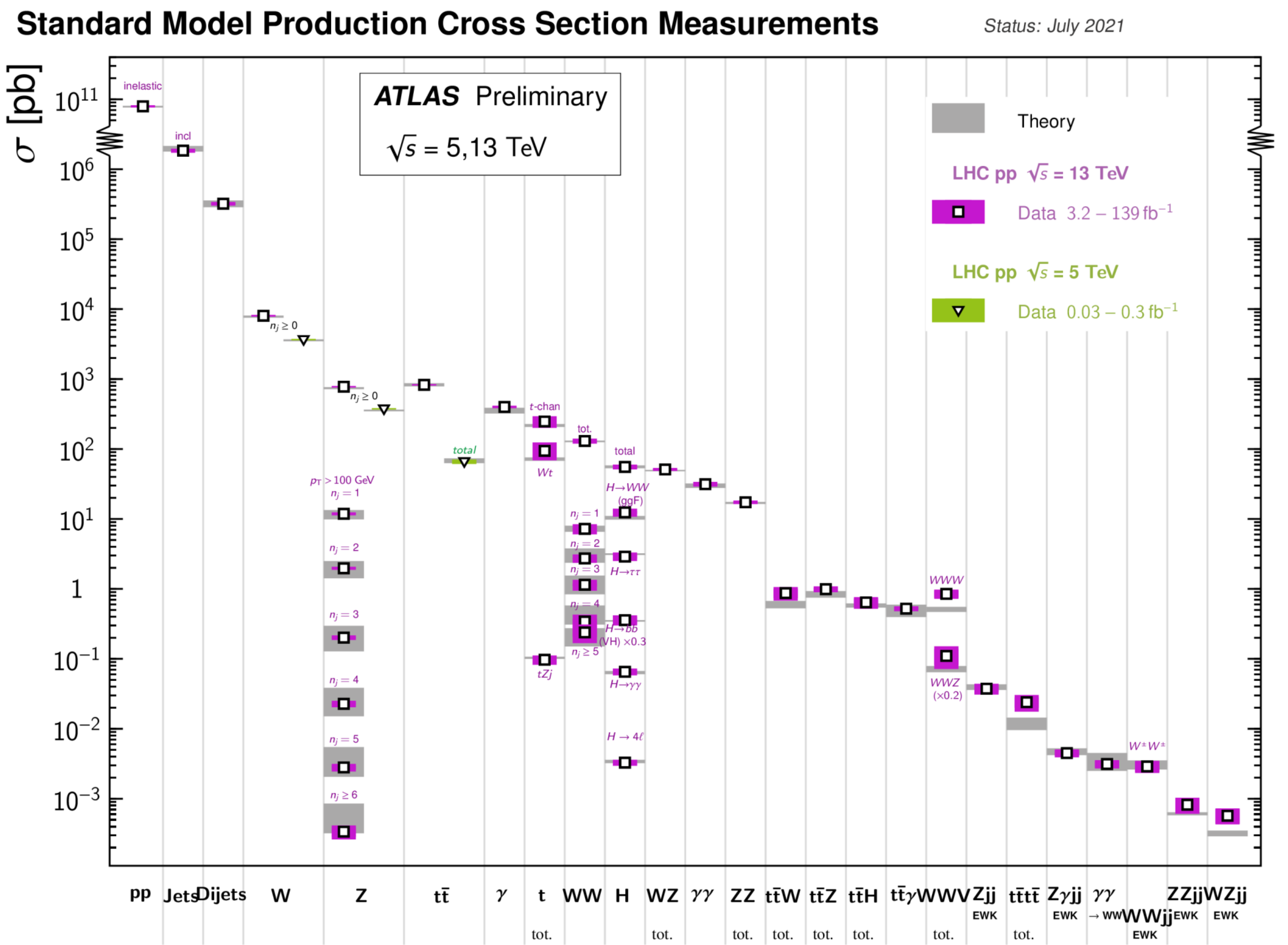

Standard Model Production Cross Section Measurements
Status: July 2021
σ [pb]
ATLAS Preliminary
√s = 5,13 TeV
Theory
LHC pp √s = 13 TeV
Data 3.2 – 139 fb⁻¹
LHC pp √s = 5 TeV
Data 0.03 – 0.3 fb⁻¹
inelastic
incl
nj ≥ 0
nj ≥ 0
pT > 100 GeV
nj = 1
nj = 2
nj = 3
nj = 4
nj = 5
nj ≥ 6
total
t-chan
Wt
tZj
tot.
nj = 1
nj = 2
nj = 3
nj = 4
nj ≥ 5
total
H→WW (ggF)
H→ττ
H→bb (VH) ×0.3
H→γγ
H → 4ℓ
WWW
WWZ (×0.2)
W±W±
pp
Jets
Dijets
W
Z
tt̄
γ
t tot.
WW
H
WZ tot.
γγ
ZZ tot.
tt̄W tot.
tt̄Z tot.
tt̄H tot.
tt̄γ
WWV tot.
Zjj EWK
tt̄tt̄ tot.
Zγjj EWK
γγ → WW
WWjj EWK
ZZjj EWK
WZjj EWK

B-physics

The $B_s^0 \to \mu^+\mu^-$ branching fraction is obtained to be $(2.69\,^{+\,0.37}_{-\,0.35}) \times 10^{-9}$

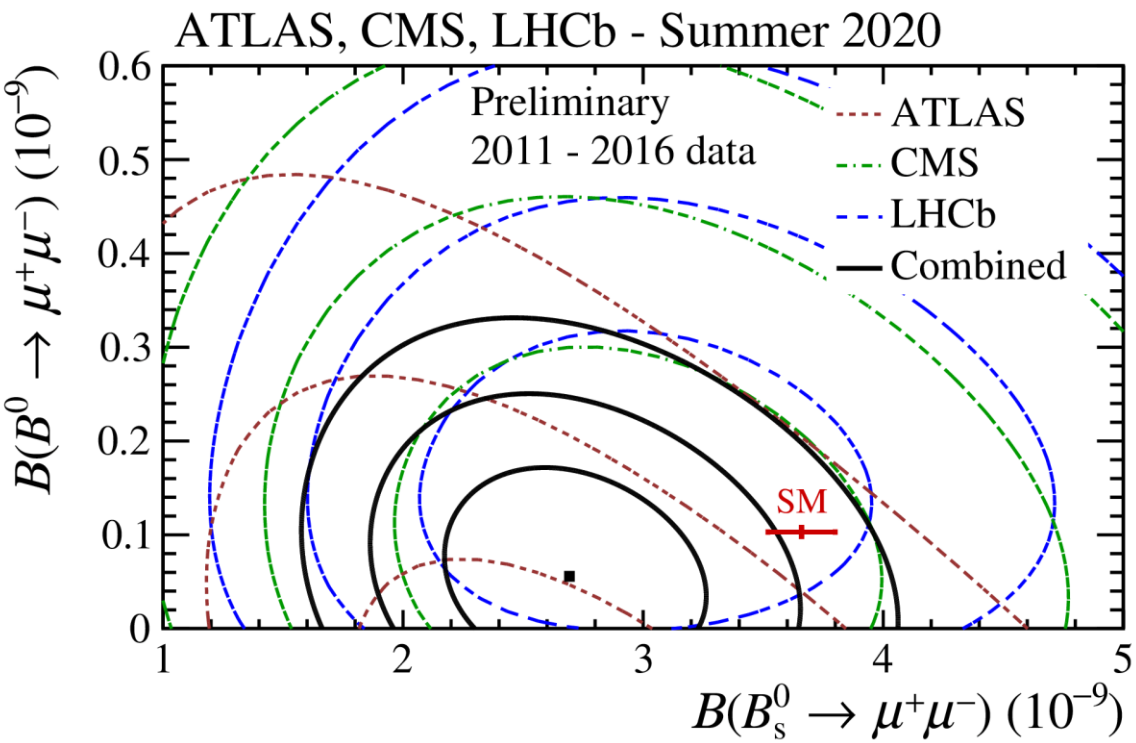

B-physics

Eur. Phys. J. C 81 (2021) 342
arXiv:2001.07115

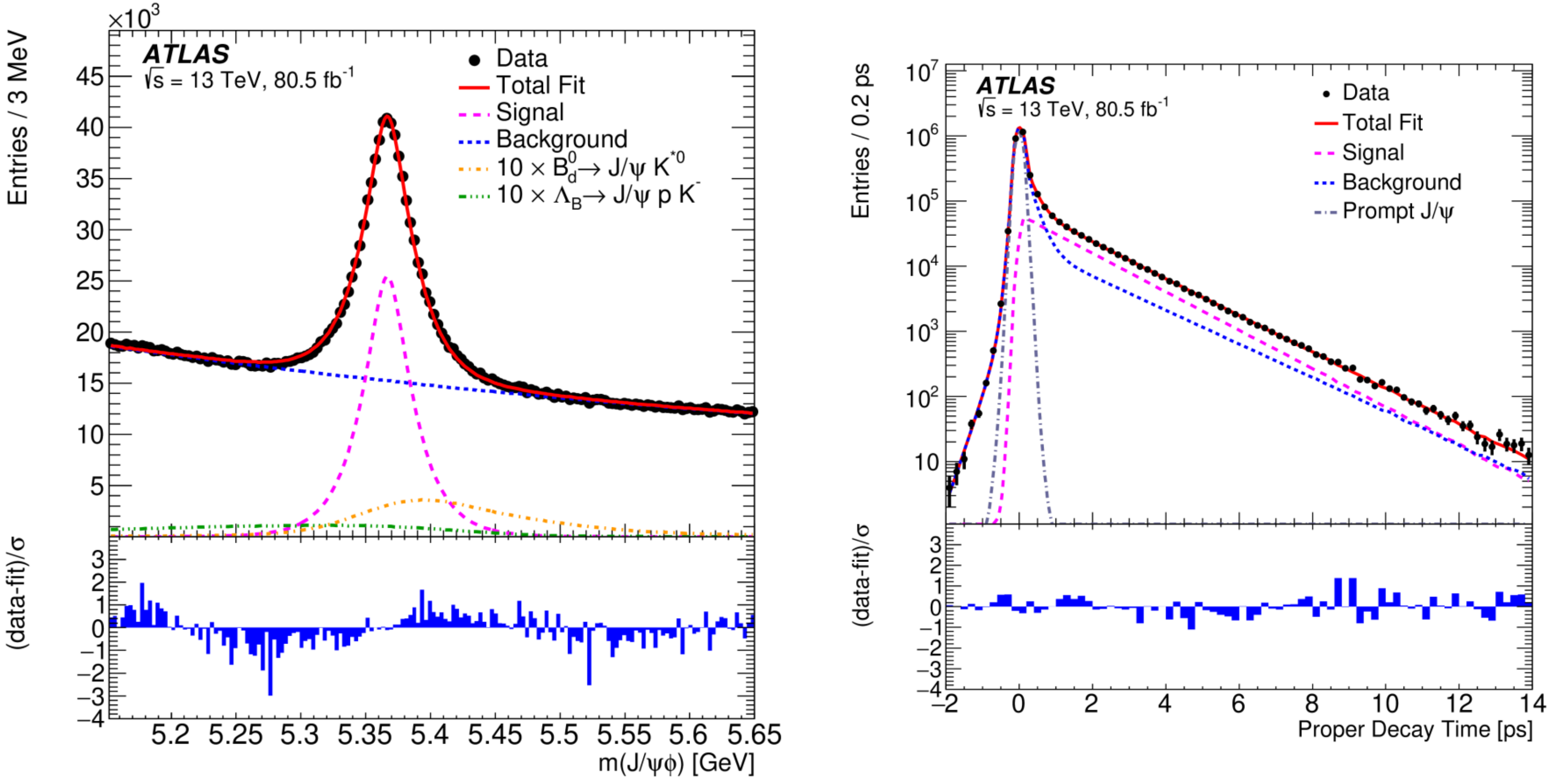

top-quark pair events with a high p_T top quark

ATLAS-CONF-2021-031

In order to evaluate
the impact of NNLO corrections, the MC setups are reweighted
at parton-level to match the NNLO QCD
+ NLO EW parton level prediction presented in Ref. [14]
The reweighting is performed on the three
variables $p_T(t)$, $p_T(t\bar{t})$ and $m(t\bar{t})$

[14] M. Czakon et al., *Top-pair production at the LHC through NNLO QCD and NLO EW*
JHEP **10** (2017) 186, arXiv: 1705.04105 [hep-ph]

Reconstruct hadronic top as reclustered R=1.0 anti-kt jet
p_T > 355 GeV, $|\eta|<2.0$, and mass $\in$ 120-220 GeV

top-quark pair events with a high p_T top quark

ATLAS-CONF-2021-031

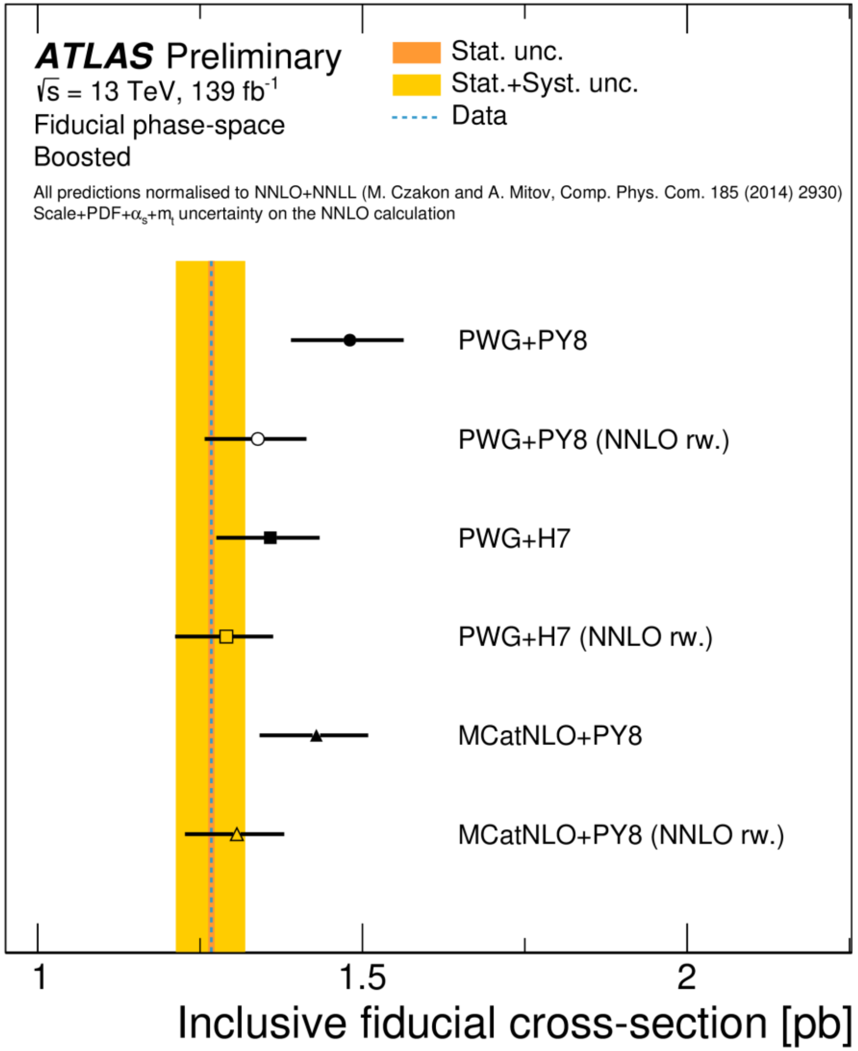

Figure 9: The fiducial cross-section at particle-level for boosted $t\bar{t}$ production measured in data (dashed line) is compared to several NLO predictions with (open markers) and without (closed markers) the NNLO reweighting applied. The yellow band represents the total uncertainty on the measured cross-section, while the orange band shows the statistical component. The uncertainties on the predictions are evaluated as the quadrature sum of the α_S, PDF, m_t and scale uncertainties present on the NNLO+NNLL prediction used to normalise all the samples. PWG+PY8 corresponds to the Powheg + Pythia sample, PWG+H7 to the Powheg + Herwig sample and MCatNLO+PY8 to the MadGraph5_aMC@NLO + Pythia sample.

top-quark pair events

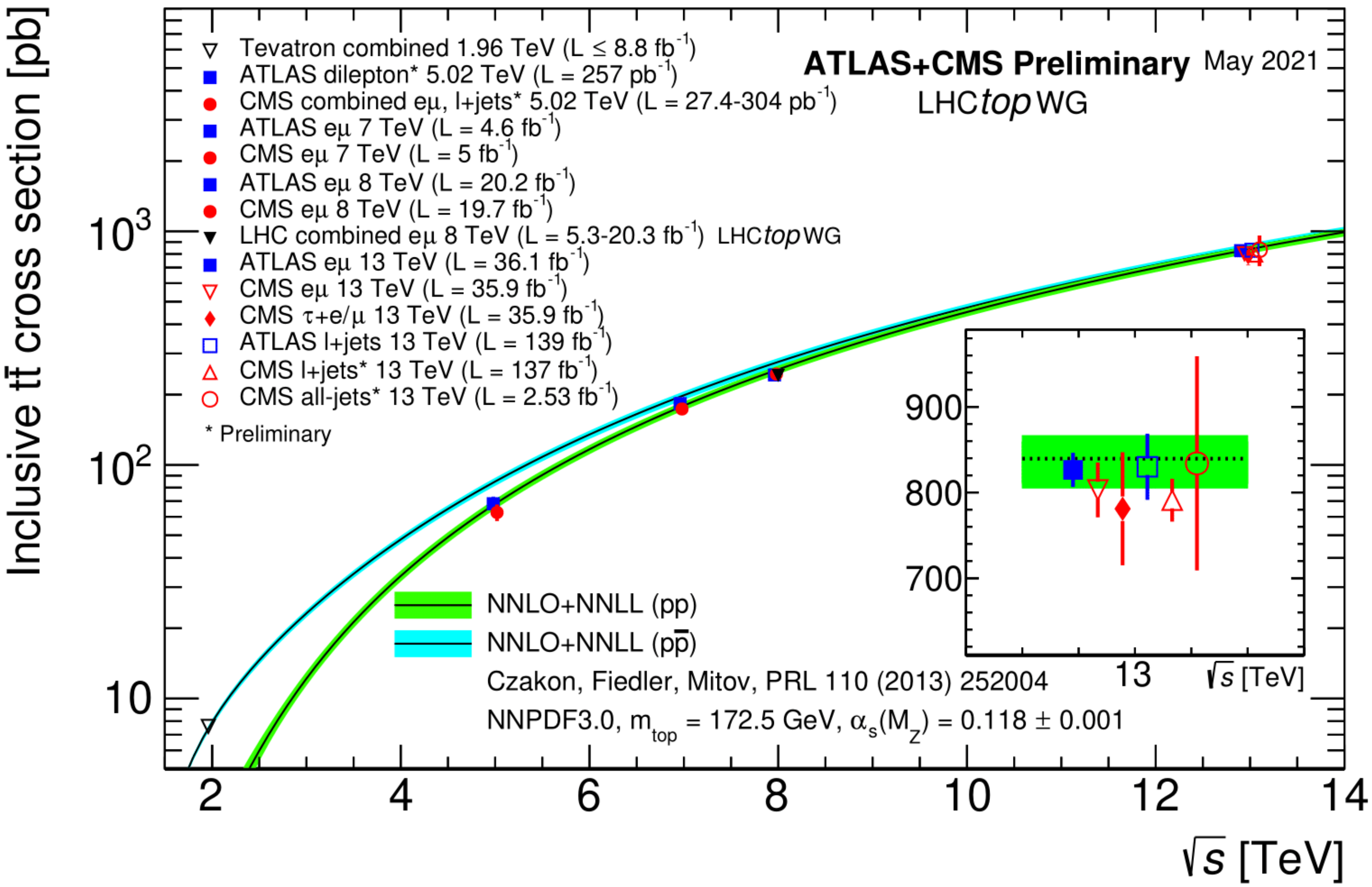

top-quark pair events

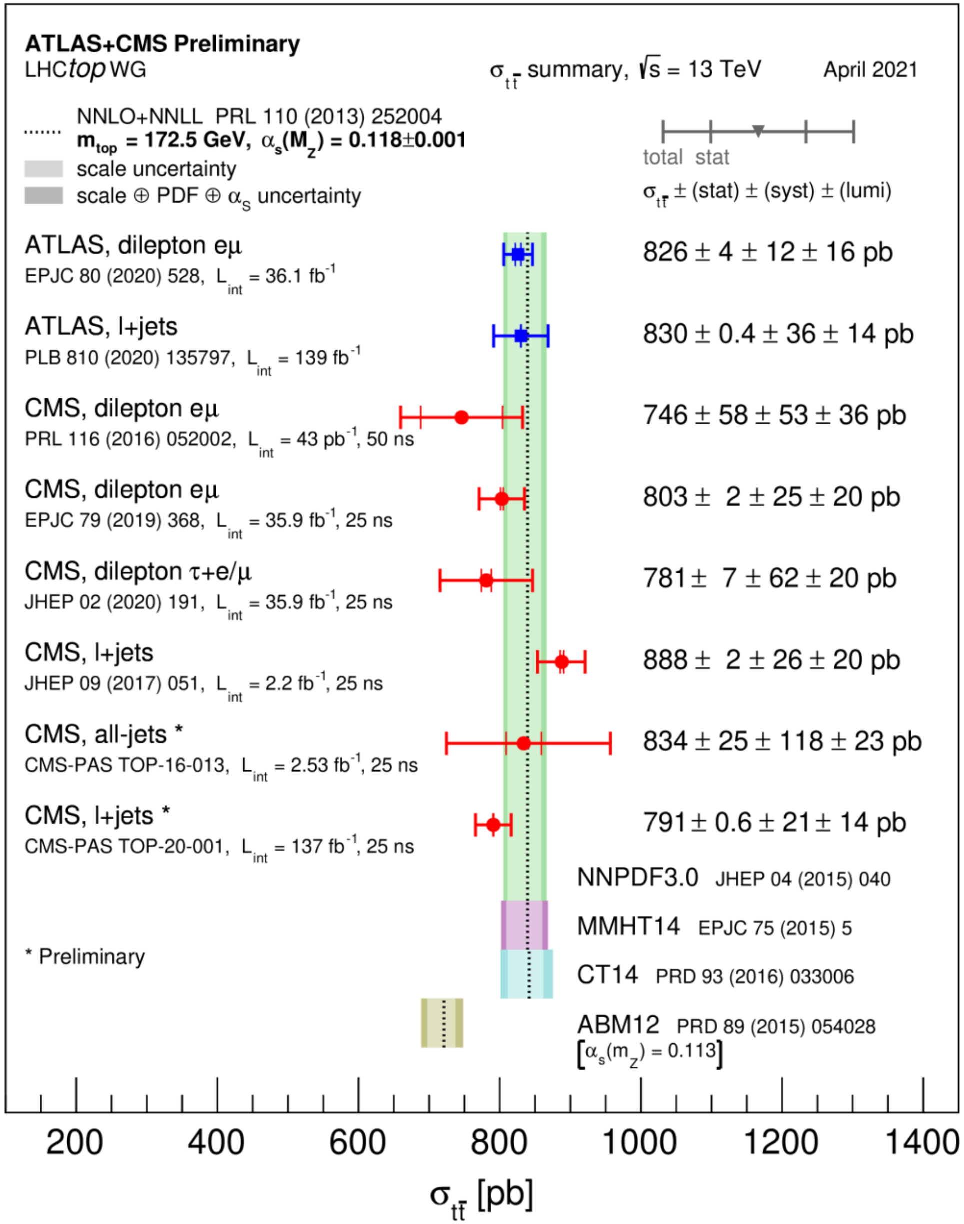

Measurement of $t\bar{t}t\bar{t}$ production cross section

arXiv:2106.11683
Eur.Phys.J.C 80 (2020) 11, 1085
M.Vincter LHCP21

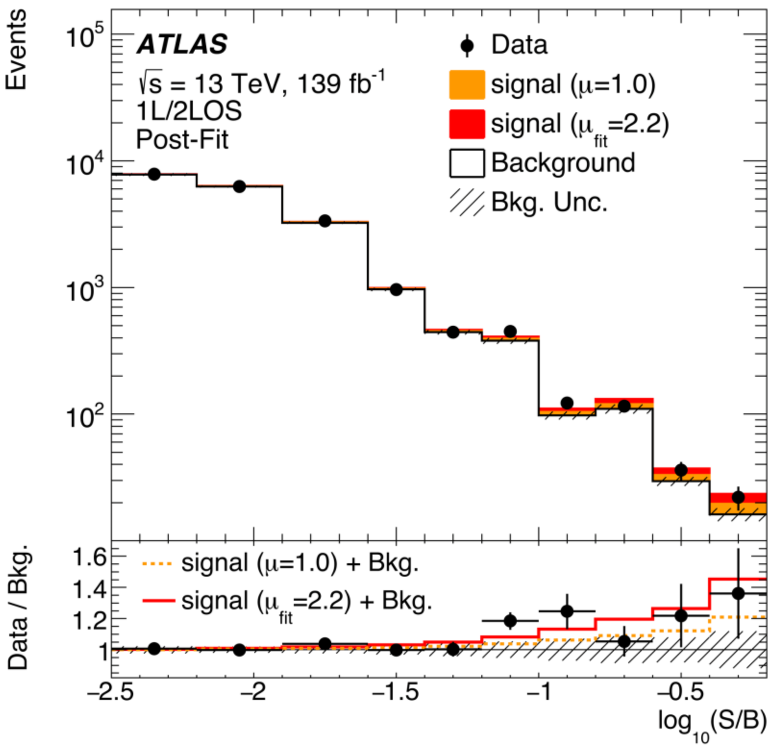

Name	Description
$\sum b$-tag	Sum of pseudo-continuous b-tagging score over the six jets with the highest score
N_{jets}	Number of jets
$\Delta R_{bb}^{\text{min}}$	Minimum ΔR between all pairs of b-tagged jets
$H_{\text{T}}^{\text{all}}$	Scalar sum of all jet and lepton transverse momenta
C^{all}	Centrality ($\sum_i p_{\text{T}i} / \sum_i E_i$) of the leptons and jets
$p_{\text{T}}^{\text{lead}}$	Transverse momentum of the leading jet
$\Delta R_{b\ell}^{\text{min}}$	Minimum ΔR between all pairs of b-tagged jets and leptons
$\Delta R_{jj}^{\text{avg}}$	Average ΔR between all pairs of jets
m_{jjj}	Invariant mass of the closest triplet of jets
$E_{\text{T}}^{\text{miss}}$	Missing transverse momentum
m_{T}^{W}	W reconstructed transverse mass $m_T(\ell, E_{\text{T}}^{\text{miss}})$ (1L)
$N_{\text{LR-jets}}$	Number of large-R jets with a mass above 100 GeV
$\sum d_{12}$	Sum of the first k_t splitting scale d_{12} of all large-R jets
$\sum d_{23}$	Sum of the second k_t splitting scale d_{23} of all large-R jets

Summary of the input variables used by the BDTs in the signal regions for the 1L and 2LOS channels. The transverse mass $m_{\text{T}}(\ell, E_{\text{T}}^{\text{miss}})$ is defined as $\sqrt{2p_{\text{T}}^{\ell} E_{\text{T}}^{\text{miss}}(1-\cos\Delta\phi)}$, where $\Delta\phi$ is the azimuthal angle between the lepton and $E_{\text{T}}^{\text{miss}}$.

Measurement of $t\bar{t}t\bar{t}$ production cross section

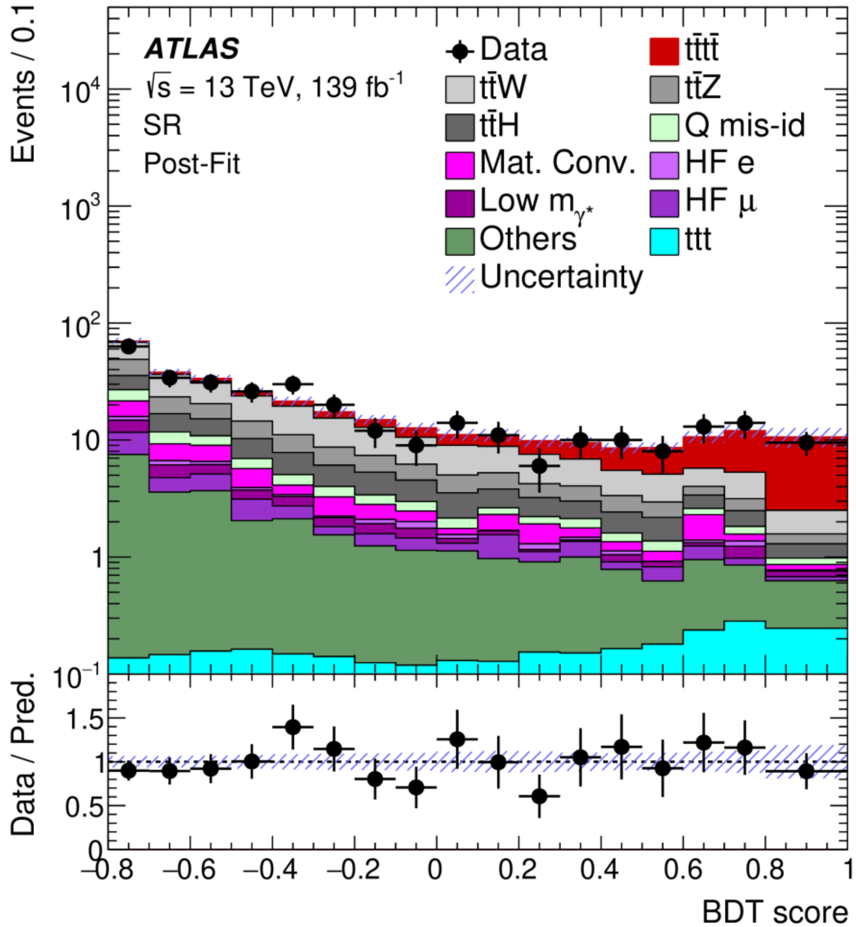

Measurement of $t\bar{t}t\bar{t}$ production cross section

Eur.Phys.J.C 80 (2020) 11, 1085

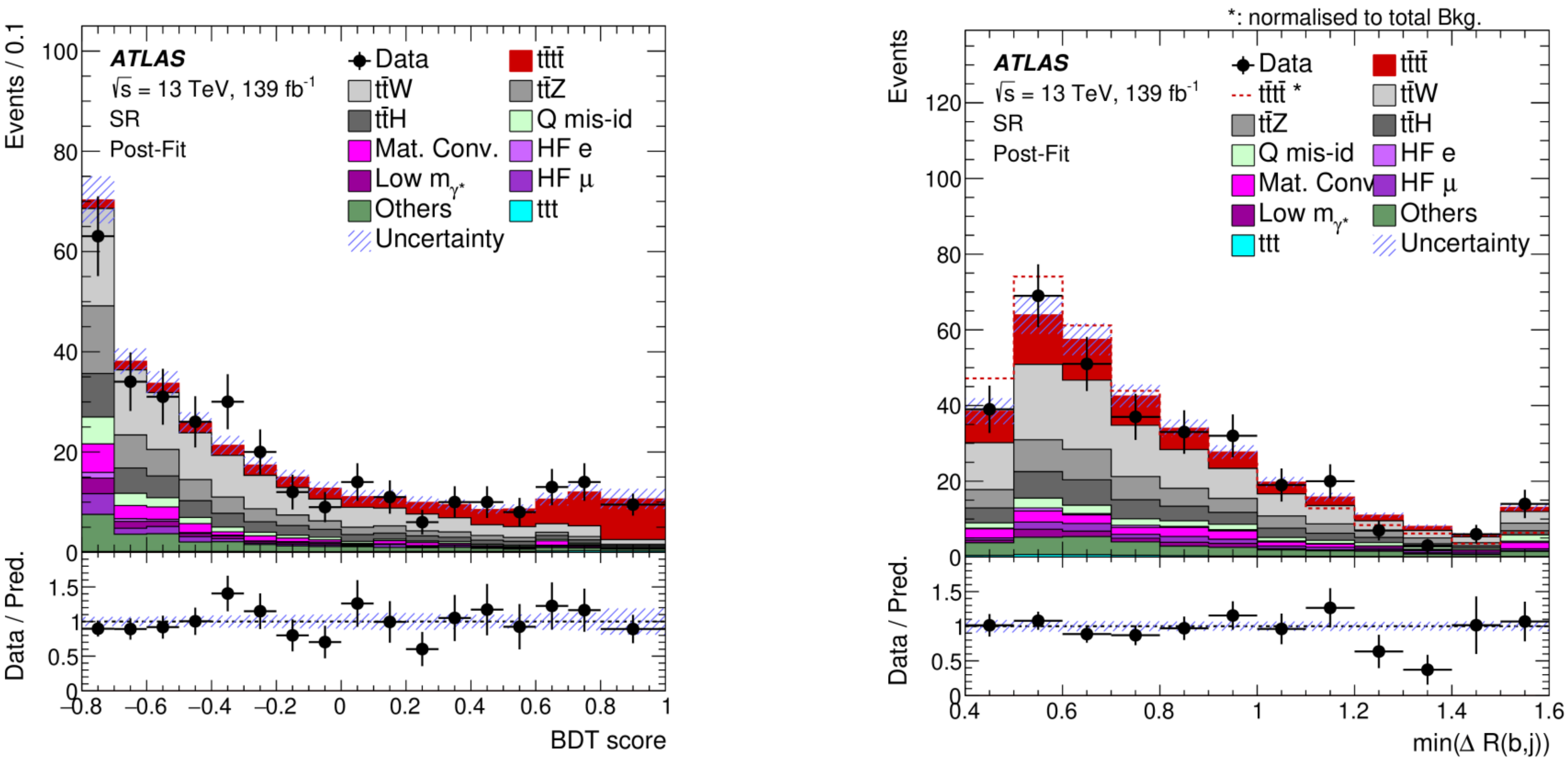

Post-fit comparison between data and prediction in the signal region for the variables used to train the multivariate discriminant: H_T excluding the leading jet p_T, the sum of distances between two leptons for all possible pairs, the maximum distance between a b-jet and a lepton among all possible pair, and the minimum distance between a jet and a b-jet among all possible pairs. The ratio of the data to the total post-fit computation is shown in the lower panel. The dashed red histogram represents the signal normalised to the total number of background events. The first and last bins contain underflow and overflow events, respectively.

4σ evidence for weak triboson production using 2015-2017 data (presented already at Corfou 2019)

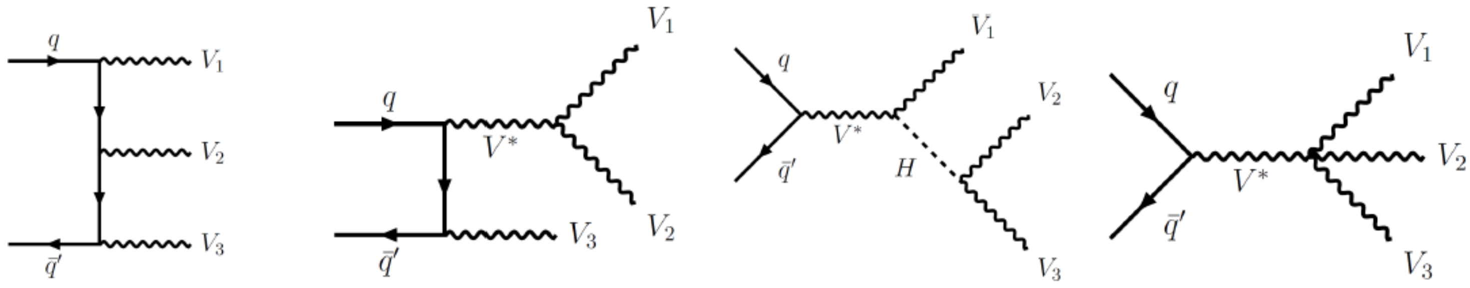

Phys. Lett. B **798** (2019) 134913

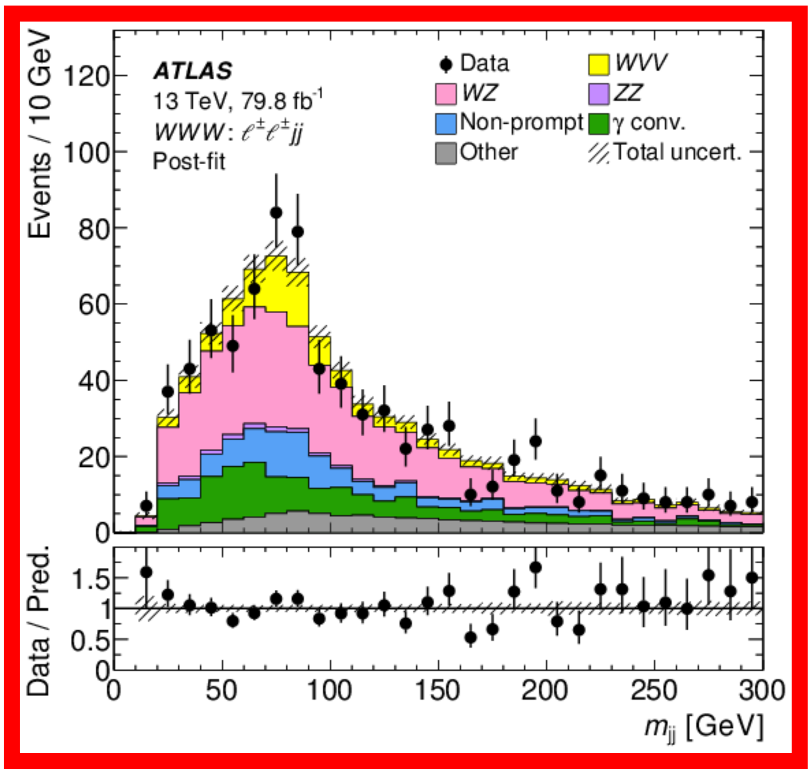

Decay channel	Significance Observed	Significance Expected
WWW combined	3.2σ	2.4σ
$WWW \to \ell\nu\ell\nu qq$	4.0σ	1.7σ
$WWW \to \ell\nu\ell\nu\ell\nu$	1.0σ	2.0σ
WVZ combined	3.2σ	2.0σ
$WVZ \to \ell\nu qq\ell\ell$	0.5σ	1.0σ
$WVZ \to \ell\nu\ell\nu\ell\ell/qq\ell\ell\ell\ell$	3.5σ	1.8σ
WVV combined	4.1σ	3.1σ

WWW production

ATLAS-CONF-2021-039

Uncertainty source	$\Delta\sigma/\sigma$ [%]
Data-driven background	5.3
Prompt-lepton-background modeling	3.3
Jets and E_T^{miss}	2.8
MC statistics	2.8
Lepton	2.1
Luminosity	1.9
Signal modeling	1.5
Pile-up modeling	0.9
Total systematic uncertainty	9.5
Data statistics	11.2
WZ normalizations	3.3
Total statistical uncertainty	11.6

Table 4: Breakdown of the uncertainty on the measured cross section for different categories. For each category, the impact is calculated by performing a fit where the nuisance parameters in the group are fixed to their best-fit values, and then subtracting the resulting uncertainty in the signal strength in quadrature from the uncertainty of the nominal fit.

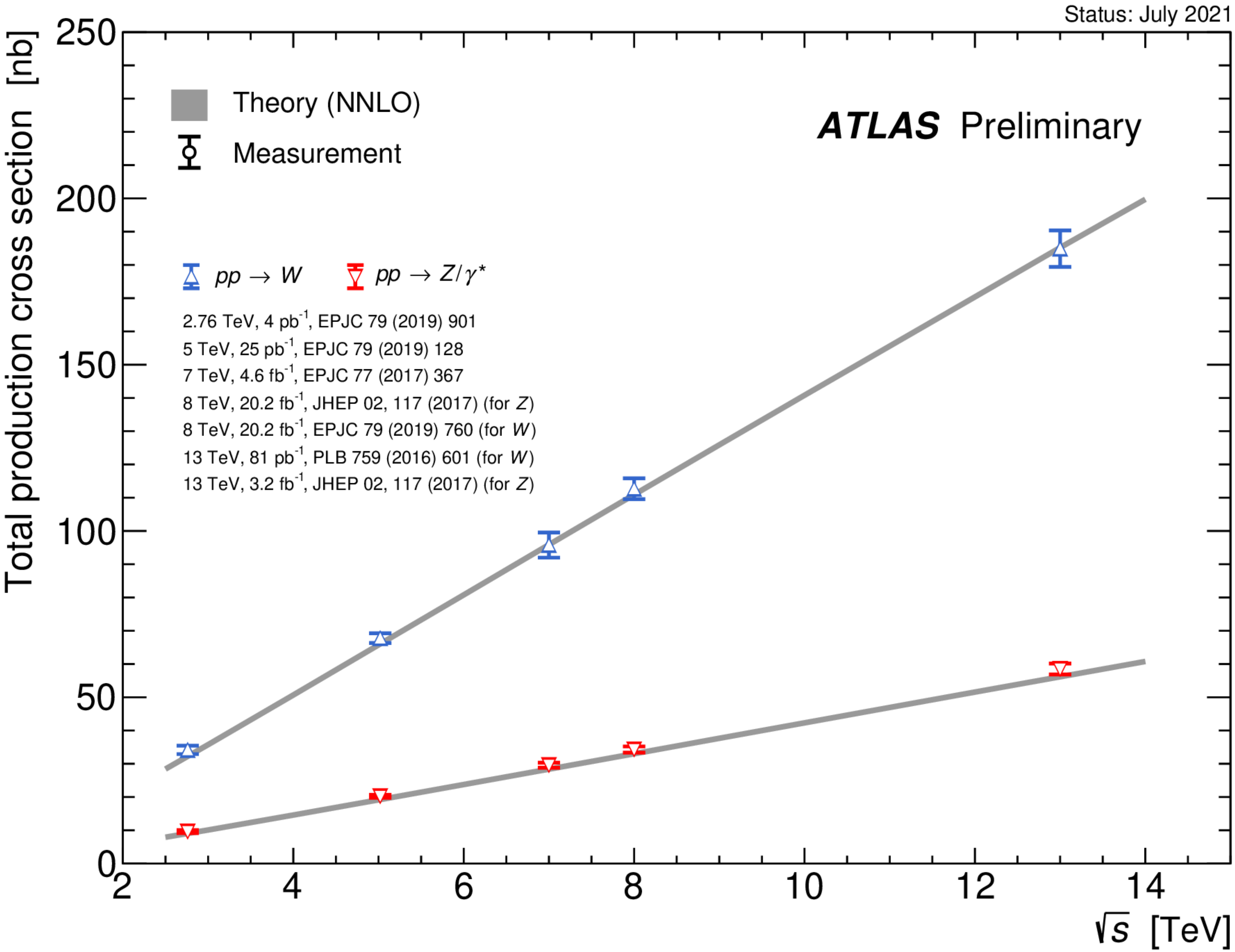
Status: July 2021
ATLAS Preliminary
Theory (NNLO)
Measurement
pp → W
pp → Z/γ*
2.76 TeV, 4 pb-1, EPJC 79 (2019) 901
5 TeV, 25 pb-1, EPJC 79 (2019) 128
7 TeV, 4.6 fb-1, EPJC 77 (2017) 367
8 TeV, 20.2 fb-1, JHEP 02, 117 (2017) (for Z)
8 TeV, 20.2 fb-1, EPJC 79 (2019) 760 (for W)
13 TeV, 81 pb-1, PLB 759 (2016) 601 (for W)
13 TeV, 3.2 fb-1, JHEP 02, 117 (2017) (for Z)
Total production cross section [nb]
√s [TeV]
0
50
100
150
200
250
2
4
6
8
10
12
14

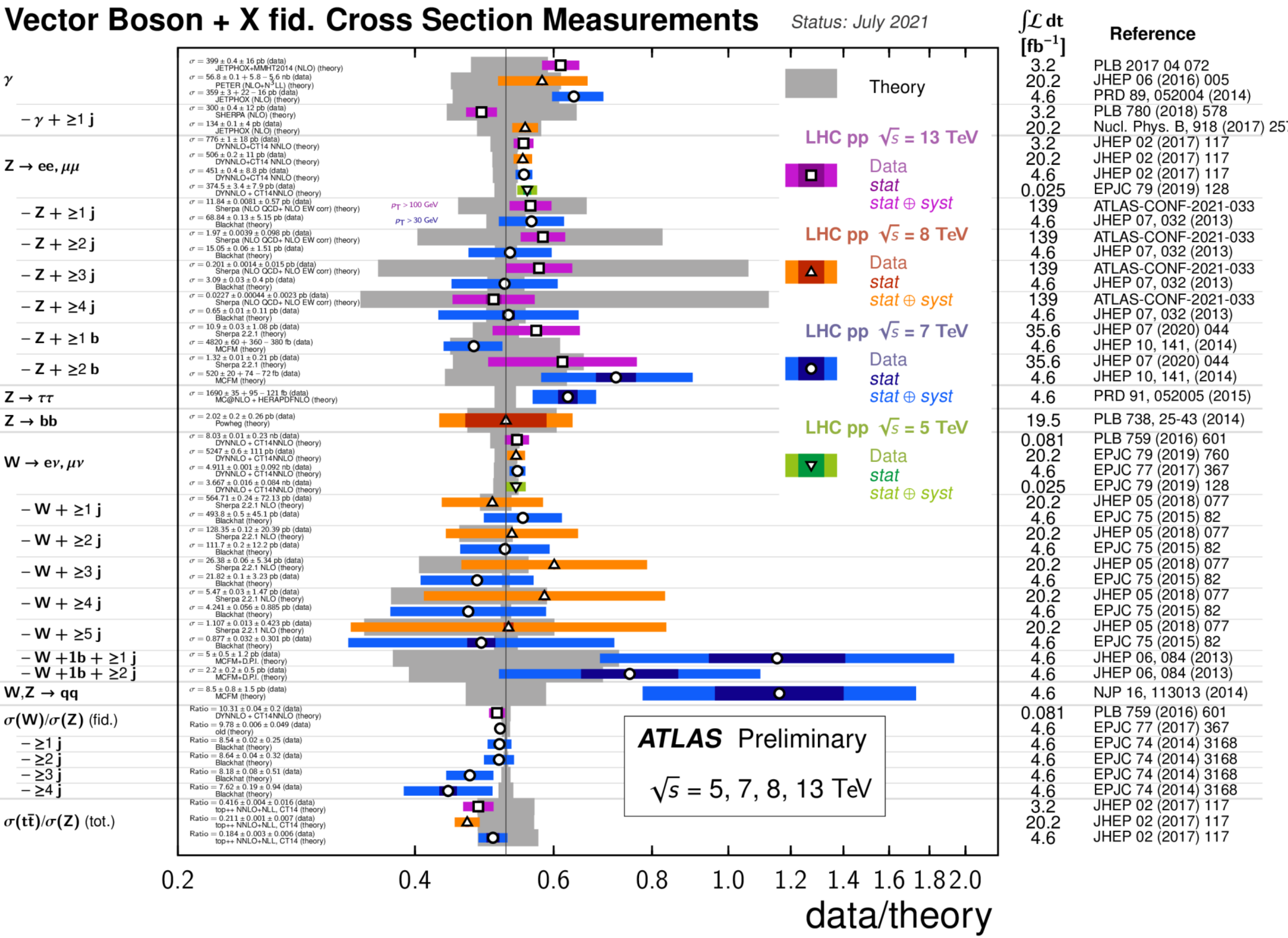
Vector Boson + X fid. Cross Section Measurements
Status: July 2021
∫L dt [fb⁻¹]
Reference
γ
− γ + ≥1 j
Z → ee, μμ
− Z + ≥1 j
− Z + ≥2 j
− Z + ≥3 j
− Z + ≥4 j
− Z + ≥1 b
− Z + ≥2 b
Z → ττ
Z → bb
W → eν, μν
− W + ≥1 j
− W + ≥2 j
− W + ≥3 j
− W + ≥4 j
− W + ≥5 j
− W +1b + ≥1 j
− W +1b + ≥2 j
W,Z → qq
σ(W)/σ(Z) (fid.)
− ≥1 j
− ≥2 j
− ≥3 j
− ≥4 j
σ(tt̄)/σ(Z) (tot.)
Theory
LHC pp √s = 13 TeV
Data
stat
stat ⊕ syst
LHC pp √s = 8 TeV
Data
stat
stat ⊕ syst
LHC pp √s = 7 TeV
Data
stat
stat ⊕ syst
LHC pp √s = 5 TeV
Data
stat
stat ⊕ syst
ATLAS Preliminary
√s = 5, 7, 8, 13 TeV
3.2 PLB 2017 04 072
20.2 JHEP 06 (2016) 005
4.6 PRD 89, 052004 (2014)
3.2 PLB 780 (2018) 578
20.2 Nucl. Phys. B, 918 (2017) 257
3.2 JHEP 02 (2017) 117
20.2 JHEP 02 (2017) 117
4.6 JHEP 02 (2017) 117
0.025 EPJC 79 (2019) 128
139 ATLAS-CONF-2021-033
4.6 JHEP 07, 032 (2013)
139 ATLAS-CONF-2021-033
4.6 JHEP 07, 032 (2013)
139 ATLAS-CONF-2021-033
4.6 JHEP 07, 032 (2013)
139 ATLAS-CONF-2021-033
4.6 JHEP 07, 032 (2013)
35.6 JHEP 07 (2020) 044
4.6 JHEP 10, 141, (2014)
35.6 JHEP 07 (2020) 044
4.6 JHEP 10, 141, (2014)
4.6 PRD 91, 052005 (2015)
19.5 PLB 738, 25-43 (2014)
0.081 PLB 759 (2016) 601
20.2 EPJC 79 (2019) 760
4.6 EPJC 77 (2017) 367
0.025 EPJC 79 (2019) 128
20.2 JHEP 05 (2018) 077
4.6 EPJC 75 (2015) 82
20.2 JHEP 05 (2018) 077
4.6 EPJC 75 (2015) 82
20.2 JHEP 05 (2018) 077
4.6 EPJC 75 (2015) 82
20.2 JHEP 05 (2018) 077
4.6 EPJC 75 (2015) 82
20.2 JHEP 05 (2018) 077
4.6 EPJC 75 (2015) 82
4.6 JHEP 06, 084 (2013)
4.6 JHEP 06, 084 (2013)
4.6 NJP 16, 113013 (2014)
0.081 PLB 759 (2016) 601
4.6 EPJC 77 (2017) 367
4.6 EPJC 74 (2014) 3168
4.6 EPJC 74 (2014) 3168
4.6 EPJC 74 (2014) 3168
4.6 EPJC 74 (2014) 3168
3.2 JHEP 02 (2017) 117
20.2 JHEP 02 (2017) 117
4.6 JHEP 02 (2017) 117
0.2 0.4 0.6 0.8 1.0 1.2 1.4 1.6 1.8 2.0
data/theory

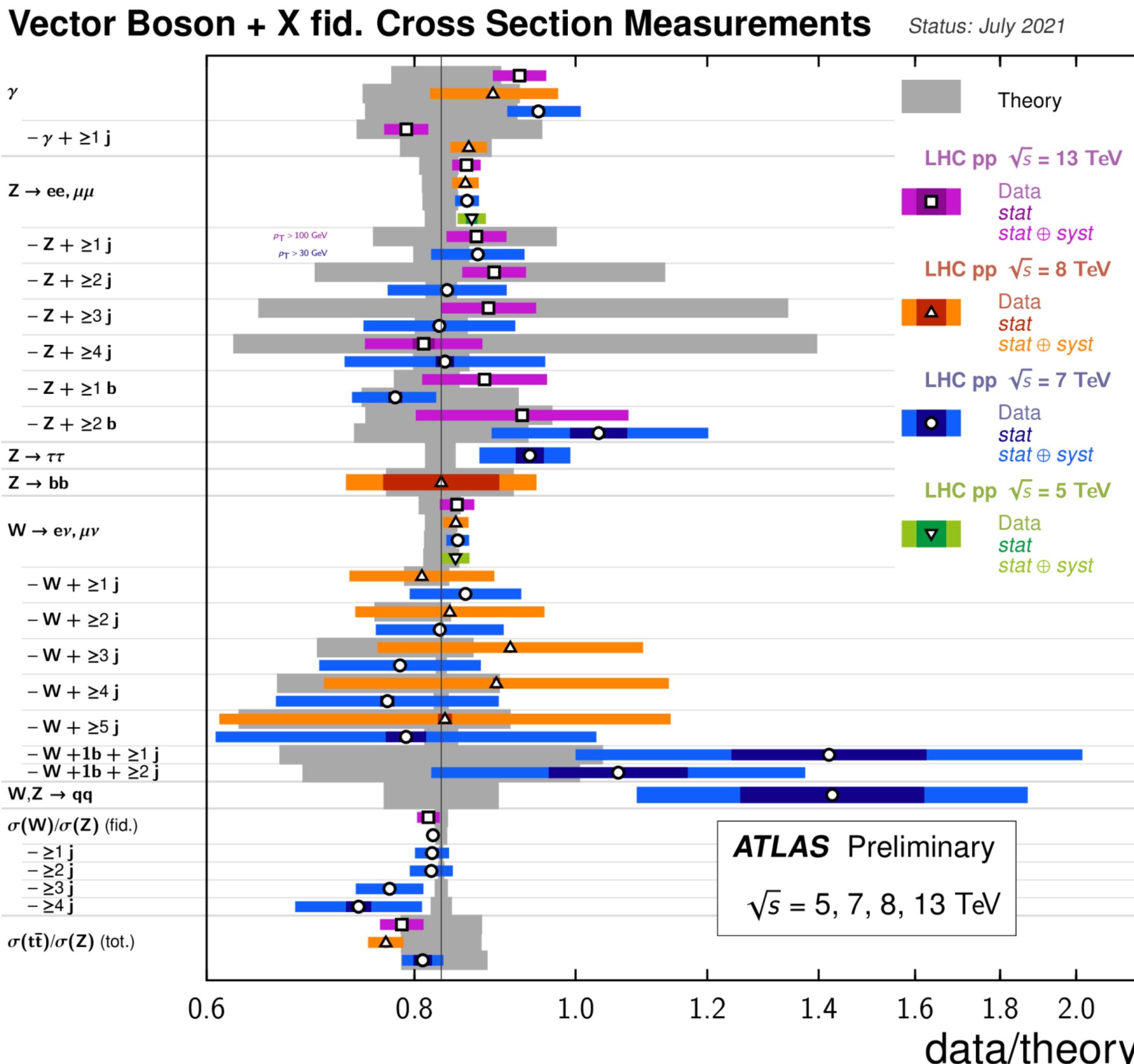
Vector Boson + X fid. Cross Section Measurements
Status: July 2021
γ
– γ + ≥1 j
Z → ee, μμ
– Z + ≥1 j
pT > 100 GeV
pT > 30 GeV
– Z + ≥2 j
– Z + ≥3 j
– Z + ≥4 j
– Z + ≥1 b
– Z + ≥2 b
Z → ττ
Z → bb
W → eν, μν
– W + ≥1 j
– W + ≥2 j
– W + ≥3 j
– W + ≥4 j
– W + ≥5 j
– W +1b + ≥1 j
– W +1b + ≥2 j
W,Z → qq
σ(W)/σ(Z) (fid.)
– ≥1 j
– ≥2 j
– ≥3 j
– ≥4 j
σ(tt̄)/σ(Z) (tot.)
Theory
LHC pp √s = 13 TeV
Data
stat
stat ⊕ syst
LHC pp √s = 8 TeV
Data
stat
stat ⊕ syst
LHC pp √s = 7 TeV
Data
stat
stat ⊕ syst
LHC pp √s = 5 TeV
Data
stat
stat ⊕ syst
ATLAS Preliminary
√s = 5, 7, 8, 13 TeV
0.6
0.8
1.0
1.2
1.4
1.6
1.8
2.0
data/theory

ATL-PHYS-PUB-2021-032

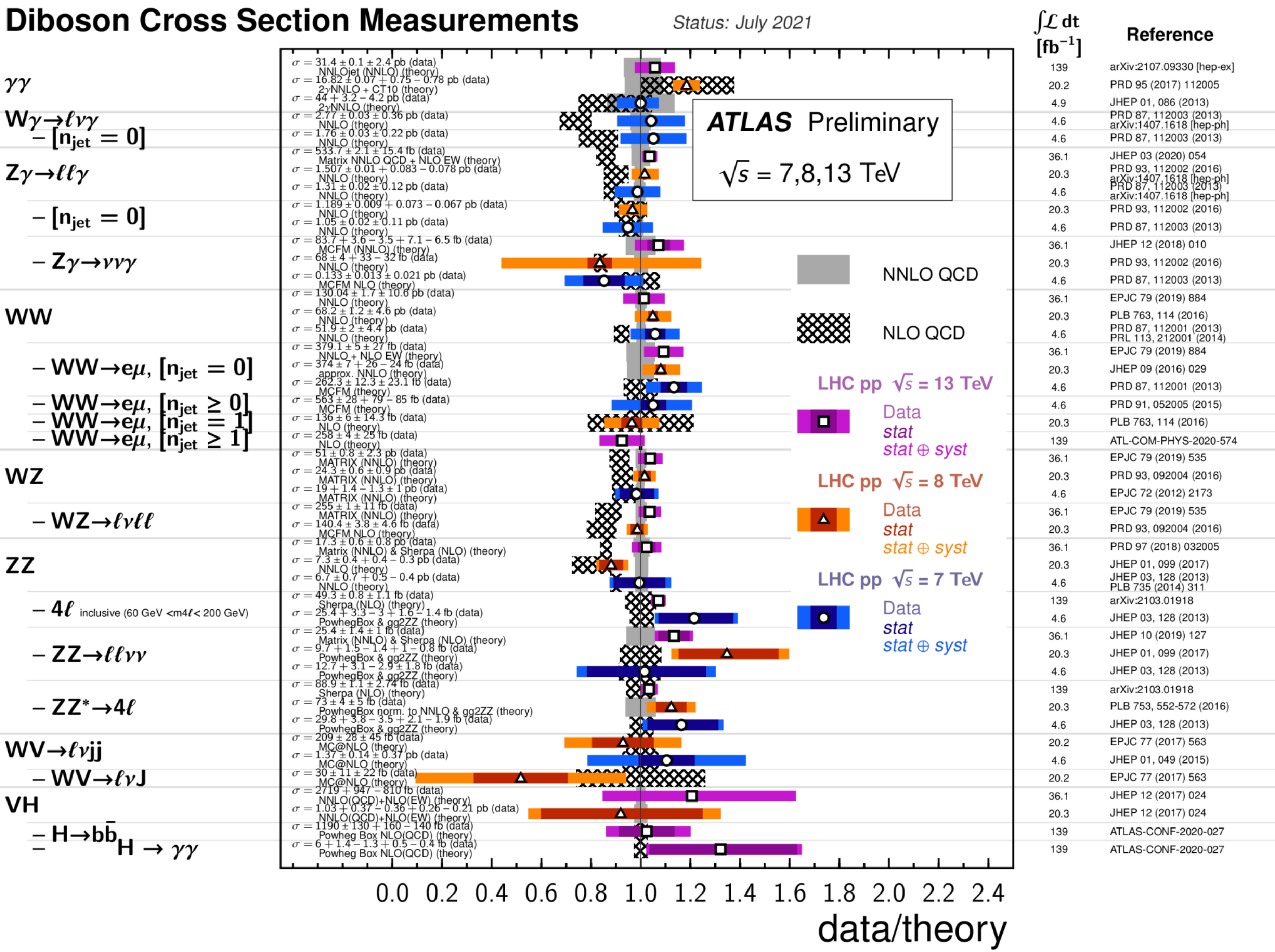

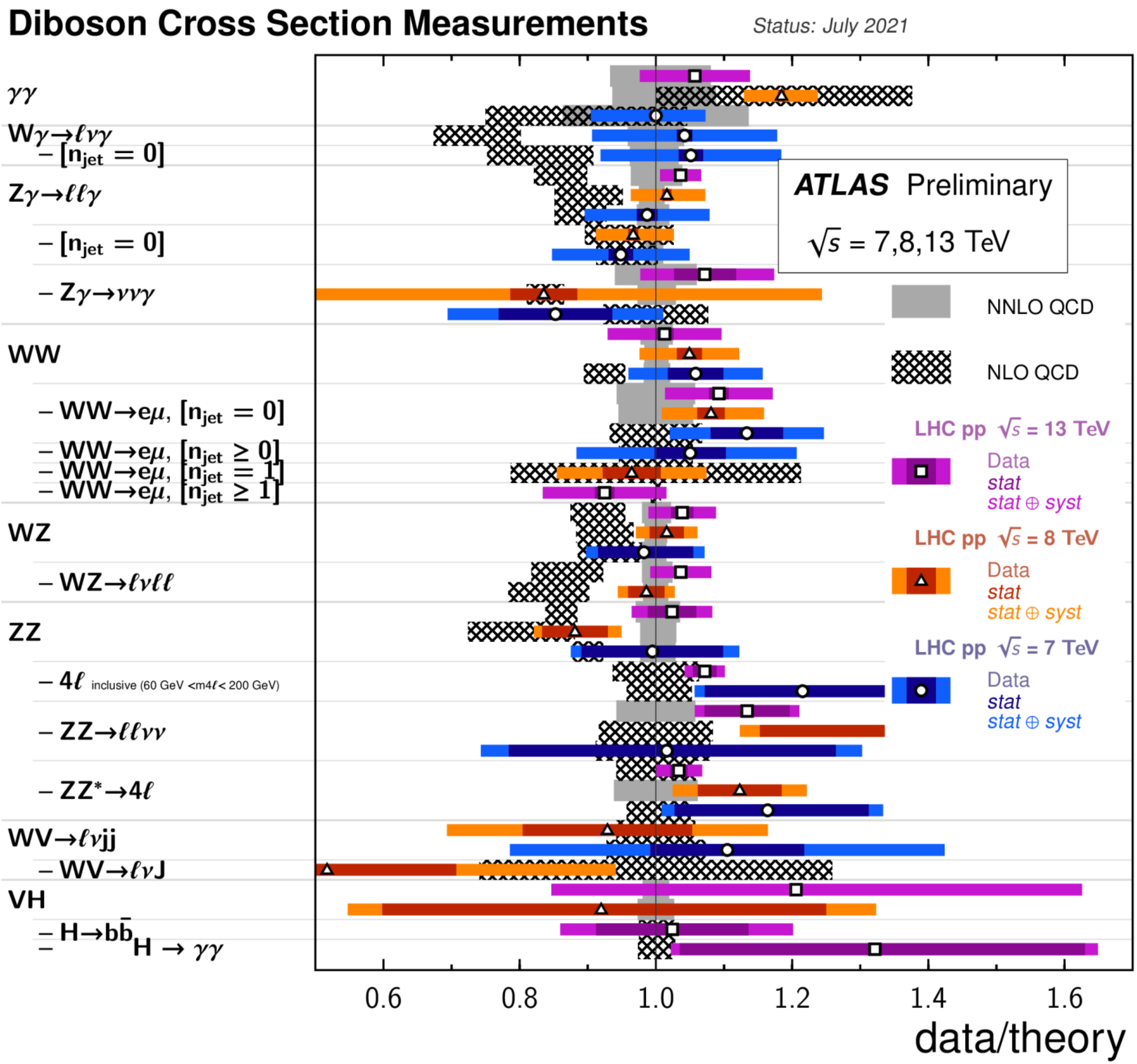
Diboson Cross Section Measurements
Status: July 2021
ATLAS Preliminary
$\sqrt{s}$ = 7,8,13 TeV
NNLO QCD
NLO QCD
LHC pp $\sqrt{s}$ = 13 TeV
Data
stat
stat ⊕ syst
LHC pp $\sqrt{s}$ = 8 TeV
Data
stat
stat ⊕ syst
LHC pp $\sqrt{s}$ = 7 TeV
Data
stat
stat ⊕ syst
$\gamma\gamma$
$W\gamma\rightarrow\ell\nu\gamma$
$-[n_{jet}=0]$
$Z\gamma\rightarrow\ell\ell\gamma$
$-[n_{jet}=0]$
$-Z\gamma\rightarrow\nu\nu\gamma$
WW
$-WW\rightarrow e\mu, [n_{jet}=0]$
$-WW\rightarrow e\mu, [n_{jet}\geq 0]$
$-WW\rightarrow e\mu, [n_{jet}=1]$
$-WW\rightarrow e\mu, [n_{jet}\geq 1]$
WZ
$-WZ\rightarrow\ell\nu\ell\ell$
ZZ
-4ℓ inclusive (60 GeV <m4ℓ< 200 GeV)
$-ZZ\rightarrow\ell\ell\nu\nu$
$-ZZ^*\rightarrow 4\ell$
$WV\rightarrow\ell\nu jj$
$-WV\rightarrow\ell\nu J$
VH
$-H\rightarrow b\bar{b}$
$-H\rightarrow\gamma\gamma$
0.6
0.8
1.0
1.2
1.4
1.6
data/theory

Z boson with high p_T jets

ATLAS-CONF-2021-033

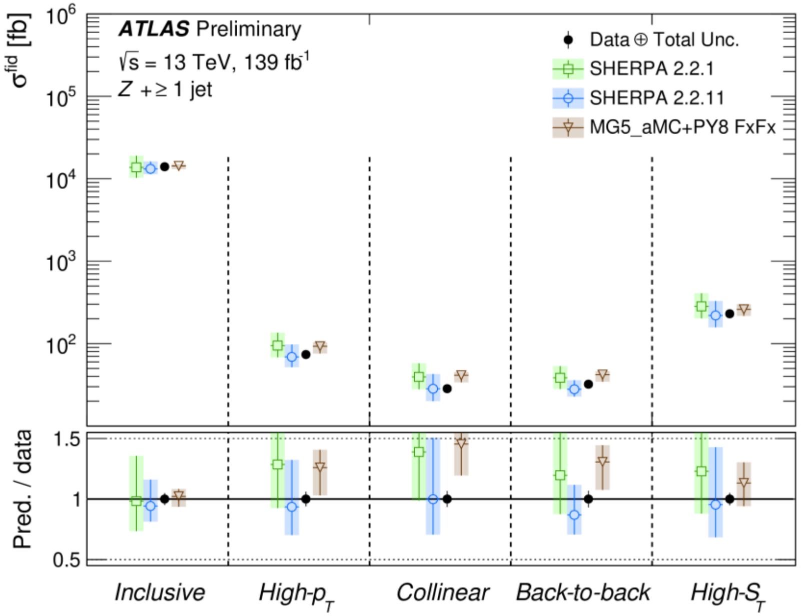

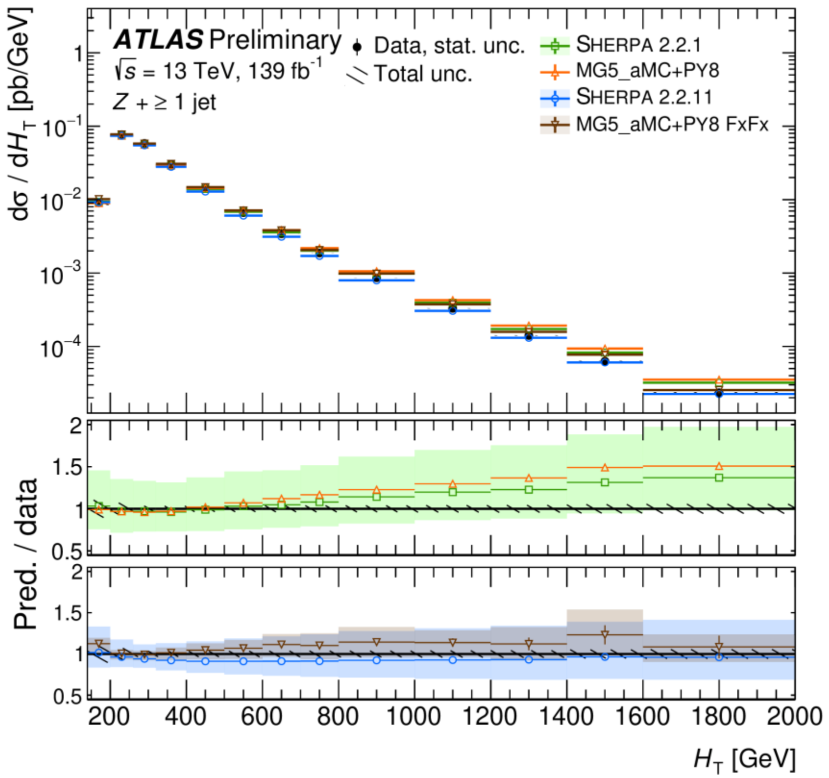

Z boson with high p_T jets

Giant QCD K-factors beyond NLO

Mathieu Rubin, Gavin P. Salam and Sebastian Sapeta arXiv:1006.2144v2 [hep-ph]

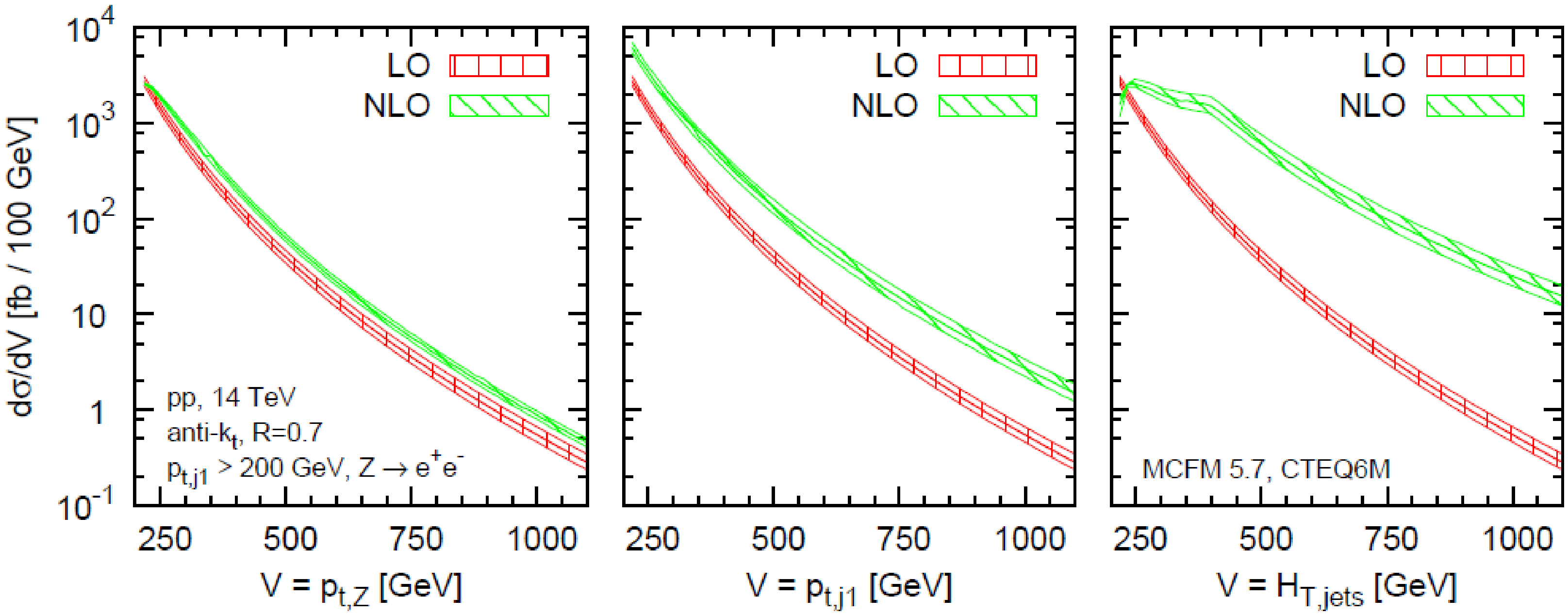

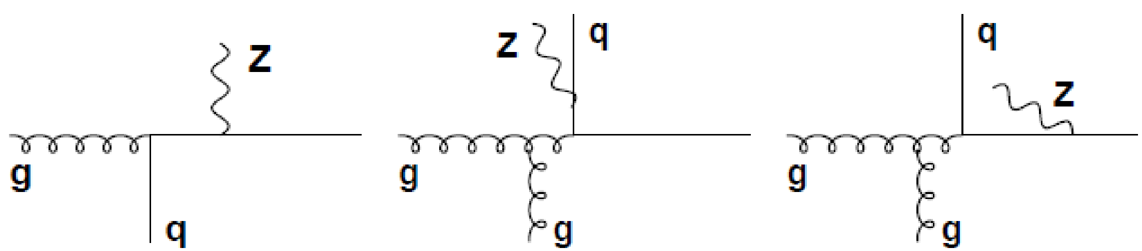

(A) (B) (C)

ATL-CONF-2018-037

EW precision measurements
Weak angle $\sin^2\theta^{l}_{eff}$

$$\frac{d\sigma}{dp_T^{\ell\ell}\, dy^{\ell\ell}\, dm^{\ell\ell}\, d\cos\theta\, d\phi} = \frac{3}{16\pi} \frac{d\sigma^{U+L}}{dp_T^{\ell\ell}\, dy^{\ell\ell}\, dm^{\ell\ell}}$$
$$\Big\{(1+\cos^2\theta) + \frac{1}{2} A_0(1-3\cos^2\theta) + A_1 \sin 2\theta \cos\phi$$
$$+\frac{1}{2} A_2 \sin^2\theta \cos 2\phi + A_3 \sin\theta \cos\phi + A_4 \cos\theta$$
$$+A_5 \sin^2\theta \sin 2\phi + A_6 \sin 2\theta \sin\phi + A_7 \sin\theta \sin\phi\Big\}$$

$$\boxed{A_{FB} = 3/8 \times A_4}$$

ATL-CONF-2018-037

EW precision measurements

Weak angle $\sin^2\theta^l_{eff}$ — W mass m_W

8 TeV data — **7 TeV data**

One wants to have measurements with uncertainties close to the results of the EW fit $\sin^2\theta_{eff} = .23153 \pm .00006$ $m_W = 80354 \pm 7$ MeV

arXiv:1803.01853

Eur.Phys.J. C78 (2018) no.2, 110,
Erratum: Eur.Phys.J. C78 (2018) no.11, 898

F-B asymmetry $q\bar{q} \rightarrow Z/\gamma^* \rightarrow \ell^+\ell^-$

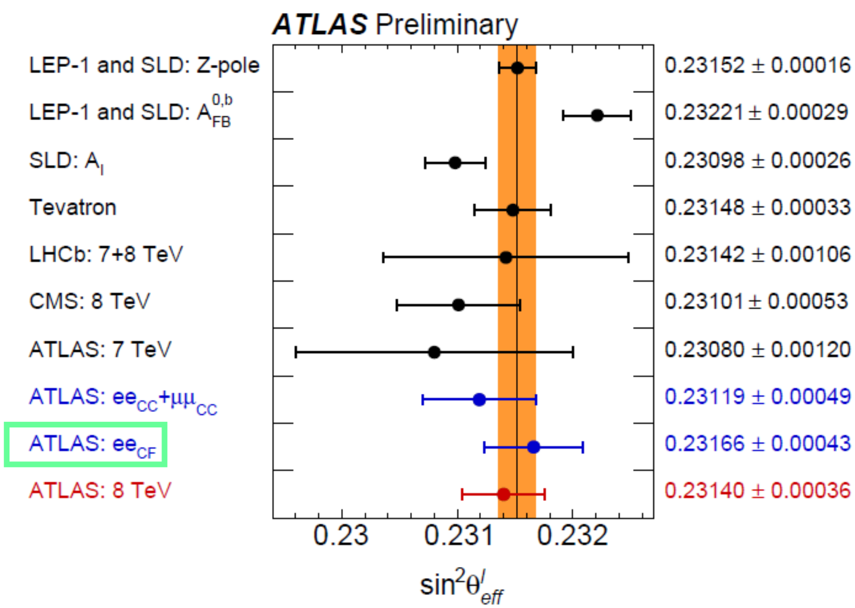

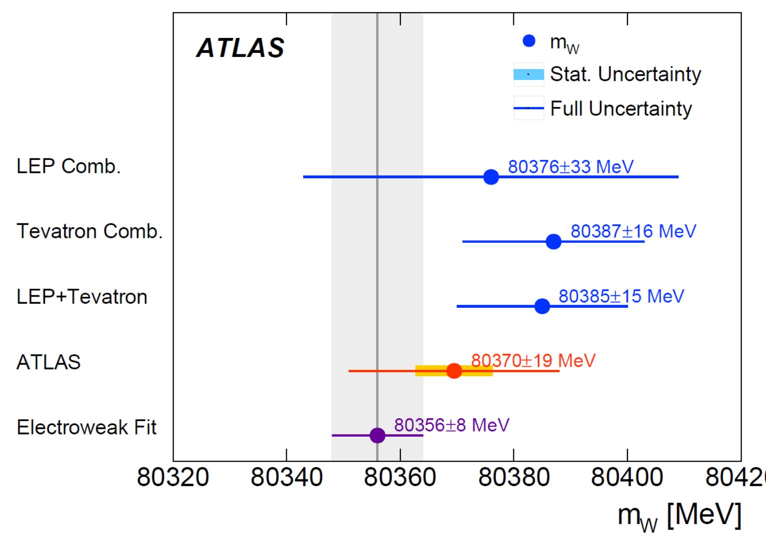

EW precision measurements

W mass m_W

arXiv:1701.07240

$$m_W = 80369.5 \pm 6.8\ \text{MeV(stat.)} \pm 10.6\ \text{MeV(exp. syst.)} \pm 13.6\ \text{MeV(mod. syst.)}$$
$$= 80369.5 \pm 18.5\ \text{MeV},$$

Combined categories	Value [MeV]	Stat. Unc.	Muon Unc.	Elec. Unc.	Recoil Unc.	Bckg. Unc.	QCD Unc.	EW Unc.	PDF Unc.	Total Unc.	χ^2/dof of Comb.
m_T-p_T^ℓ, $W^\pm$, e-μ	80369.5	6.8	6.6	6.4	2.9	4.5	8.3	5.5	9.2	18.5	29/27

EW precision measurements
W mass m_W LHCb

muon p_T based m_W measurement by LHCb *2016 dataset 1.7 fb $^{-1}$*

$$m_W = 80364 \pm 23_{\text{stat}} \pm 11_{\text{exp}} \pm 17_{\text{theory}} \pm 9_{\text{PDF}}\ \text{MeV}$$

Measurement uncertainty summary

Source	Size [MeV]	
Parton distribution functions	**9.0**	Average of NNPDF31, CT18, MSHT20
Theory (excl. PDFs) total	**17.4**	
Transverse momentum model	12.0	Envelope from five different models
Angular coefficients	9.0	"Uncorrelated" 31 point scale variation
QED FSR model	7.2	Envelope of Pythia, Photos and Herwig
Additional electroweak corrections	5.0	Test with POWHEGew
Experimental total	**10.6**	
Momentum scale and resolution modelling	7.5	Includes simple statistical contributions, dependence on external inputs and details of the methods.
Muon ID, trigger and tracking efficiency	6.0	
Isolation efficiency	3.9	
QCD background	2.3	
Statistical	**22.7**	
Total	**31.7**	

Zγjj EW

ATLAS-CONF-2021-038

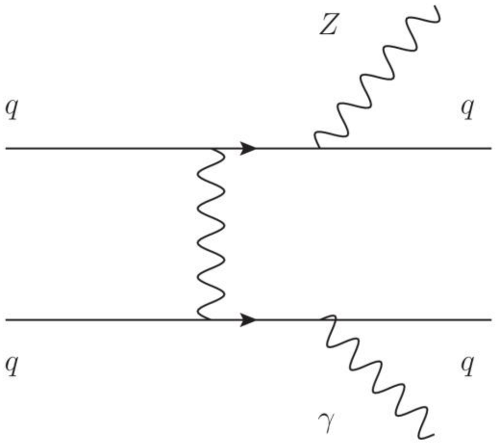

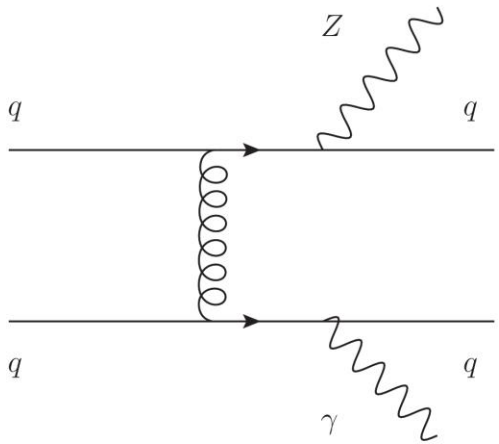

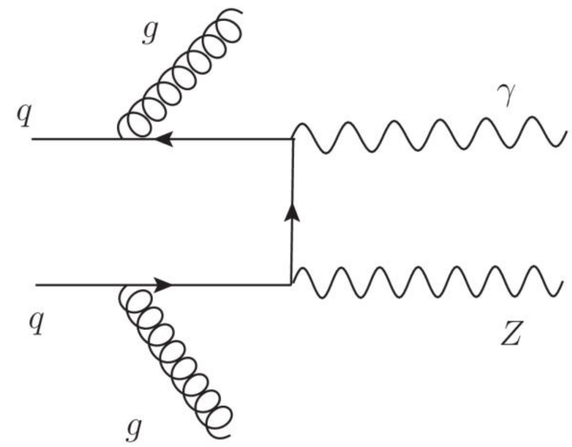

electroweak non-VBS signal

QCD-induced backgrounds with

gluon exchange

gluon radiation

$Z\gamma jj$ EW (CMS)

arXiv:2106.11082

EW $Z\gamma jj$ production is $5.21 \pm 0.52\,(\text{stat}) \pm 0.56\,(\text{syst})$ fb

$$= 5.21 \pm 0.76\,\text{fb}$$

observed and expected signal significances are well in excess of 5 standard deviations

♪ ***Results***

- ***detector***
- ***SM (including multibosons and VBS)***
- ***BSM***
- ***(B-E)H***

SUSY Electroweak

arXiv:2108.07586

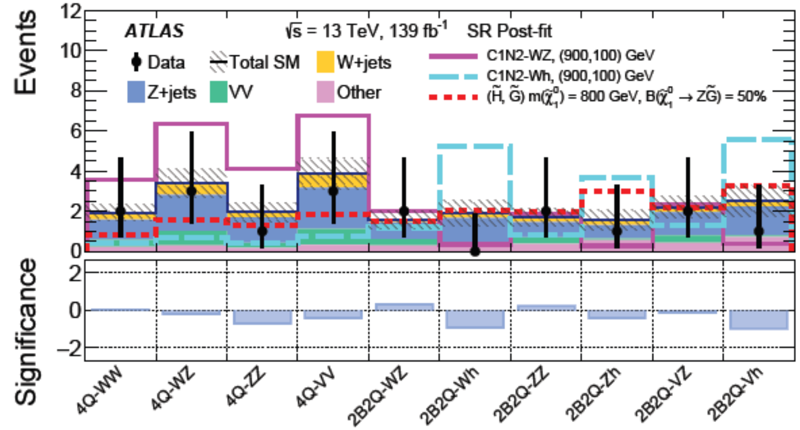

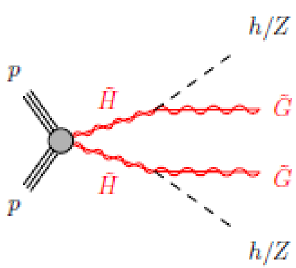

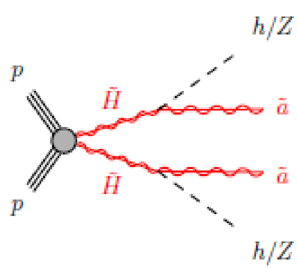

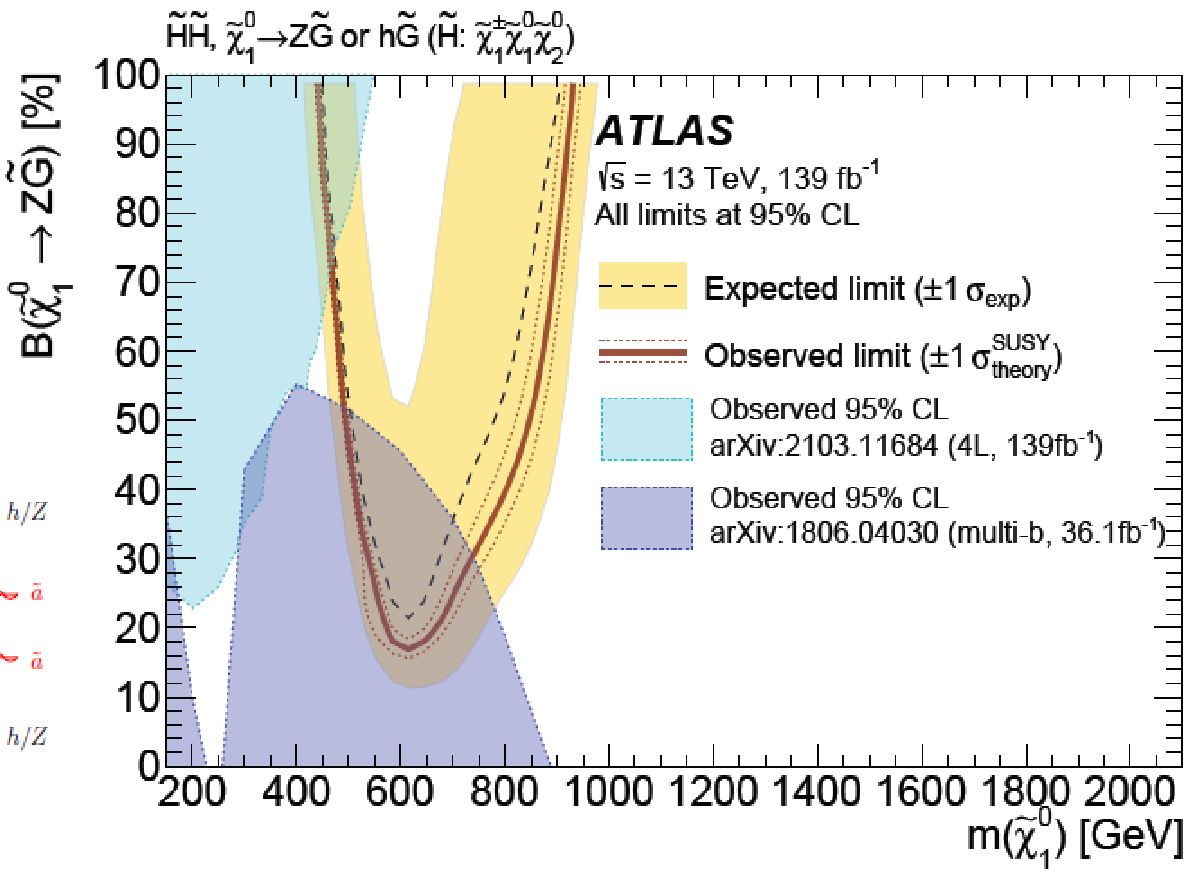

Flavour anomalies and vector leptoquarks

$LQ_3^V \to b\tau$ / $t\nu_\tau$

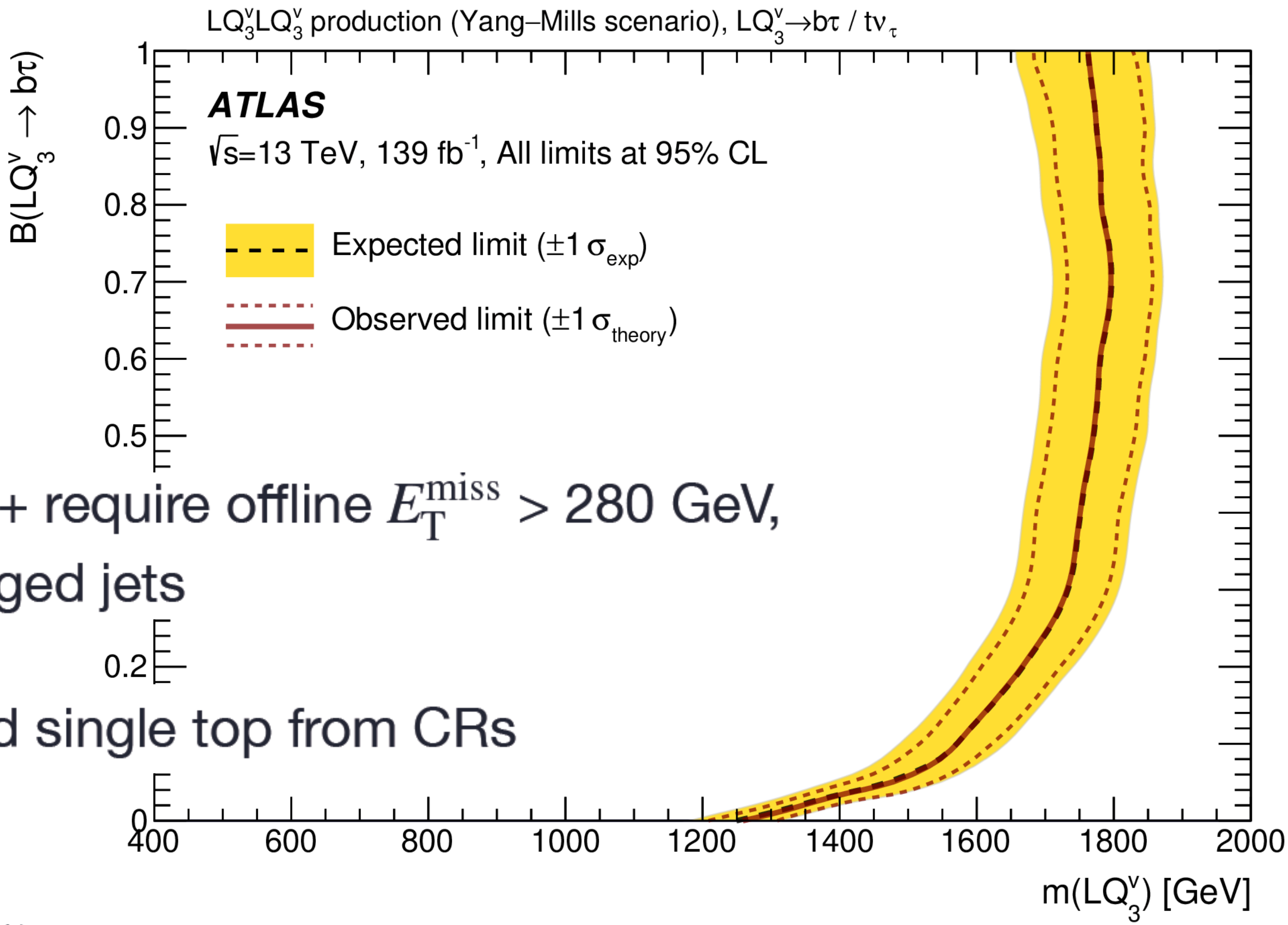

Trigger on E_T^{miss} + require offline E_T^{miss} > 280 GeV,

1 τ_{had}, ≥ 2 b-tagged jets

Main bkg: $t\bar{t}$ and single top from CRs

Addresses $R(D^{(*)})$ anomaly at ~expected scale

https://atlas.web.cern.ch/Atlas/GROUPS/PHYSICS/PAPERS/SUSY-2019-18/

♪ ***Results***

- ***detector***
- ***SM (including multibosons and VBS)***
- ***BSM***
- ***(B-E)H***

1 Additional BEH bosons $\gamma\gamma$ excess at 95 GeV

CMS PAS HIG-17-013

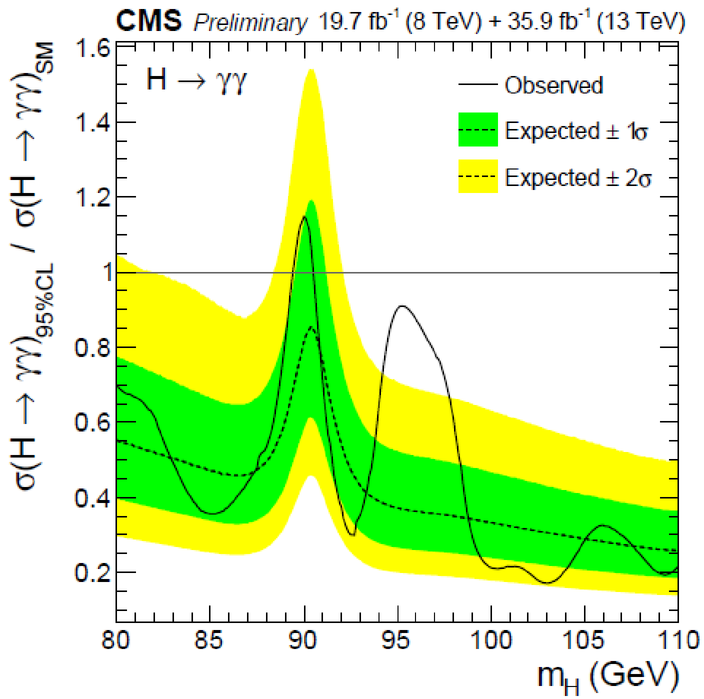

these yield an excess with approximately 2.8σ local (1.3σ global) significance for the same hypothesis mass as for the 13 TeV dataset alone, mass of 95.3 GeV.

1 Additional BEH bosons $\gamma\gamma$ excess at 95 GeV

CMS PAS HIG-17-013

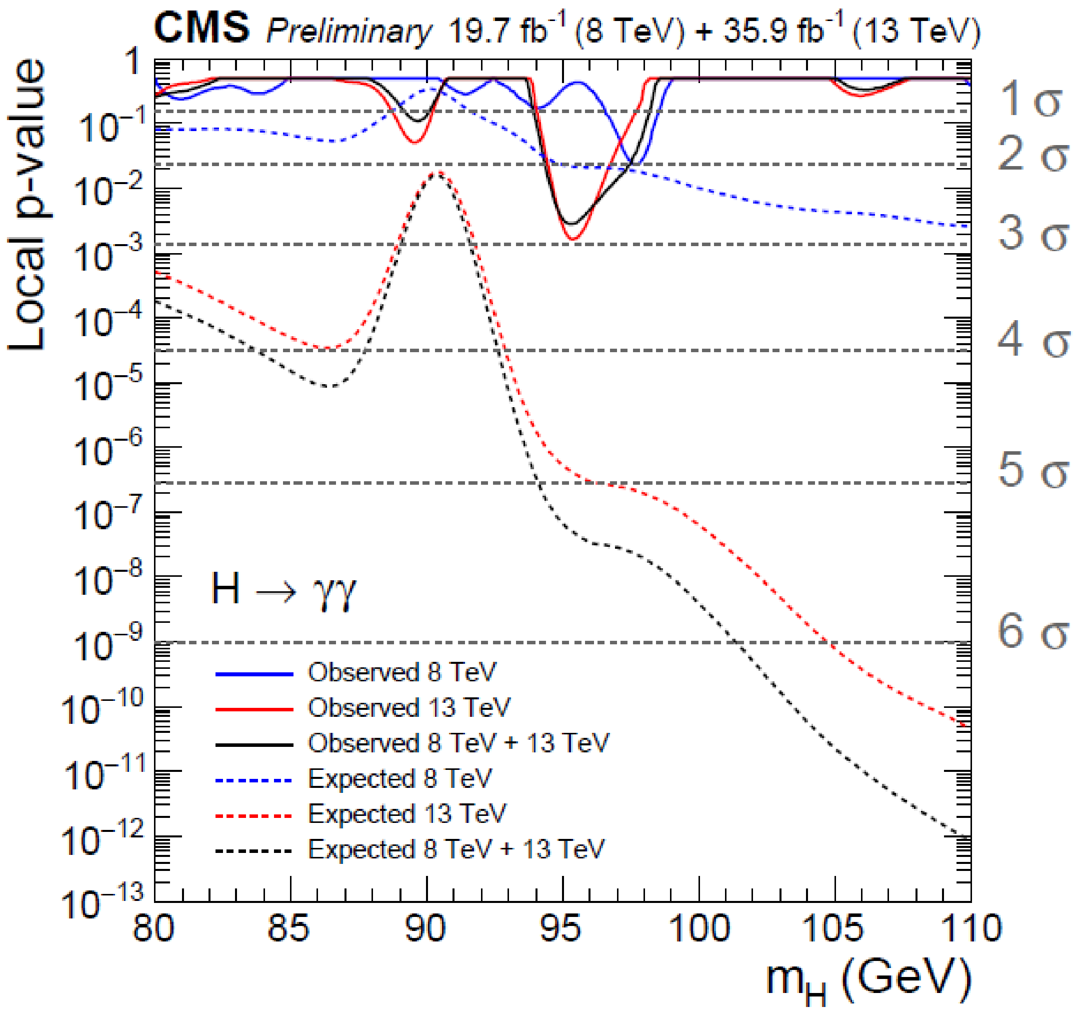

1 Additional BEH bosons $\gamma\gamma$ excess at 95 GeV

CMS PAS HIG-17-013

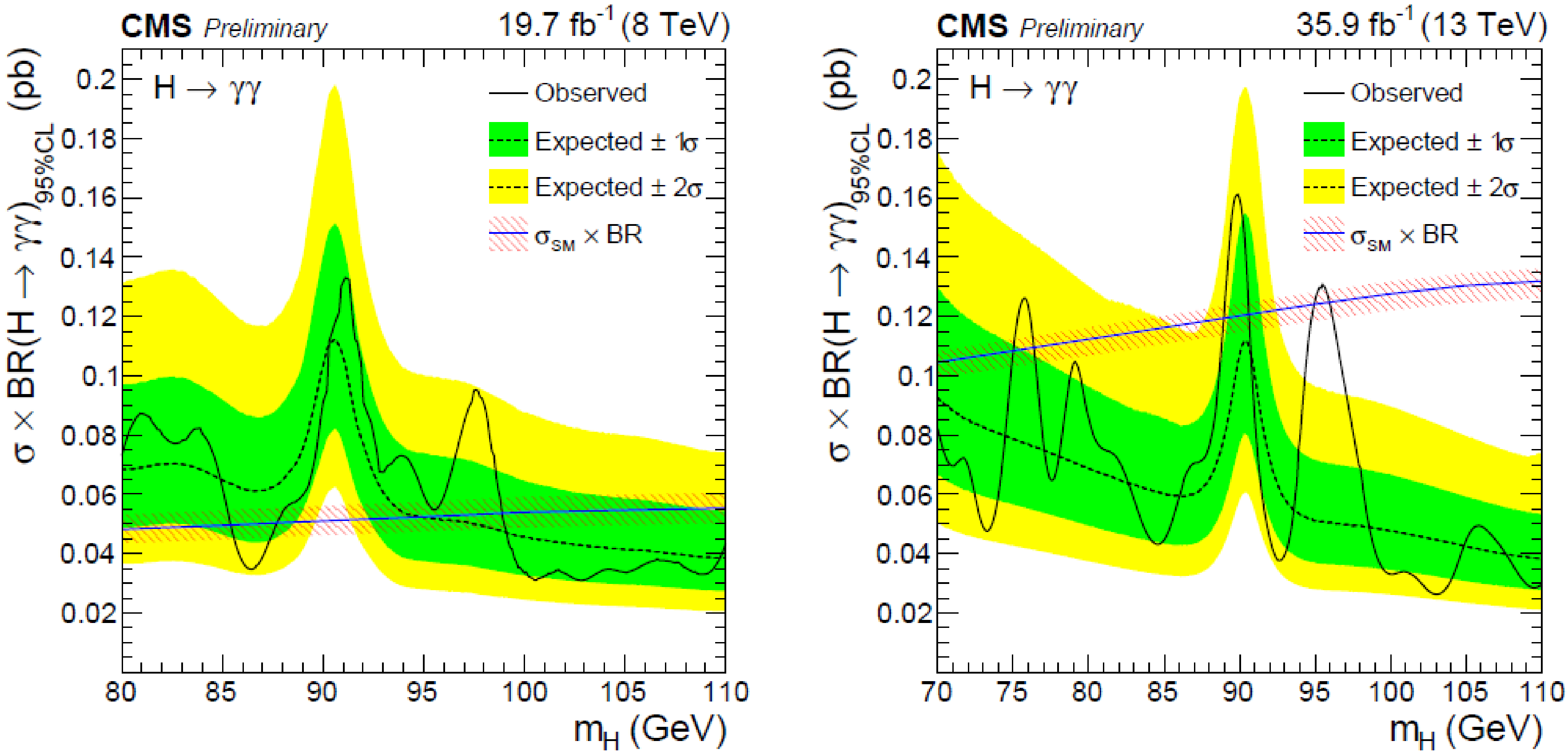

1 Additional BEH bosons $\gamma\gamma$ excess at 95 GeV

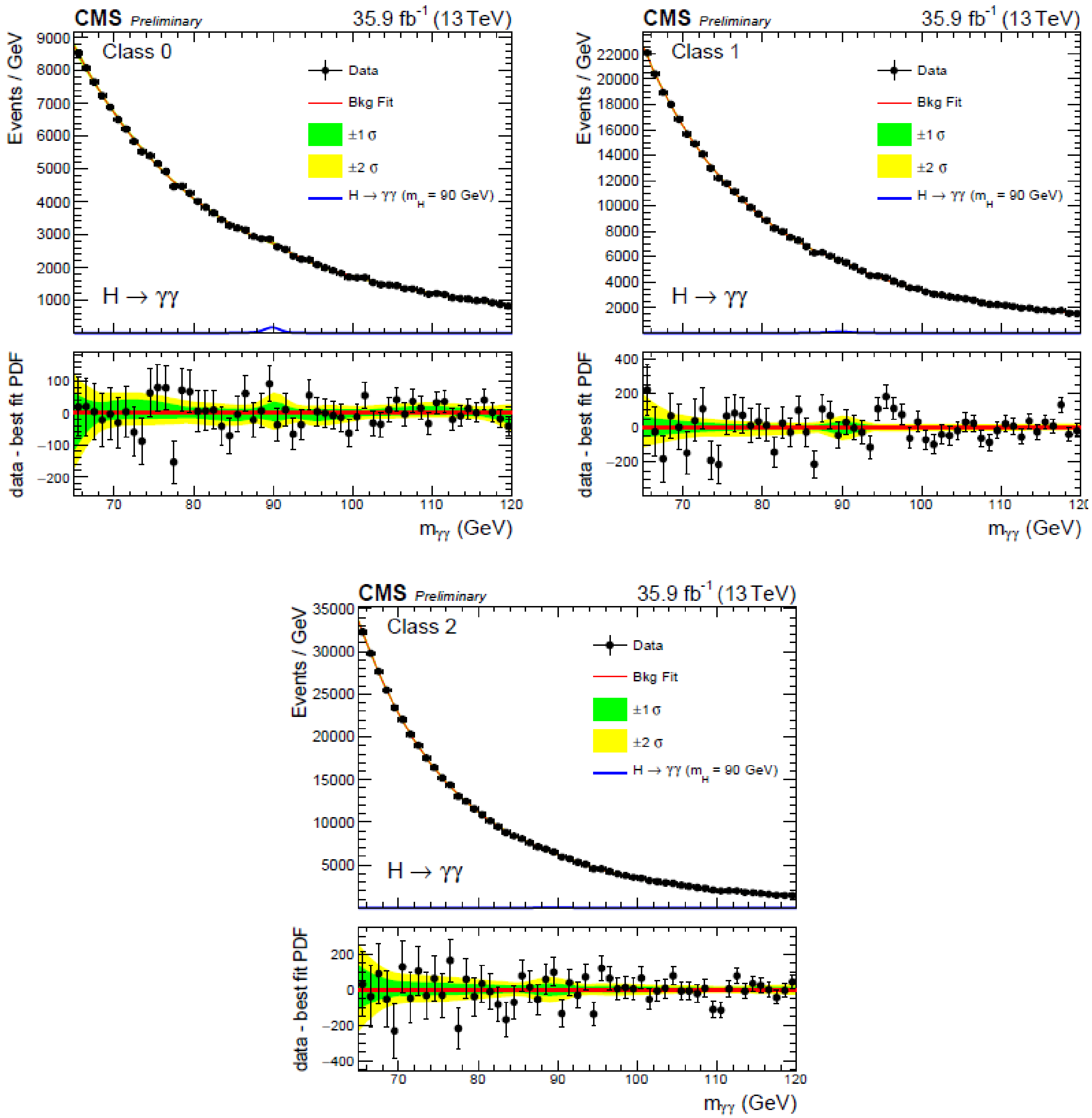

CMS PAS HIG-17-013

1 Additional BEH bosons $\gamma\gamma$ excess at 95 GeV

CMS PAS HIG-17-013

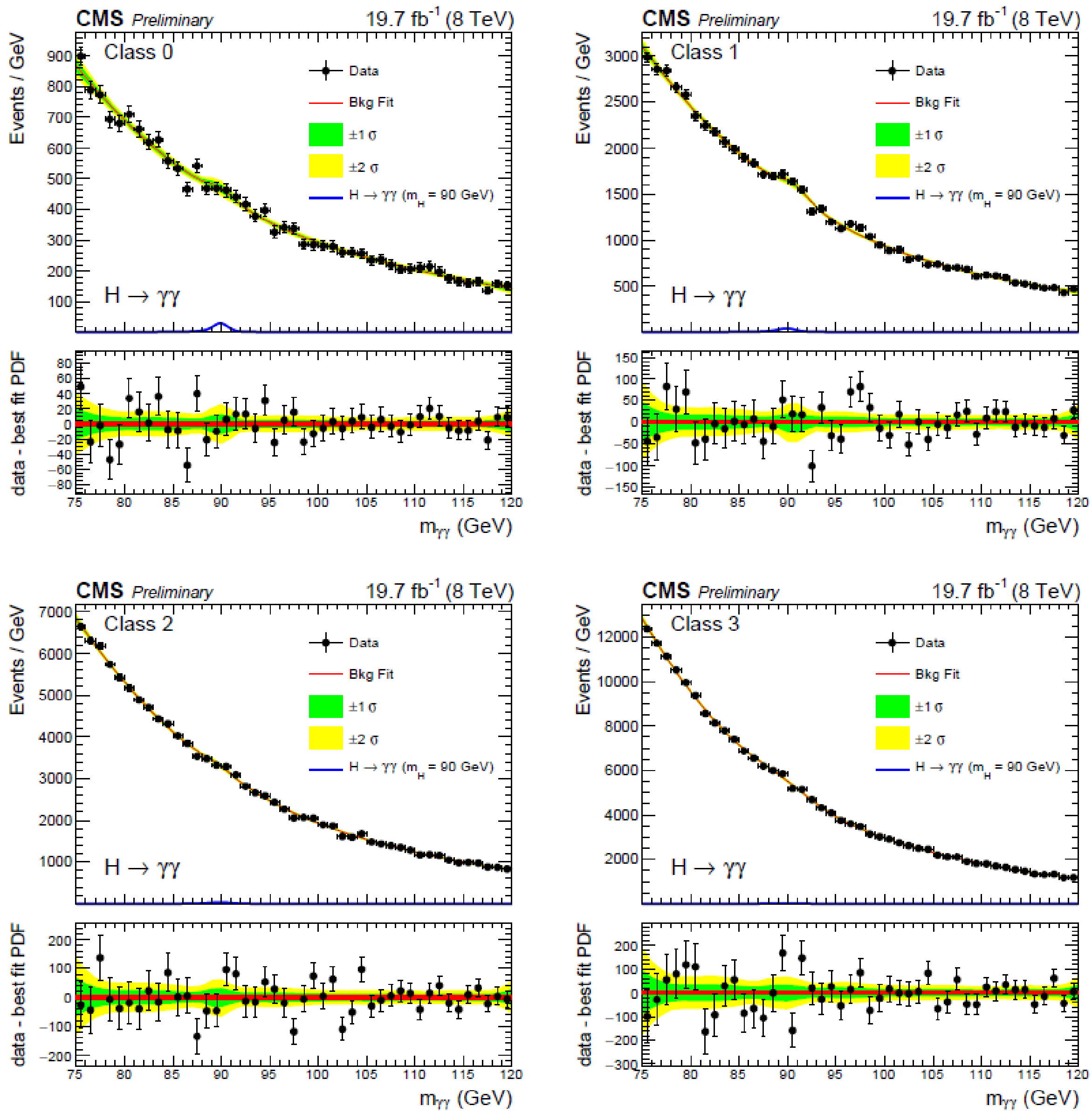

Search for the standard model Higgs boson at LEP

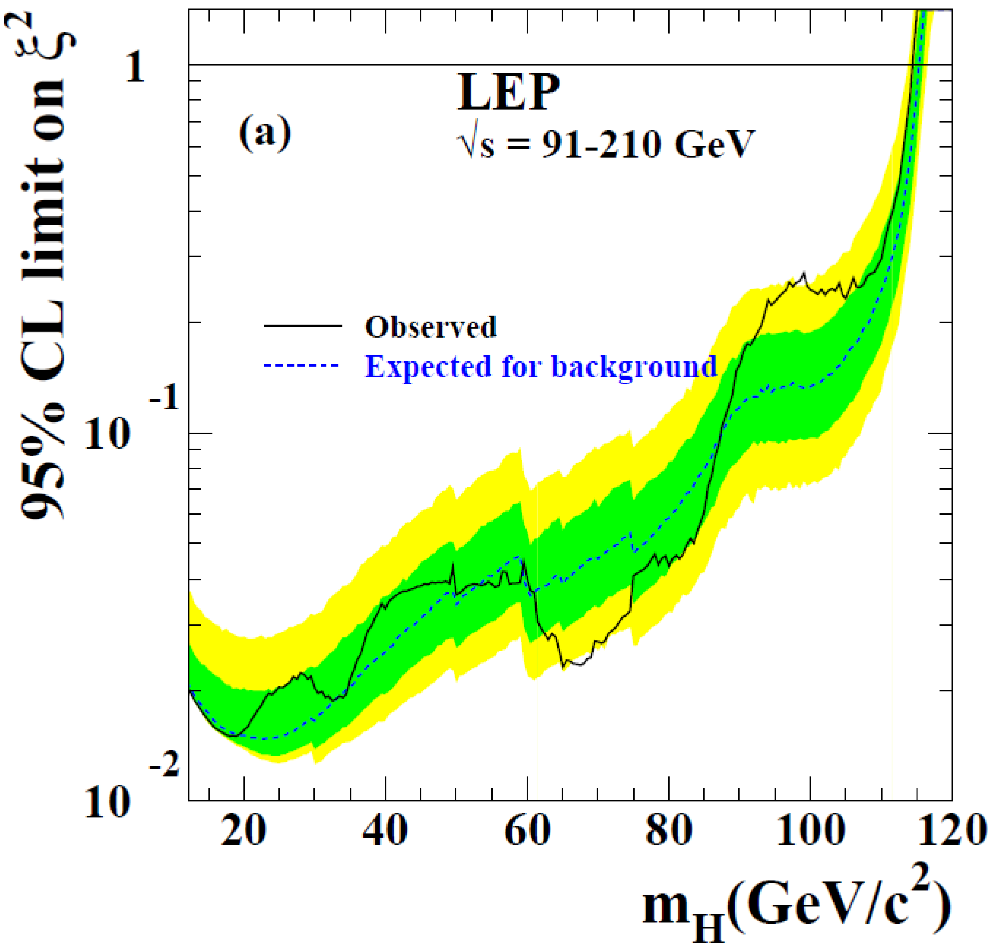

Phys.Lett. B565 (2003) 61-75

1 Additional BEH bosons $\gamma\gamma$ excess at 95 GeV

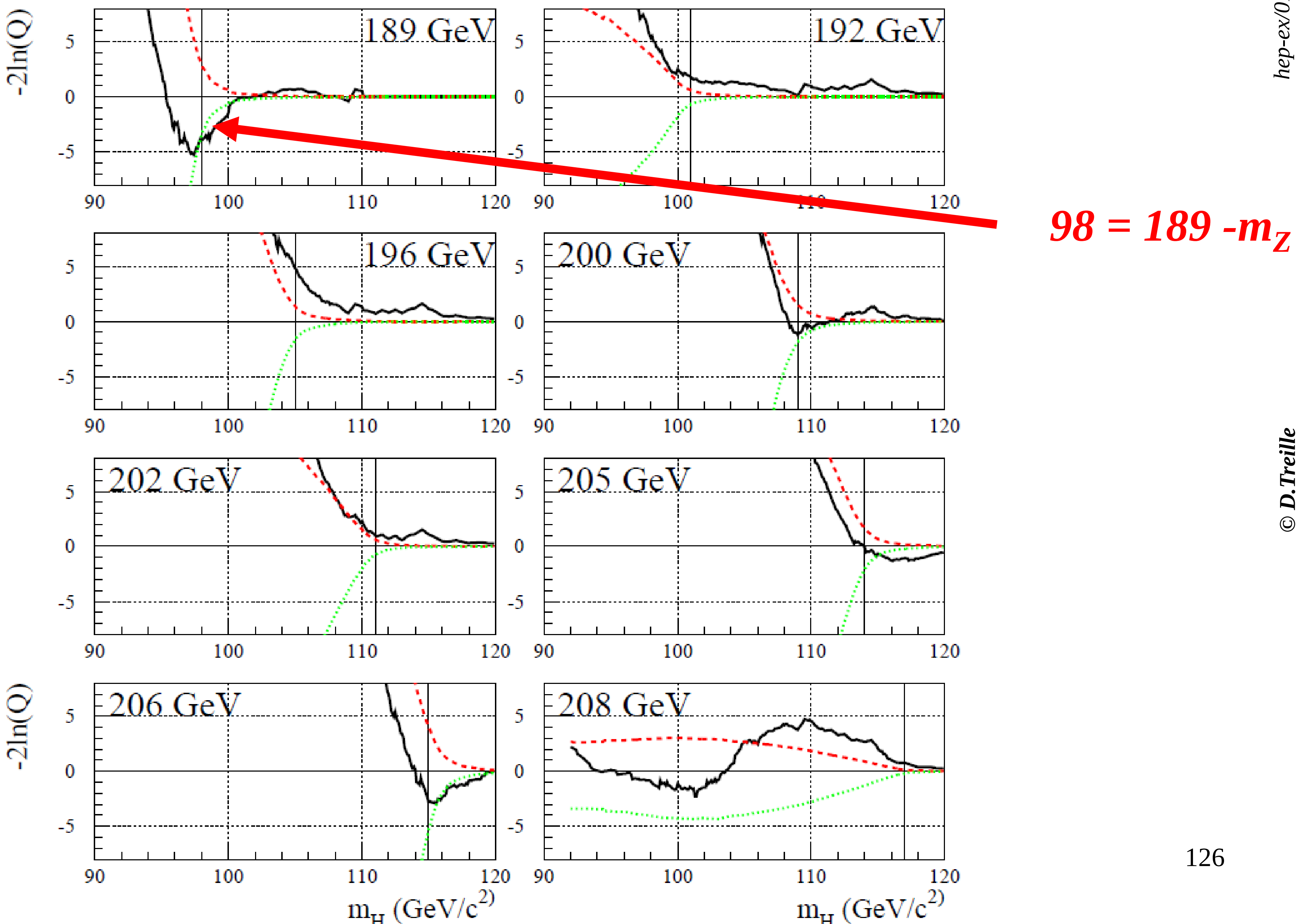

hep-ex/0107029

1 exotic decays of standard BEH boson

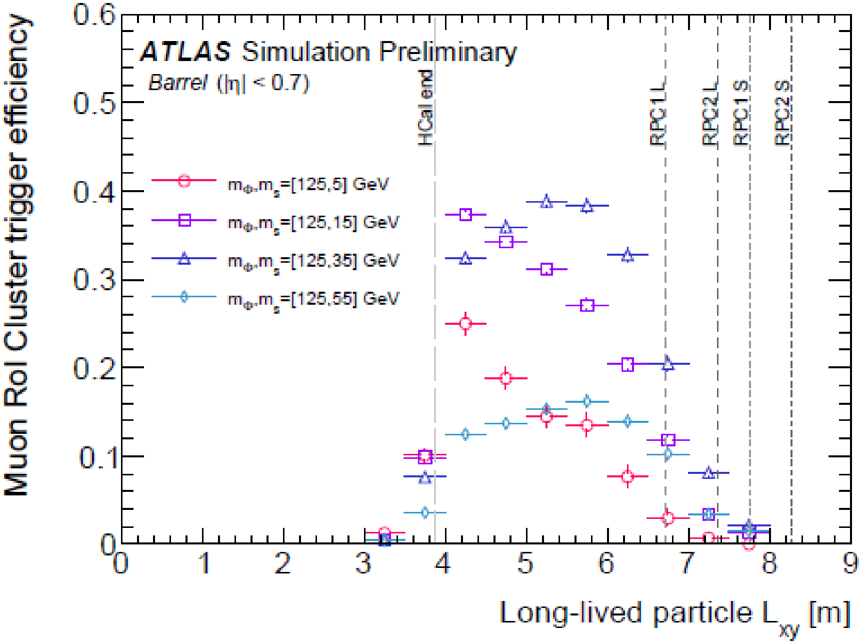

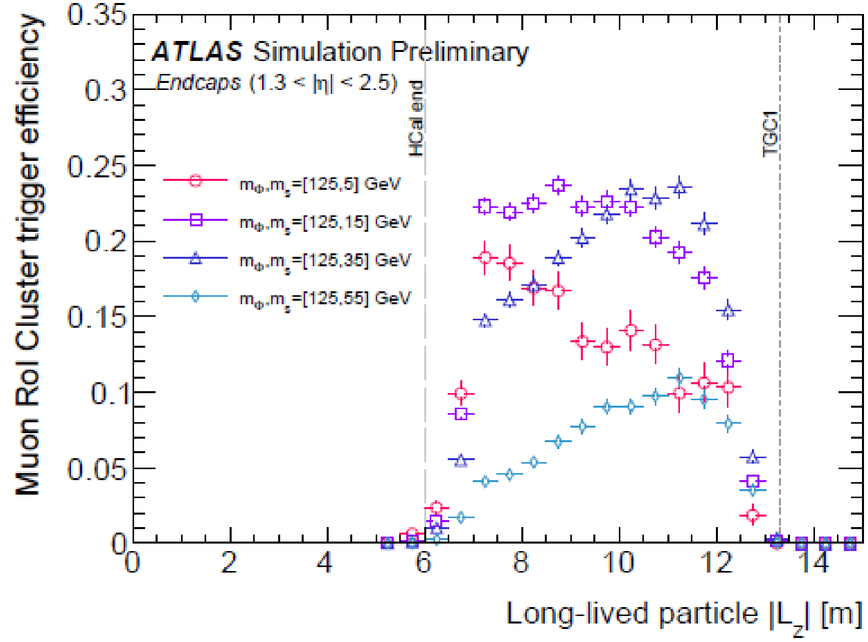

1 Additional BEH bosons $\gamma\gamma$ excess at 95 GeV

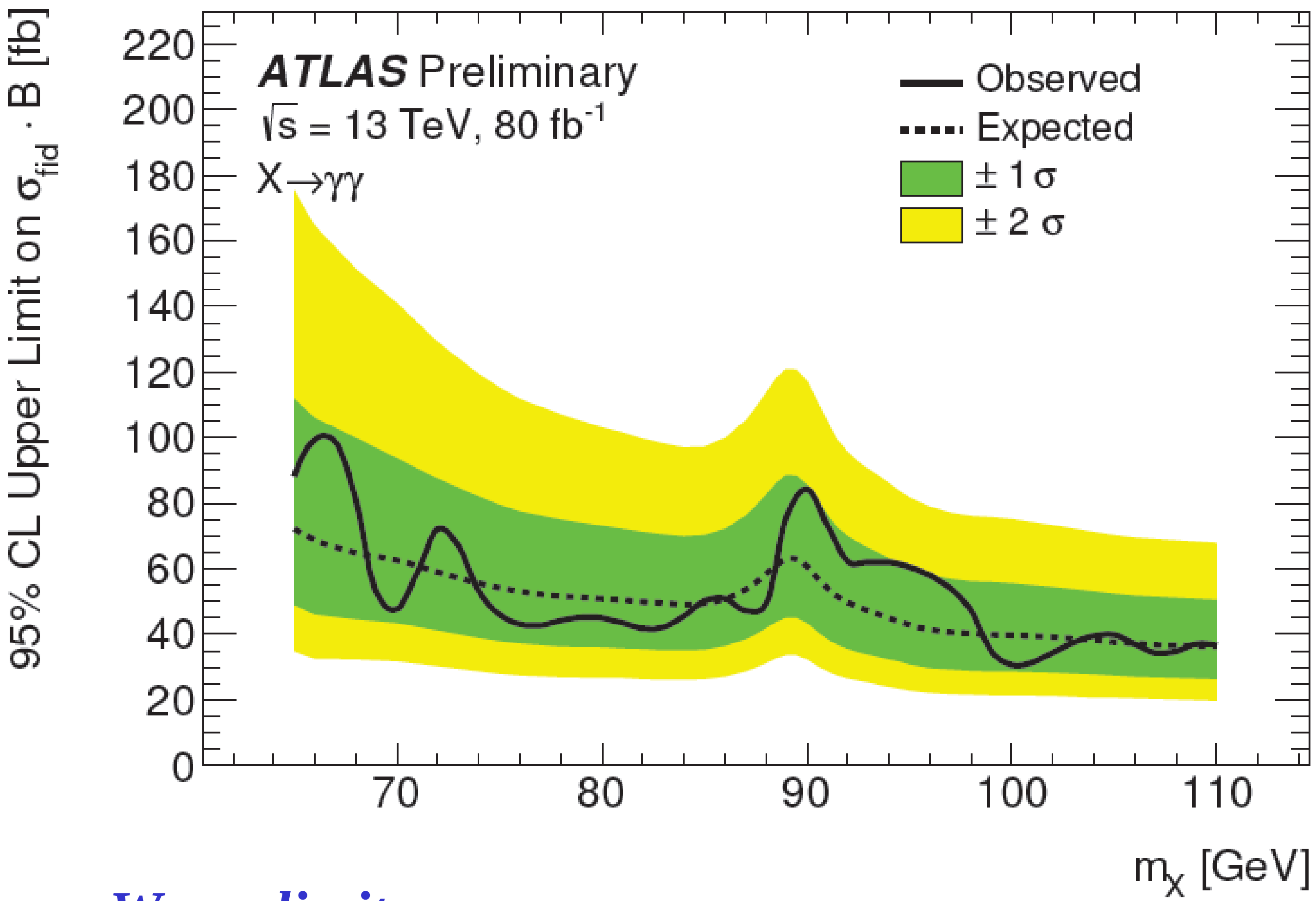

ATLAS-CONF-2018-025

.. ***Worse limit***

2 The SM BEH boson

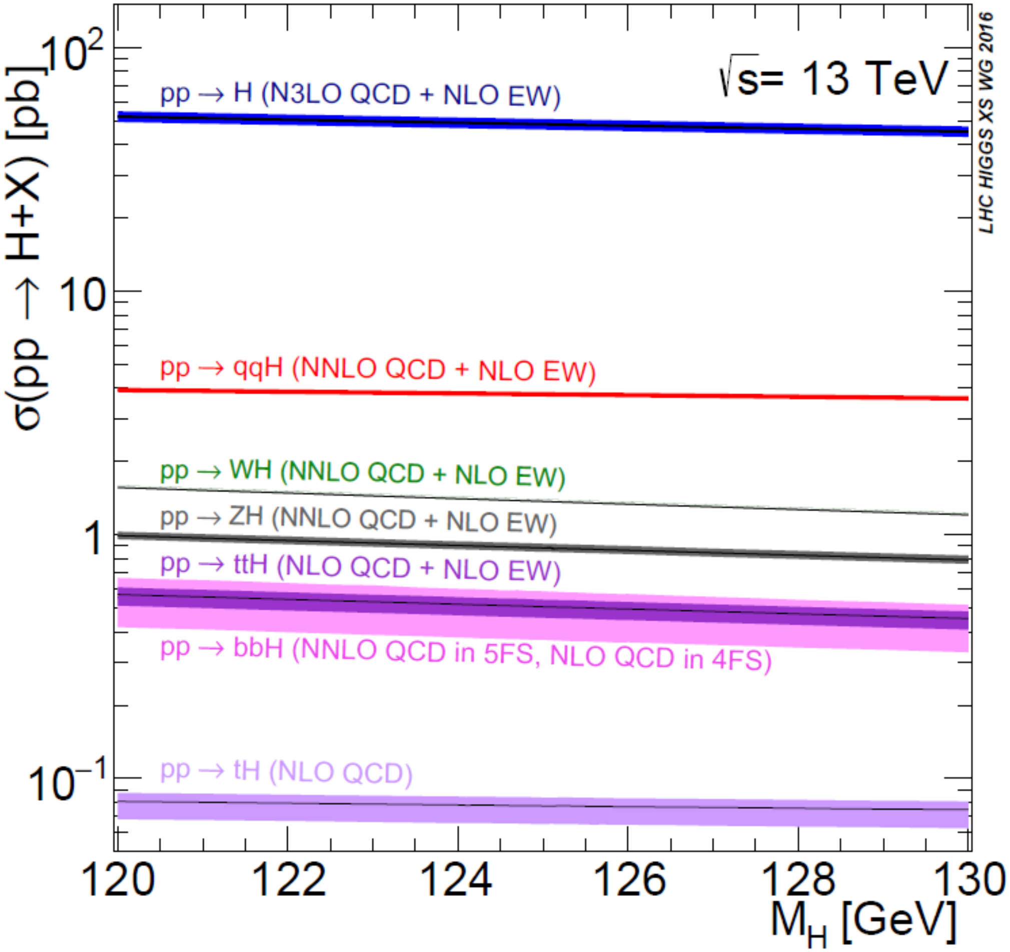

arXiv:1610.07922

2 The SM BEH boson

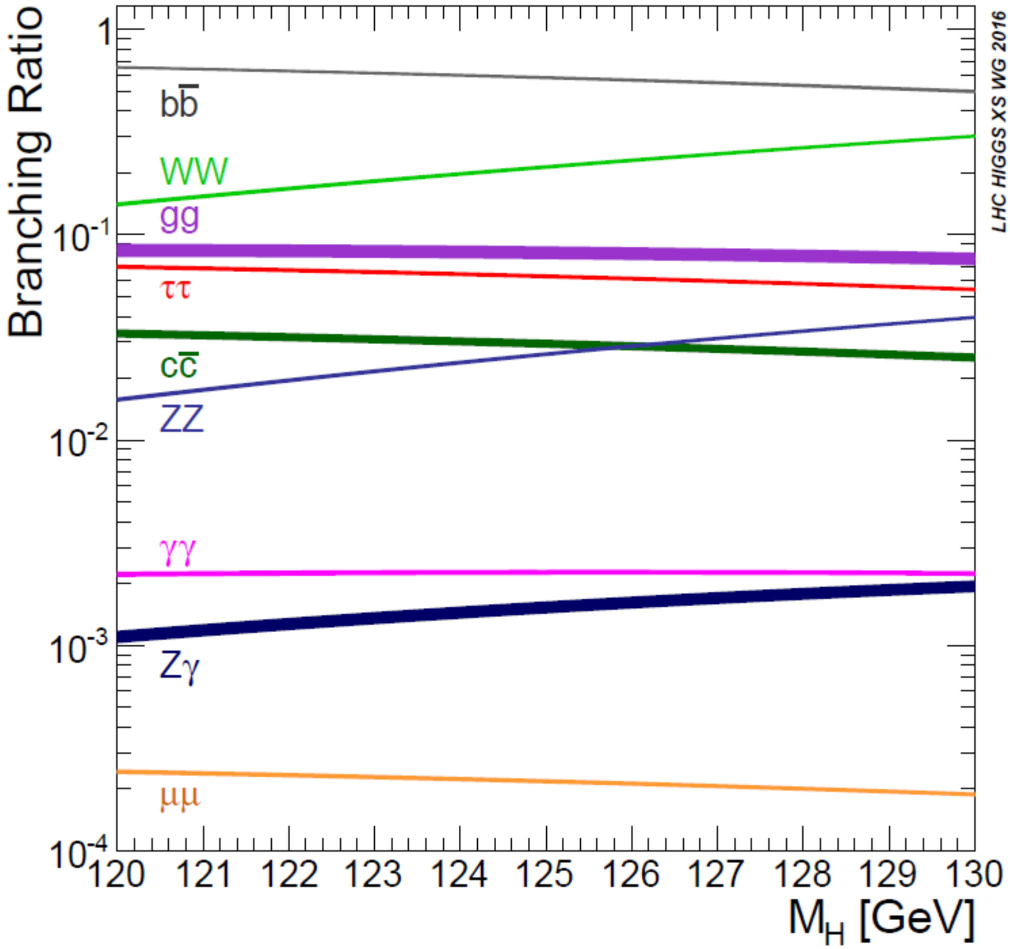

arXiv:1610.07922

2 The SM BEH boson

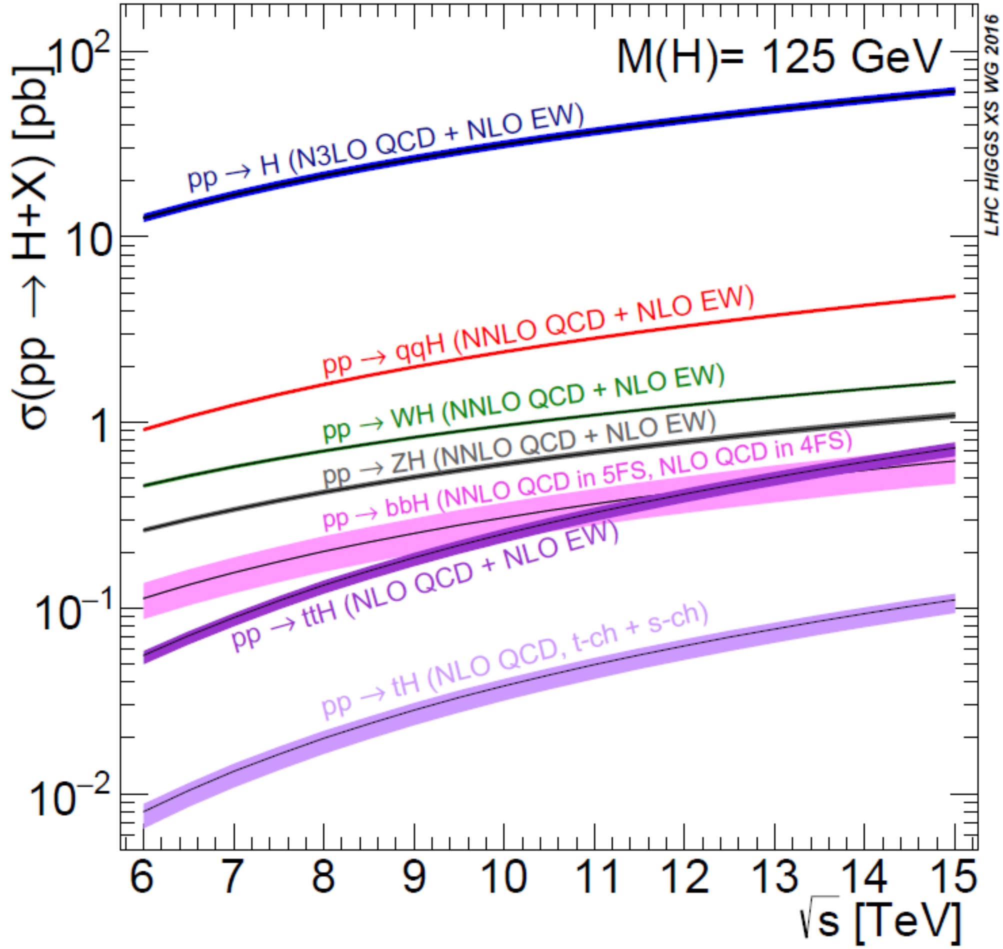

arXiv:1610.07922

2 The SM BEH boson (final Run-1 ATLAS + CMS result)

PRL **114,** 191803 (2015)

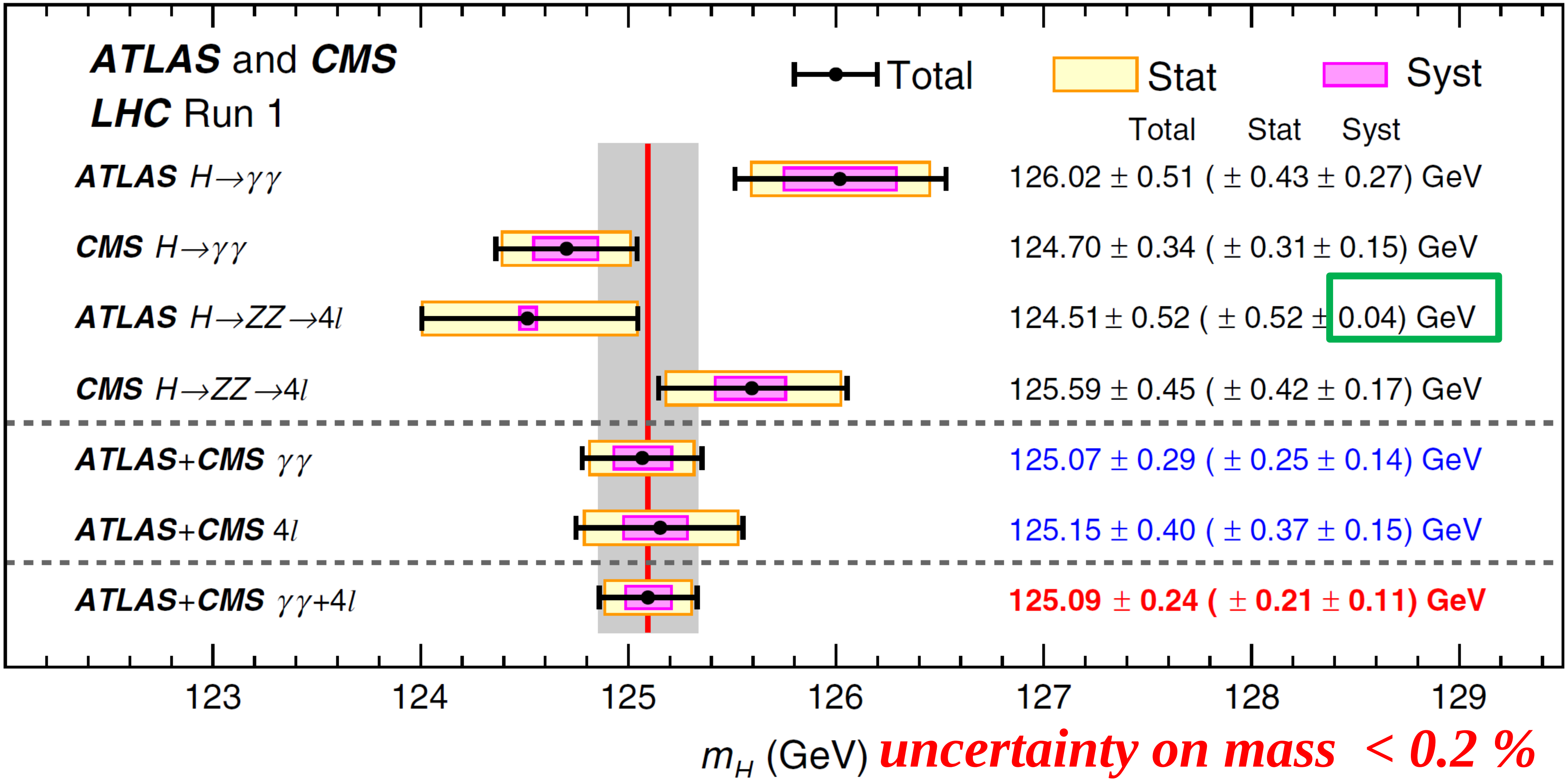

uncertainty on mass < 0.2 %

Remember ATLAS has an uncertainty on W mass of 19 MeV *Eur.Phys.J. C78 (2018) no.2, 110*

note that $\Delta m_H = 0.1$ GeV $\rightarrow \Delta(BR(H\rightarrow ZZ)) / BR(H\rightarrow ZZ) \sim 1\%$

At longer term uncertainty will be dominated by 4l

(for $H\rightarrow \gamma\gamma$: need to extrapolate from e to γ !)

2 The SM BEH boson $H \to \gamma\gamma$

ATLAS-CONF-2020-026

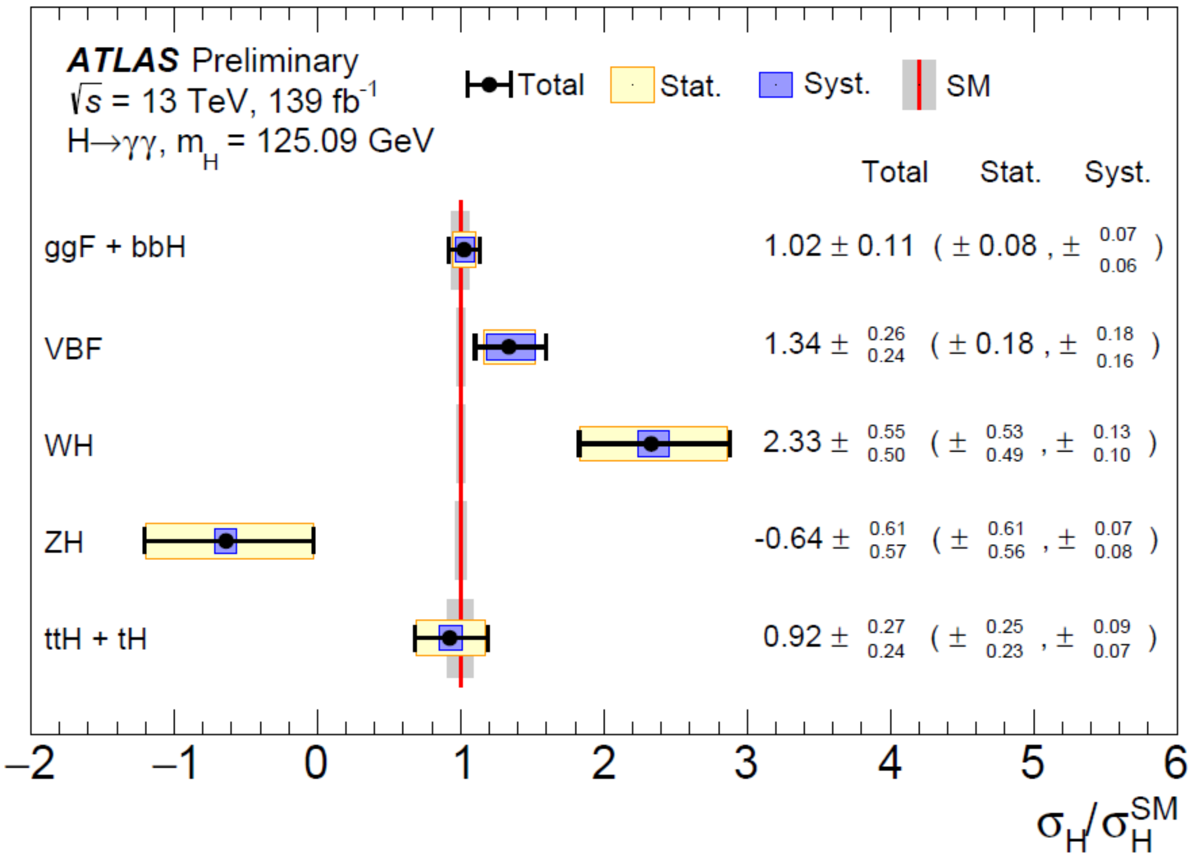

2 The SM BEH boson Interference in $\gamma\gamma$ (between signal and background)

start to be sensitive to **subtle effects** *like interference*

(between signal and background) in $\gamma\gamma$

Martin, Dixon and Li Phys.Rev.Lett. 111 (2013) 11180

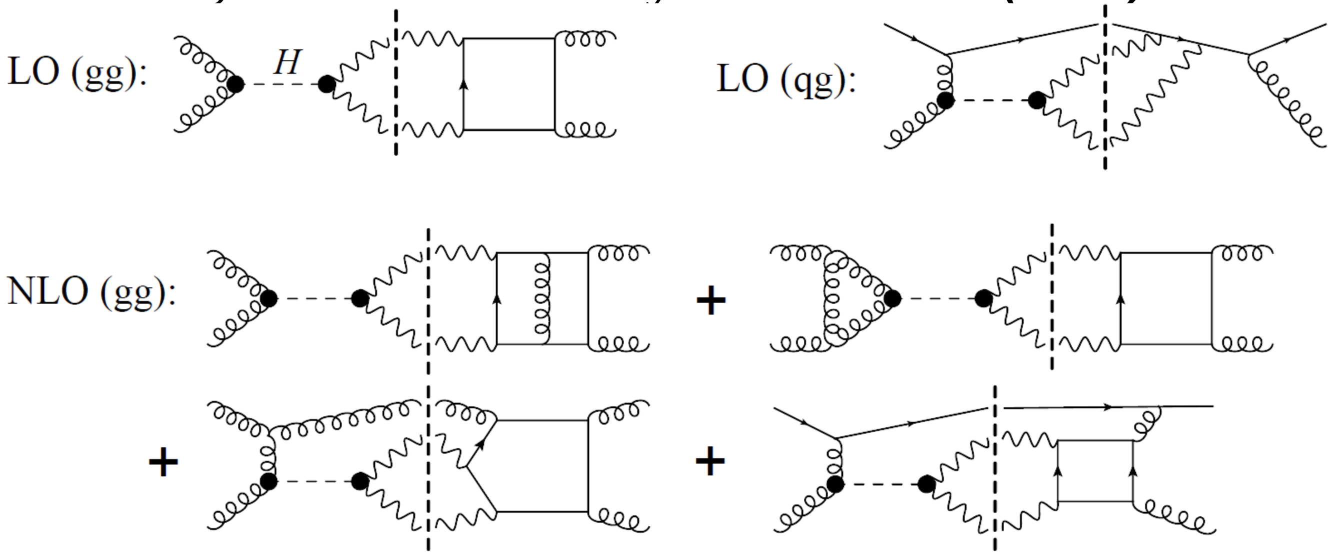

Interference depends of S/B , therefore is <u>*smaller at high p_T(H)*</u> *where S/B is larger*

some work can be done at high pT (H+2j) see for instance Phys.Rev. D92 (2015) no.1, 013004

2 The SM BEH boson Mass shift

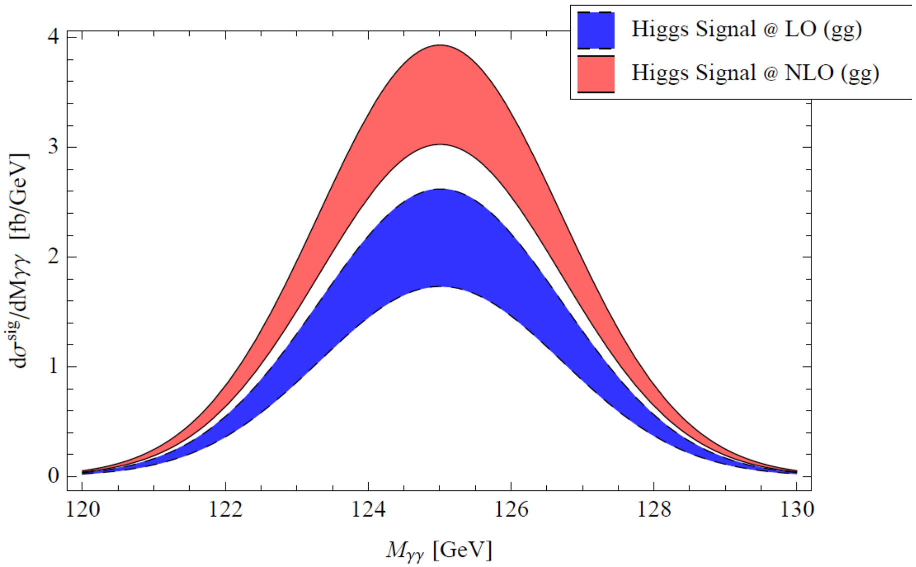

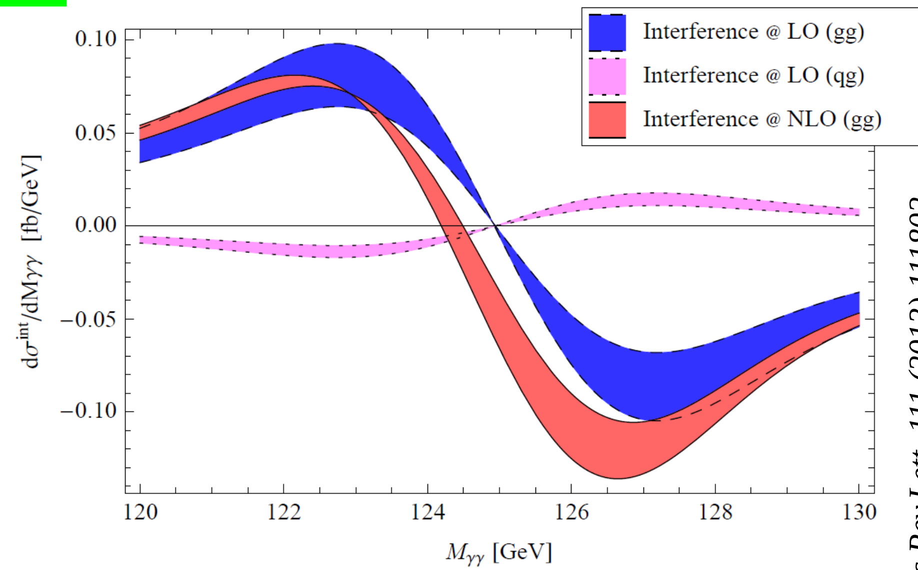

L.Dixon and Y.Li Phys.Rev.Lett. 111 (2013) 111802

The expected median mass shift is found to be $\Delta m_H = -35 \pm 9$ MeV assuming a Standard Model width of 4 MeV for the Higgs boson

ATL-PHYS-PUB-2016-009

However the effect is larger for larger H width
→ could constrain the H width

There is also an effect on the cross-section measurement (few %) to be taken into account

2 The SM BEH boson $H \to l\, l\, \gamma$

Phys. Lett. B 819 (2021) 136412
C.Tackmann EPS 21

Low invariant mass range: $m_{\ell\ell} < 30$ GeV, dominated by $H \to \gamma^* \gamma$

Dedicated trigger and identification of low-$m_{\ell\ell}$ electron pairs

- Overlapping showers in electromagnetic calorimeter
- Performance validated with low-R converted photons

Background parametrized by analytic functions

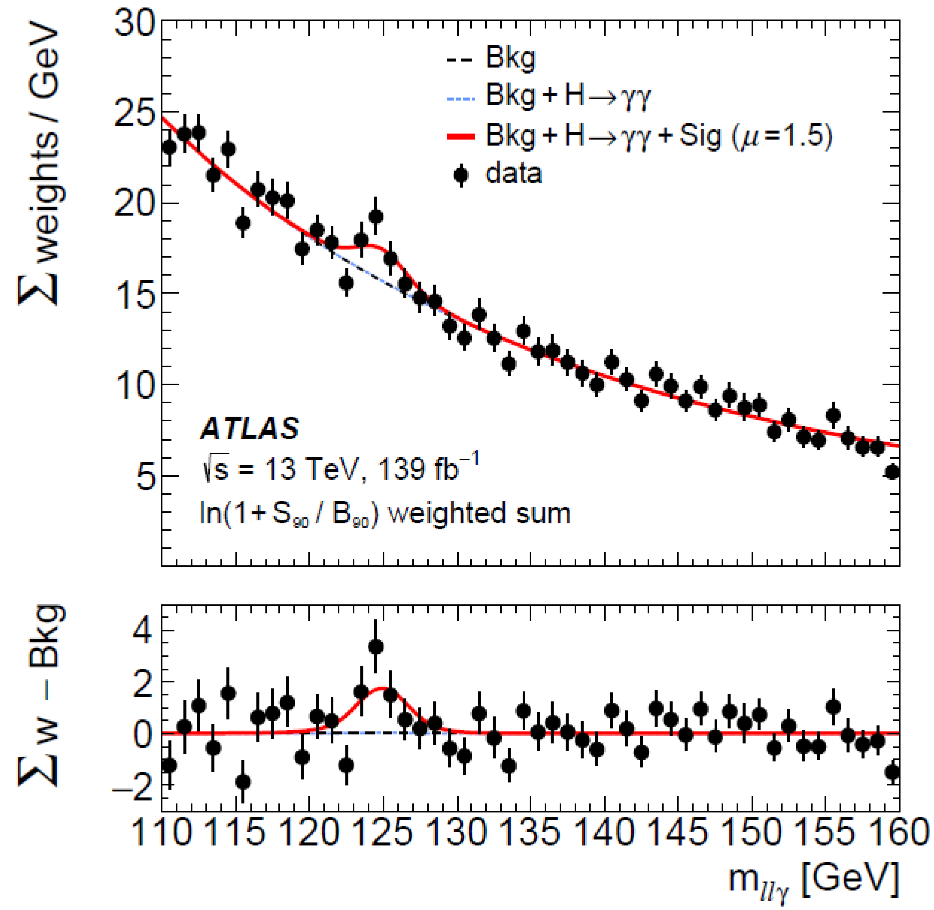

Significance: 3.2 σ obs. (2.1 σ exp.)

2 The SM BEH boson $H\to l\, l\, \gamma$

Phys. Lett. B 819 (2021) 136412

C.Tackmann EPS 21

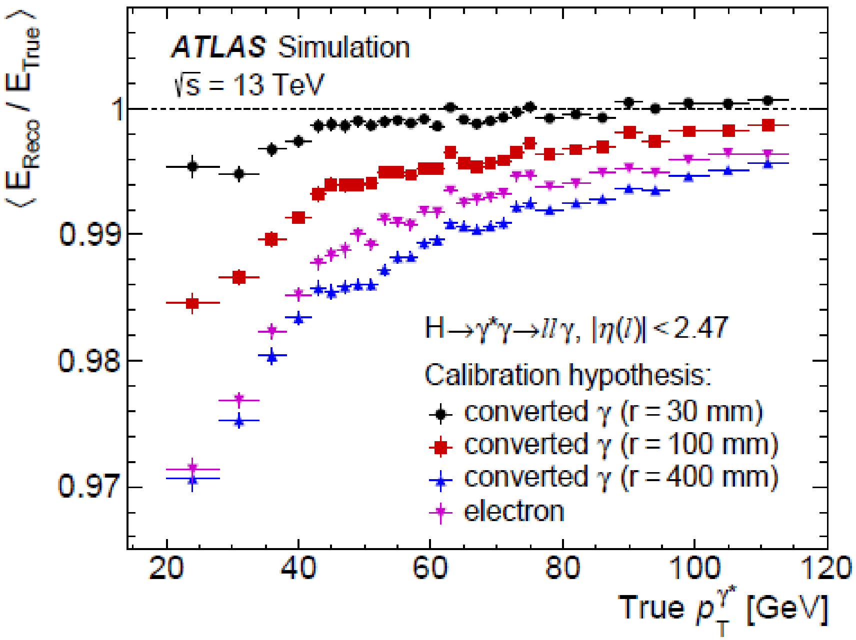

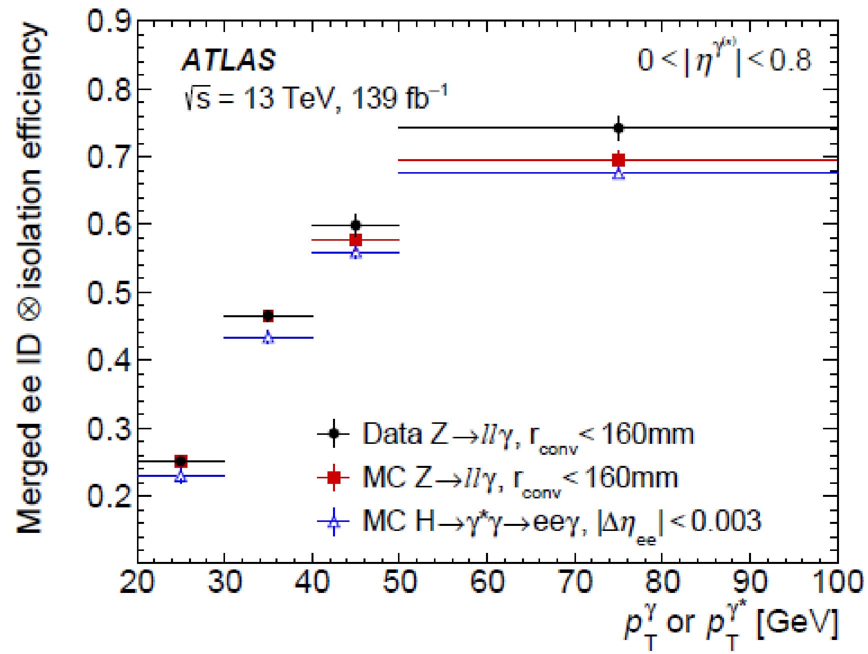

2 The SM BEH boson $H \to Z\gamma$

Phys.Lett.B 809 (2020) 135754

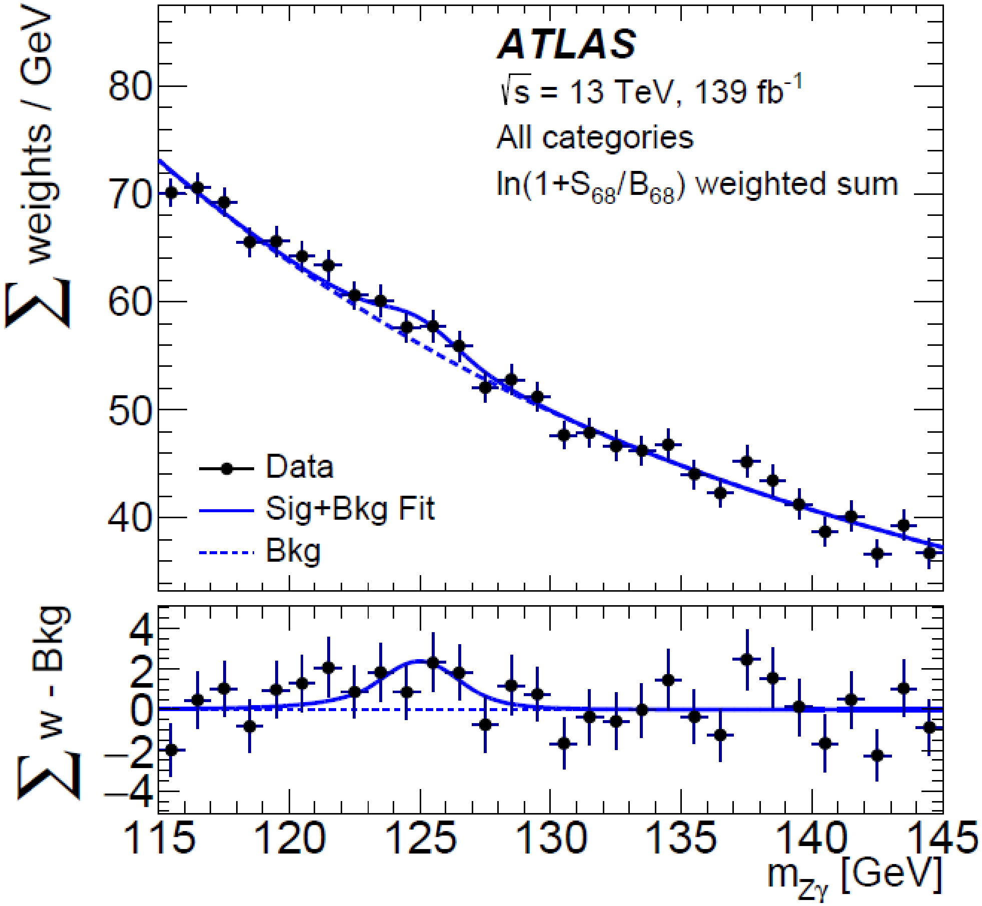

Significance: 2.2 σ obs. (1.2 σ exp.)

value for the signal yield normalised to the Standard Model prediction is $2.0^{+1.0}_{-0.9}$

2 The SM BEH boson ($H \to \tau\tau$) τ reconstruction

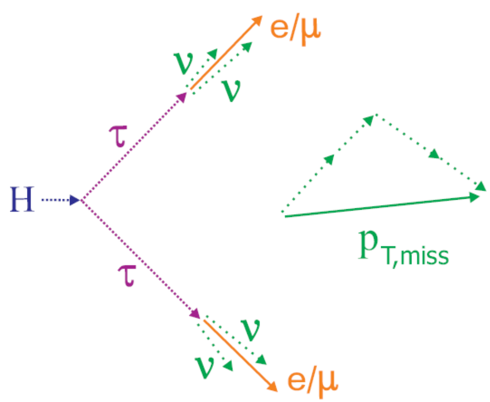

reconstruction of Higgs mass with collinear approximation and angle between the two τ

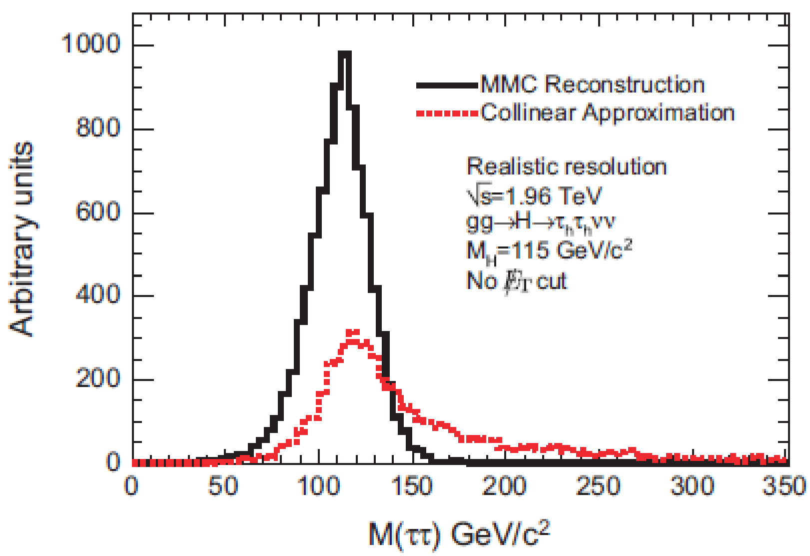

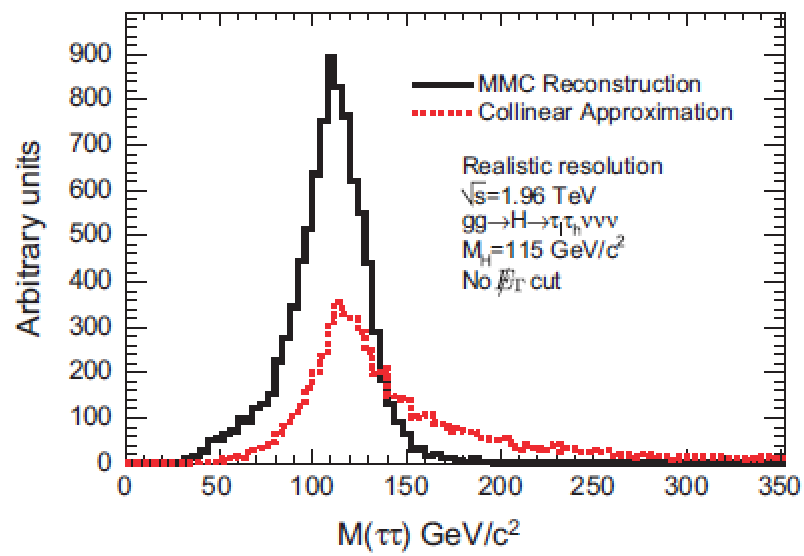

Nucl.Instrum.Meth. A654 (2011) 481-489

Improvement comes from requiring that the relative orientations of the neutrinos and other decay products are consistent with the mass and kinematics of a τ lepton decay

2 The SM BEH boson $H \to \tau\tau$

Source of uncertainty	Impact on $\Delta\sigma / \sigma(pp \to H \to \tau\tau)$ [%] Observed	Expected
Theoretical uncertainty in signal	8.1	8.6
Jet and $\vec{E}_T^{miss}$	4.2	4.1
Background sample size	3.7	3.4
Hadronic τ decays	2.0	2.1
Misidentified τ	1.9	1.8
Luminosity	1.7	1.8
Theoretical uncertainty in Top processes	1.4	1.2
Theoretical uncertainty in Z+jets processes	1.1	1.1
Flavor tagging	0.5	0.5
Electrons and muons	0.4	0.3
Total systematic uncertainty	11.1	11.0
Data sample size	6.6	6.3
Total	12.8	12.5

2 The SM BEH boson $H \to \tau\tau$

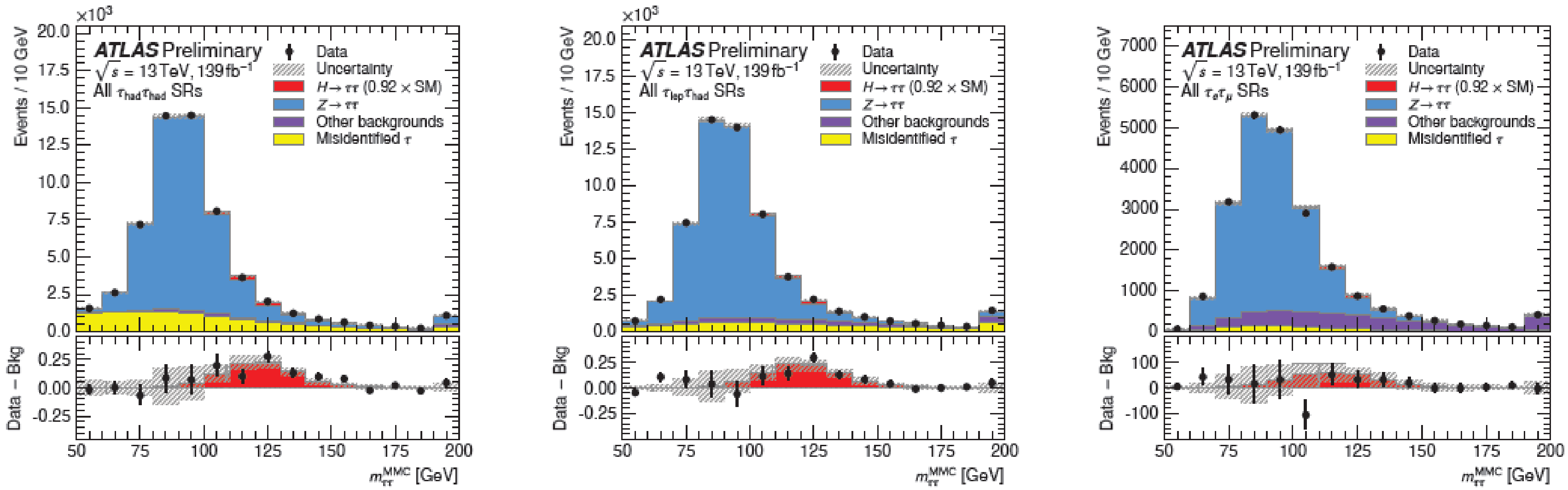

(a) $\tau_{had}\tau_{had}$ (b) $\tau_{lep}\tau_{had}$ (c) $\tau_e\tau_\mu$

Figure 9: Distribution of the reconstructed di-τ invariant mass ($m_{\tau\tau}^{MMC}$) for all events in the (a) $\tau_{had}\tau_{had}$, (b) $\tau_{lep}\tau_{had}$ and (c) $\tau_e\tau_\mu$ signal regions. The bottom panel shows the differences between observed data events and expected background events (black points). The observed Higgs-boson signal, corresponding to $(\sigma \times B)/(\sigma \times B)_{SM} = 0.92$, is shown with a filled red histogram. Entries with values above the x-axis range are shown in the last bin of each distributions. The prediction for each sample is determined from the likelihood fit performed to measure the total $pp \to H \to \tau\tau$ cross-section.

2 The SM BEH boson $H \to \tau\,\tau$

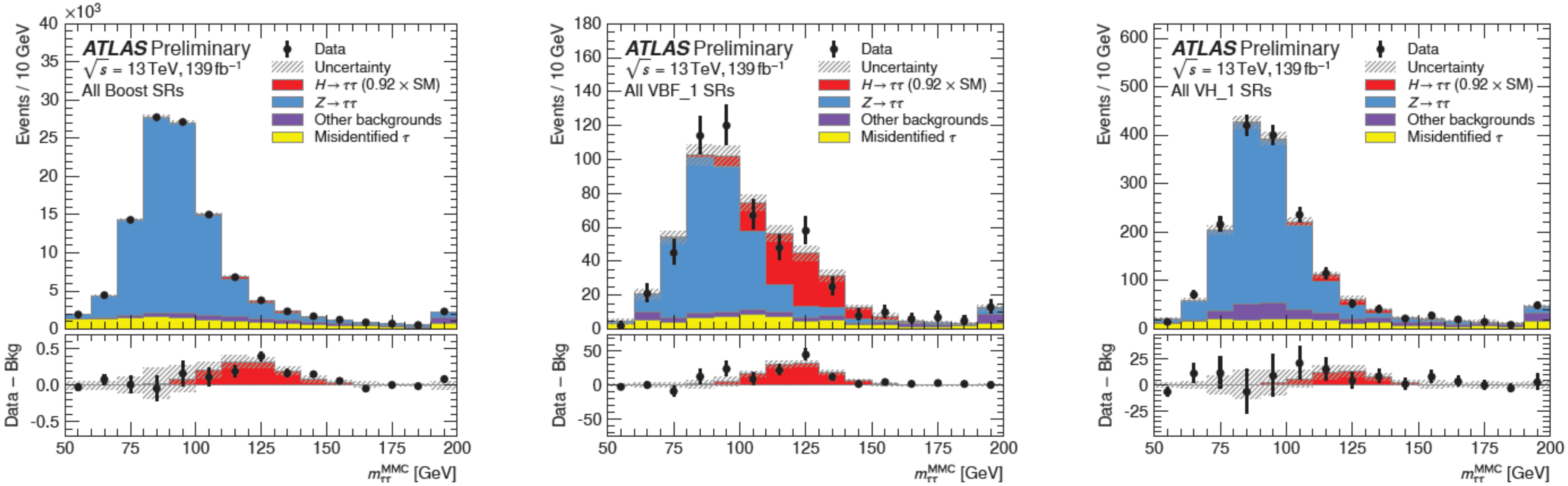

(a) boost (b) VBF_1 (c) VH_1

Figure 10: Distribution of the reconstructed di-τ invariant mass ($m_{\tau\tau}^{\mathrm{MMC}}$) for all events in the (a) boost, (b) VBF_1 and (c) VH_1 signal regions. The bottom panel shows the differences between observed data events and expected background events (black points). The observed Higgs-boson signal, corresponding to $(\sigma \times B)/(\sigma \times B)_{\mathrm{SM}} = 0.92$, is shown with a filled red histogram. Entries with values above the x-axis range are shown in the last bin of each distributions. The prediction for each sample is determined from the likelihood fit performed to measure the total $pp \to H \to \tau\tau$ cross-section.

ATLAS-CONF-2021-044

2 The SM BEH boson $H \rightarrow \tau\,\tau$

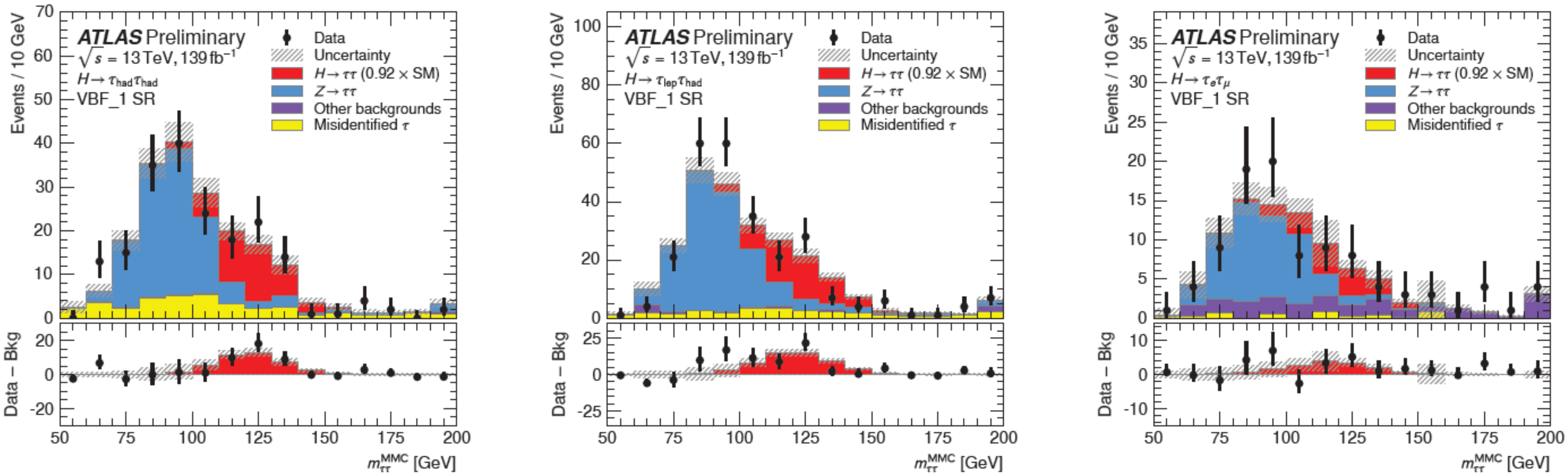

(a) $\tau_{\text{had}}\tau_{\text{had}}$ (b) $\tau_{\text{lep}}\tau_{\text{had}}$ (c) $\tau_e\tau_\mu$

Figure 11: Distribution of the reconstructed di-τ invariant mass ($m_{\tau\tau}^{\text{MMC}}$) for all events in the VBF_1 categories of (a) $\tau_{\text{had}}\tau_{\text{had}}$, (b) $\tau_{\text{lep}}\tau_{\text{had}}$ and (c) $\tau_e\tau_\mu$ signal regions. The bottom panel shows the differences between observed data events and expected background events (black points). The observed Higgs-boson signal, corresponding to $(\sigma \times B)/(\sigma \times B)_{\text{SM}} = 0.92$, is shown with a filled red histogram. Entries with values above the x-axis range are shown in the last bin of each distributions. The prediction for each sample is determined from the likelihood fit performed to measure the total $pp \rightarrow H \rightarrow \tau\tau$ cross-section.

2 *The SM BEH boson H → τ τ (CMS)*

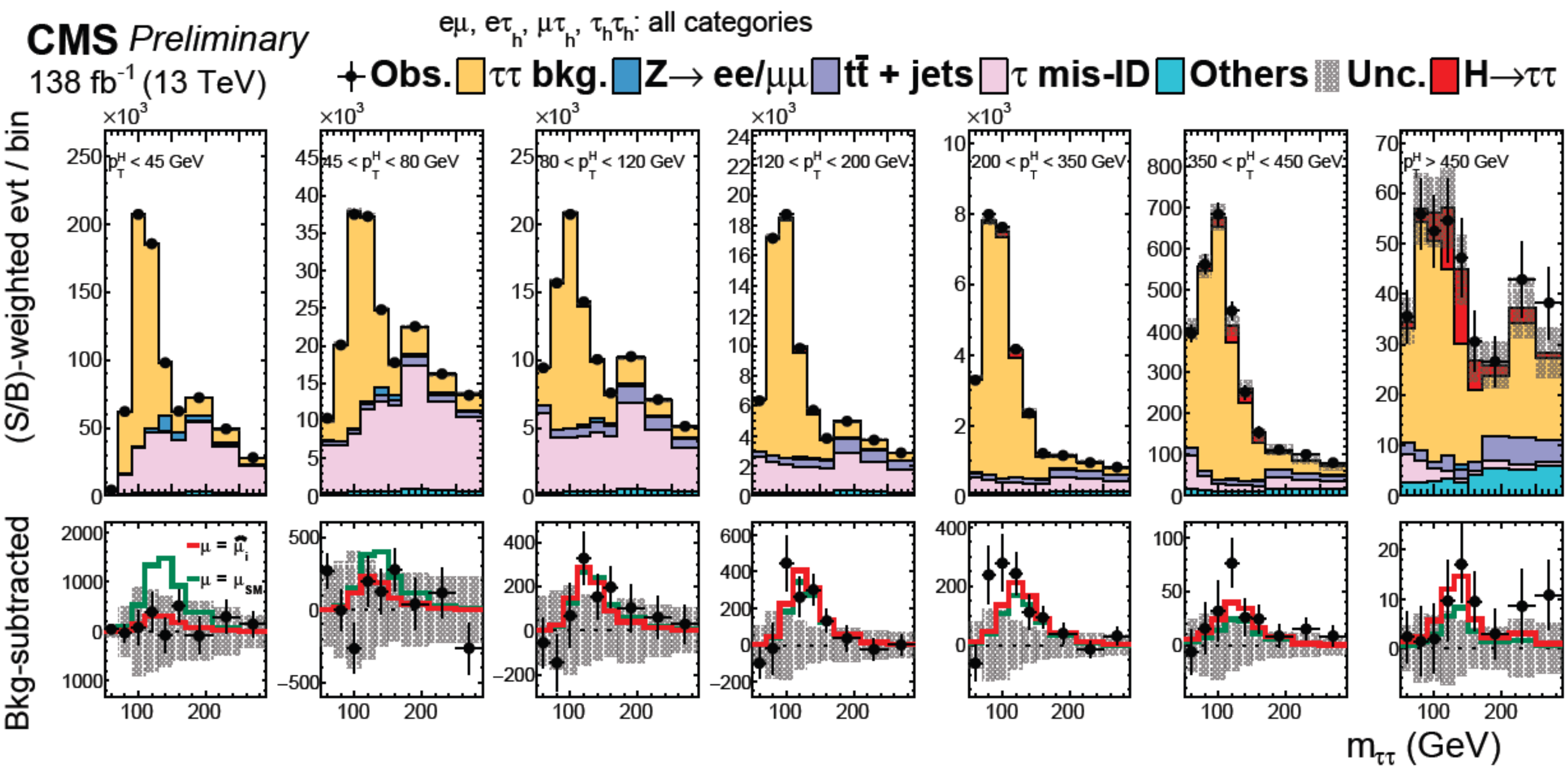

Inclusive fiducial measurement

(by summing N_{jet} bins)

$$\sigma_{\mathrm{fid}} = 426 \pm 102\ \mathrm{fb}$$

$$\sigma_{\mathrm{fid}}^{\mathrm{SM}} = 408 \pm 27\ \mathrm{fb}$$

2 The SM BEH boson $H \to cc$

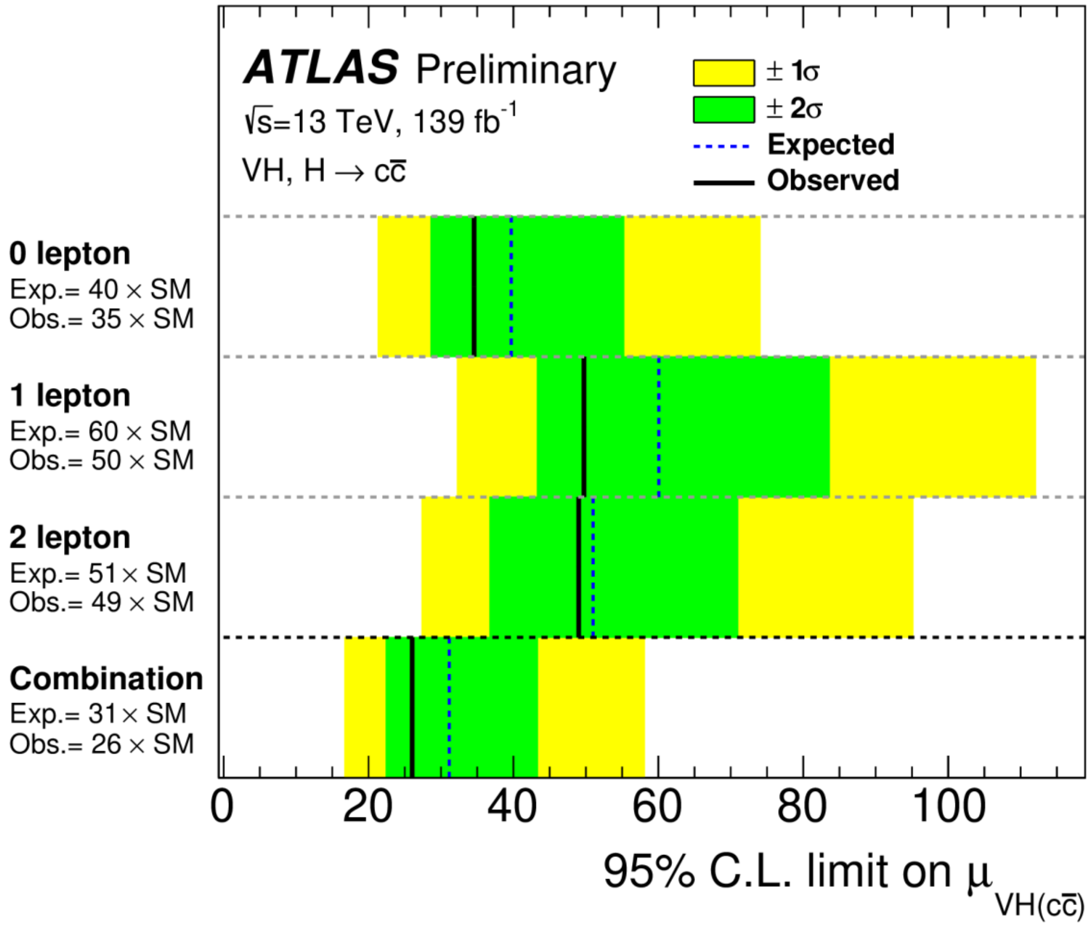

2 The SM BEH boson $H \rightarrow cc$

ATLAS-CONF-2021-021

Target VH production to suppress backgrounds and trigger

Challenges:

- ⋆ c-tagging: multivariate algorithm
- ⋆ Large backgrounds: categorize in terms of number of leptons, number of c-tags, p_T^V

Limit on $H \to c\bar{c}$: $\mathbf{26}$ ($\mathbf{31^{+12}_{-8}}$) $\times$ SM 95% CL

$|\kappa_c| < \mathbf{8.5}$ ($\mathbf{12.4}$) obs. (exp.) at 95% CL

$$\mu_{VH(c\bar{c})}(\kappa_c) = \frac{\kappa_c^2}{1 + B^{\mathrm{SM}}_{H\to c\bar{c}}(\kappa_c^2 - 1)}$$

2 The SM BEH boson $H \to cc$

ATLAS-CONF-2021-021

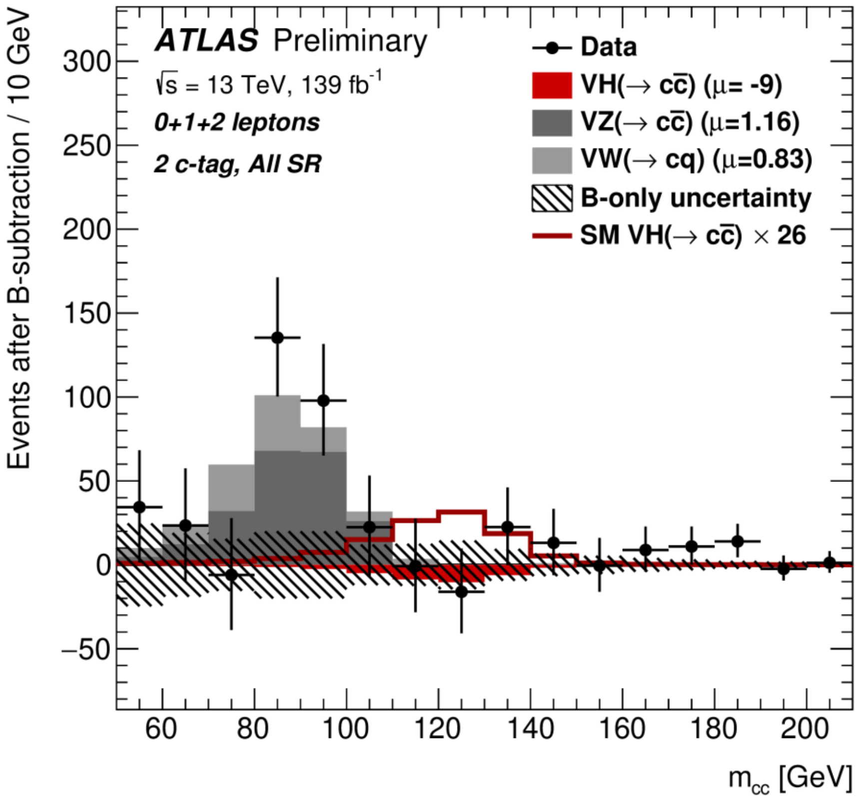

Simultaneous measurement of $VW(\to cq)$ and $VZ(\to c\bar{c})$ as control channels

- ⋆ 3.8 σ (4.6 σ) and 2.6 σ (2.2 σ) obs. (exp.) significance

2 The SM BEH boson $H \to \mu\mu$

Phys. Lett. B 812 (2021) 135980 arXiv:2007.07830

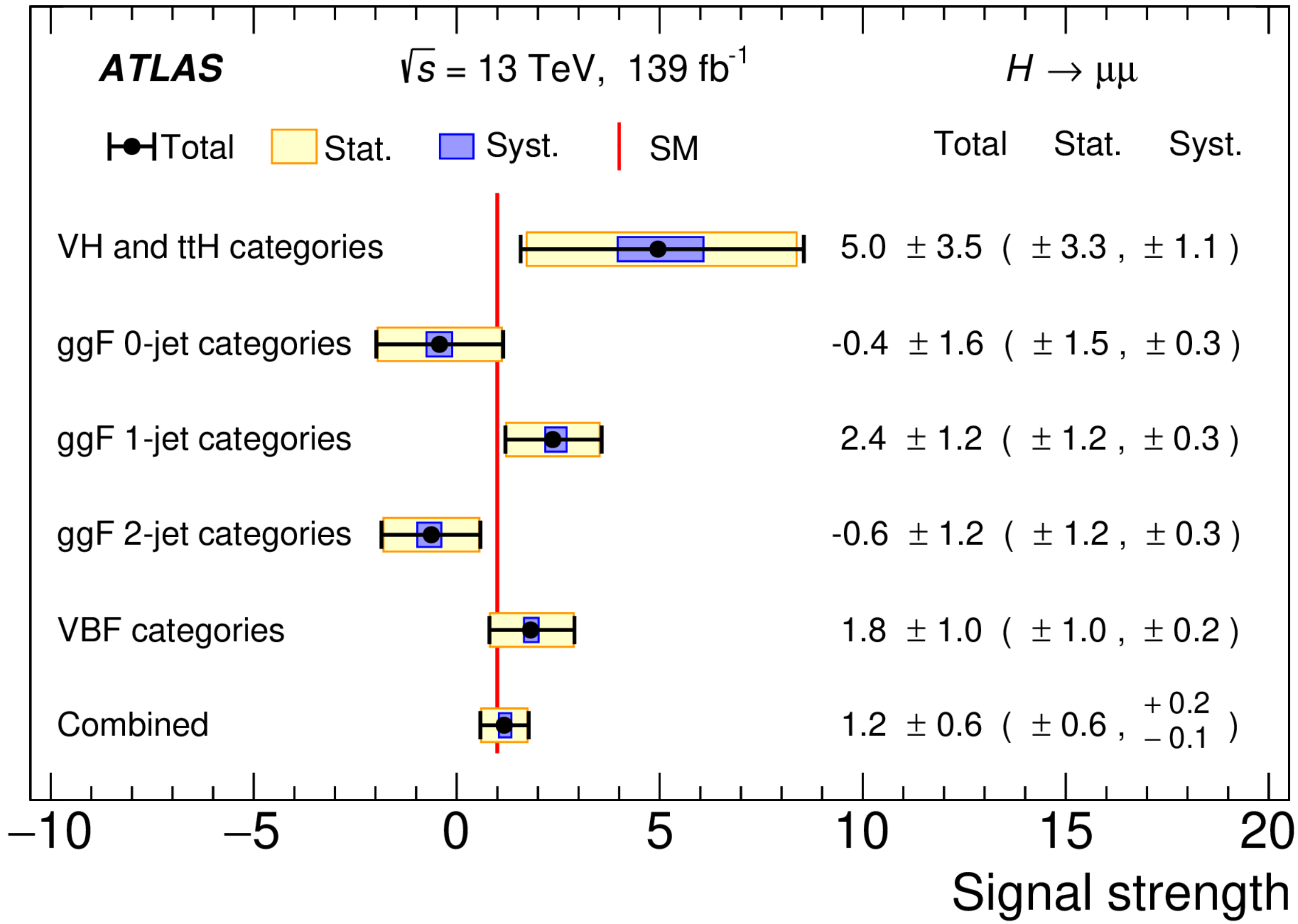

2 The SM BEH boson $H \to W W^* \to e\,\nu\,\mu\,\nu$

ATLAS-CONF-2021-014

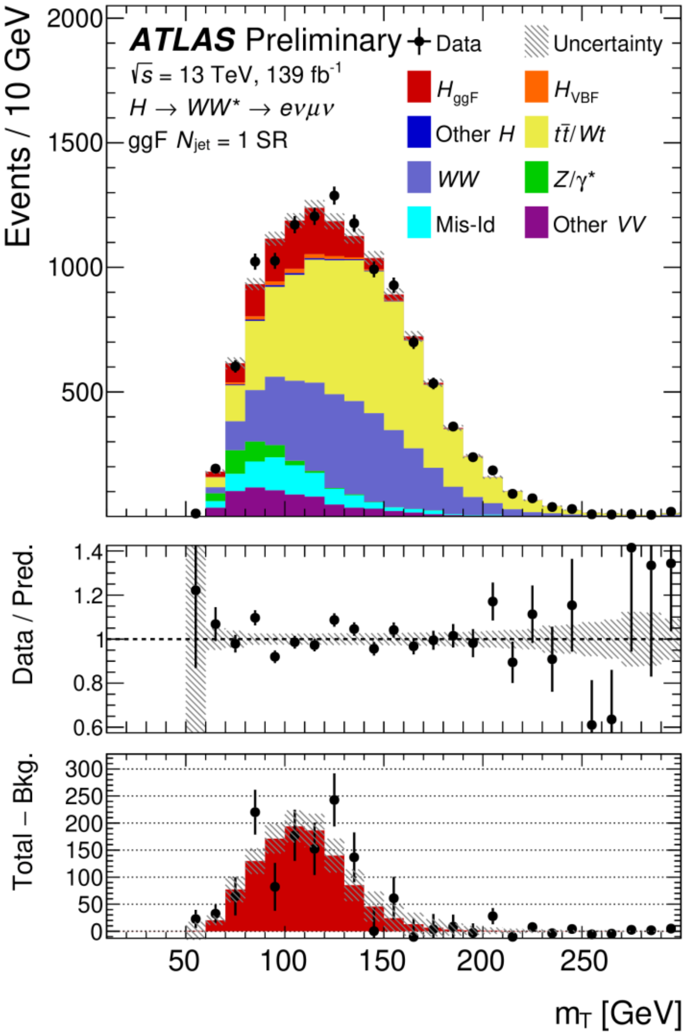

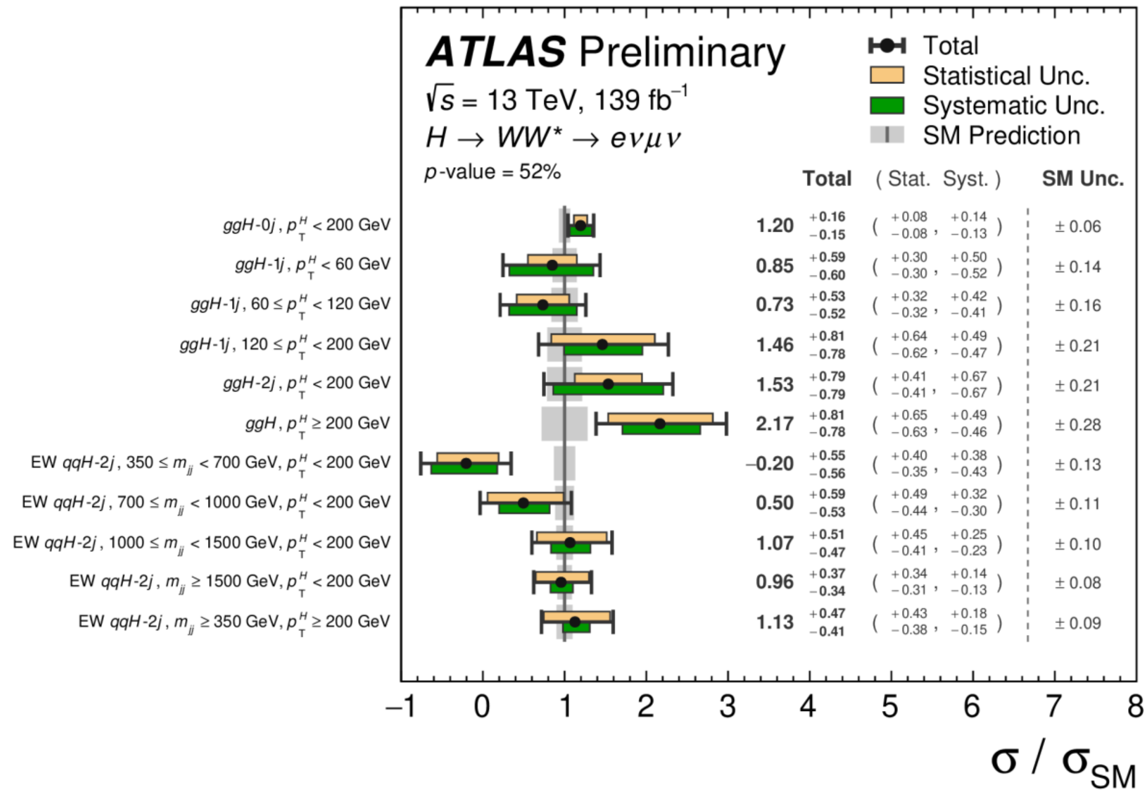

2 The SM BEH boson combined $H \to 4l$ and $H \to \gamma\gamma$

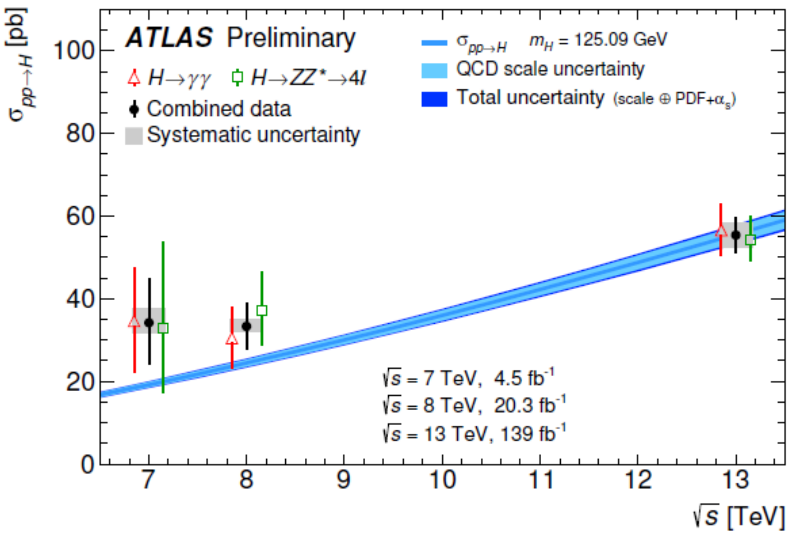

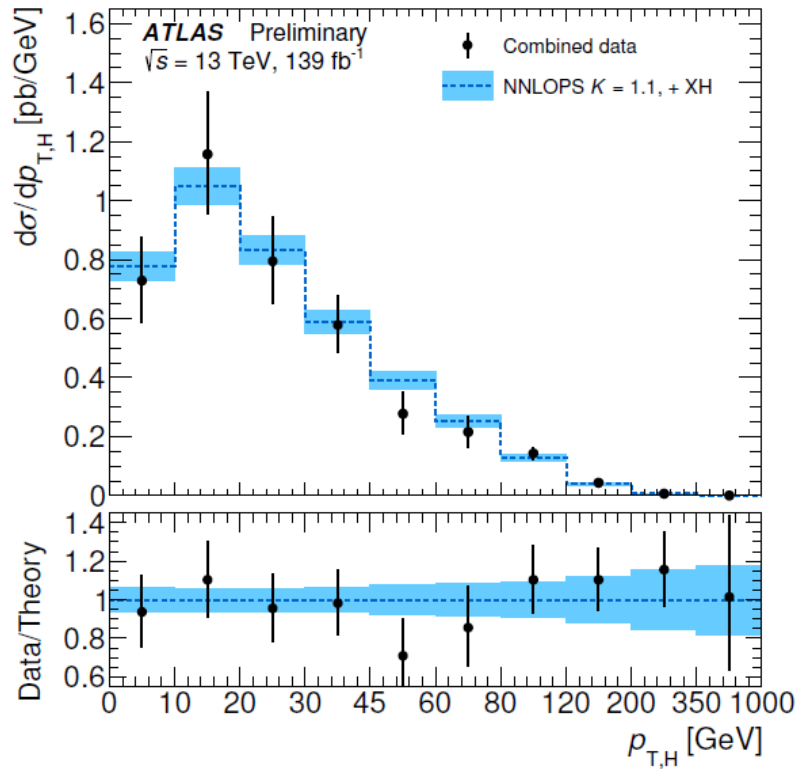

ATLAS-CONF-2019-032

Combined inclusive $pp \to H$ cross section

$$55.4^{+4.3}_{-4.2}\ \text{pb}\ (\ \pm 3.1(\text{stat.})\ ^{+3.0}_{-2.8}(\text{sys.})\ )$$

$$SM = 55.6 \pm 2.5\ \text{pb}$$

2 The SM BEH boson H → bb
(already at Corfou 2019***)***

Combination of VH channels gives significance obs(exp) of 5.3 σ (4.8 σ)

H→bb

Main analysis is targetting VH but also start to look at ggH and VBF modes

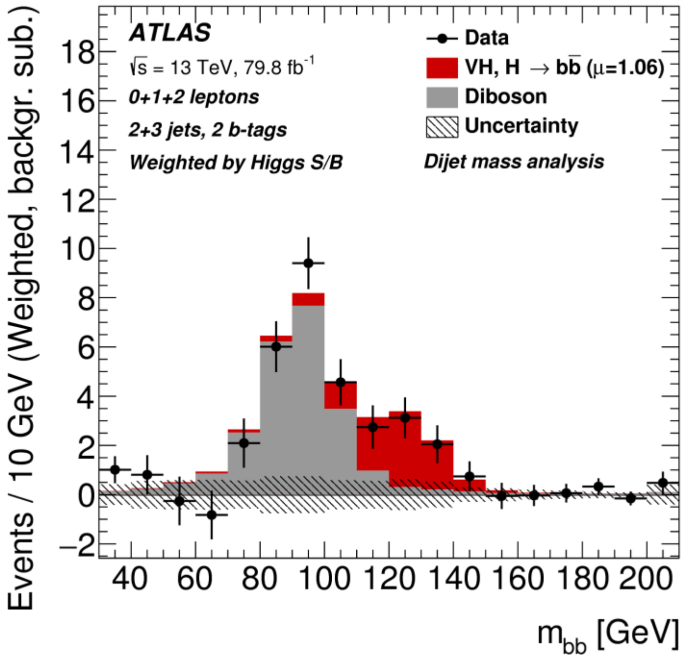

Phys.Lett. B786 (2018) 59-86

H→ bb : 5.4 σ obs 5.5 σ exp

$$\mu = 1.01 \pm 0.12(\text{stat.})^{+0.16}_{-0.15}(\text{syst.})$$

2 The SM BEH boson WH and ZH $H \to bb$

Eur.Phys.J.C 81 (2021) 2, 178

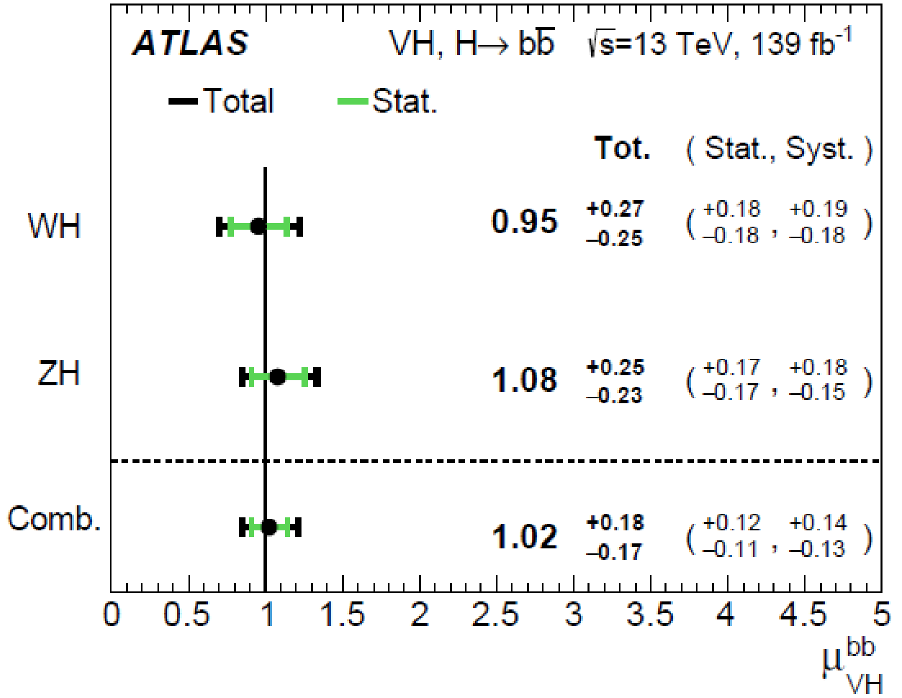

The production of a Higgs boson in association with a W or Z boson is established with observed (expected) significances of 4.0 (4.1) and 5.3 (5.1) standard deviations, respectively

2 The SM BEH boson WH and ZH $H \to bb$

Eur.Phys.J.C 81 (2021) 2, 178

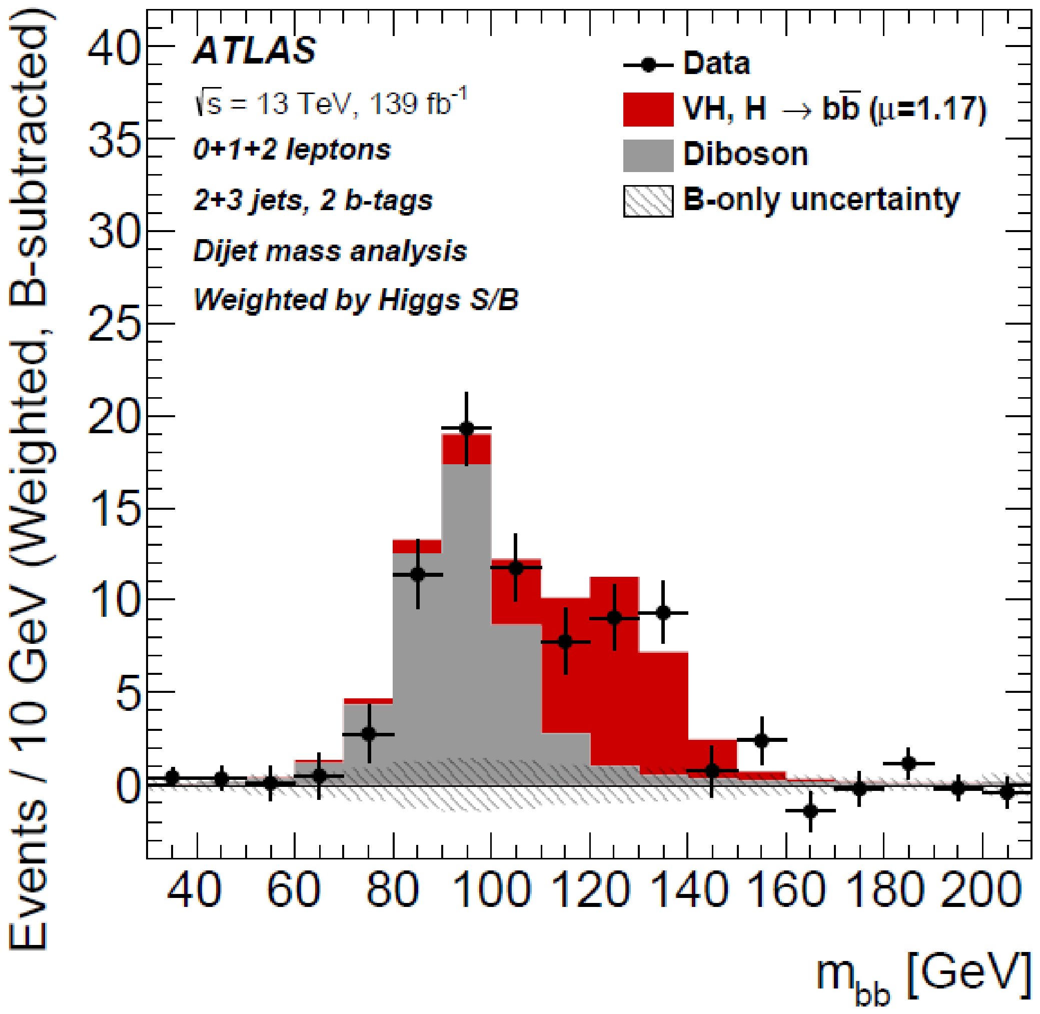

2 The SM BEH boson WH and ZH $H \to bb$

Eur.Phys.J.C 81 (2021) 2, 178

Table 2: Summary of the event selection and categorisation in the 0-, 1- and 2-lepton channels.

Selection	0-lepton	1-lepton		2-lepton
		e sub-channel	μ sub-channel	
Trigger	E_T^{miss}	Single lepton	E_T^{miss}	Single lepton
Leptons	0 *loose* leptons	Exactly 1 *tight* electron 0 additional *loose* leptons $p_T > 27$ GeV	Exactly 1 *tight* muon 0 additional *loose* leptons $p_T > 25$ GeV	Exactly 2 *loose* leptons $p_T > 27$ GeV Same-flavour Opposite-sign charges ($\mu\mu$)
E_T^{miss}	> 150 GeV	> 30 GeV	–	–
$m_{\ell\ell}$	–	–	–	$81\ \text{GeV} < m_{\ell\ell} < 101\ \text{GeV}$
Jet p_T	> 20 GeV for $\|\eta\| < 2.5$ > 30 GeV for $2.5 < \|\eta\| < 4.5$			
b-jets	Exactly 2 b-tagged jets			
Leading b-tagged jet p_T	> 45 GeV			
Jet categories	Exactly 2 / Exactly 3 jets	Exactly 2 / Exactly 3 jets		Exactly 2 / ≥ 3 jets
H_T	> 120 GeV (2 jets), > 150 GeV (3 jets)	–		–
$\min[\Delta\phi(\boldsymbol{E}_T^{miss}, \textbf{jets})]$	$> 20°$ (2 jets), $> 30°$ (3 jets)	–		–
$\Delta\phi(\boldsymbol{E}_T^{miss}, \boldsymbol{bb})$	$> 120°$	–		–
$\Delta\phi(\boldsymbol{b}_1, \boldsymbol{b}_2)$	$< 140°$	–		–
$\Delta\phi(\boldsymbol{E}_T^{miss}, \boldsymbol{p}_T^{miss})$	$< 90°$	–		–
p_T^V regions	– $150\ \text{GeV} < p_T^V < 250\ \text{GeV}$ $p_T^V > 250$ GeV	– $150\ \text{GeV} < p_T^V < 250\ \text{GeV}$ $p_T^V > 250$ GeV		$75\ \text{GeV} < p_T^V < 150\ \text{GeV}$ $150\ \text{GeV} < p_T^V < 250\ \text{GeV}$ $p_T^V > 250$ GeV
Signal regions	$\Delta R(\boldsymbol{b}_1, \boldsymbol{b}_2)$ signal selection			
Control regions	High and low $\Delta R(\boldsymbol{b}_1, \boldsymbol{b}_2)$ side-bands			

2 The SM BEH boson WH and ZH $H \to bb$ cross check WZ and ZZ $Z \to bb$

Eur.Phys.J.C 81 (2021) 2, 178

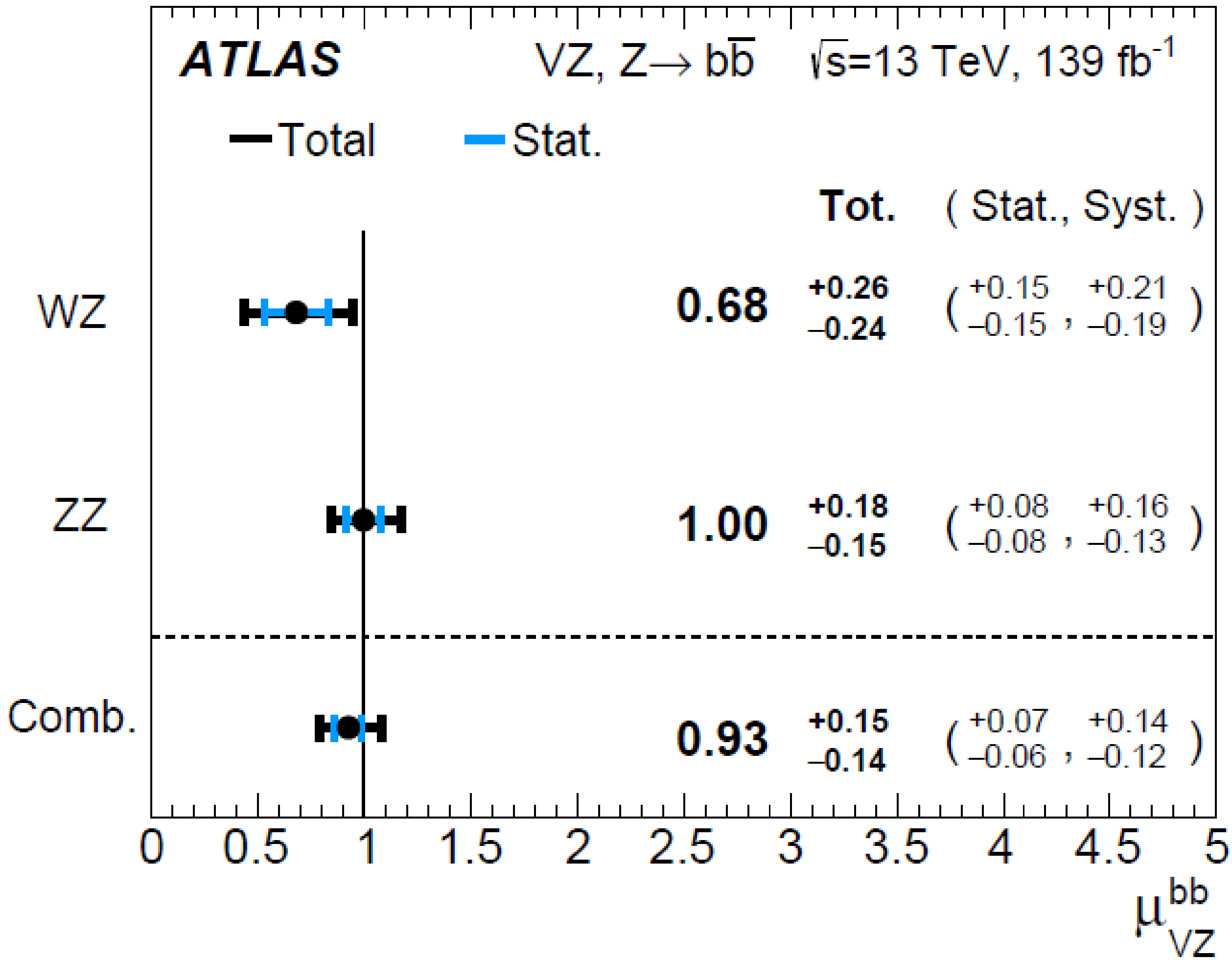

2 The SM BEH boson VBF $H \to bb$

Eur. Phys. J. C. 81 (2021) 537

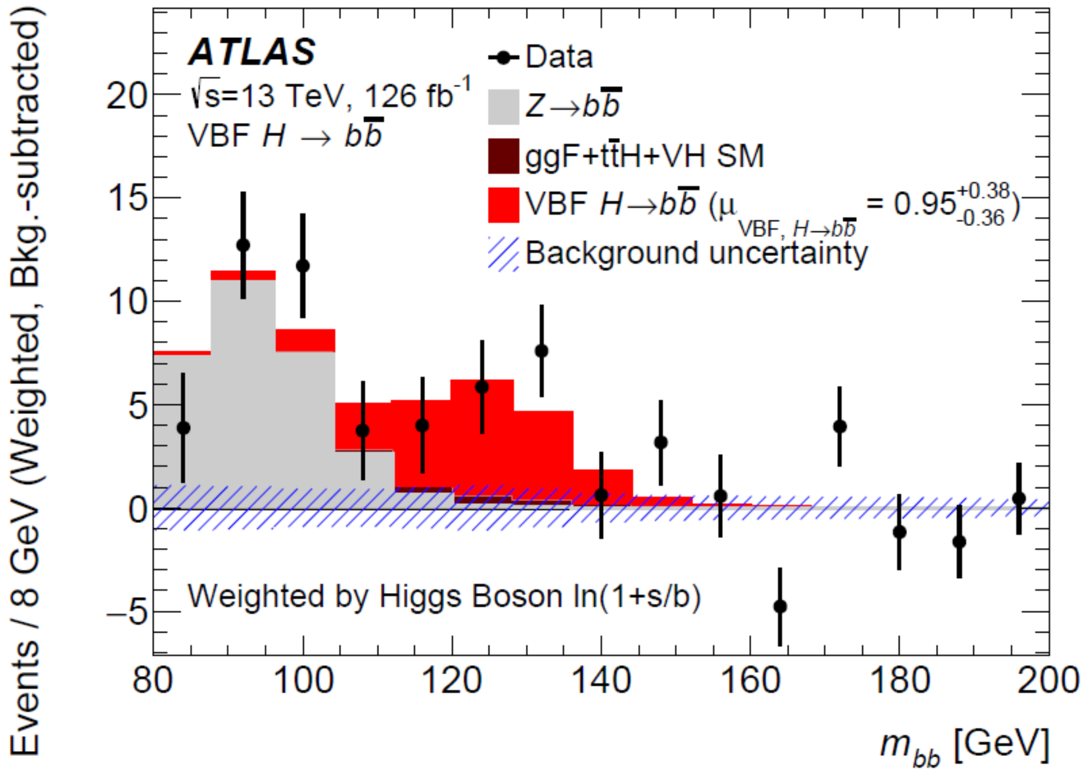

observed (expected) significance of 2.6 (2.8) standard deviations from the background only hypothesis

2 The SM BEH boson
3 VBF (H → bb) + γ

JHEP 03 (2021) 268

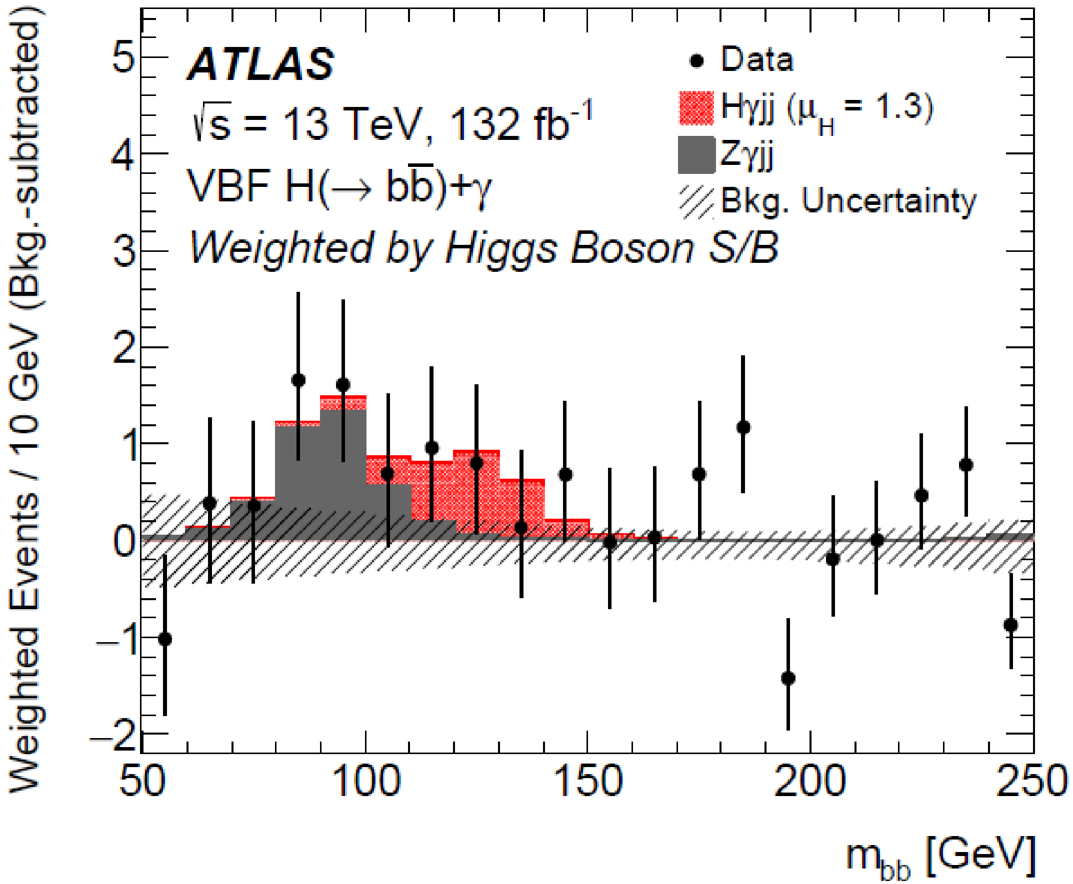

The measured Higgs boson signal yield in this final-state signature is 1.3 ± 1.0 times the Standard Model prediction. The observed significance of the Higgs boson signal above the background is 1.3 standard deviations, compared to an expected significance of 1.0 standard deviations.

2 The SM BEH boson H combination

ATLAS-CONF-2020-027

Analysis decay channel	Target Prod. Modes	$\mathcal{L}$ [fb^{-1}]
$H \to \gamma\gamma$	ggF, VBF, $WH, ZH, t\bar{t}H, tH$	139
$H \to ZZ^*$	ggF, VBF, $WH, ZH, t\bar{t}H(4\ell)$	139
	$t\bar{t}H$ excl. $H\to ZZ^*\to 4\ell$	36.1
$H \to WW^*$	ggF, VBF	36.1
	$t\bar{t}H$	
$H \to \tau\tau$	ggF, VBF	36.1
	$t\bar{t}H$	
$H \to b\bar{b}$	VBF	24.5 – 30.6
	WH, ZH	139
	$t\bar{t}H$	36.1
$H \to \mu\mu$	ggF, VBF, $VH, t\bar{t}H$	139
$H \to inv$	VBF	139

2 The SM BEH boson H combination

ATLAS-CONF-2020-027

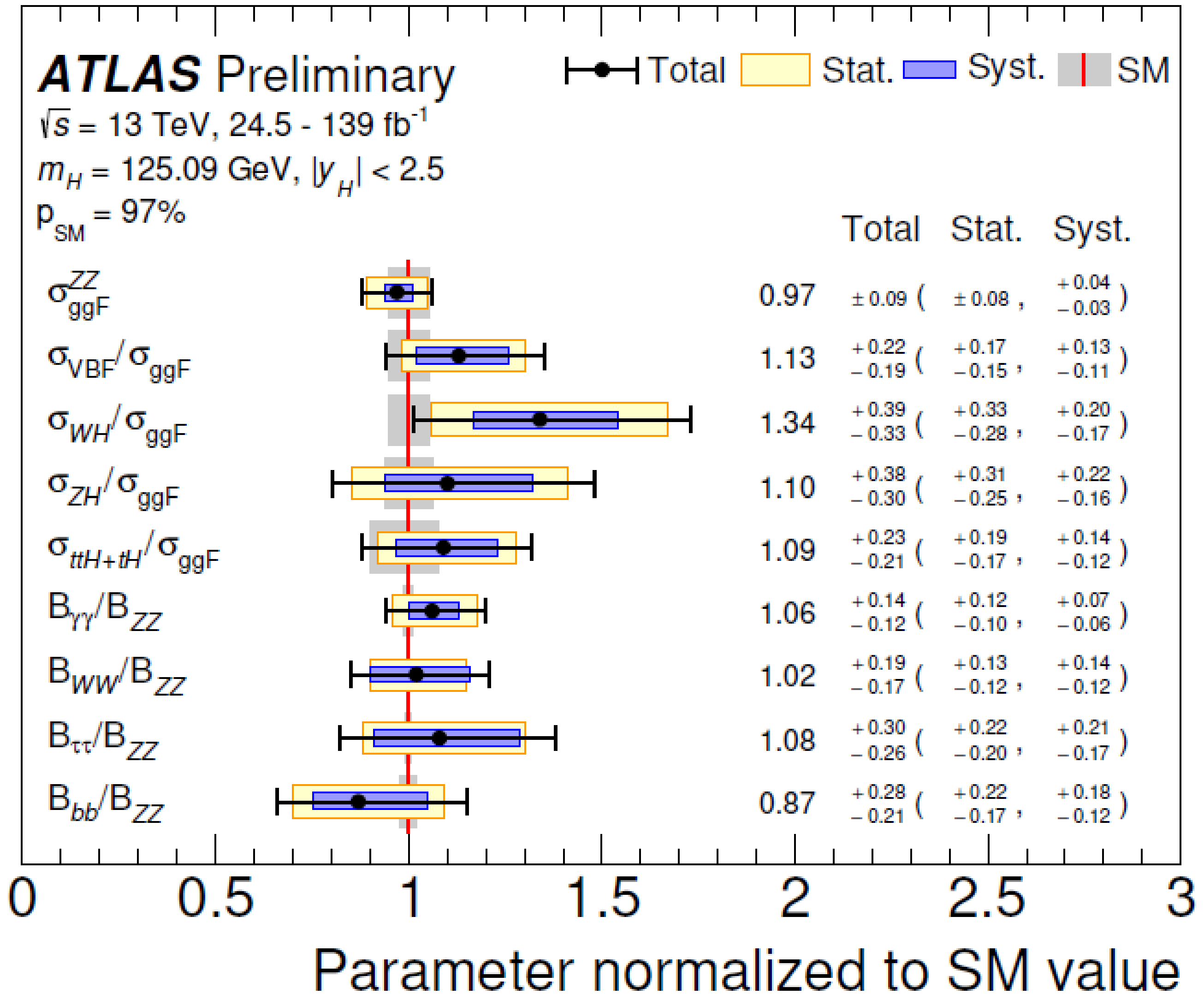

2 The SM BEH boson H combination

ATLAS-CONF-2020-027

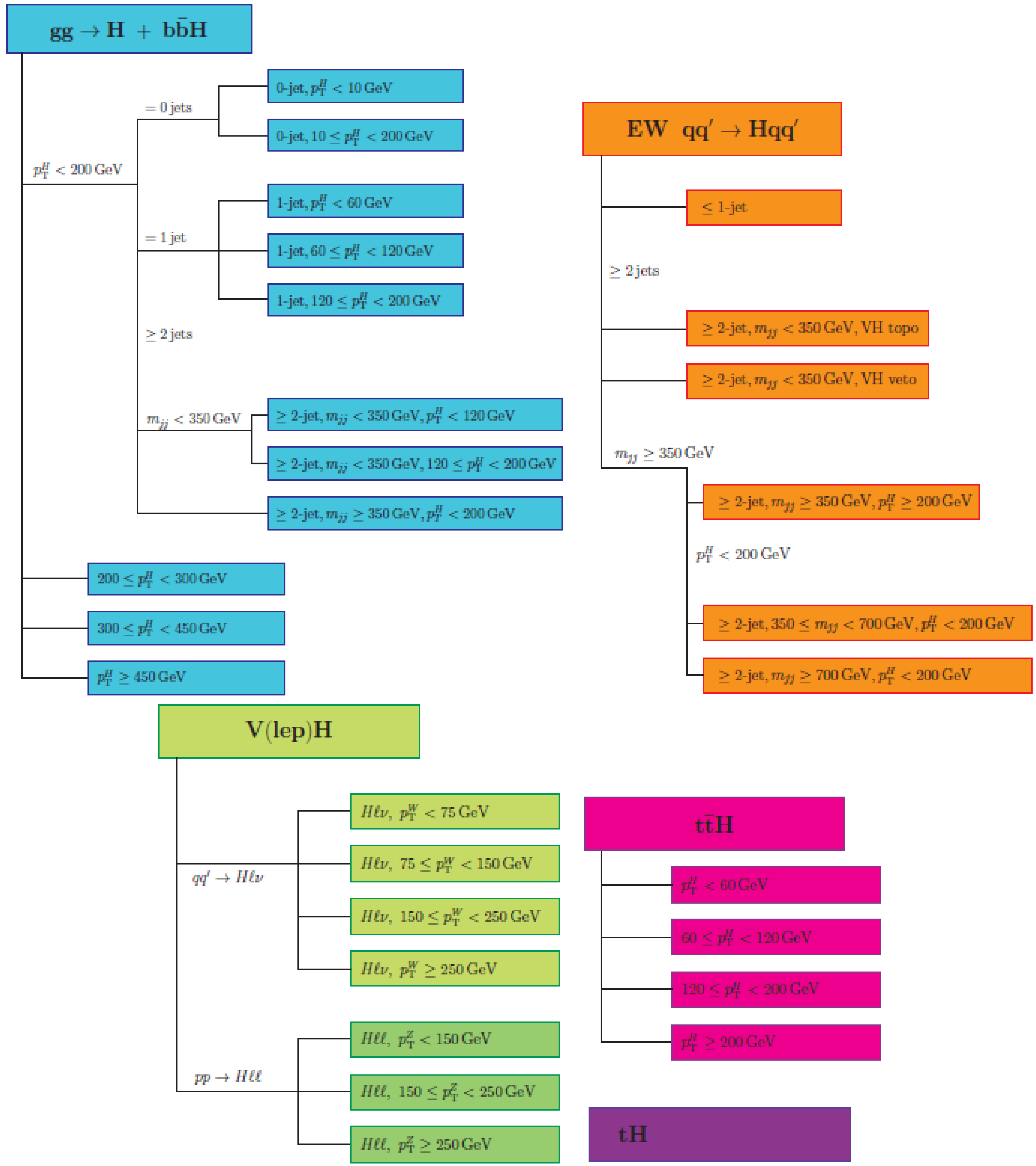

2 The SM BEH boson STXS = simplified template cross sections
(transparency already shown at Corfou 2019)

designed to measure the different Higgs boson production processes in specific regions of phase space and in a way that can be easily combined with other decay channels

Compared to the signal strength measurements they provide finer granularity

theory uncertainties are smaller

In fact there are 31 STXS , but measure 9 (lack of statistics)

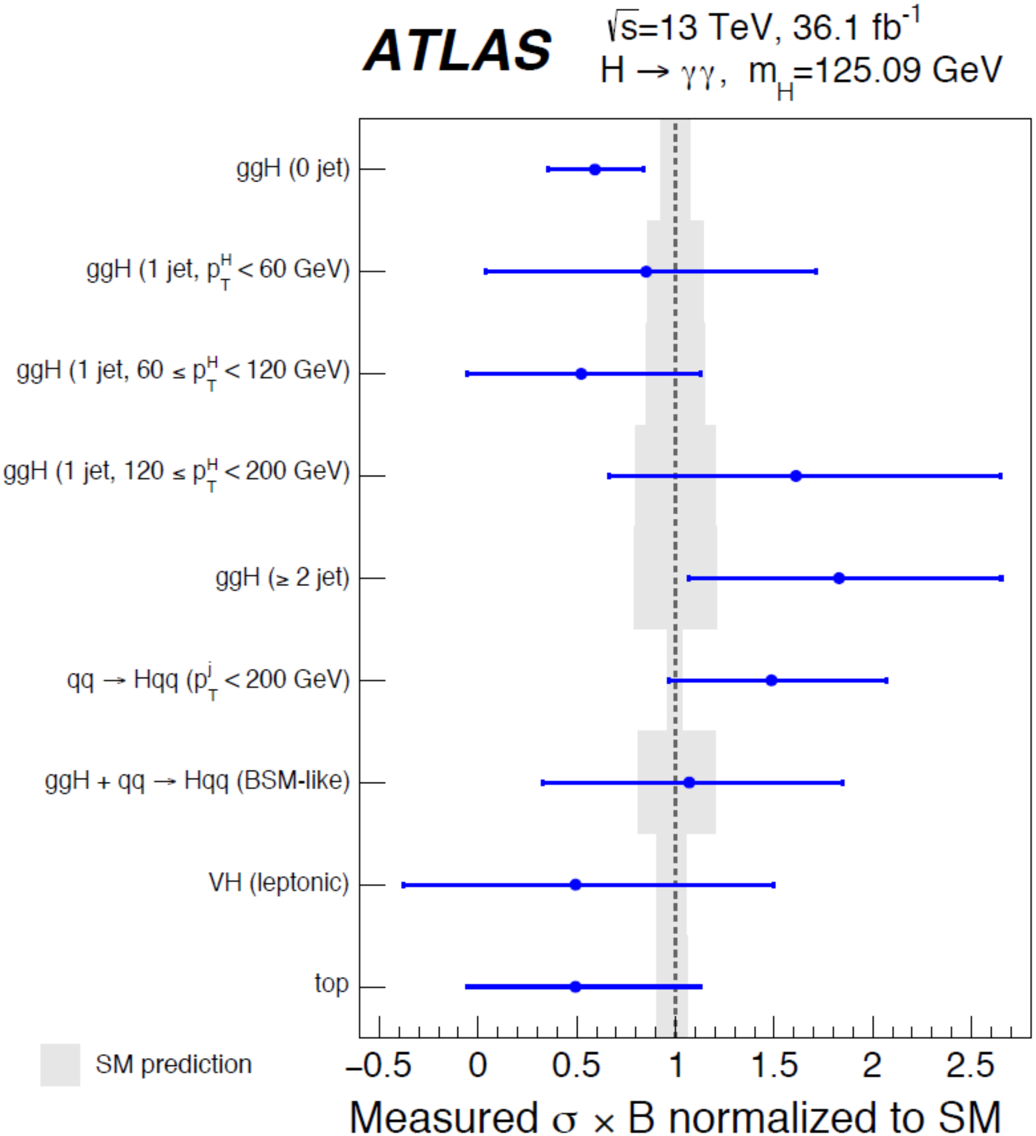

arXiv:1802.04146

2 The SM BEH boson H combination

ATLAS-CONF-2020-027

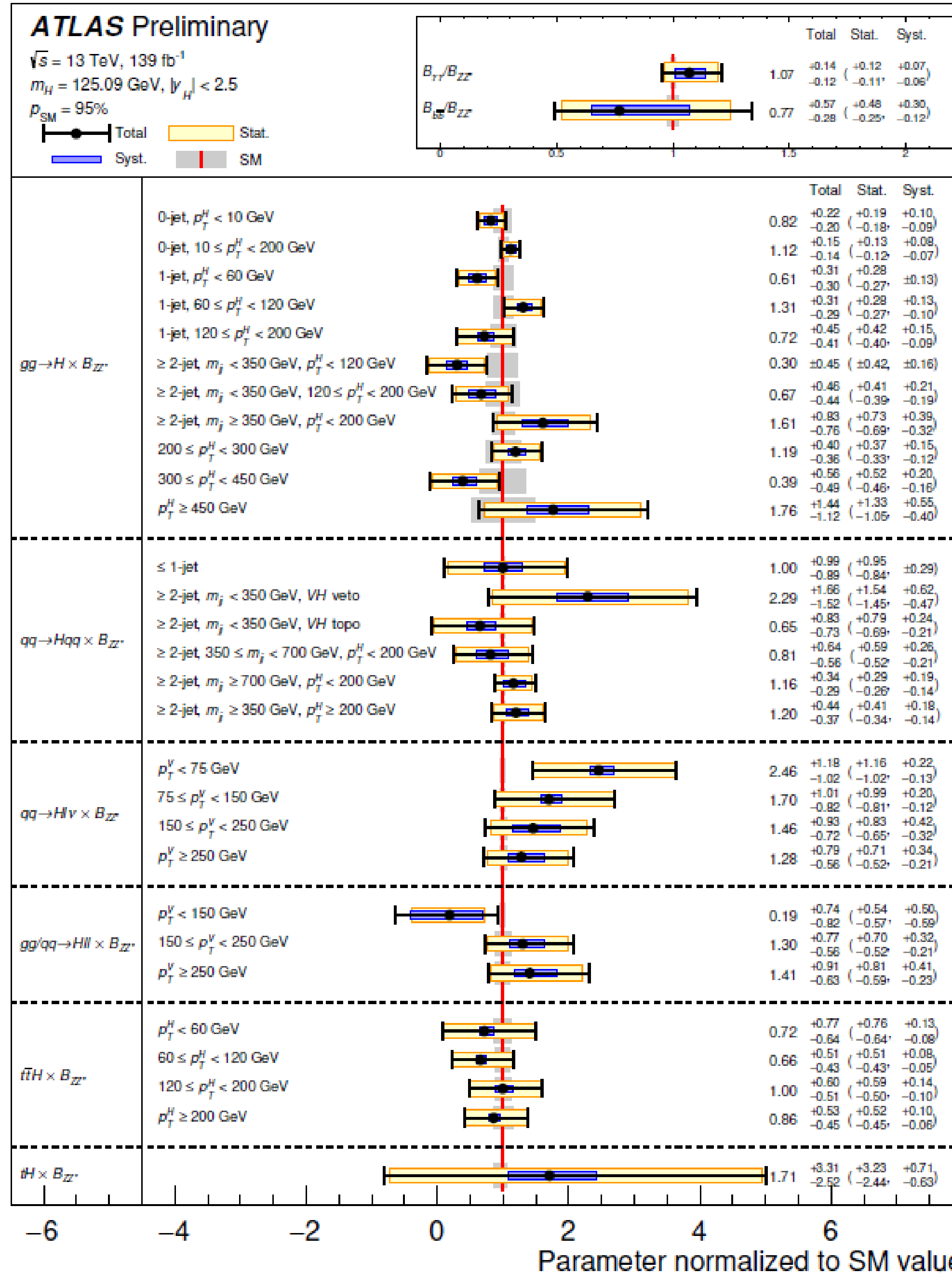

- Invisible decays: decays which are identified through an $E_{\mathrm{T}}^{\mathrm{miss}}$ signature in the analyses described in Section 3.5. In the SM, the branching fraction of invisible decays is predicted to be 0.1%, exclusively from the $H \to ZZ^* \to 4\nu$ process. The BSM contribution to this branching fraction is denoted as $B_{\mathrm{i.}}$.
- Undetected decays: decays to which none of the analyses included in this combination are sensitive, such as decays to light quarks which have not yet been resolved, or undetected BSM particles without a sizable $E_{\mathrm{T}}^{\mathrm{miss}}$ in the final state. For the former, the SM contribution of these undetected decays is already included in Γ^{SM}, and amounts to 11%, mainly driven by the decays to gluon pairs. The BSM contribution to the undetected branching fraction is denoted as $B_{\mathrm{u.}}$. Note that deviations of the partial width of the input measurements of this analysis are separately included by scaling their partial width by κ_j.

2 The SM BEH boson H combination interpretation

ATLAS-CONF-2020-053

Two interpretations of these measurements are presented here, based on an Effective Field Theory (EFT) framework of the Standard Model (SM), as well as a minimal supersymmetric extension of the Standard Model (MSSM).

six benchmarks

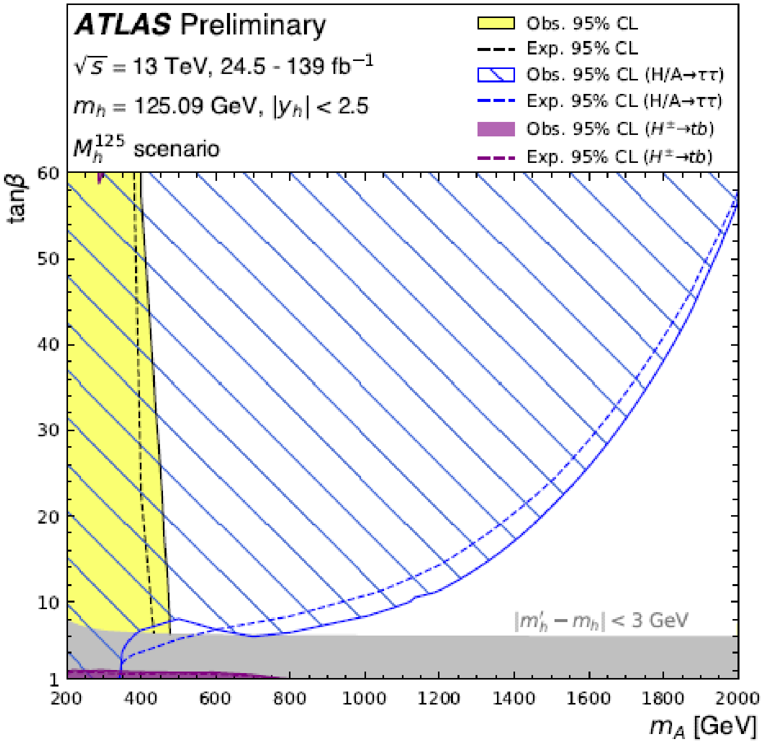

1. M_h^{125} **scenario:** All superparticles are chosen to be so heavy that production and decays of the MSSM Higgs bosons are only mildly affected by their presence. The loop-induced SUSY contribution to the couplings of the light CP-even scalar are small, and the heavy Higgs bosons with masses up to 2 TeV decay only to SM particles.

2 The SM BEH boson Z H invisible

ATLAS-CONF-2021-029

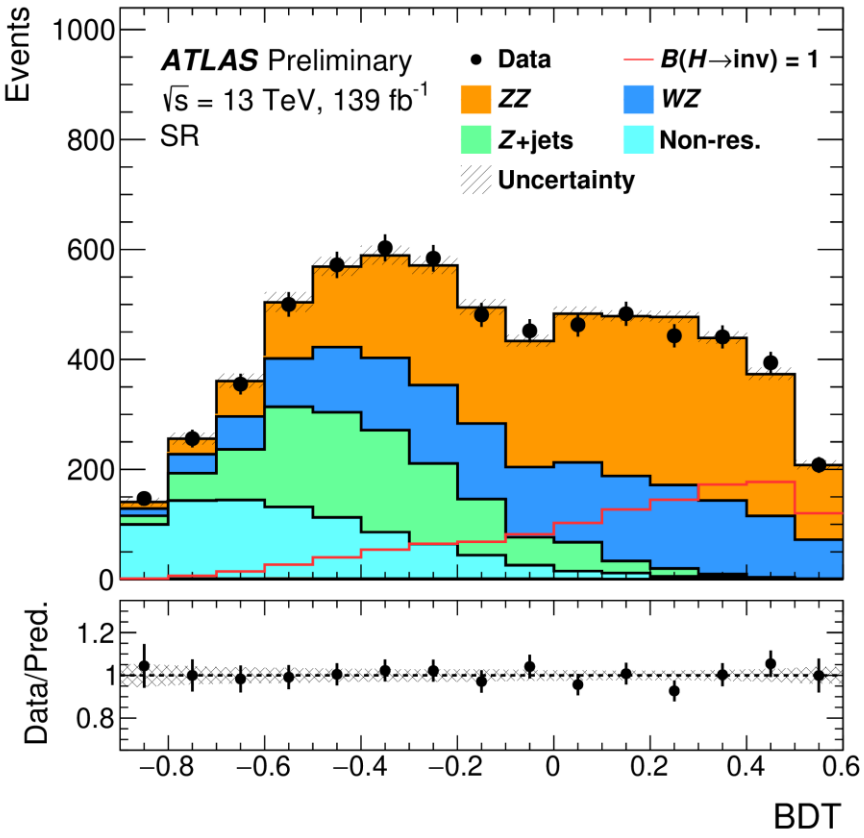

3 Search for a pair of BEH bosons

ATL-PHYS-PUB-2021-031

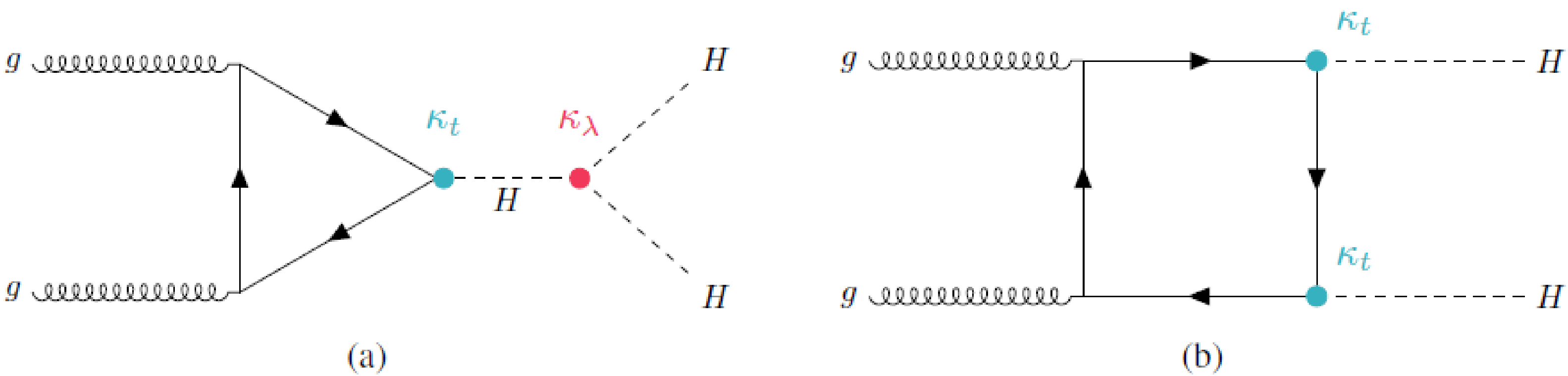

Figure 1: The LO Feynman diagrams for HH production via gluon-gluon fusion. The label κ_λ represents the Higgs boson self-coupling modifier and κ_t represents the top quark Yukawa coupling modifier.

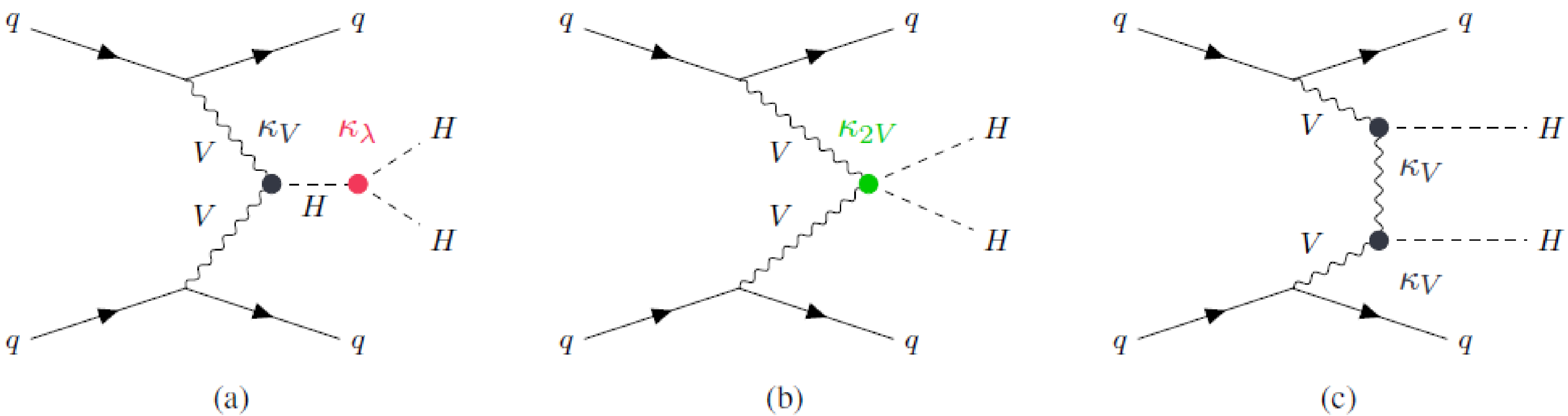

Figure 2: The LO Feynman diagrams for HH production via vector-boson fusion. The label κ_λ represents the Higgs boson self-coupling modifier, κ_{2V} represents the $HHVV$ coupling modifier and κ_V represents the HVV coupling modifier.

3 Search for a pair of BEH bosons

ATL-PHYS-PUB-2021-031

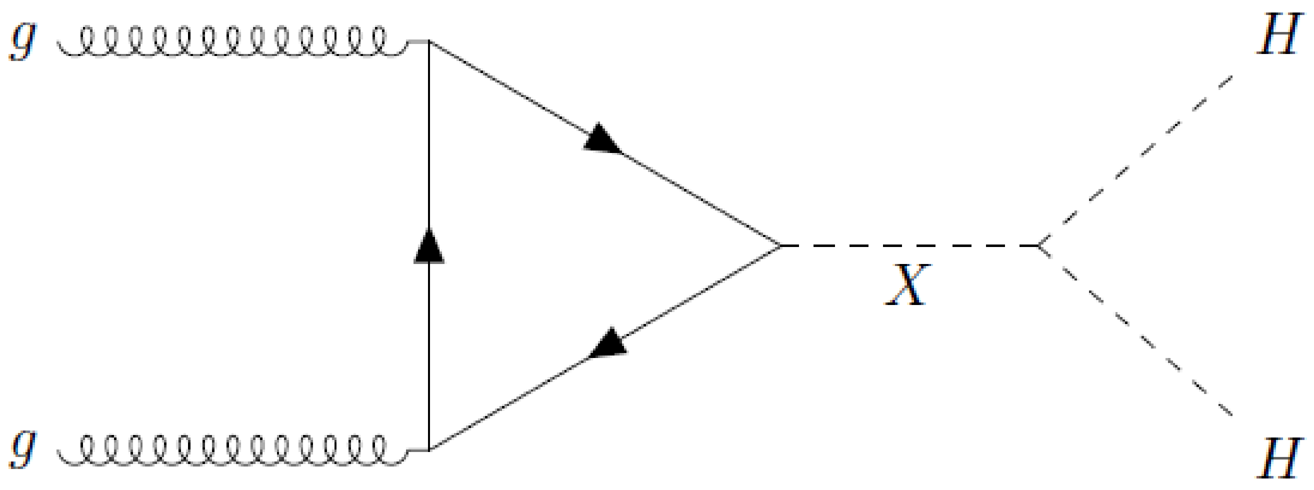

Figure 3: The LO Feynman diagram for gluon-gluon fusion production of a heavy scalar resonance decaying in Higgs boson pair.

3 Search for a pair of BEH bosons

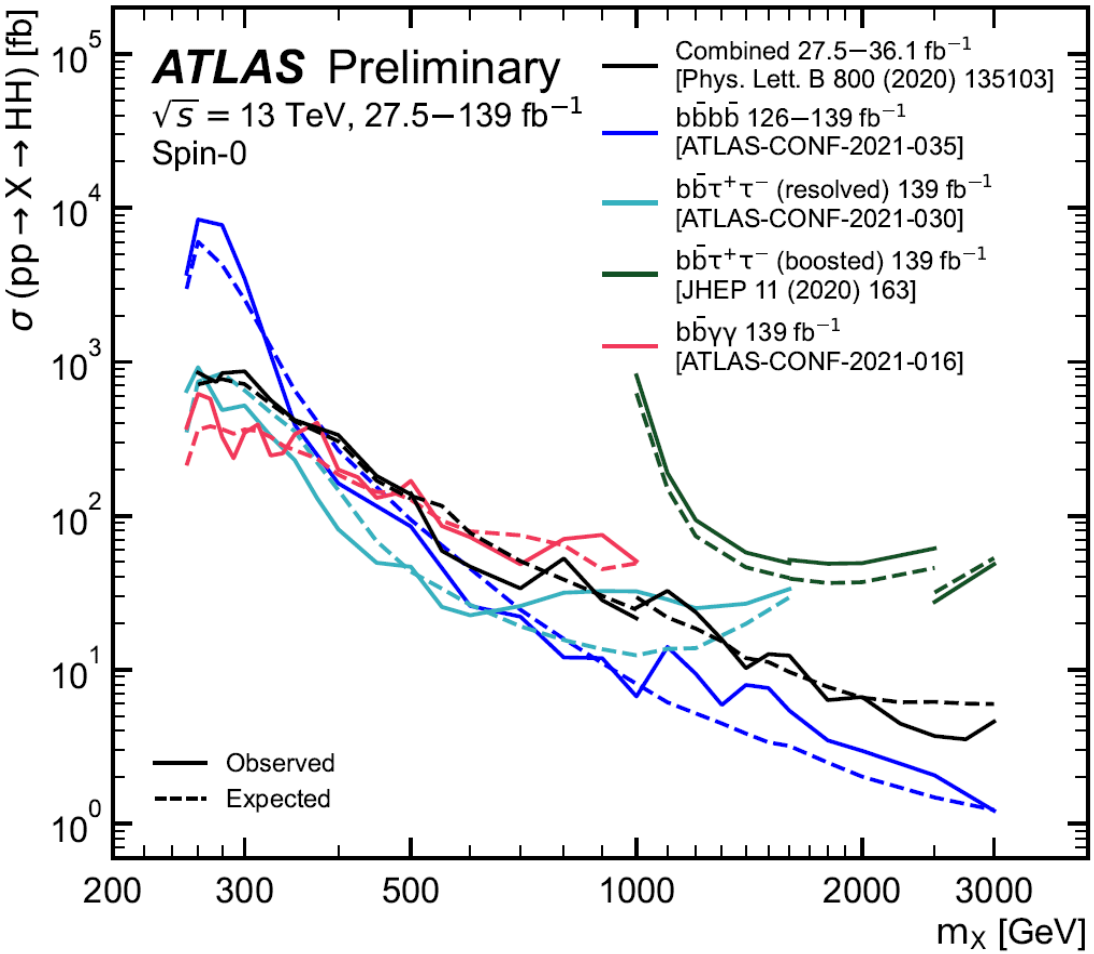

Figure 5: Upper limits at 95% confidence level (CL) on the resonant HH production cross-section as a function of the mass for a narrow-width scalar resonance. Results are shown from the statistical combination of the $b\bar{b}\tau^+\tau^-$, $b\bar{b}b\bar{b}$, $b\bar{b}\gamma\gamma$, $W^+W^-W^+W^-$, $W^+W^-\gamma\gamma$ and $b\bar{b}W^+W^-$ searches with 36 fb^{-1} and from the searches using 139 fb^{-1} in the $b\bar{b}\gamma\gamma$, resolved $b\bar{b}\tau^+\tau^-$, boosted $b\bar{b}\tau^+\tau^-$, and $b\bar{b}b\bar{b}$ channels.

HH → bb ττ

ATLAS-CONF-2021-030

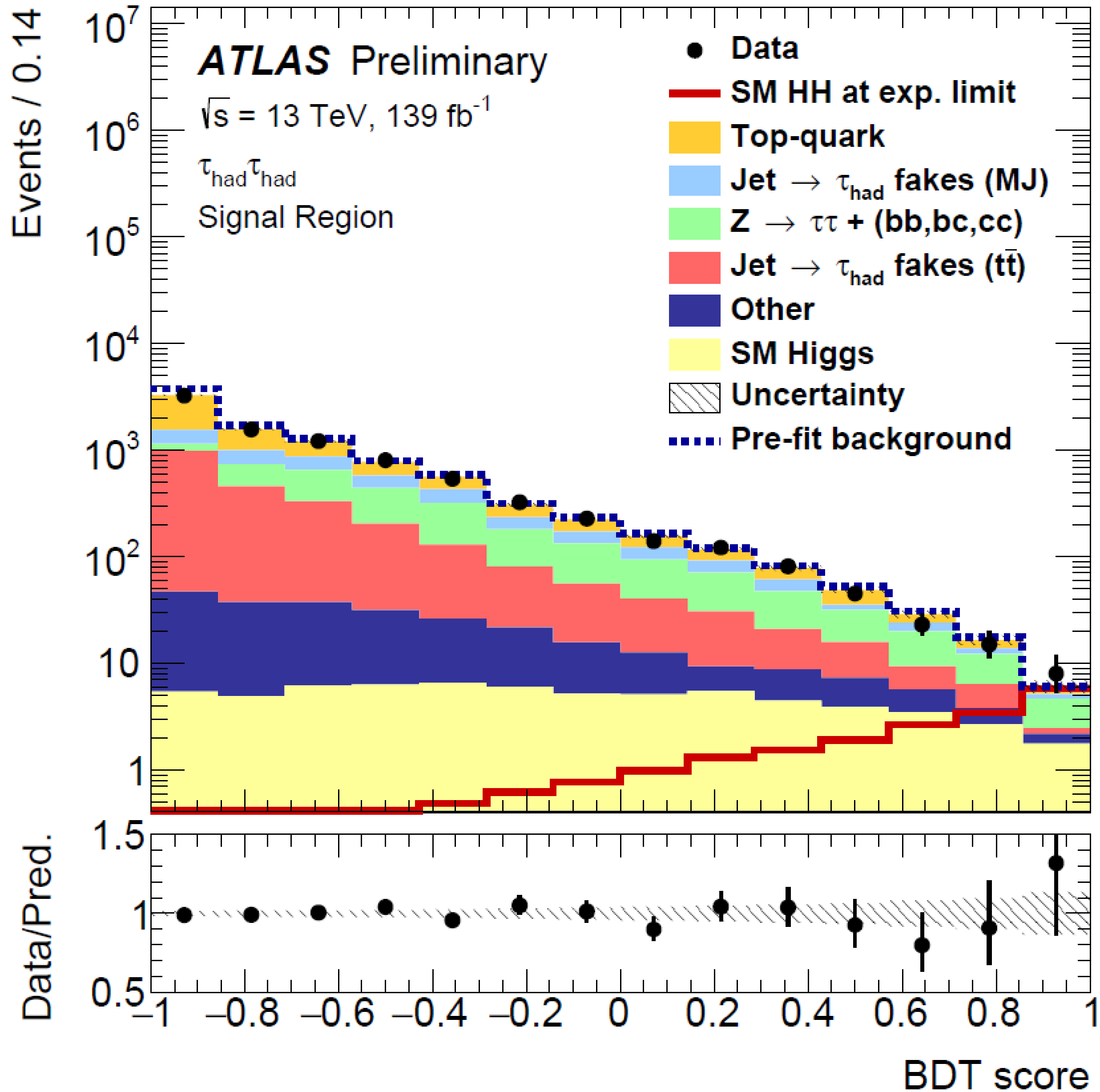

- ***Historical introduction , Setting the stage***
- ***Results***
- ***Future of ATLAS , Run-3 , HL-LHC***
- ***Conclusions***
- ***Backup***

- ♪ *Historical introduction , Setting the stage*
- ♪ *Results*
- ♪ *Future of ATLAS , Run-3 , HL-LHC*
- ♪ ***Conclusions***
- ♪ *Backup*